RAOUL PIETERSZ

Pricing models for Bermudan-style interest rate derivatives

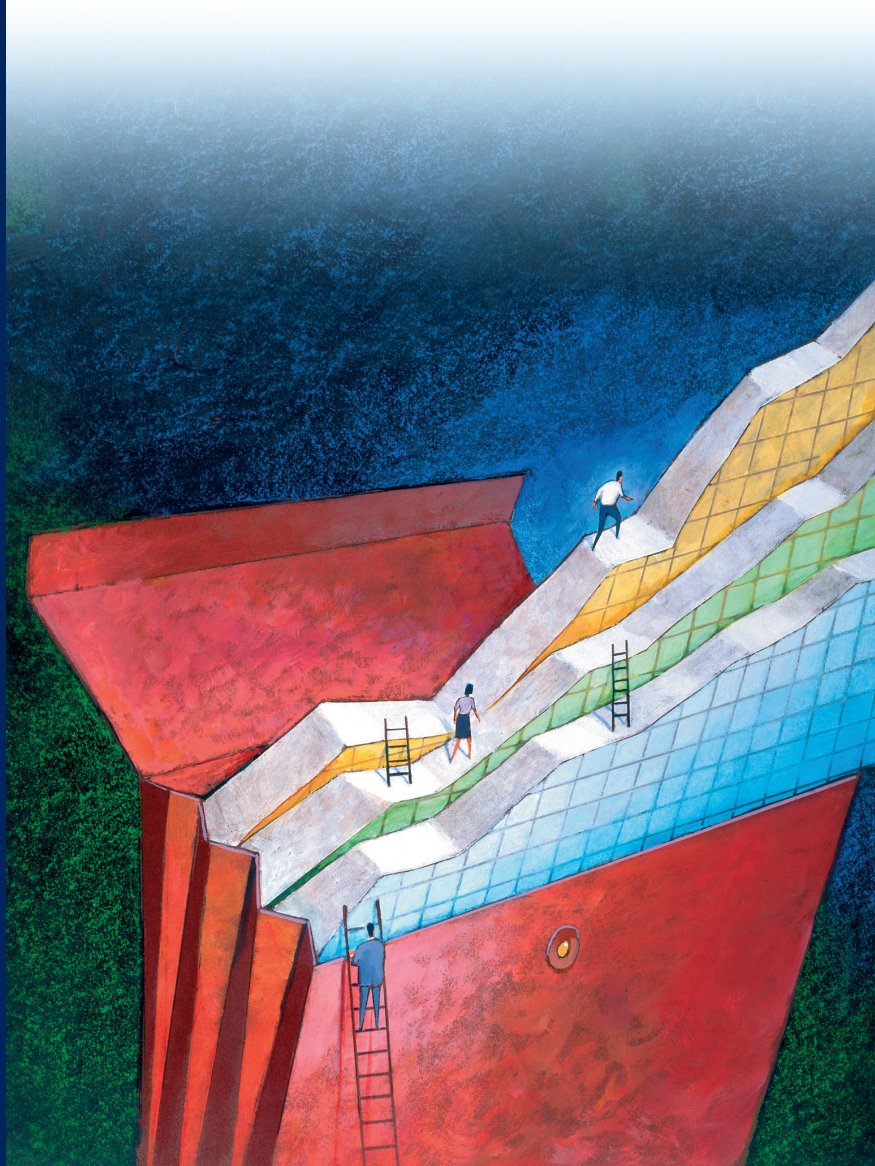

Pricing Models for Bermudan-Style Interest Rate Derivatives

Pricing Models for Bermudan-Style Interest Rate Derivatives

Waarderingsmodellen voor Bermuda-stijl rente derivaten

Proefschrift

ter verkrijging van de graad van doctor aan de
Erasmus Universiteit Rotterdam
op gezag van de
rector magnificus

Prof.dr. S.W.J. Lamberts

en volgens besluit van het College voor Promoties.

De openbare verdediging zal plaatsvinden op

donderdag 8 december 2005 om 16.00 uur

door

Raoul Pietersz
geboren te Rotterdam

Promotiecommissie

Promotoren:
Prof.dr. A.A.J. Pelsser
Prof.dr. A.C.F. Vorst

Overige leden:
Prof.dr. P.J.F. Groenen
Prof.dr. F.C.J.M. de Jong
Dr.ir. M.P.E. Martens

Erasmus Research Institute of Management (ERIM)
Erasmus University Rotterdam
Internet: http://www.erim.eur.nl

ERIM Ph.D. Series Research in Management 71

ISBN 90-5892-099-2

Voor Beata, Karsten en Daniël

Acknowledgements

First and foremost, I would like to thank my promotor Antoon Pelsser. His guidance throughout the Ph.D. period has been excellent. Chapters 2, 5 and 6 were written in cooperation with Antoon. The research benefitted greatly from his invaluable suggestions, and he truly is an inspirator. Thank you Antoon.

Second, I thank my promotor and former employer Ton Vorst. He is the one who suggested me to start the Ph.D. track with Antoon Pelsser, and who part-time employed me at ABN AMRO Bank, Quantitative Risk Analytics (at the time "Market Risk – Modelling and Product Analysis"), for the period September 2001 till June 2004. For all this, I am very grateful.

Third, many thanks go to the other members of the small committee; Patrick Groenen, Frank de Jong, and, Martin Martens. Also, I express my gratitude to the other members of the committee; Lane Hughston, Farshid Jamshidian, and, Thierry Post.

Fourth, special thanks go to Marcel van Regenmortel, for teaching me many technical and exciting aspects of interest rate derivatives pricing, and for part-time employing me at Product Development Group, Quantitative Analytics, ABN AMRO Bank, from July 2004 onwards. Chapters 5 and 7 were written in cooperation with Marcel.

Fifth, I am grateful to Patrick Groenen, for co-authoring Chapter 3.

Sixth, I thank Igor Grubišić for co-authoring Chapter 4.

I am much obliged to my colleagues at Erasmus University Rotterdam: Jaap Spronk for support through the Erasmus Center for Financial Research (ECFR); Martin Martens for his help while I was co-teaching one of his example classes and for suggesting me as a lecturer at the Rotterdam School of Management (RSM); Winfried Hallerbach for help with preparation of RSM lectures; Wilfred Mijnhardt for guiding me through the publication process; Tineke Kurtz, Tineke van der Vhee, Elli Hoek van Dijke, and Ella Boniuk, for efficiently aiding me in administrative matters; and, Mariëlle Sonnenberg, for being a pleasant room-mate.

During the Ph.D. period I have been able to present my work at leading international conferences. I am very grateful for the financial support that made this possible, received from Erasmus Research Institute of Management (ERIM), from the Econometric Institute (EI), and from ECFR.

A special thank you to past and present managers at ABN AMRO Bank: Ton Vorst, Dick Boswinkel, Nam Kyoo Boots, Marcel van Regenmortel, Bernt van Linder and Geert Ceuppens. Thank you to past and present colleagues at Product Development Group: Nicolas Carré in Amsterdam, and Thilo Roßberg and Russell Barker in London. Thanks to members of CAL: Nancy Appels, Reinier Bosman, Danny Wester, Frank Putman, André Roukema, Jelper Striet, and Willem van der Zwart. Thank you to past and present colleagues at 'Product Analysis': Steffen Lukas, Benjamin Schiesslé, Martijn van der Voort, Lukas Phaf, Alice Gee, Rutger Pijls, Drona Kandhai, and Alex Zilber. A thank you to colleagues that have become friends: Dion Hautvast, Bram Warmenhoven, and Glyn Baker.

I am also grateful to a number of anonymous referees and to Riccardo Rebonato and Mark Joshi who provided valuable comments and suggestions to earlier versions of the papers that form the basis for this thesis. Many thanks to Frank de Jong and Joanne Kennedy for providing much appreciated feedback to my research proposal.

Finally, I would like to thank my parents for always being there for me. I thank my son Karsten for bringing so much joy to my life. I thank Beata for her love, support, and kindness.

Raoul Pietersz
February 7th 2005, Amsterdam

Contents

List of Figures

List of Tables

Notation

s A lower case italic denotes a scalar.

$\mathbf{v}$ A lower case bold denotes a vector.

$\mathbf{M}$ An upper case bold denotes a matrix.

α Day count fraction.

β Correlation parameter, see (2.4).

γ Weights; correlation parameters.

$\mathbf{\Gamma}$ Lagrange multipliers.

δ Delta: risk sensitivity with respect to underlying rate or asset price.

$\mathbf{\Delta}$ Tangent vector for geometric programming.

ε Perturbation size; convergence criterium.

η Pay $(+1)$/receive (-1) fixed index; caplet $(+1)$/floorlet (-1) index.

θ Drift in short rate models.

λ Largest eigenvalue of $\mathbf{B}$.

$\mathbf{\Lambda}$ Diagonal eigenvalues matrix.

μ Drift.

ν Vega: risk sensitivity with respect to volatility.

π Realized numeraire relative payoff.

ρ Target correlation, matrix form: $\mathbf{P}$.

$\varrho^{(p,s)}$ Performance ratio for algorithm s on test problem p.

σ Volatility.

τ_i Discretization time point. Time discretization: $\tau_1 < \cdots < \tau_m$.

ϕ Cumulative normal distribution function; performance profile.

φ Objective function for rank reduction of correlation matrices.

χ Auxiliary majorization function.

$\mathbf{\Psi}$ Error per-entry in correlation matrix: $\mathbf{\Psi} = \mathbf{Y}\mathbf{Y}^T - \mathbf{P}$.

ω Outcome of probability space, $\omega \in \Omega$.

Ω Probability space.

S^n Sphere in $\mathbb{R}^{n+1}$.

$\mathbb{E}$ Expectation.

$\mathbb{P}$ Real-world probability measure.

$\mathbb{Q}$ Arbitrage-free pricing measure.

$\mathbb{R}$ Set of real numbers.

$\mathbb{S}_n$ Set of real $n \times n$ symmetric matrices.

$\mathcal{F}$ Filtration.

$\mathcal{N}$ Normal distribution.

$\mathcal{O}$ Order.

$\mathcal{S}$ Swap market model.

a Model parameter.

b Discount bond price; model parameter.

b_i Price of a discount bond maturing at time t_i.

$\mathbf{B}$ Helper matrix for majorization.

c Model parameter.

$\mathbf{C}$ Correlation matrix.

d Number of stochastic factors; the usual d_1, d_2 in Black-type formulas.

e End index of a forward rate.

f Forward rate.

$i(t)$ Spot LIBOR index at time t, see (2.3).

$\mathbf{I}$ Identity matrix.

k Strike rate.

m Number of discretization time points.

n Number of forward rates; numeraire value.

o Option price.

p PVBP, present value of a basis point, see (2.1).

$\mathbf{P}$ Target correlation matrix, $\mathbf{P} = (\rho_{ij})_{ij}$.

$\mathbf{Q}$ Orthogonal matrix, $\mathbf{Q}\mathbf{Q}^T = \mathbf{I}$, with $\mathbf{I}$ the identity matrix.

r Short rate; instantaneous continuously compounded interest rate.

s Swap rate; start index of a forward rate; asset price.

t Time.

t_i Tenor time. Tenor structure: $0 = t_0 < \cdots < t_n$.

v Value of a security, asset or derivative.

w Brownian motion; weight coefficient.

$\mathbf{Y}$ Decomposition matrix: $\mathbf{Y}\mathbf{Y}^T = \mathbf{P}$, with $\mathbf{P}$ a correlation matrix.

z Normally distributed random variable.

$_i$ (Subscript i) Associated with the period $[t_i, t_{i+1}]$ (e.g., f_i, σ_i, α_i); associated with t_i (e.g, b_i).

$_{s:e}$ (Subscript $s : e$) Associated with the period $[t_s, t_e]$ (e.g., $f_{s:e}, \sigma_{s:e}$).

$^{(i+1)}$ (Superscript $(i + 1)$) Associated with the forward measure for which b_{i+1} is the numeraire.

d Infinitesimal differential.

bp Basis point, 0.01%.

P&L Profit and loss.

xNCy x non-call y option, exercisable on an underlying with a maturity of x years from today but callable only after y years.

$\cdot$ Scalar product of vectors.

$\langle \cdot, \cdot \rangle$ Scalar product of vectors; quadratic cross-variation.

$\langle \cdot \rangle$ Quadratic variation.

Var Variance.

Cov Covariance.

$\|.\|$ Vector length: Square root of sum of squares of vector entries.

$\| \cdot \|_F$ Frobenius norm, $\|\mathbf{Y}\|_F^2 := \mathrm{tr}(\mathbf{Y}\mathbf{Y}^T)$ for matrices $\mathbf{Y}$.

$\ll$ Much smaller than.

^{T} (Superscript T) Matrix transpose.

Outline

The purpose of this thesis is to further knowledge of efficient valuation and risk management of interest rate derivatives (mainly of Bermudan-style but other types are also included) by extending the theory on market models. Here, we provide an outline of the thesis. Readers that are non-experts in the field of interest rate derivatives pricing could skip the outline at first reading and return here after reading the introductory Chapter 1.

A schematic outline of the thesis is given in Figure 1.

Chapter 2 investigates various popular calibration choices for the LIBOR market model and their effect on the quality of risk sensitivities of Bermudan swaptions. The results show that care should be taken when selecting a calibration method: Certain choices, e.g., so-called *time-homogeneous volatility*, may lead to non-efficient estimates of risk sensitivities. Poor and unstable estimates of risk, in turn, lead to fluctuations in a hedge portfolio that are spurious and have no economic meaning, and the risk associated with the derivative is not adequately reduced. The results however also show that so-called *constant volatility* leads to efficient and stable estimates of risk sensitivities. The combined results are important and valuable to financial institutions that need to select a calibration method for market models, with the aim to risk manage Bermudan swaptions and other interest rate derivatives.

Chapter 2 has been published in the Journal of Derivatives, see Pietersz & Pelsser (2004*a*). An extended abstract of the chapter has been published in Risk Magazine, see Pietersz & Pelsser (2004*b*). The Risk article has been republished as part of a Risk book, see Pietersz & Pelsser (2005*b*).

Chapters 3 and 4 solve the same problem in two completely different ways. The problem is the so-called *rank reduction of correlation matrices*, and occurs as a key part of calibrating multi-factor market models to correlation. Mathematically formulated, rank reductions of correlation matrices are non-convex optimization problems, which are known to be difficult to solve: The problem is to minimize, over low-rank correlation matrices attainable by the model, an objective value, which is the *error* with the original given correlation matrix. We present two elegant solution algorithms. The benefit over existing algorithms is the enhanced efficiency: In terms of computational speed, the algorithms of Chapters 3 and 4 outperform existing algorithms, in the numerical tests we considered.

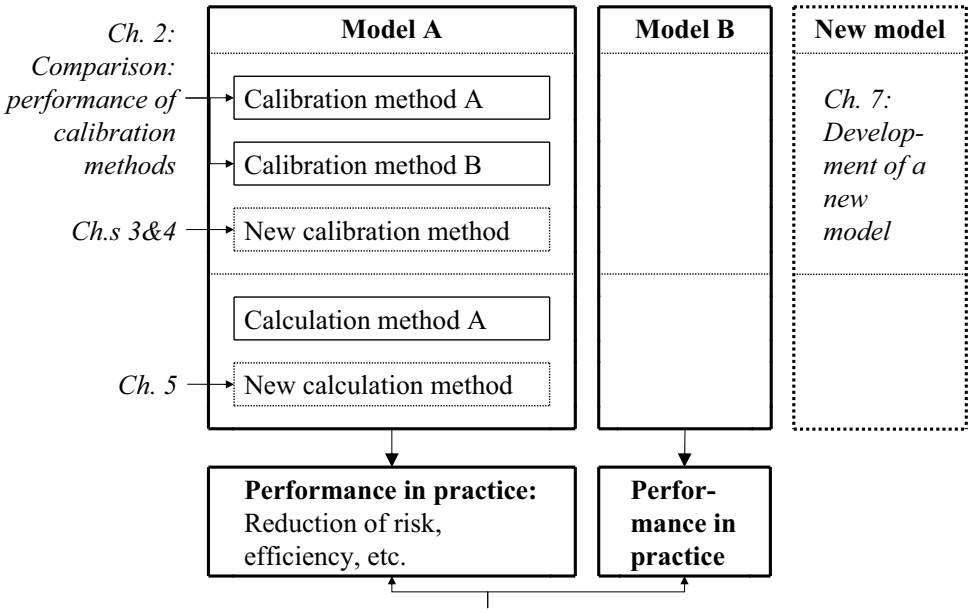

Figure 1: Outline of the thesis. Here, models A and B denote market models and Markov-functional models, respectively. The new model denotes CMS and generic market models.

Chapter 3 presents a solution for rank reduction of correlation matrices, based on *majorization*, which is a general technique from optimization. We perform the task of showing that majorization can be applied to rank reduction of correlation matrices. The resulting algorithm is globally convergent (i.e., from any starting point) to a local minimum. The algorithm is shown to be straightforward to implement, which makes its use accessible to non-experts. The majorization algorithm is extremely efficient, because of its low cost per iterate.

Chapter 3 has been published in Quantitative Finance, see Pietersz & Groenen (2004*b*). An extended abstract of the chapter has been published in Risk Magazine, see Pietersz & Groenen (2004*a*).

Chapter 4 develops a solution for rank reduction of correlation matrices based on *geometric programming*, which is optimization over curved space (*manifolds*). The manifold-equivalents of Newton and conjugate gradient optimization algorithms are presented for the problem of rank reduction of correlation matrices. By carefully selecting the manifold, we are able to bring the gradient and Hessian to natural forms, enabling an efficient implementation. The geometric curved algorithms enjoy the same super-linear local convergence properties as their Euclidean flat counterparts: Quadratic convergence for Newton and m-steps quadratic convergence for conjugate gradient, where m denotes the dimension of the manifold. Additionally, we develop a novel method to immediately check whether a stationary point is a global minimum, by extending the Lagrange multiplier results of Zhang & Wu (2003) and Wu (2003). This feature is very rare for non-convex optimisation problems, and makes the problem of rank reduction of correlation matrices all the more interesting. Extensive numerical tests show that geometric programming compares favourably with other existing algorithms, in terms of computational speed.

Chapter 4 has been submitted. For the working paper version, see Grubišić & Pietersz (2005).

Chapter 5 introduces a new discretization for the LIBOR market model, the *Brownian bridge discretization*. Discretizations are required for implementation of a pricing algorithm. The benefit of Brownian bridge is its accuracy when single or large time steps are used. For single time steps, we show that it is least-squares optimal to use Brownian bridge (in a to be defined natural sense). This is also confirmed in the numerical LIBOR-in-arrears test extended from Hunter, Jäckel & Joshi (2001). As a multi step discretization, we show that Brownian bridge converges weakly with order one. The multi step convergence is illustrated by numerical tests. Finally, we show that a single time step discretization combined with a *separability* assumption on the volatility, allows for an even more efficient implementation via pricing on a grid or on a recombining lattice, instead of Monte Carlo.

Chapter 5 has been published in the Journal of Computational Finance, see Pietersz, Pelsser & van Regenmortel (2004). An extended abstract has been published in Wilmott Magazine, see Pietersz, Pelsser & van Regenmortel (2005).

Chapter 6 presents novel empirical comparisons on the performance of models in terms of reduction of risk. The profit and loss (P&L) of hedge portfolios of Bermudan swaptions are recorded for USD swap rates and swaptions data over a one year period. We compare LIBOR and swap market models, and the Markov-functional model of Hunt, Kennedy & Pelsser (2000). The Markov-functional model is representative of single-factor models, such as short rate models. The market models are representative of multi-factor interest rate pricing models. Both market models and Markov-functional models can be calibrated to relevant interest rate correlations. Therefore, correlation pricing effects can be captured in both model types. The three main conclusions of the hedge tests are quite remarkable:

First, delta hedging is compared to delta and vega hedging. Delta hedging is theoretically justified by the replication argument of Black & Scholes (1973) and Merton (1973), of continuous trading in the underlying asset. Vega hedging is the offsetting of volatility risk by trading in underlying options. Vega hedging is not based on a replication argument, and it is considered a financial engineering trick, widely applied by traders and practitioners. We show that delta and vega hedging significantly outperforms delta hedging, in terms of reduction of variance of P&L.

Second, the algorithm of Longstaff & Schwartz (2001) for estimating the optimal exercise decision of American options in Monte Carlo is investigated. This algorithm is required for market models, but not for the Markov-functional model. We show that the algorithm contains a discontinuity, which renders convergence of finite difference estimates of risk sensitivities to be slower, see, for example, Glasserman (2004, Section 7.1). The hedge tests show that the less effective estimation of risk sensitivities adversely affects reduction of variance of P&L. Moreover, we propose a novel adjustment of the Longstaff & Schwartz (2001) algorithm, termed *constant exercise decision method*. With our proposed modification, a far greater reduction of variance of P&L is attained than with the original algorithm. The reduction is comparable to the reduction in the Markov-functional model. Our proposal thus enables market models to function properly as risk management tools of callable derivatives.

Third, the effect of the number of stochastic factors and correlation specification is investigated. The hedge tests show no significant differences in terms of reduction of variance of P&L, across: models, number of factors and correlation specification.

Finally, the effect of smile on pricing is investigated. *Volatility smile* is the phenomenon that different Black (1976) implied volatilities are quoted for different strikes of otherwise equal options. The results show that the impact of smile can be much larger than the impact of correlation. Also, the impact of smile is similar in both market models and Markov-functional models.

Chapter 6 has been submitted. For a working paper version, see Pietersz & Pelsser (2005*a*).

In Chapter 7, new *CMS and generic market models* are developed, which allow for ease of volatility calibration for a whole new range of derivatives, such as fixed-maturity Bermudan swaptions and Bermudan CMS swaptions. CMS and generic market models allow for a choice of forward rates other than the classical LIBOR and swap rates in the LIBOR and swap market models, respectively. We present a theoretical result with necessary and sufficient conditions for an arbitrary structure of forward rates to be arbitrage-free at all possible states of the model. CMS and generic drift terms for the forward rates are derived, by use of matrix notation, for both terminal and spot measures. A fast algorithm is presented that approximately, but accurately, calculates forward rates over time steps for CMS market models.

Chapter 7 has been submitted. For a working paper version, see Pietersz & van Regenmortel (2005).

Chapter 1

Introduction

Bermudan-style interest rate derivatives are an important class of options. Many banking and insurance products, such as mortgages, cancellable bonds, and life insurance products, contain Bermudan interest rate options associated with early redemption or cancellation of the contract. The abundance of these options makes evident that their proper valuation and risk measurement are important to banks and insurance companies. Risk measurement allows for offsetting market risk by hedging with underlying liquidly traded assets and options.

The purpose of this thesis is to further knowledge of efficient valuation and risk management of Bermudan-style interest rate derivatives. In this chapter, we provide a historic background and comprehensive framework for the chapters that are to follow.

The outline of this chapter is as follows. First, we introduce the use of models for arbitrage-free pricing. Second, we briefly describe interest rate markets and options. Third, we provide an overview of interest rate derivatives pricing models relevant to the thesis. Fourth, American option pricing with Monte Carlo simulation is discussed.

1.1 Arbitrage-free pricing

In this thesis, pricing models produce *relative valuations*. The relative valuation of an asset (most often a derivative) is in terms of other asset prices. Pricing models are thus viewed as an 'extrapolation tool' that aim to extrapolate derivative prices from underlying assets.

Key to relative valuation models is the exclusion of arbitrage. An *arbitrage* is an opportunity to make a risk-less profit with positive probability, with no costs at time of execution. If an arbitrage opportunity occurs, then many investors buy the arbitrage opportunity, driving up the arbitrage price. Eventually, this causes the arbitrage to

disappear. Arbitrage opportunities are therefore not likely to occur in an efficient and competitive economy.

When we construct a relative valuation model, then we usually do so by specifying dynamics of certain base asset prices in a frictionless arbitrage-free market. We then consider, for example, derivatives whose values derive from these base assets. A *self-financing portfolio* is a portfolio without injection or withdrawal of funds. A derivative that we added to the model is said to be *attainable* if its payoff can be exactly replicated by a dynamically managed self-financing portfolio of the base assets. We call a model *complete* if all the derivatives that we added to the model are attainable. In a complete model, any added derivative is effectively redundant (in this theoretical world), since it is merely a particular dynamic portfolio of the base assets. The added derivatives are said to be *spanned* by the underlying assets. In a complete model, any derivative price is already known when the current underlying prices and their dynamics are known: The current derivative price is simply equal to the current value of a replicating portfolio.

Next to absence of arbitrage, we also assume *absence of transaction costs*: there is no difference in price when buying or selling an asset. This assumption obviously does not reflect reality. In the presence of transaction costs, arbitrageurs cannot exploit all theoretical arbitrage opportunities, since transaction costs make some of these no longer profitable. However, for large market participants, transaction costs are sufficiently low relative to transaction sizes. In effect, the assumption of zero transaction costs is quite accurate for the market as a whole. Moreover, the assumption of absence of transaction costs leads to a theory that is still sufficiently accurate, but much more tractable.

Model dynamics of returns on asset prices, in the real-world measure, consist of two parts: An average part (*drift*) and a random part (*diffusion*). The diffusion part can be modelled as either continuous (e.g., Brownian motion) or discontinuous (e.g., jumps as in Merton (1976)). The use of continuous diffusion models is widespread, foremost because continuous models provide a more than sufficiently accurate description of reality, and also because of analytical tractability. This thesis therefore considers only continuous diffusion models. If it is then assumed that asset returns over disjoint time periods are independent, then it follows from the Lévy-Khinchin theorem that the diffusion term is a (time- and state-dependent) *volatility* coefficient times a Brownian motion.

We summarize these concepts in terms of stochastic differential equations (SDEs). We consider a model with a filtered probability space $(\Omega, \mathbb{P}, \mathcal{F})$ with filtration $\mathcal{F} = (\mathcal{F}(t))_{t\geq 0}$, on which is defined a $\mathcal{F}$-adapted Brownian motion w. Here, $\mathbb{P}$ denotes the real-world measure. The asset price is denoted by s, its $\mathcal{F}$-adapted drift by μ and its $\mathcal{F}$-adapted volatility by σ. A realization in Ω is denoted by ω. We have:

$$\frac{\mathrm{d}s(t)}{s(t)} = \mu(t,\omega)\mathrm{d}t + \sigma(t,\omega)\mathrm{d}w(t).$$

Also, we assume the existence of a money market account with price b and return $r(t, \omega)$:

$$\frac{\mathrm{d}b(t)}{b(t)} = r(t, \omega)\mathrm{d}t.$$

The *market price of risk* (or *Sharpe ratio*, see Sharpe (1964)) is defined to be the excess average return over the risk free rate divided by the volatility of the asset. In other words, it is (drift-[risk free rate])/volatility and $(\mu - r)/\sigma$, see, e.g., Baxter & Rennie (1996, page 119). A sufficient condition for no-arbitrage is equality of market prices of risk for all assets, e.g., Hull (2000, Equation (19.6)). The actual levels of market prices of risk then turn out not to matter for valuation.

We introduce some key concepts of arbitrage-free pricing. A *numeraire* is an asset with a strictly positive value at all times. Asset prices may be denominated in terms of amounts of the numeraire. A *martingale* is a process with zero drift. Suppose we can construct a new measure (the so-called *risk neutral measure*) such that all numeraire-expressed asset prices become martingales. It can be shown (e.g., Hunt & Kennedy (2000, Theorem 7.32)) that the assumption of existence of such a measure automatically implies that the model is arbitrage-free. Moreover, if there exists a single unique risk neutral measure, then it can be shown (e.g., Hunt & Kennedy (2000, Theorem 7.41)) that the model is *complete*, i.e., every derivative security is attainable by a replicating portfolio in the underlying assets.

Given the assumption of equality of all market prices of risk, we may apply Girsanov's theorem (e.g., Øksendal (1998, Theorem 8.6.4)) to construct the risk-neutral measure. Under the risk neutral measure, market prices of risk then turn out to disappear. Therefore these do not affect arbitrage-free pricing.

The martingale property of numeraire-relative asset prices implies that their future expectations take today's value. If s and n denote prices of an asset and a numeraire, respectively, then

$$\frac{s(0)}{n(0)} = \mathbb{E}\left[\frac{s(t)}{n(t)}\right], \text{ for } t \geq 0.$$

where the expectation is with respect to the risk-neutral measure. The price v of a derivative (also an asset), necessarily sharing the same market price of risk, then satisfies

$$v(0) = n(0)\mathbb{E}\left[\frac{v(t)}{n(t)}\right], \text{ for } t \geq 0, \tag{1.1}$$

which is the fundamental arbitrage-free pricing formula, see, e.g., Björk (2004, Theorem 10.18). We note that the market price of risk does not occur in this formula. If we calculate (1.1) for a call option on a stock that is modelled as geometric Brownian motion, then we obtain the famous formula of Black & Scholes (1973).

In practice, we directly model under a risk-neutral measure, by specifying the part that stems from the real-world measure, the diffusion part. No-arbitrage requirements then fully fix the drift term. In fact, for European call and put options, traders quote the diffusion part: so-called *implied volatility*. It is the volatility to be used in the Black-Scholes formula to obtain the European option price. A *European* option is an option that is exercisable only at a single point in time (usually during a single trading day).

The reason that the derivative price is fully fixed by (1.1) is *replication* by a self-financing portfolio. Suppose amounts δ_s of s and δ_b of b are held, then the value v is given by:

$$v = s\delta_s + b\delta_b, \tag{1.2}$$

The change in value v of a self-financing portfolio thus satisfies (e.g, Joshi (2003*a*, Equations (5.58) and (5.59))):

$$\mathrm{d}v = \delta_s \mathrm{d}s + \delta_b \mathrm{d}b. \tag{1.3}$$

In other words, value changes due to trading in the asset s and risk-free asset b cancel exactly:

$$s\mathrm{d}\delta_s + b\mathrm{d}\delta_b = 0.$$

A *replicating portfolio* is a dynamically managed self-financing portfolio of underlying assets s and b, which has a value equal to the payoff of derivative v, in all possible future states of the economy.

The replicating portfolio holds a dynamic amount of δ_s of the underlying asset s. The amount δ_s can be calculated from (1.2), (1.3), and from *Itô's formula*: If s is a stochastic process, and $v : \mathbb{R} \to \mathbb{R}$ is a function, then for the process $v(s)$ we have:

$$\mathrm{d}v = \frac{\partial v}{\partial s}\mathrm{d}s + \frac{1}{2}\frac{\partial^2 v}{\partial s^2}\mathrm{d}\langle s\rangle, \tag{1.4}$$

see, for example, Karatzas & Shreve (1991, Theorem 3.3.3). Here, angle brackets $\langle\cdot\rangle$ denote quadratic variation, see, e.g., Øksendal (1998, Exercise 2.17). By rewriting (1.4) in the form of (1.3), we can show that

$$\delta_s = \frac{\partial v}{\partial s}. \tag{1.5}$$

The quantity δ_s is called the *delta*, and it is an example of a *risk sensitivity*: the risk sensitivity with respect to the underlying asset price.

1.1.1 Use of models in practice

A dynamic hedge of the derivative v consists of taking an opposite position in the replicating portfolio. In practice, the hedge is not re-balanced on a continuous basis, rather at

discrete points in time. Re-balancing usually takes place when delta risk exceeds a certain threshold level. The adaption from continuous-time to discrete-time hedging works extremely well in practice, and forms the basis for the success of arbitrage-free pricing models.

While we use risk-neutral pricing models as relative valuation and hedging tools, it is interesting to note that these models also make assertions on real-world price dynamics, through the connection with the real-world measure. Risk-neutral models can thus also be viewed as *economic models*, attempting to model economic reality. Though modelling of real-world price dynamics is a vital aspect of risk-neutral models, it is not the most important aspect. More important to risk-neutral models are:

1. To produce sensible prices of derivatives, and to reproduce prices of underlying assets and options exactly.

2. To adequately reduce variance of profit and loss (P&L), when a hedge is set up.

3. To efficiently produce prices, i.e., within a limited amount of computational time.

The difference between the use of a model as a *hedging tool* or economic model has important implications. For example, consider modelling the term structure of interest rates. Extensive empirical research has shown that the term structure is driven by more than one stochastic factors, see the review article of Dai & Singleton (2003). For an economic model, we should thus use at least two factors, and a single-factor model is simply not acceptable. However, for a model used as hedging tool, it is perfectly sensible to consider a single-factor model, as long as it satisfies the above three properties.

The necessity that pricing models need reproduce prices of underlying assets and options has two further implications:

First, option price data (implied volatility) determines the diffusion part (or, equivalently, *volatility*) of the model, rather than time-series estimates from historic data on asset returns. The reason is straightforward: Certain features of a derivative may become redundant during the life of the derivative, which may render the derivative equivalent to (or almost equivalent to) a market traded option. In that case, the model should produce a derivative price equal to the market traded option price, otherwise the financial institution holding the derivative can incur arbitrage, which should be avoided. The only way to avoid arbitrage is to make the model consistent with prices of underlying options, i.e., to use implied volatility for the diffusion term in the model. The process of making the model consistent with market prices is called *calibration*.

Second, a pricing model is re-calibrated to the most recent implied volatility data, whenever the derivative needs be valued. The important reason is again that of no-arbitrage, and is the same as above for the use of implied volatility in models. Implied

volatility quotes change over time. The practice of re-calibration to unpredictably changing volatility is not consistent with most pricing models (excluding stochastic volatility models), since most models assume volatility to be known over the model time horizon.

When implied volatility changes, then a derivative value may change too, due to the practice of re-calibration. As a result, derivative traders face volatility risk (*vega*). The risk may be offset by vega hedging. If σ denotes the volatility, and o the price of an underlying option, then the following portfolio has zero volatility risk (for small changes in σ):

$$\text{one derivative } (v) \text{ and } -\frac{\partial v/\partial \sigma}{\partial o/\partial \sigma} \text{ options } (o). \tag{1.6}$$

A delta hedge with the underlying asset as in (1.5) can then be applied to the vega-neutral portfolio in (1.6).

Vega hedging is out-of-model hedging, since we hedge parameters that are input to the model. Delta hedging with the underlying asset in (1.5) is in-model hedging, since the underlying asset price is a state variable of the model. Nonetheless, vega hedging is not inconsistent with arbitrage-free pricing models: We are only holding a different portfolio of derivatives and options that needs to be delta hedged. From an arbitrage-free pricing perspective though, there is simply no need to add the additional options (though such addition *is* allowed): the original derivative is already perfectly delta-replicable in the theoretical model world. In practice however, vega hedging enables a significant additional reduction of variance of P&L, and it thus contributes to wealth preservation.

Another practice for arbitrage-free pricing models is that of customizing a model to a certain product. We construct the model in such way that all parts of economic reality, relevant to the product, are incorporated into the model. The benefit is that the product is priced correctly, while not having to fully model all parts of the market, thereby often attaining a more efficient implementation.

1.2 Interest rate markets and options

In interest rate markets, participants trade primarily in interest rate agreements. An *interest rate agreement* is an agreement to borrow or lend money, over an agreed period of time, against agreed periodical payments (*interest rate payments*) that are in some form denoted as a percentage (*interest rate*) of the underlying borrowed or lent amount (*notional amount*).

We refer to the length of an interest rate agreement as its *tenor*. Different tenors may attract different interest rates, which gives rise to the so-called *term structure of interest rates*.

The above description of an interest rate agreement includes money market deposits, bonds, forward interest rate agreements, and swaps. Money market deposits, bonds, and swaps are of particular relevance to this thesis, therefore we explain their workings in some detail.

1.2.1 Linear products: Deposits, bonds, and swaps

Money market deposits usually have a maturity of one year or less. The two parties agree on an interest rate and one party deposits the notional amount. At the end of the agreement (at *maturity*), the other party returns the notional and makes the agreed interest rate payments.

A bond is an agreement between two parties, the borrower and the lender, on a designated notional amount. At initiation, the borrower receives a pre-negotiated amount for the bond (not necessarily equal to the notional amount). During the life of the bond, the borrower makes coupon payments on the notional amount, usually on the basis of a fixed contractually agreed rate, but the coupon payments could also be based on a floating interest rate. By a *floating interest rate*, we mean the prevailing market interest rate for the tenor spacing between the floating interest rate payments. We discuss the method for determining this floating interest rate below. If there are no coupon payments during the life of the bond, then we call such a bond a *zero coupon bond*. At maturity of a bond, the borrower returns the notional amount to the lender.

Interest rate swaps typically have a maturity of two years or more. Interest rate swaps involve only exchanges of interest rate payments, but normally do *not* involve exchanges of notional. The two parties agree on an interest rate. Periodically, one party pays this agreed interest rate (the *fixed rate*), while the other party pays a floating interest rate. We remark that the frequency of fixed and floating payments may differ. Typical frequencies are annually, semi-annually, quarterly, and monthly.

The fixed rate at which market participants can enter into a swap agreement at otherwise zero cost is called the *swap rate*. Swap rates can be seen as long term borrowing and lending rates. In fact, the swap rate for a swap with a particular tenor is more or less the interest rate for that particular tenor. The reason is that a swap can be used to create a synthetic borrowing or lending agreement at a single interest rate over the tenor period of the swap: Suppose we borrow money through deposits with floating interest rates, and we enter into a swap in which we pay fixed, on a notional equal to the amount borrowed from the deposit. At the end of each deposit, we borrow the same amount again in the deposit market, in order to pay back the notional from the previous deposit agreement. Rolling over money market deposits in such way, the resulting deposit interest payments cancel against the floating interest we receive from the swap; the fixed swap payments remain. Effectively, we then pay a fixed interest rate on our loan over the life of the swap.

The two parties in a swap determine the floating interest rate usually via a reference interest rate. Reference rates are used to calculate payments not only of swaps, but also of other securities, such as interest rate derivatives. A *reference interest rate* is a rate that is set by a financial authority or calculation agent. Examples are:

LIBOR: London inter-bank offered rate, published by the British Bankers' Association (BBA), each trading day at noon (12.00am) London time.

EURIBOR: Euro inter-bank offered rate, published by the European Banking Federation (FBE) and by the Financial Markets Association (ACI), each trading day at around 11.00am central European time.

These reference rates are published for several tenors and currencies. Upon publication of the reference rate, practitioners say that the rate then *fixes*.

Financial authorities determine reference rates normally along the following lines: A number of panel banks are consulted. Each panel bank provides rates at which it conceives it possible to borrow money in the inter-bank market, for various tenors and currencies. For each tenor and currency, some percentile of the top and bottom of the quotes are discarded. The remaining quotes are averaged to form the reference rate for that tenor and currency. It is interesting to note there is now an interest rate derivatives pricing model that bears the name of a reference rate: the *LIBOR market model*, see Section 1.3.

An interesting note is that the first major swap took place only in 1981, between IBM and the World Bank, see Valdez (1997, pages 269–270).

1.2.2 Interest rate options: Caps, floors, and swaptions

The plain-vanilla European interest rate options most relevant to this thesis are (i) caps and floors, and, (ii) swaptions. A cap consists of a sequence of consecutive caplets, and, likewise, a floor consists of a sequence of consecutive floorlets. Caplets and floorlets are call and put options, respectively, on LIBOR rates. Swaptions are options on swap rates.

A caplet (respectively, a floorlet) gives its holder at expiry the right, but not the obligation, to enter into a borrowing deposit (lending deposit) at a pre-arranged strike rate. If an option holder claims the option right, then we say that he or she *exercises* the option. If LIBOR fixes below (above) the respective strike rate, then it is cheaper to borrow (more rewarding to lend) in the market; whereby it is sensible *not* to exercise the caplet (floorlet) and it ends worthless. If LIBOR fixes above (below) the respective strike rate, then it is sensible to exercise the caplet (floorlet), since we then receive the positive difference LIBOR minus strike (strike minus LIBOR) at the deposit payment date. The option gains at the deposit payment date as dependent on realized LIBOR are displayed in Figure 1.1.

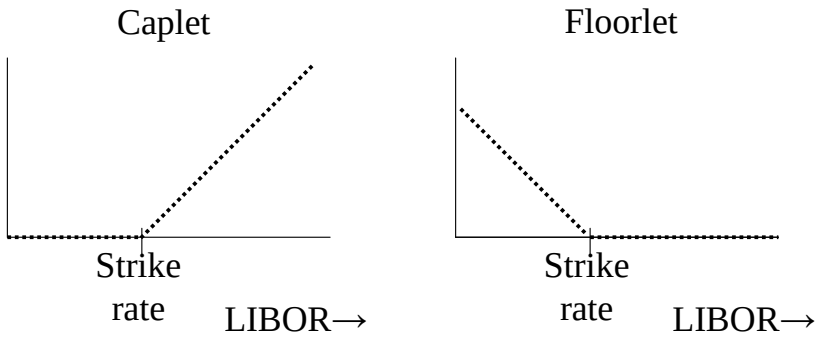

Figure 1.1: Payoffs of caplets and floorlets versus realized LIBOR.

A European swaption gives its holder at expiry the right, but not the obligation, to enter into a swap with a fixed rate equal to a pre-arranged strike rate. Market participants invariably indicate the direction of swap cash flows from the point of view of whether fixed payments are payed or received. Thus, if we hold a swaption that gives us the right to enter into a swap for which we pay or receive fixed, then such a swaption is a *payer* or *receiver* swaption, respectively. A payer (respectively, a receiver) swaption corresponds to a call option (put option). The payoff structures for payer and receiver swaptions are similar to those of caplets and floorlets in Figure 1.1: instead of 'LIBOR' read 'swap rate', and instead of 'caplet' or 'floorlet' read 'payer swaption' or 'receiver swaption'.

Cash settled contracts differ from normal option contracts, in that they pay the relevant difference between realized rate and strike, if this is positive. For a cash settled swaption at expiry, both parties need to agree on 'the' swap rate manifest in the market. Usually, again a reference rate is used. An example of a reference swap rate is ISDAFIX, published for various tenors and currencies by the International Swaps and Derivatives Association (ISDA). Financial authorities calculate swap reference rates more or less in the same way as deposit reference rates are set; via consultation of a group of panel banks.

From Figure 1.1, we find that an option always provides a nonnegative cash flow, with a positive probability to provide a positive cash flow, therefore we require a positive premium for the option. To calculate cap and floor or swaption premiums, market participants initially used a Black-type formula that is based on assuming a log-normal distribution for the LIBOR or swap rate at expiry. This approach however lacked a theoretical justification for long, but the approach later turned out to be valid. Moreover, an assumption of jointly log-normal LIBOR and swap rates is inconsistent. Many researchers therefore considered the use of the Black formula for caps and floors or swaptions to be unsound for a considerable period: While the Black swaptions approach had already been justified in 1990, articles establishing its validity kept appearing at least until 1997, see Rebonato (2004*a*, Section 4(d)).

We present the Black approach for caps and floors; the approach is similar for swaptions. Prior to that, we introduce some terminology: We set out by specifying a *tenor structure*, $0 = t_0 < t_1 < \cdots < t_{n+1}$. Let α_i denote the *day count fraction* for the period $[t_i, t_{i+1}]$. A *discount bond* is a hypothetical security that pays one unit of currency at its maturity, and has no other cash flows. The time-t price of a discount bond with maturity t_i is denoted by $b_i(t)$.

To present the Black approach for caps and floors, we consider two tenor points $0 < t_1 < t_2$. LIBOR fixes at time t_1 and interest is paid at time t_2. We define the *forward LIBOR rate* $f_1(t)$ by

$$f_1(t) = \frac{b_1(t) - b_2(t)}{\alpha_1 b_2(t)}. \tag{1.7}$$

We consider the *forward measure*, which is the measure associated with the discount bond b_2 maturing at the payment date of the LIBOR deposit. By the assumption of absence of arbitrage, it follows that f_1 is a martingale under its forward measure. To see this, note that $f_1(t)$ in (1.7) is the value of a portfolio $((b_1(t) - b_2(t))/\alpha_1)$ expressed in terms of amounts of the numeraire $b_2(t)$.

Continuing, we assume that the forward LIBOR rate is a *log-normal* martingale under its forward measure:

$$\frac{\mathrm{d}f_1(t)}{f_1(t)} = \sigma_1 \mathrm{d}w(t), \text{ equivalently, } f_1(t) = f_1(0)\exp\left(-\frac{1}{2}\sigma_1^2 t + \sigma_1 w(t)\right), \tag{1.8}$$

where σ_1 is a scalar constant. The payoff $v(t_2)$ at time t_2 of a caplet with strike rate k is then given by $\alpha_1 \max(f_1(t_1) - k, 0)$. From (1.1), we find for the caplet value $v(0)$:

$$\begin{aligned} v(0) &= n(0)\mathbb{E}\left[\frac{v(t_2)}{n(t_2)}\right] = b_2(0)\mathbb{E}\left[\frac{\alpha_1 \max(f_1(t_1) - k, 0)}{b_2(t_2)}\right] \\ &\overset{(*)}{=} \alpha_1 b_2(0)\mathbb{E}\big[\max(f_1(t_1) - k, 0)\big]. \end{aligned} \tag{1.9}$$

Equality $(*)$ holds since $b_2(t_2) = 1$. If we calculate (1.9) in full, we obtain the formula of Black (1976):

$$\begin{aligned} v(0) &= \alpha_1 b_2(0)\eta\Big\{f_1(0)\phi\big(\eta d_1\big) - k\phi\big(\eta d_2\big)\Big\}, \\ d_{1,2} &= \frac{\ln\left(\frac{f_1(0)}{k}\right) \pm \frac{1}{2}\sigma_1^2 t_1}{\sigma_1\sqrt{t_1}}. \end{aligned}$$

Here, η denotes $+1$ for a caplet, and -1 for a floorlet; $\phi(\cdot)$ denotes the cumulative normal distribution function.

1.3 Interest rate derivatives pricing models

Up to here we have examined options on a single interest rate, such as caps, floors and European swaptions. There are however many interesting interest rate derivatives that depend not only on a single interest rate, but on multiple interest rates. Examples include Bermudan-style interest rate derivatives. *Bermudan* means that the derivative is exercisable (equivalently: *callable*) at multiple discrete time points, usually separated by, e.g., annual or semi-annual periods.

Exercise of a Bermudan derivative is a trade-off between taking the option gains now or holding onto the option at possibly more favourable option gains later. Inherently, values of Bermudan interest rate derivatives therefore depend on multiple interest rates. There are of course also many non-Bermudan interest rate derivatives that dependent on

multiple interest rates. To value such multi-rate dependent products, we need a model that features dynamics for the whole term structure of interest rates. Preferably, such dynamic term structure models need be consistent with the Black formula for caps, floors and swaptions.

1.3.1 Short rate models

Historically, the first dynamic term structure models are *short rate models*. The *short rate* r is a hypothetical rate: it is the instantaneous rate of interest for the floating money market account (equivalently: *bank account*) with value n:

$$\frac{\mathrm{d}n}{n} = r\mathrm{d}t, \text{ equivalently, } n(t) = n(0)\exp\left(\int_0^t r(s)\mathrm{d}s\right).$$

In a short rate model, we select the bank account as numeraire. Discount bond prices satisfy, by the fundamental arbitrage-free pricing formula (1.1):

$$b_i(t,r) = \mathbb{E}\left[\underbrace{b_i\big(t_i, r(t_i)\big)}_{=1}\frac{n(t)}{n(t_i)}\middle| r(t) = r\right] = \mathbb{E}\left[\exp\left(-\int_t^{t_i} r(s)\mathrm{d}s\right)\middle| r(t) = r\right], \text{ for } t < t_i. \tag{1.10}$$

From (1.10), we can calculate discount bond prices, once the arbitrage-free dynamics of the short rate are known. For most main-stream short rate models, we can find explicit and analytical formulas for (1.10) for discount bond prices given the associated short rate. Short rate models are characterized by their specification of dynamics for the short rate. Examples of short rate models are given in Table 1.1 (this table is not complete).

As can be seen from Table 1.1, there are many short rate models. Next to short rate models, there are many more other interest rate derivatives pricing models. The reason for this abundance of interest rate models stems from different specifications of the interest rate market, as explained below.

To specify discount bond price dynamics, we need only specify the volatility term $\sigma_i^{(b)}$, the drift term then follows from no-arbitrage restrictions, as explained in Section 1.1. Therefore, we omit the drift, and focus on the diffusion term:

$$\frac{\mathrm{d}b_i}{b_i} = \cdots + \sigma_i^{(b)}(t,\omega)\mathrm{d}w(t). \tag{1.11}$$

The bond price volatility may thus be state-dependent.

A set of discount bond prices may be alternatively given by a set of interest rates. For example, discount bond prices may be given (implicitly or explicitly) in terms of a set of forward LIBOR rates $\mathbf{f} = (f_1, \ldots, f_n)$:

$$1 + \alpha_i f_i = \frac{b_i}{b_{i+1}}, \tag{1.12}$$

Table 1.1: Some short rate models and their specification of short rate dynamics. Here, the scalars a, b, and c denote model parameters.

Model	Specification
Merton (1973)	$\mathrm{d}r = b\mathrm{d}t + \sigma\mathrm{d}w$
Vasicek (1977)	$\mathrm{d}r = (b - ar)\mathrm{d}t + \sigma\mathrm{d}w$
Dothan (1978)	$\mathrm{d}r = ar\mathrm{d}t + \sigma r\mathrm{d}w$
Brennan & Schwartz (1979)	$\mathrm{d}r = (b - ar)\mathrm{d}t + \sigma r\mathrm{d}w$
Cox, Ingersoll & Ross (1985)	$\mathrm{d}r = (b - ar)\mathrm{d}t + \sigma\sqrt{r}\mathrm{d}w$
Ho & Lee (1986)	$\mathrm{d}r = \theta(t)\mathrm{d}t + \sigma\mathrm{d}w$
Hull & White (1990)	$\mathrm{d}r = (\theta(t) - ar)\mathrm{d}t + \sigma\mathrm{d}w$
	$\mathrm{d}r = (\theta(t) - ar)\mathrm{d}t + \sigma\sqrt{r}\mathrm{d}w$
Black, Derman & Toy (1990)	$\mathrm{d}r = \theta(t)r\mathrm{d}t + \sigma r\mathrm{d}w$
Black & Karasinski (1991)	$\mathrm{d}r = (ar - br\log r)\mathrm{d}t + \sigma r\mathrm{d}w$
Pearson & Sun (1994)	$\mathrm{d}r = (b - ar)\mathrm{d}t + \sigma\sqrt{r - c}\,\mathrm{d}w$

or in terms of the short rate r, see (1.10). Dynamics for a set of forward LIBOR rates or for the short rate give rise to dynamics for discount bond prices, and vice versa. In fact, it is the requirement of deterministic and known volatility for an interest rate specification that determines a model. Thus, if we require volatility to be only time dependent $\sigma(t)$, and not state dependent, for one of the specifications, then we obtain stochastic volatility for the other specifications:

$$\frac{\mathrm{d}b_i}{b_i} = \cdots + \sigma_i^{(b)}(t)\,\mathrm{d}w(t) \quad \Rightarrow \quad \begin{cases} \frac{\mathrm{d}r}{r} = \cdots + \sigma^{(r)}(t,\omega)\,\mathrm{d}w(t) \\ \frac{\mathrm{d}f_i}{f_i} = \cdots + \sigma_i^{(f)}(t,\omega)\,\mathrm{d}w(t) \end{cases} \tag{1.13}$$

$$\frac{\mathrm{d}r}{r} = \cdots + \sigma^{(r)}(t)\,\mathrm{d}w(t) \quad \Rightarrow \quad \begin{cases} \frac{\mathrm{d}f_i}{f_i} = \cdots + \sigma_i^{(f)}(t,\omega)\,\mathrm{d}w(t) \\ \frac{\mathrm{d}b_i}{b_i} = \cdots + \sigma_i^{(b)}(t,\omega)\,\mathrm{d}w(t) \end{cases} \tag{1.14}$$

$$\frac{\mathrm{d}f_i}{f_i} = \cdots + \sigma_i^{(f)}(t)\,\mathrm{d}w(t) \quad \Rightarrow \quad \begin{cases} \frac{\mathrm{d}b_i}{b_i} = \cdots + \sigma_i^{(b)}(t,\omega)\,\mathrm{d}w(t) \\ \frac{\mathrm{d}r}{r} = \cdots + \sigma^{(r)}(t,\omega)\,\mathrm{d}w(t) \end{cases} \tag{1.15}$$

Specification (1.13) corresponds to the extension of Black & Scholes (1973) from stocks to bonds, (1.14) corresponds to short rate models, and (1.15) to the LIBOR market model. We restrict our exposition to these model classes. More specifications are available: in fact, Rebonato (2004*a*, Section 3) lists five specifications.

Bond options can be viewed as caplets and floorlets, see Hull (2000, Equation 20.10). The straight extension of the model of Black & Scholes (1973) from stocks to bonds, i.e., deterministic and known instantaneous bond volatility, suffers however from the problem that discount bond prices do not necessarily converge to one at maturity. There are also other related problems, see Rebonato (2004*a*, Section 4(b)). Therefore a direct application of Black & Scholes (1973) to bond prices yields an interest rate derivatives pricing model with many undesirable features.

The initial success of short rate models is mainly due to their analytical tractability and numerical efficiency. There are, however, also some drawbacks to short rate models: They are, in a sense, difficult to calibrate, as model parameters need be implied from market option prices via non-straightforward numerical procedures. The resulting numerical calibration procedures can be instable and computationally costly. The reason is that short rate models are formulated in terms of an artificial short rate that is not directly observable in the market. Moreover, deterministic volatility for an abstract short rate in (1.14) does not correspond to market practice of quoting implied volatility for LIBOR and swap rates, see Section 1.2. Consequently, model parameters need to be tweaked to ensure the model fits to the relevant market rates and volatilities.

An example of the indirect calibration of short rate models is when they are calibrated to swaption volatility: we then have to resort to the formula of Jamshidian (1989): A swaption is viewed as an option on a coupon paying bond. Jamshidian (1989) decomposes the option on the coupon paying bond into several options on discount bonds.

Another disadvantageous feature of short rate models is that they produce an arbitrary volatility smile. *Volatility smile* is the phenomenon that different implied volatility is quoted for options that have different strikes but that are otherwise identical. The classical model of Black & Scholes (1973) exhibits a so-called *flat* volatility smile, in the sense that the implied volatility is independent of strike. We thus expect from any interest rate model that aims to be the equivalent of Black & Scholes (1973) for interest rates to also produce a flat volatility smile. Such is, as stated before, not the case for short rate models. Smile volatility is more realistic than flat volatility, since we can observe a pronounced volatility smile in interest rate markets. However, the produced smile ought to correspond also qualitatively to the observed smile, and such is not the case for short rate models: the latter exhibit rather arbitrary smiles, and smile shapes are not controllable by model users, at least not without further modification.

Typically, short rate models have only a single stochastic driver, although some two factor short rate models exist too, see, for example, Longstaff & Schwartz (1992) and Ritchken & Sankarasubramanian (1995). An advantage of single factor models is that recombining lattices can be used to efficiently price mildly path-dependent derivatives, including American-type options. A disadvantage is the resulting difficulty to model instantaneous de-correlation.

For a more extensive discussion on advantages and disadvantages of short rate models (e.g., positivity of interest rates and non-explosiveness of short rate models), the reader is referred to Cairns (2004, Section 4.1).

1.3.2 Market models

In recent years, a successful class of models has appeared in the literature known as *market models* (LIBOR and swap market models, also referred to as BGM models, see Brace, Gątarek & Musiela (1997), Miltersen, Sandmann & Sondermann (1997) and Jamshidian (1997)) or *string models* (see Santa-Clara & Sornette (2001) and Longstaff, Santa-Clara & Schwartz (2001)). Kerkhof & Pelsser (2002) show that the two formulations are equivalent. Market models correspond to specification (1.15). For an arbitrage-free construction of the LIBOR market model starting from discount bond dynamics (1.11), see Pietersz (2001, Section 3.2). It is specification (1.15) with which traders quote prices of underlying options (caps and swaptions). Market models therefore allow for straightforward calibration to prices of underlying options: the model parameter is simply equal to the market quoted volatility.

Market models are based on the forward measure technique for caplets, presented in Section 1.2. Moreover, market models are the equivalent of Black & Scholes (1973) for interest rates, because the LIBOR and swap market model produce flat volatility for caps and swaptions, respectively. Positivity of interest rates is guaranteed for the deterministic volatility LIBOR market model, since forward LIBOR rates are log-normal martingales.

In LIBOR market models, forward swap rates are generally not log-normally distributed. This seems to imply that the LIBOR market model produces non-flat swaption volatility, and is thus not a canonical model for swaptions. Such deviation from the log-normal paradigm however turns out to be extremely small in the LIBOR market model, see Chapter 2.5. Fortunately for the LIBOR market model, there also exist extremely accurate approximate formulas for swaption implied volatility. Consequently, the LIBOR market model can be calibrated to swaption volatility. This joint cap-swaption calibration potential of the LIBOR market model has very much contributed to its success. An interesting use of the approximate swaption volatility calibration via semidefinite programming is given in Brace & Womersley (2000) and D'Aspremont (2003).

The ease of calibration of market models allows for modelling of other market aspects, such as time homogeneity of cap and swaption volatility. *Time homogeneity of volatility* means that the model preserves the cap or swaption volatility curves as model-time progresses. In Chapter 2, we investigate the effect of including such time homogeneous calibration procedures on the quality of risk sensitivities produced by the model.

Market models correspond to (1.15), and are thus based on a set of forward rates. These forward rates are, in fact, the state variables of the model. The number of state

variables can grow large for particular trades: For a thirty years model with semi-annual forward rates, the model has sixty forward rates. This means that market models have large dimensionality. We address reduction of dimensionality in Chapters 3 and 4.

Due to the dimensionality of market models, Monte Carlo simulation has to be used to value derivatives, which is non-efficient compared to recombining lattices used in short rate models. Technological computer hardware developments have however recently enabled the use of Monte Carlo as a sufficiently efficient pricing and risk management tool. In Chapter 5, we study an efficient and accurate approximation of the LIBOR market model that enables pricing on a recombining lattice.

Though some derivatives can be valued without Monte Carlo when a short rate or Markov-functional model is used, the trend shows a growing complexity in derivatives. Certain derivatives have become so complex and strongly path-dependent, that these can only be valued with Monte Carlo anyway, whether a low factor (short rate or Markov-functional) or multi factor model is used.

Volatility smile can be incorporated in the LIBOR market model, see, for example, Andersen & Andreasen (2000).

The traditional LIBOR market model is based on a set of forward LIBOR rates. Jamshidian (1997) extends the market model technology to a set of forward swap rates that co-end at the same final date. Hunt & Kennedy (2000, Section 18.4) and Galluccio & Hunter (2004) extend with a set of forward swap rates that co-start at the same initial date, which is useful for, e.g., European options on interest rate spreads. An *interest rate spread* is a difference between separate interest rates. In Chapter 7, we extend market models to include forward constant maturity swap (CMS) rates and other generic specifications of rates. The derivation methodology is fully generic and includes the previous market model specifications. The CMS market model is key to the pricing of, for example, fixed maturity Bermudan swaptions and Bermudan CMS swaptions.

1.3.3 Markov-functional models

A model class that combines some of the features of short rate models and market models is the Markov-functional model of Hunt et al. (2000), see also Hunt & Kennedy (2000, Section 19) and Pelsser (2000, Section 9). Markov-functional models can be calibrated to interest rate option volatility much like market models, and they do *not* suffer from the drawback of short rate models of producing an arbitrary smile: Volatility smile is very much controllable in Markov-functional models, and a flat volatility smile can be achieved. Moreover, Markov-functional models do *not* suffer from the computational burden of market models, and pricing can be efficiently performed on, e.g., a grid.

The numerical efficiency of pricing on a grid comes however with a price: a single stochastic Markov driver implies that the model has difficulty in attaining instantaneous

de-correlation between interest rates. A question that has not yet been addressed in the academic literature so far, is whether a lack of de-correlation causes a significant impact on the pricing and hedge performance of a model. In Chapter 6, we address this research question by empirical comparison of market models and Markov-functional models, in terms of pricing and hedge performance.

1.4 American option pricing with Monte Carlo simulation

American options feature a period during which the option can be exercised. *Bermudan options* can be exercised at several discrete points in time. Bermudan options are thus somewhat in between European and American options.

The valuation of American options typically involves a backward induction routine, while Monte Carlo simulation is of forward induction type. An efficient algorithm for pricing American options in Monte Carlo was therefore not known in the literature for long. The problem is that we need to know, at a simulation node, the value of holding onto the option. This conditional expectation value is not known, and to calculate it would, in principle, require simulation within simulation, which is most inefficient. Only recently has efficient American option valuation with Monte Carlo been enabled by novel *regression-based* methods, see, for example, Longstaff & Schwartz (2001). The key is to make use of cross-sectional information present in the simulation, by regressing the hold-on value onto functions of explanatory variables present in the simulation. The regression-based approximate hold-on value may then be used to formulate an exercise decision.

The regression based techniques have been generalized to *stochastic mesh methods* by Broadie & Glasserman (2004) and Avramidis & Matzinger (2004). Other American option pricing techniques include the dual approach of Rogers (2002), see also Jamshidian (2003), and the high-dimensional grid approach of Berridge & Schumacher (2003).

In Chapter 6, we show that the regression-based algorithm of Longstaff & Schwartz (2001) leads to inefficiently estimated risk sensitivities. We propose a modification of the algorithm, deemed the *constant exercise method*, that enhances the quality of risk sensitivity estimates.

Chapter 2

Risk-managing Bermudan swaptions in a LIBOR model

[1] This chapter presents a new approach to calculating swap vega per bucket in a LIBOR model. It shows that for some forms of volatility an approach based on recalibration may make estimated swap vega very uncertain, as the instantaneous volatility structure may be distorted by recalibration. This does not happen in the case of constant swap rate volatility.

An alternative approach not based on recalibration comes out of comparison with the swap market model. It accurately estimates vegas for any volatility function in few simulation paths. The key to the method is that the perturbation in LIBOR volatility is distributed in a clear, stable, and well-understood fashion, while in the recalibration method the change in volatility is hidden and potentially unstable.

2.1 Introduction

The LIBOR interest rate model discussed in Section 1.3.2 is popular among both academics and practitioners alike. We will call this the BGM model.

One reason the LIBOR BGM model is popular is that it can risk-manage interest rate derivatives that depend on both the cap and swaption markets, which would make it a *central interest rate model*. It features lognormal LIBOR and almost lognormal swap rates,

[1] This chapter has been published in different form as Pietersz, R. & Pelsser, A. A. J. (2004*a*), 'Risk-managing Bermudan swaptions in a LIBOR model', *Journal of Derivatives* **11**(3), 51–62. An extended abstract of this chapter appeared as Pietersz, R. & Pelsser, A. A. J. (2004*b*), 'Swap vega in BGM: pitfalls and alternatives', *Risk Magazine* pp. 91–93. March issue. This Risk article was republished as part of a Risk book, as Pietersz, R. & Pelsser, A. A. J. (2005*b*), Swap vega in BGM: pitfalls and alternatives, *in* N. Dunbar, ed., 'Derivatives Trading and Option Pricing', Risk Books, London, UK, pp. 277–285.

and thus also the market-standard Black formula for caps and swaptions. Approximate swaption volatility formulas such as in Hull & White (2000) have been shown to be of high quality (see Brace, Dun & Barton (1998)).

There remain a number of issues to be resolved to use BGM as a central interest rate model. One issue is the calculation of swap vega. A common and usually very successful method for calculating a Greek in a model equipped with a calibration algorithm is to perturb market input, recalibrate, and then revalue the option. The difference in value divided by the perturbation size is then an estimate for the Greek.

If this technique is applied to the calculation of swap vega in the LIBOR BGM model, however, it may (depending on the volatility function) yield estimates with high uncertainty. In other words, the standard error of the vega is relatively high. The uncertainty disappears, of course, if we increase the number of simulation paths, but the number required for clarity can far exceed 10,000, which is probably the maximum in a practical environment.

For a constant-volatility calibration, however, the vega is estimated with low uncertainty. The number of simulation paths needed for clarity of vega thus depends on the chosen calibration. The reason is that for certain calibrations, under a perturbation, the additional volatility is distributed unevenly and one might even say unstably over time. For a constant-volatility calibration, of course, this additional volatility is naturally distributed evenly over time. It follows that there is higher correlation between the discounted payoffs along the original path and perturbed volatility. As the vega is the expectation of the difference between these payoffs (divided by the perturbation size), the standard error will be lower.

We develop a method that is not based on recalibration to compute swap vega per bucket in the LIBOR BGM model. It may be used to calculate swap vega in the presence of any volatility function, with predictability at 10,000 or fewer simulation paths. The strength of the method is that it accurately estimates swap vegas for any volatility function and in few simulation paths.

The key to the method is that the perturbation in the LIBOR volatility is distributed in a clear, stable, and well-understood fashion, while in the recalibration method the change in volatility is hidden and potentially unstable. The method is based on keeping swap rate correlation fixed but increasing the instantaneous volatility of a single swap rate evenly over time, while all other swap rate volatilities remain unaltered.

It is important to verify that a calculation method reproduces the correct numbers when the answer is known. We benchmark our swap vega calculation method using Bermudan swaptions for two reasons. First, a Bermudan swaption is a complicated enough (swap-based) product (in a LIBOR-based model) that depends non-trivially on the swap rate volatility dynamics; for example, its value depends also on swap rate correlation. Second, a Bermudan swaption is not as complicated as some other more exotic interest

rate derivatives, and some intuition exists about its vega behavior. We show for Bermudan swaptions that our method yields almost the same swap vega as found in a swap market model.

Glasserman & Zhao (1999) provide efficient algorithms for calculating risk sensitivities, given a perturbation of LIBOR volatility. Our problem differs from theirs in that we derive a method to calculate the perturbation of LIBOR volatility to obtain the correct swap rate volatility perturbation for swaption vega. The Glasserman and Zhao approach may then be applied to efficiently compute the swaption vega, with the LIBOR volatility perturbation we find using our method.

2.2 Recalibration approach

We first consider examples of the recalibration approach to computing swap vega. Three calibration methods are considered. We show that, for two of the three methods, the resulting vega is hard to estimate and many simulation paths are needed for clarity.

Each forward rate is modeled as a geometric Brownian motion under its forward measure:

$$\frac{\mathrm{d}f_i(t)}{f_i(t)} = \boldsymbol{\sigma}_i(t) \cdot \mathrm{d}\mathbf{w}^{(i+1)}(t), \text{ for } 0 \leq t \leq t_i,$$

The positive integer d is referred to as the *number of factors* of the model. The function $\boldsymbol{\sigma}_i : [0, t_i] \to \mathbb{R}^d$ is the volatility vector function of the i-th forward rate. The k-th component of this vector corresponds to the k-th Wiener factor of the Brownian motion. $\mathbf{w}^{(i+1)}$ is a d-dimensional Brownian motion under the forward measure $\mathbb{Q}^{(i+1)}$.

A discount bond pays one unit of currency at maturity. From (1.12), the forward rates are related to discount bond prices as follows:

$$f_i(t) = \frac{1}{\alpha_i}\left\{\frac{b_i(t)}{b_{i+1}(t)} - 1\right\}.$$

The swap rate corresponding to a swap starting at t_i and ending at t_j is denoted by $s_{i:j}$. The swap rate is related to discount bond prices as follows:

$$s_{i:j}(t) = \frac{b_i(t) - b_j(t)}{p_{i:j}(t)},$$

where p denotes the *present value of a basis point*:

$$p_{i:j}(t) = \sum_{k=i}^{j-1} \alpha_k b_{k+1}(t). \tag{2.1}$$

It is understood that $p_{i:j} \equiv 0$ whenever $j \leq i$.

We consider the swap rates $s_{1:n+1}, \ldots, s_{n:n+1}$ corresponding to the swaps underlying a coterminal Bermudan swaption.[2] Swap rate $s_{i:n+1}$ is a martingale under its forward swap measure $\mathbb{Q}^{(i:n+1)}$. We may thus implicitly define its volatility vector $\boldsymbol{\sigma}_{i:n+1}$ by:

$$\frac{\mathrm{d}s_{i:n+1}(t)}{s_{i:n+1}(t)} = \boldsymbol{\sigma}_{i:n+1}(t) \cdot \mathrm{d}\mathbf{w}^{(i:n+1)}(t), \text{ for } 0 \leq t \leq t_i. \tag{2.2}$$

In general, $\boldsymbol{\sigma}_{i:n+1}$ will be stochastic because swap rates are not lognormally distributed in the BGM model, although they are very close to lognormal as shown, for example, by Brace et al. (1998). Because of near lognormality, the Black formula approximately holds for European swaptions. There are closed-form formulas for the swaptions Black implied volatility; see, for example, Hull & White (2000).

We model LIBOR instantaneous volatility as constant in between tenor dates (piecewise-constant). A volatility structure $\{\boldsymbol{\sigma}_i(\cdot)\}_{i=1}^n$ is *piece wise-constant* if:

$$\boldsymbol{\sigma}_i(t) = (\text{const}), \quad t \in [t_{i-1}, t_i).$$

The volatility will sometimes be modeled as time-homogeneous. To define this, first define a fixing to be one of the time points $t_1, \ldots, t_n$. Define $i : [0, t_n] \to \{1, \ldots, n\}$:

$$i(t) = 1 + \#\big\{\text{fixings in } [0, t]\big\}. \tag{2.3}$$

A volatility structure is said to be time-homogeneous if it depends only on the index to maturity $i - i(t)$.

Three volatility calibration methods are considered:

1. (THFRV)—*Time-homogeneous forward rate volatility.* This approach is based on ideas of Rebonato (2001). Because of the time-homogeneity restriction, there are as many parameters as market swaption volatilities. A Newton-Rhapson sort of solver may be used to find the exact calibration solution (if there is one).

2. (THSRV)—*Time-homogeneous swap rate volatility.* The algorithm for calibrating with such a volatility function is a two-stage bootstrap. The first and the second stage are described in Equation (6.20) and Section 7.4 of Brigo & Mercurio (2001).

3. (CONST)—*Constant forward rate volatility.* The corresponding calibration algorithm is similar to the second stage of the two-stage bootstrap. We note that constant forward rate volatility implies constant swap rate volatility.

[2] A coterminal Bermudan swaption is an option to enter into an underlying swap at several exercise opportunities. The holder of a Bermudan swaption has the right at each exercise opportunity to either enter into a swap or hold the option; all the underlying swaps that may possibly be entered into have the same ending date.

Table 2.1: Market European swaption volatilities.

Expiry (Y)	1	2	3	...	28	29	30
Tenor (Y)	30	29	28	...	3	2	1
Swaption Volatility	15.0%	15.2%	15.4%	...	20.4%	20.6%	20.8%

All calibration methods have in common that the forward rate correlation structure is calibrated to a historical correlation matrix using principal components analysis (PCA); see Hull & White (2000). Correlation is assumed to evolve time-homogeneously over time.

We consider a 31NC1 coterminal Bermudan payers swaption deal struck at 5% with annual compounding. The notation $x\text{NC}y$ denotes an "x non-call y" Bermudan option, which is exercisable into a swap with a maturity of x years from today but is callable only after y years. The option is callable annually.

The BGM tenor structure is $0 < 1 < 2 < \cdots < 31$. All forward rates are taken to equal 5%. The time zero forward rate instantaneous correlation is assumed following Rebonato (1998, p. 63) as:

$$\rho_{ij}(0) = e^{-\beta|t_i - t_j|}, \tag{2.4}$$

where β is chosen to equal 5%. The market European swaption volatilities were taken as displayed in Table 2.1.

To determine the exercise boundary, we use the Longstaff & Schwartz (2001) least squares Monte Carlo method. Only a single explanatory variable is considered, namely, the swap net present value (NPV). Two regression functions are employed, a constant and a linear term.

For each bucket a perturbation $\Delta\sigma(\approx 10^{-8})$ is applied to the swaption volatility in the calibration input data.[3] The model is recalibrated, and we check to see that the calibration error for all swaption volatilities is a factor 10^6 lower than the volatility perturbation. The Bermudan swaption is repriced through Monte Carlo simulation using the exact same random numbers.

Denote the original price by v and the perturbed price by $v_{i:n+1}$. Then the recalibration method of estimating swap vega $\nu_{i:n+1}$ for bucket i is given by:

$$\nu_{i:n+1} = \frac{v_{i:n+1} - v}{\Delta\sigma}. \tag{2.5}$$

[3]It was verified that the resulting vega is stable for a wide range of volatility perturbation. For very extreme perturbation, the vega is unstable. At high levels of perturbation, vega-gamma terms affect the vega. At too low levels of volatility perturbation, floating point number round-off errors affect the vega.

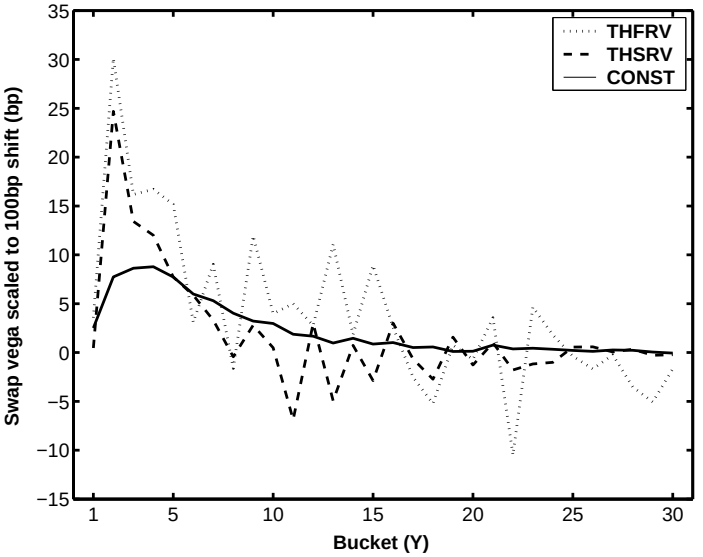

Figure 2.1: Recalibration swap vega results for 10,000 simulation paths.

Usually the swap vega is denoted in terms of a shift in the swaption volatility. For example, consider a 100 basis point (bp) shift in the swaption volatility. The swap vega scaled to a 100 bp shift $\nu_{i:n+1}^{100\text{bp}}$ is then defined by

$$\nu_{i:n+1}^{100\text{bp}} = (0.01) \cdot \nu_{i:n+1}.$$

Swap vega results for a Monte Carlo simulation of 10,000 scenarios are displayed in Figure 2.1. The standard errors (SEs) are displayed separately in Figure 2.2. The levels of SE for THFRV and CONST are 6.00 and 0.25, respectively. The number of paths needed for THFRV to obtain the same SE as CONST is thus $(6/0.25)^2 \times 10,000 = 5.8M$. For THSRV, we find 1.4M paths are needed.

Figure 2.3 displays the THFRV vega for 1 million simulation paths.

2.3 Explanation

The key to explanation of the vega results under recalibration is the change in swap rate instantaneous variance after recalibration. For the THFRV and THSRV recalibration approaches, the instantaneous variance increment (in the limit) is completely different from a constant- volatility increment. This holds for all buckets.

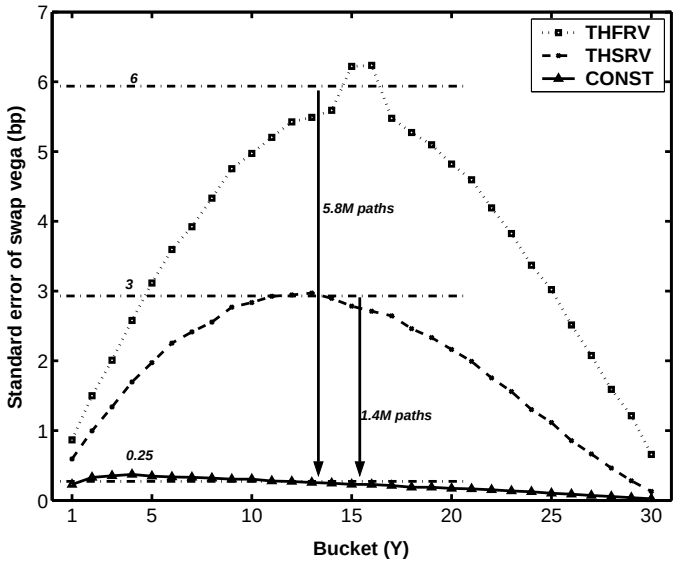

Figure 2.2: Empirical standard errors of vega for 10,000 simulation paths.

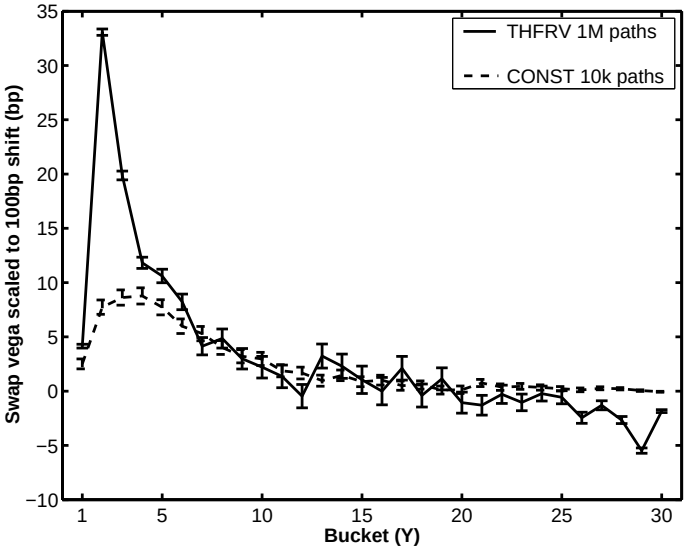

Figure 2.3: Recalibration THFRV vega results for 1 million simulation paths.

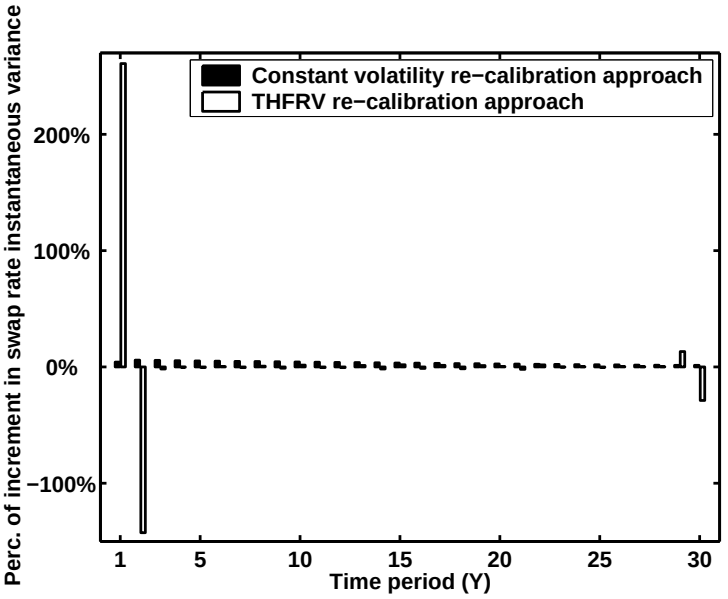

Figure 2.4: Observed change in swap rate instantaneous variance for THFRV and CONST recalibration approach.

For illustration, we consider the volatility perturbation shown in Figure 2.4, which is associated with the calculation of swap vega corresponding to bucket 30. The price differential has to be computed in the limit of the 30×1 swaption implied volatility perturbation $\Delta\sigma$ tending to zero. This implies a swap rate instantaneous variance increment of $30\Delta\sigma^2$. This total variance increment has to be distributed over all time periods. We note that for both data sets the sum of the variance increments equals 100%. For THFRV, the distribution of the variance increment is concentrated in the begin and end time periods, and is even negative in the second time period. This is at variance with the natural and intuitive even distribution in the CONST recalibration.

From (2.5), it follows that the simulation variance of the vega is given by

$$\mathrm{Var}\big[\nu_{i:n+1}^{100\mathrm{bp}}\big] = c^2\mathrm{Var}\big[\pi_{i:n+1} - \pi\big] = c^2\Big\{\mathrm{Var}\big[\pi_{i:n+1}\big] - 2\mathrm{Cov}\big[\pi_{i:n+1}, \pi\big] + \mathrm{Var}\big[\pi\big]\Big\}, \quad (2.6)$$

where π and $\pi_{i:n+1}$ are the payoffs along the path of the original and the perturbed model, respectively. Here $c := 0.01/\Delta\sigma_{i:n+1}$.

The vega standard error is thus minimized if there is high covariance between the discounted payoffs in the original and the perturbed model. This does *not* occur for a

perturbation such as dictated by THFRV, because the stochasticity in the simulation is basically moved around to other time periods (in our case from period 2 to period 1). Because the rate increments over different time periods are *independent*, this leads to a reduced covariance, leading in turn to a higher standard error of the vega.

There is higher covariance between the payoffs under the perturbations of variance implied by the CONST calibration, because then each independent time period maintains approximately the same level of variance; no stochasticity is moved to other random sources. From (2.6), it then follows that the standard error is lower.

2.4 Swap vega and the swap market model

An alternative method for calculating swap vega has the advantage that the estimates of vega have a low standard error for any volatility function. The first step is to study the definition of swap vega in the swap market model, which we will extend to the LIBOR BGM model. This will give us an alternative method to calculate swap vega per bucket.

How much our dynamically managed hedging portfolio should hold in European swaptions is essentially determined by the swap vega per bucket. The latter is the derivative of the exotic price with respect to the Black swaption implied volatility.

We consider a swap market model $\mathcal{S}$. In the model, swap rates are lognormally distributed under their forward swap measure. This means that all swap rate volatility functions $\boldsymbol{\sigma}_{i:n+1}(\cdot)$ of (2.2) are deterministic. The Black implied swaption volatility $\sigma_{k:n+1}$ is given by

$$\sigma_{k:n+1} = \sqrt{\frac{1}{t_k}\int_0^{t_k} |\boldsymbol{\sigma}_{k:n+1}(s)|^2 \mathrm{d}s}.$$

As may be seen in this equation, there are an uncountable number of perturbations of the swap rate instantaneous volatility that produce the same perturbation as the Black implied swaption volatility. There is, however, a natural one-dimensional parameterized perturbation of the swap rate instantaneous volatility, namely, a simple proportional increment. This is illustrated in Figure 2.5.

We define swap vega in the swap market model as follows. Denote the price of an interest rate derivative in a swap market model $\mathcal{S}$ by v. We consider a perturbation of the swap rate instantaneous volatility given by

$$\boldsymbol{\sigma}^{\varepsilon}_{k:n+1}(\cdot) = (1+\varepsilon)\boldsymbol{\sigma}_{k:n+1}(\cdot), \tag{2.7}$$

where the shift applies only to $k : n+1$. Denote the corresponding swap market model by $\mathcal{S}_{k:n+1}(\varepsilon)$. We note that the implied swaption volatility in $\mathcal{S}_{k:n+1}(\varepsilon)$ is given by $\sigma^{\varepsilon}_{k:n+1} = (1+\varepsilon)\sigma_{k:n+1}$. Denote the price of the derivative in $\mathcal{S}_{k:n+1}(\varepsilon)$ by $v_{k:n+1}(\varepsilon)$. Then the swap

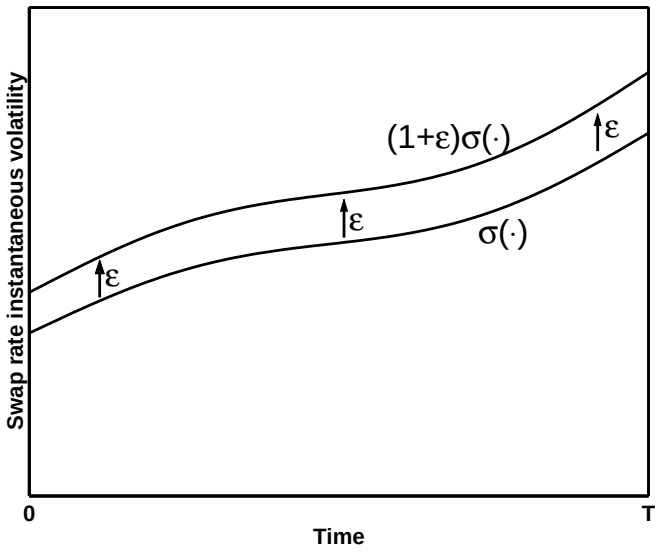

Figure 2.5: Natural increment of Black implied swaption volatility.

vega per bucket $\nu_{k:n+1}$ is defined as

$$\nu_{k:n+1} = \lim_{\varepsilon \to 0} \frac{v_{k:n+1}(\varepsilon) - v}{\varepsilon \sigma_{k:n+1}}. \tag{2.8}$$

Equation (2.8) is the derivative of the exotic price with respect to the Black implied swaption volatility. In conventional notation we may write

$$\nu_{k:n+1} = \frac{\partial v}{\partial \sigma_{k:n+1}} = \lim_{\Delta\sigma_{k:n+1} \to 0} \frac{v(\sigma_{k:n+1} + \Delta\sigma_{k:n+1}) - v(\sigma_{k:n+1})}{\Delta\sigma_{k:n+1}} \tag{2.9}$$

In (2.8) $\varepsilon\sigma_{k:n+1}$ is equal to the swaption volatility perturbation $\Delta\sigma_{k:n+1}$, and $v_{k:n+1}(\varepsilon)$ and v denote the prices of the derivative in models where the k-th swaption volatility equals $\sigma_{k:n+1} + \Delta\sigma_{k:n+1}$ and $\sigma_{k:n+1}$, respectively.

The swap rate volatility perturbation in (2.7) defines a relative shift. It is also possible to apply an absolute shift in the form of

$$\boldsymbol{\sigma}^{\varepsilon}_{k:n+1}(\cdot) = \left(1 + \frac{\varepsilon}{\|\boldsymbol{\sigma}_{k:n+1}(\cdot)\|}\right) \boldsymbol{\sigma}_{k:n+1}(\cdot), \tag{2.10}$$

where the shift applies only to $k : n+1$. This ensures that the absolute level of the swap rate instantaneous volatility is increased by an amount ε. We note that the relative and

absolute perturbation are equivalent when the instantaneous volatility is constant over time.

The method for calculating swap vega per bucket is largely the same for both relative and absolute perturbation (but we will point out any differences). The first difference is in the change in swaption implied volatility $\Delta\sigma_{k:n+1}$ of (2.9); namely, straightforward calculations reveal that the perturbed volatility satisfies

$$\sigma^{\varepsilon}_{k:n+1} = \sigma_{k:n+1} + \varepsilon \frac{\frac{1}{t_k}\int_0^{t_k} \|\bar{\sigma}_{k:n+1}(s)\| \mathrm{d}s}{\sigma_{k:n+1}} + \mathcal{O}\big(\varepsilon^2\big).$$

2.5 Alternative method for calculating swap vega

An alternative method for calculating swap vega in the BGM framework may be applied to any volatility function to yield accurate vega with a small number of simulation paths. The method is based on a perturbation in the forward rate volatility to match a constant swap rate volatility increment. Rebonato (2002) also derives this method in terms of covariance matrices, but our derivation is explicitly in terms of volatility vectors.

Swap rates are not lognormally distributed in the LIBOR BGM model. This means that swap rate instantaneous volatility is stochastic. The stochasticity is almost invisible as shown empirically, for example, by Brace et al. (1998). D'Aspremont (2002) shows that the swap rate is uniformly close to a lognormal martingale.

Hull & White (2000) show that the swap rate volatility vector is a weighted average of forward LIBOR volatility vectors:

$$\boldsymbol{\sigma}_{i:n+1}(t) = \sum_{j=i}^{n} w_j^{i:n+1}(t)\boldsymbol{\sigma}_j(t), \quad w_j^{i:n+1}(t) = \frac{\alpha_j \gamma_j^{i:n+1}(t) f_j(t)}{1+\alpha_j f_j(t)}, \tag{2.11}$$

$$\gamma_j^{i:n+1}(t) = \frac{b_i(t)}{b_i(t) - b_{n+1}(t)} - \frac{p_{i:j}(t)}{p_{i:n+1}(t)},$$

where the weights $w^{i:n+1}$ are in general state-dependent.

Hull and White derive an approximating formula for European swaption prices that is based on evaluating the weights in (2.11) at time zero. This is a good approximation by virtue of the near lognormality of swap rates in the LIBOR BGM model. We denote the resulting swap rate instantaneous volatility by $\boldsymbol{\sigma}^{\mathrm{HW}}_{i:n+1}$ as follows:

$$\boldsymbol{\sigma}^{\mathrm{HW}}_{i:n+1}(t) = \sum_{j=i}^{n} w_j^{i:n+1}(0)\boldsymbol{\sigma}_j(t). \tag{2.12}$$

When we write $w_j^{i:n+1} := w_j^{i:n+1}(0)$ and adopt the convention that

$$\boldsymbol{\sigma}_i(t) = \boldsymbol{\sigma}_{i:n+1}(t) = 0 \text{ when } t > t_i,$$

a useful form of (2.12) is:

$$\begin{array}{rcccccc} \boldsymbol{\sigma}^{\mathrm{HW}}_{1:n+1}(t) & = & w_1^{1:n+1}\boldsymbol{\sigma}_1(t) & + & \dots & + & w_n^{1:n+1}\boldsymbol{\sigma}_n(t) \\ \vdots & & & & \ddots & & \vdots \\ \boldsymbol{\sigma}^{\mathrm{HW}}_{n:n+1}(t) & = & & & & & w_n^{n:n+1}\boldsymbol{\sigma}_n(t) \end{array} \tag{2.13}$$

If $\mathbf{W}$ is the upper triangular non-singular weight matrix (with upper triangular inverse $\mathbf{W}^{-1}$), these volatility vectors can be jointly related through the matrix equation:

$$\big[\boldsymbol{\sigma}_{\cdot:n+1}\big] = \mathbf{W}\big[\boldsymbol{\sigma}_{\cdot}\big].$$

The swap rate volatility under relative perturbation (2.7) of the k-th volatility is

$$\big[\boldsymbol{\sigma}_{\cdot:n+1}\big] \to \big[\boldsymbol{\sigma}_{\cdot:n+1}\big] + \varepsilon\big[\begin{array}{ccccccc} 0 & \dots & 0 & \boldsymbol{\sigma}_{k:n+1} & 0 & \dots & 0 \end{array}\big]^{\top}.$$

We note that the swap rate correlation is left unaltered. The corresponding perturbation in the BGM volatility vectors is given by

$$\big[\boldsymbol{\sigma}_{\cdot}\big] \to \big[\boldsymbol{\sigma}_{\cdot}\big] + \varepsilon\mathbf{W}^{-1}\big[\begin{array}{ccccccc} 0 & \dots & 0 & \boldsymbol{\sigma}_{k:n+1} & 0 & \dots & 0 \end{array}\big]^{\top}. \tag{2.14}$$

We note that only the volatility vectors $\boldsymbol{\sigma}_k(t), \dots, \boldsymbol{\sigma}_n(t)$ are affected (due to the upper triangular nature of $\mathbf{W}^{-1}$), which are the vectors that underlie $\boldsymbol{\sigma}_{k:n+1}(t)$ in the Hull and White approximation. With the new LIBOR volatility vectors, prices can be recomputed in the BGM model and the vegas calculated.

2.6 Numerical results

We demonstrate the algorithm in a simulation with 10,000 paths. The results are displayed in Figure 2.6. We note that the approach yields slightly negative vegas for buckets 17-30.

In Appendix 2.A, we show that negative values are not a spurious result. That is, for the analytically tractable setup of a two-stock Bermudan option, negativity of vega occurs with correlation $\approx$1, and volatilities for short expiration dates are higher than volatilities at longer expiration dates—this of course is in a typical interest rate setting.

The vegas were also calculated for the absolute perturbation method in results not displayed. The differences in the vegas for the two methods are minimal; for any vega with absolute value above 1 bp, the difference is less than 4%, and for any vega with absolute value below 1 bp, the difference is always less than a third of a basis point.

2.7 Comparison with the swap market model

The swap market model (SMM) is the canonical model for computing swap vega per bucket. We compare the LIBOR BGM model and a swap market model with the very

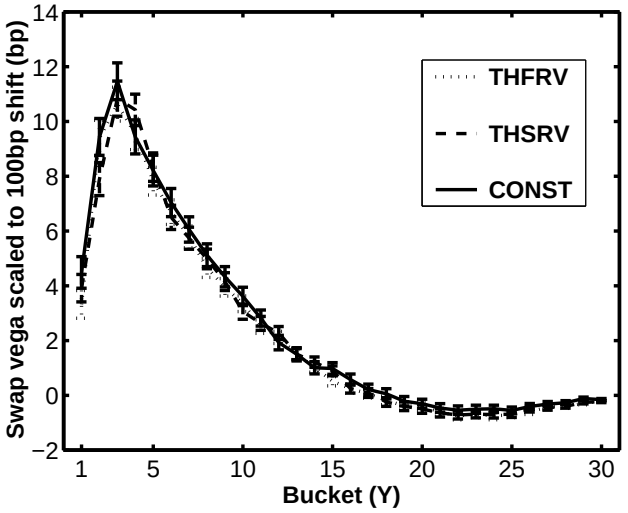

Figure 2.6: Swap vega results for 10,000 simulation paths. Error bars denote 95% confidence bound based on the standard error.

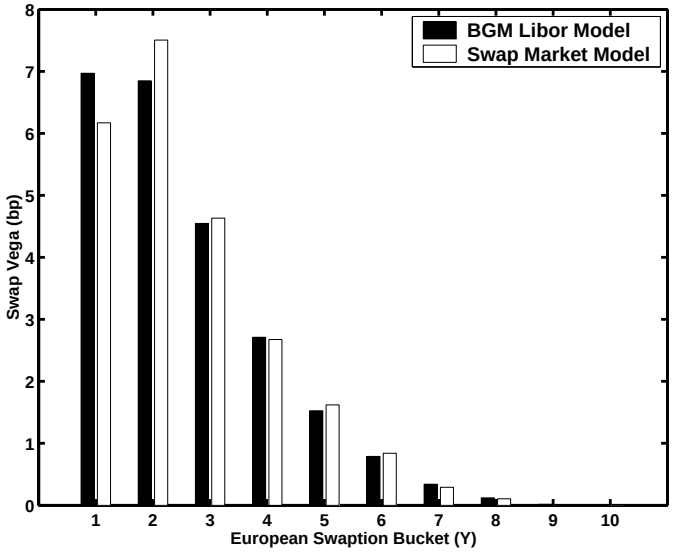

Figure 2.7: Comparison of LMM and SMM for swap vega per bucket, 5% strike.

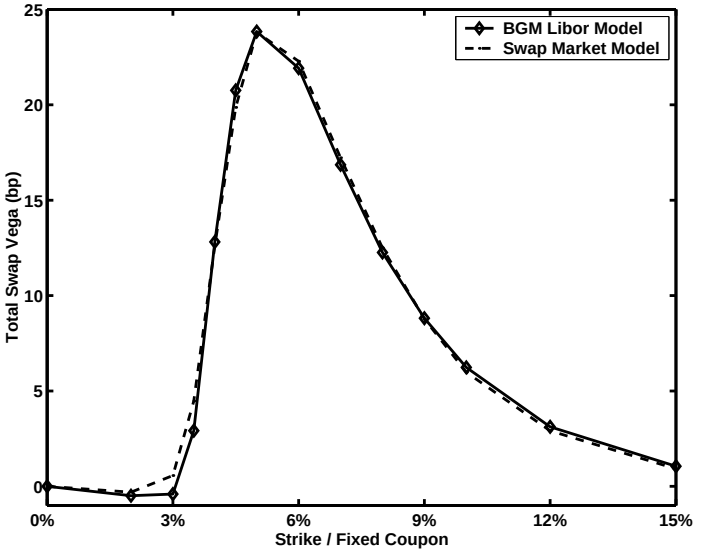

Figure 2.8: Comparison of LMM and SMM for total swap vega against strike.

same swap rate quadratic cross-variation structure. Approximate equivalence between the two models has been established by Joshi & Theis (2002, Equation (3.8)).

We perform the test for an 11NC1 pay-fixed Bermudan option on a swap with annual fixed and floating payments. A single-factor LIBOR BGM model is used with constant volatility calibrated to the euro cap volatility curve of October 10, 2001. The zero rates were taken to be flat at 5%. In the Monte Carlo simulation of the SMM we apply the discretization suggested in Lemma 5 of Glasserman & Zhao (2000).

Results appear in Table 2.2, and are displayed partially in Figures 2.7 and 2.8. In this particular case, the BGM LIBOR model reproduces the swap vegas of the swap market model very accurately.

2.8 Conclusions

We have presented a new approach to calculating swap vega per bucket in the LIBOR BGM model. We show that for some forms of the volatility an approach based on re-calibration may lead to great uncertainty in estimated swap vega, as the instantaneous volatility structure may be distorted by recalibration. This does not happen in the case of constant swap rate volatility.

Table 2.2: Swap vega per bucket test results for varying strikes—10,000 simulation paths.

BGM LIBOR MODEL

Fixed Rate	2%	3%	3.5%	4%	4.5%	5%	6%	7%	8%	9%	10%	12%	15%
Value	2171	1476	1138	829	585	410	210	112	64	36	21	8	2
	(4)	(5)	(5)	(5)	(5)	(4)	(3)	(2)	(2)	(1)	(1)	(1)	(0)
1Y	-2.0	-2.0	2.6	10.9	11.1	7.0	1.2	0.1	0.0	0.0	0.0	0.0	0.0
2Y	1.5	1.6	1.0	2.6	5.7	6.8	4.0	1.0	0.0	0.0	0.0	0.0	0.0
3Y	0.0	0.0	-0.3	0.1	2.5	4.5	4.1	2.1	1.0	0.3	0.0	0.0	0.0
4Y	0.0	0.0	-0.1	-0.1	1.1	2.7	4.4	3.6	2.0	1.1	0.5	0.2	0.1
5Y	0.0	0.0	-0.1	-0.2	0.4	1.5	3.7	3.6	2.7	1.5	1.0	0.3	0.1
6Y	0.0	0.0	-0.1	-0.2	0.1	0.8	2.1	2.5	2.0	1.7	1.2	0.3	0.2
7Y	0.0	0.0	-0.1	-0.2	0.0	0.3	1.3	1.8	1.8	1.6	1.1	0.5	0.0
8Y	0.0	0.0	0.0	-0.1	-0.1	0.1	0.7	1.3	1.5	1.3	1.3	0.9	0.3
9Y	0.0	0.0	0.0	-0.1	-0.1	0.0	0.3	0.7	0.8	0.8	0.8	0.6	0.3
10Y	0.0	0.0	0.0	0.0	0.0	0.0	0.1	0.3	0.3	0.4	0.4	0.3	0.2
Total Vega	-0.5	-0.4	2.9	12.8	20.8	23.8	21.9	16.9	12.3	8.8	6.2	3.1	1.0

SWAP MARKET MODEL

Fixed Rate	2%	3%	3.5%	4%	4.5%	5%	6%	7%	8%	9%	10%	12%	15%
Value	2172	1480	1146	841	592	411	204	109	61	34	19	7	1
	(6)	(6)	(6)	(5)	(5)	(4)	(4)	(3)	(2)	(1)	(1)	(1)	(0)
1Y	-1.9	-0.7	4.4	11.3	11.5	6.2	0.4	0.0	0.0	0.0	0.0	0.0	0.0
2Y	1.6	1.6	1.1	2.2	5.2	7.5	3.6	0.5	0.0	0.0	0.0	0.0	0.0
3Y	0.0	-0.1	-0.4	0.0	2.0	4.6	4.7	2.2	0.6	0.2	0.0	0.0	0.0
4Y	0.0	-0.1	-0.2	-0.1	0.9	2.7	4.8	3.7	1.7	0.8	0.3	0.1	0.0
5Y	0.0	0.0	-0.2	-0.2	0.4	1.6	3.7	3.0	2.3	1.2	0.5	0.1	0.0
6Y	0.0	0.0	-0.1	-0.2	0.1	0.8	2.6	3.3	3.1	2.3	1.2	0.2	0.0
7Y	0.0	0.0	-0.1	-0.2	-0.1	0.3	1.3	2.0	1.9	1.3	1.4	0.8	0.1
8Y	0.0	0.0	0.0	-0.1	-0.1	0.1	0.8	1.3	1.5	1.5	1.2	0.6	0.2
9Y	0.0	0.0	0.0	-0.1	-0.1	0.0	0.4	0.9	1.0	1.0	0.9	0.7	0.3
10Y	0.0	0.0	0.0	0.0	0.0	0.0	0.1	0.3	0.4	0.5	0.5	0.4	0.3
Total Vega	-0.3	0.6	4.5	12.6	19.9	23.8	22.3	17.2	12.5	8.8	6.0	2.9	0.9

We derive an alternative approach that is not based on recalibration, using the swap market model. The method accurately estimates swaption vegas for any volatility function and at a small number of simulation paths.

The key to the method is that the perturbation in the LIBOR volatility is distributed in a clear, stable, and well-understood fashion, but in the recalibration method the change in volatility is hidden and potentially unstable. We also show for a Bermudan swaption deal that our method yields almost the same swap vega as a swap market model.

2.A Appendix: Negative vega for two-stock Bermudan options

We examine a two-stock Bermudan option to show that its vega per bucket is negative in certain situations. The holder of a two-stock Bermudan option has the right to call the first stock s_1 at strike k_1 at time t_1; if the holder decides to hold the option, the right remains to call the second stock s_2 at strike k_2 at time t_2; if this right is not exercised, then the option becomes worthless. Here $t_1 < t_2$.

The Bermudan option is valued under standard Black-Scholes conditions. Under the risk-neutral measure, the stock prices satisfy the stochastic differential equations:

$$\frac{\mathrm{d}s_i}{s_i} = r\mathrm{d}t + \sigma_i \mathrm{d}w_i, \quad i = 1, 2, \quad \mathrm{d}w_1 \mathrm{d}w_2 = \rho \mathrm{d}t,$$

where σ_i is the volatility of the i-th stock, and w_i, $i = 1, 2$, are Brownian motions under the risk-neutral measure, with correlation ρ. It follows that the time t_1 stock prices are distributed as follows:

$$s_i(t_1) = f\big(s_i(0), 0; t_1\big) \exp\left\{\sigma_i \sqrt{t_1} z_i - \frac{1}{2}\sigma_i^2 t_1\right\}, \quad i = 1, 2, \tag{2.15}$$

where the pair (z_1, z_2) is standard bivariate normally distributed with correlation ρ and where

$$f(s, t; u) := s \exp\big\{r(u - t)\big\}, \tag{2.16}$$

is the time t forward price for delivery at time u of a stock with current price s.

At time t_1, the holder of the Bermudan option will choose whichever of two alternatives has a higher value: either calling the first stock, or holding the option on the second stock; the value of the latter is given by the Black-Scholes formula. on conditioning and involves a one-dimensional numerical integration over the Black formula.

Therefore the (cash-settled) payoff $v(s_1(t_1), s_2(t_1), t_1)$ of the Bermudan at time t_1 is given by:

$$\max\Big\{\big(s_1(t_1) - k_1\big)_+, \mathrm{BS}_2\big(s_2(t_1), t_1\big)\Big\}, \tag{2.17}$$

Table 2.3: Deal description.

Spot price for stock 1	$s_1(0)$	150
Spot price for stock 2	$s_2(0)$	140
Strike price for stock 1	k_1	100
Strike price for stock 2	k_2	100
Exercise time for stock 1	t_1	1Y
Exercise time for stock 2	t_2	2Y
Volatilities	σ_i	Variable
Correlation	ρ	0.9
Risk-free rate	r	5%

where BS is the Black-Scholes formula:

$$\begin{aligned} \mathrm{BS}_i(s,t) &= e^{-r(t_i-t)}\Big\{ f(s,t;t_i)\phi\Big(d_1^{(i)}\Big) - k_i\phi\Big(d_2^{(i)}\Big)\Big\}, \\ d_{1,2}^{(i)}(s,t) &= \frac{\ln\big(f(s,t;t_i)/k_i\big) \pm \frac{1}{2}\sigma_i^2 t}{\sigma_i\sqrt{t}}, \end{aligned}$$

where $\phi(\cdot)$ is the cumulative normal distribution function.

The time zero value $v(s_1, s_2, 0)$ of the Bermudan option may thus be computed by a bivariate normal integration of the discounted version of the payoff in (2.17):

$$v(s_1, s_2, 0) = e^{-rt_1}\mathbb{E}\Big[v\big(t_1, s_1(t_1), s_2(t_1)\big)\Big].$$

The vega per bucket ν_i is defined as

$$\nu_i := \frac{\partial v(s_1, s_2, 0)}{\partial \sigma_i}, \quad i = 1, 2.$$

The vega may be numerically approximated by finite differences:

$$\nu_i = \frac{v(s_1, s_2, 0; \sigma_i + \Delta\sigma_i) - v(s_1, s_2, 0; \sigma_i)}{\Delta\sigma_i} + \mathcal{O}\big(\Delta\sigma_i^2\big), \quad i = 1, 2,$$

for a small volatility perturbation $\Delta\sigma_i \ll 1$.

We note that the vega per bucket may possibly be negative for both the first and the second bucket. As an example of vega negativity, we compute the vega per bucket for the deal described in Table 2.3. Results are displayed in Table 2.4. The volatility is perturbed by a small amount.

Table 2.4: Results for negative vega per bucket for two-stock Bermudan option.

	σ_1	σ_2	price	$\nu_1^{100\text{bp}}$	$\nu_2^{100\text{bp}}$
Scenario 1	10%	30%	64.53	-0.45	0.56
Scenario 2	30%	10%	65.11	0.56	-0.44

The resulting vega is insensitive to either the perturbation size or the density of the 2D integration grid. In several instances a vega per bucket is negative, in both the first and the second bucket.

To ensure that the negative vega is not due to an implementation error, we develop an alternative valuation of the two-stock Bermudan option (available upon request). It is based on conditioning and involves a one-dimensional numerical integration over the Black formula. The alternative method yields the exact same results.

We note in Table 2.4 that the negative vegas occur in the case of high correlation and for the bucket with the lowest volatility. In the case of high correlation and one stock with significantly higher volatility than the other, we contend that the only added value of the additional option on the low-volatility stock lies in offering protection against a down move of both stocks (recall that the stocks are highly correlated). There are two scenarios:

- *Up move.* Both stocks move up. Because the high-volatility stock moves up much more than the low-volatility stock, the high-volatility call will be exercised.
- *Down move.* Both stocks move down. Because the high-volatility stock moves down much more than the low-volatility stock, the high-volatility call becomes out of the money, and the low-volatility call will be exercised.

If now the volatility of the low-volatility stock is increased by a small amount, then in these scenarios the exercise strategy remains unchanged. Also, in the case of an up move, the payoff remains unaltered. In the case of a down move, however, the low-volatility stock (volatility slightly increased) moves down more than in the unperturbed case. Therefore, the payoff of the protection call is reduced. In total, the Bermudan option is thus worth less.

We give an alternative explanation of the source of vega negativity for Bermudan swaptions. We consider a European maximum option on the two highly correlated stocks s_1 and s_2, struck at $k > 0$, with payoff:

$$\max(s_1 - k,\ s_2 - k,\ 0).$$

We deem the risk behaviour of this option to be similar to the risk behaviour of a Bermudan swaption, since the choice of calling either s_1 or s_2 corresponds to the choice of exercising at the first or second exercise opportunity. We have:

$$\max(s_1 - k,\ s_2 - k,\ 0) = \max(s_1 - k,\ 0) + 1_{\{s_1 > k\}} \max(s_2 - s_1,\ 0).$$

The maximum option is thus the sum of an ordinary European call option and a (conditional) European spread option. If the volatility of the first stock increases then the volatility of the spread $s_2 - s_1$ decreases (for highly correlated stocks), by which the value of the European spread option decreases. This causes a negative component in the total composition of the vega. However the ordinary call option value increases when the volatility of the first stock increases, which thus constitutes a positive component of the vega.

The same argument can be applied to show that an increase in volatility of the second stock causes a negative component in the vega. The spread option argument carefully shows a negative component in the vega of a Bermudan swaption, however it does not explain that this negative component can sometimes outweigh the other positive components of the vega. This outweighing of the negative component is explained in the up and down moves argument above.

Chapter 3

Rank reduction of correlation matrices by majorization

[1] A novel algorithm is developed for the problem of finding a low-rank correlation matrix nearest to a given correlation matrix. The algorithm is based on majorization and, therefore, it is globally convergent. The algorithm is computationally efficient, is straightforward to implement, and can handle arbitrary weights on the entries of the correlation matrix. A simulation study suggests that majorization compares favourably with competing approaches in terms of the quality of the solution within a fixed computational time. The problem of rank reduction of correlation matrices occurs when pricing a derivative dependent on a large number of assets, where the asset prices are modelled as correlated log-normal processes. Such an application mainly concerns interest rates.

3.1 Introduction

In this chapter, we study the problem of finding a low-rank correlation matrix nearest to a given (correlation) matrix. First we explain how this problem occurs in an interest rate derivatives pricing setting. We will focus on interest rate derivatives that depend on several rates such as the 1 year LIBOR deposit rate, the 2 year swap rate, etc. An example of such a derivative is a Bermudan swaption. A Bermudan swaption gives its holder the right to enter into a fixed maturity interest rate swap at certain exercise dates. At an exercise opportunity, the holder has to choose between exercising then or holding onto the option with the chance of entering into the swap later at more favourable interest rates.

[1] This chapter has been published in different form as Pietersz, R. & Groenen, P. J. F. (2004*b*), 'Rank reduction of correlation matrices by majorization', *Quantitative Finance* **4**(6), 649–662. An extended abstract of this chapter appeared as Pietersz, R. & Groenen, P. J. F. (2004*a*), 'A major LIBOR fit', *Risk Magazine* p. 102. December issue.

Evidently, the value depends not only on the current available swap rate but, amongst others, also on the forward swap rates corresponding to future exercise dates. In contrast, an example of a derivative that is dependent on a single interest rate is a caplet, which can be viewed as a call option on LIBOR. In this case, the value of the caplet depends only on a single forward LIBOR rate.

Here, we will focus on derivatives depending on several rates. Our discussion can however also be applied to the situation of a derivative depending on several *assets*. To do so a model is set up that specifies the behaviour of the asset prices. Each of the asset prices is modelled as a log-normal martingale under its respective forward measure. Additionally, the asset prices are correlated. Suppose we model n correlated log-normal price processes,

$$\frac{\mathrm{d}s_i}{s_i} = \ldots \mathrm{d}t + \sigma_i \mathrm{d}\tilde{w}_i, \quad \langle \mathrm{d}\tilde{w}_i, \mathrm{d}\tilde{w}_j \rangle = \rho_{ij}, \tag{3.1}$$

under a single measure. Here s_i denotes the price of the i^{th} asset, σ_i its volatility and $\tilde{w}_i$ denotes the associated driving Brownian motion. Brownian motions i and j are correlated with coefficient ρ_{ij}, the correlation coefficient between the returns on assets i and j. The matrix $\mathbf{P} = (\rho_{ij})_{ij}$ should be positive semidefinite and should have a unit diagonal. In other words, $\mathbf{P}$ should be a true correlation matrix. The term $\ldots \mathrm{d}t$ denotes the drift term that stems from the change of measure under the non-arbitrage condition.

The models that fit into the framework of (3.1) and which are most relevant to our discussion are the LIBOR and swap market models for valuation of interest rate derivatives, as introduced in Section 1.3.2. These models were developed by Brace et al. (1997), Jamshidian (1997) and Miltersen et al. (1997). In this case, an asset price corresponds to a forward LIBOR or swap rate. For example, if we model a 30 year Bermudan swaption with annual call and payment dates, then our model would consist of 30 annual forward LIBOR rates or 30 co-terminal forward swap rates. In the latter case, we consider 30 forward starting annual-paying swaps, starting at each of the 30 exercise opportunities and all ending after 30 years. Model (3.1) could however be applied to a derivative depending on a number of, for example, stocks, too.

Given the model (3.1), the price of any derivative depending on the assets can be calculated by non-arbitrage arguments. Because the number of assets is assumed to be high and the derivative is assumed complex in this exposition, the derivative value can be calculated only by Monte Carlo simulation. To implement scheme (3.1) by Monte Carlo we need a decomposition $\mathbf{P} = \mathbf{Y}\mathbf{Y}^T$, with $\mathbf{Y}$ an $n \times n$ matrix. In other words, if we denote the i^{th} row vector of $\mathbf{Y}$ by $\mathbf{y}_i$, then the decomposition reads $\langle \mathbf{y}_i, \mathbf{y}_j \rangle = \rho_{ij}$, where $\langle ., . \rangle$ denotes the scalar product. We then implement the scheme

$$\frac{\mathrm{d}s_i}{s_i} = \ldots \mathrm{d}t + \sigma_i \big\{ \, y_{i1}\mathrm{d}w_1 + \cdots + y_{in}\mathrm{d}w_n \, \big\}, \quad \langle \mathbf{y}_i, \mathbf{y}_j \rangle = \rho_{ij}, \tag{3.2}$$

where the w_i are now independent Brownian motions. Scheme (3.2) indeed corresponds to scheme (3.1) since both volatility and correlation are implemented correctly. The instantaneous variance is $\langle \mathrm{d}s_i/s_i \rangle = \sigma_i^2 \mathrm{d}t$ since $\|\mathbf{y}_i\| = \rho_{ii} = 1$ and volatility is the square root of instantaneous variance divided by $\mathrm{d}t$. Moreover, for the instantaneous covariance we have $\langle \mathrm{d}s_i/s_i, \mathrm{d}s_j/s_j \rangle = \sigma_i \sigma_j \langle \mathbf{y}_i, \mathbf{y}_j \rangle \mathrm{d}t = \sigma_i \sigma_j \rho_{ij} \mathrm{d}t$.

For large interest rate correlation matrices, usually almost all variance (say 99%) can be attributed to only 3–6 stochastic Brownian factors. Therefore, (3.2) contains a large number of almost redundant Brownian motions that cost expensive computational time to simulate. Instead of taking into account all Brownian motions, we would wish to do the simulation with a smaller number of factors, d say, with $d < n$ and d typically between 2 and 6. The scheme then becomes

$$\frac{\mathrm{d}s_i}{s_i} = \ldots \mathrm{d}t + \sigma_i \big\{ \; y_{i1} \mathrm{d}w_1 + \cdots + y_{id} \mathrm{d}w_d \; \big\}, \quad \langle \mathbf{y}_i, \mathbf{y}_j \rangle = \rho_{ij}. \tag{3.3}$$

The $n \times d$ matrix $\mathbf{Y}$ is a decomposition of $\mathbf{P}$. This approach immediately implies that the rank of $\mathbf{P}$ be less than or equal to d. For financial correlation matrices, this rank restriction is generally not satisfied. It follows that an approximation be required. We could proceed in two possible ways. The first way involves approximating the covariance matrix $(\sigma_i \sigma_j \rho_{ij})_{ij}$. The second involves approximating the correlation matrix while maintaining an exact fit to the volatilities. In a derivatives pricing setting, usually the volatilities are well-known. These can be calculated via a Black-type formula from the European option prices quoted in the market, or mostly these volatilities are directly quoted in the market. The correlation is usually less known and can be obtained in two ways. First, it can be estimated from historical time series. Second, it can be implied from correlation sensitive market-traded options such as spread options. A spread option is an option on the difference between two rates or asset prices. Such correlation sensitive products are not traded as liquidly as the European plain-vanilla options. Consequently, in both cases of historic or market-implied correlation, we are more confident of the volatilities. For that reason, in a derivative pricing setting, we approximate the correlation matrix rather than the covariance matrix.

The above considerations lead to solving the following problem:

$$\begin{array}{rl} \text{Find} & \mathbf{Y} \in \mathbb{R}^{n \times d}, \\ \text{to minimize} & \varphi(\mathbf{Y}) := \frac{1}{c} \sum_{i<j} w_{ij} \big(\rho_{ij} - \langle \mathbf{y}_i, \mathbf{y}_j \rangle \big)^2, \\ \text{subject to} & \|\mathbf{y}_i\|_2 = 1, \;\; i = 1, \ldots, n. \end{array} \tag{3.4}$$

Here w_{ij} are nonnegative weights and $c := 4 \sum_{i<j} w_{ij}$. The objective value φ is scaled by the constant c in order to make it independent of the problem dimension n. Because each term $\rho_{ij} - \langle \mathbf{y}_i, \mathbf{y}_j \rangle$ is always between 0 and 2, it follows for the choice of c that φ is always between 0 and 1.

An interesting alternative is to approximate the covariance matrix while keeping variance fixed[2]. If $\tilde{\mathbf{P}} = (\tilde{\rho}_{ij})_{ij}$ denotes the instantaneous covariance matrix, and $\boldsymbol{\sigma}$ denotes the vector of volatilities, then

$$\tilde{\mathbf{P}} = \mathbf{Diag}(\boldsymbol{\sigma})\ \mathbf{P}\ \mathbf{Diag}(\boldsymbol{\sigma}),$$

where $\mathbf{Diag}(\boldsymbol{\sigma})$ denotes a diagonal matrix with the diagonal filled with the vector $\boldsymbol{\sigma}$. Approximating the covariance matrix while ensuring a perfect fit to variance amounts to solving the following problem (we leave out weights w and the scalar factor c, from (3.4), for clarity of presentation):

$$\begin{array}{rl} \text{Find} & \tilde{\mathbf{Y}} \in \mathbb{R}^{n\times d}, \\ \text{to minimize} & \tilde{\varphi}(\tilde{\mathbf{Y}}) := \sum_{i<j} \left(\tilde{\rho}_{ij} - \langle \tilde{\mathbf{y}}_i, \tilde{\mathbf{y}}_j \rangle\right)^2, \\ \text{subject to} & \|\tilde{\mathbf{y}}_i\|_2^2 = \tilde{\rho}_{ii},\ \ i = 1, \ldots, n. \end{array} \tag{3.5}$$

Here, $\tilde{\mathbf{y}}_i$ relates to $\mathbf{y}_i$ in (3.3) via

$$\tilde{\mathbf{y}}_i = \sigma_i \mathbf{y}_i.$$

Approximating covariance with fixed variance as in (3.5) yields, in general, different results than approximating correlation as in (3.4), since the added variance may change the importance of certain factors. We carefully state "in general" and "may change", since if all variances are equal to one, then problems (3.4) (with constant weights) and (3.5) are obviously identical. We note that the majorization algorithm in this chapter, and the geometric programming algorithm in Chapter 4, can be applied to the covariance approximating problem in (3.5) by setting the weights in (3.4) as $w_{ij} = \sigma_i^2 \sigma_j^2$. The *covariance* problem (3.5) is thus a special case of the *correlation* problem (3.4), therefore we focus on (3.4) in the remainder of the thesis.

The weights w_{ij} in (3.4) have been added for three reasons:

- For squared differences, a large difference constitutes a far greater part of the total error in (3.4) than a small difference. The weights for small differences can then be appropriately increased to adjust for this.

- Financial reasons may sometimes compel us to assign higher weights to particular correlation pairs. For example, we could be more confident about the correlation between the 1 and 2 year swap rates than about the correlation between the 8 and 27 year swap rates.

- The objective function with weights has been considered before in the literature. See for example Rebonato (1999*c*, Section 10). Rebonato (2002, Section 9) provides an excellent discussion of the pros and cons of using weights.

[2]Many thanks to Ton Vorst for pointing out this alternative.

The simplest case of φ is $\varphi(\mathbf{Y}) := c^{-1}\|\mathbf{P} - \mathbf{Y}\mathbf{Y}^T\|_F^2$, where $\|\cdot\|_F$ denotes the Frobenius norm, $\|\mathbf{Y}\|_F^2 := \mathrm{tr}(\mathbf{Y}\mathbf{Y}^T)$ for matrices $\mathbf{Y}$. This objective function (which we shall also call 'Frobenius norm') fits in the framework of (3.4); it corresponds to the case of all weights equal. The objective function in (3.4) will be referred to as 'general weights'.

In the literature, there exist six other algorithms for minimizing φ defined in (3.4). These methods are outlined in the next section and are shown to have several disadvantages, namely none of the methods is simultaneously

(i) efficient,

(ii) straightforward to implement,

(iii) able to handle general weights and

(iv) guaranteed to converge to a local minimum.

In this chapter, we develop a novel method to minimize φ that simultaneously has the four mentioned properties. The method is based on iterative majorization that has the important property of guaranteed convergence to a stationary point. The algorithm is straightforward to implement. We show that the method can efficiently handle general weights. We investigate empirically the efficiency of majorization in comparison to other methods in the literature. The benchmark tests that we will consider are based on the performance given a fixed small amount of computational time. This is exactly the situation in practice: decisions based on derivative pricing calculations have to be made in a limited amount of time.

The remainder of this chapter is organized as follows. First, we provide an overview of the methods available in the literature. Second, the idea of majorization is introduced and the majorizing functions are derived. Third, an algorithm based on majorization is given along with reference to associated MATLAB code. Global convergence and the local rate of convergence are investigated. Fourth, we present empirical results. The chapter ends with some conclusions.

3.2 Literature review

We describe seven existing algorithms available in the literature for minimizing φ. Because a review of the majorization method is interesting from the point of view of Chapter 4 (Rank reduction by geometric programming), we include here the discussion of the majorization method itself. For each of the seven algorithms, it is indicated whether it can handle general weights. If not, then the most general objective function it can handle stems from the weighted Frobenius norm $\|\cdot\|_{F,\mathbf{\Omega}}$ with $\mathbf{\Omega}$ a symmetric positive

definite matrix, where $\|\mathbf{Y}\|^2_{F,\mathbf{\Omega}} := \mathrm{tr}(\mathbf{Y}\mathbf{\Omega}\mathbf{Y}^T\mathbf{\Omega})$. The objective function $\varphi(\mathbf{Y}) := c^{-1}\|\mathbf{R} - \mathbf{Y}\mathbf{Y}^T\|^2_{F,\mathbf{\Omega}}$ will be referred to as 'weighted Frobenius norm' too.

3.2.1 Modified PCA

First, we mention the 'modified principal component analysis (PCA)' method. For ease of exposition, we restrict to the case of the Frobenius norm, however the method can be applied to the weighted Frobenius norm as well though not for general weights. Modified PCA is based on an eigenvalue decomposition $\mathbf{P} = \mathbf{Q}\mathbf{\Lambda}\mathbf{Q}^T$, with $\mathbf{Q}$ orthogonal and $\mathbf{\Lambda}$ the diagonal matrix with eigenvalues. If the eigenvalues are ordered descendingly then a low-rank decomposition with associated approximated matrix close to the original matrix is found by

$$\{\mathbf{Y}_{\mathrm{PCA}}\}_i = \frac{\mathbf{z}}{\|\mathbf{z}\|_2}, \tag{3.6}$$

$$\mathbf{z} := \left\{\mathbf{Q}_d\mathbf{\Lambda}_d^{1/2}\right\}_i, \quad i = 1, \ldots, n. \tag{3.7}$$

Here $\{\mathbf{X}\}_i$ denotes the i^{th} row of a matrix $\mathbf{X}$, $\mathbf{Q}_d$ the first d columns of $\mathbf{Q}$, and $\mathbf{\Lambda}_d$ the principal sub-matrix of $\mathbf{\Lambda}$ of degree d. Ordinary PCA stops with (3.7) and it is the scaling in (3.6) that is the 'modified' part, ensuring that the resulting correlation matrices have unit diagonal. Modified PCA is popular among financial practitioners and implemented in numerous financial institutions. The modification of PCA in this way is believed to be due to Flury (1988). For a description in finance related articles, see, for example, Sidenius (2000) and Hull & White (2000). Modified PCA is easy to implement, because almost all that is required is an eigenvalue decomposition. The calculation is almost instant, and the approximation is reasonably accurate. A strong drawback of modified PCA is its non-optimality: generally one may find decompositions $\mathbf{Y}$ (even locally) for which the associated correlation matrix $\mathbf{Y}\mathbf{Y}^T$ is closer to the original matrix $\mathbf{P}$ than the PCA-approximated correlation matrix $\mathbf{Y}_{\mathrm{PCA}}\mathbf{Y}_{\mathrm{PCA}}^T$. The modified PCA approximation becomes worse when the magnitude of the left out eigenvalues increases.

Throughout this chapter we choose the starting point of any method considered (beyond modified PCA) to be the modified PCA solution.

3.2.2 Majorization

Second, we mention the majorization approach of Pietersz & Groenen (2004*a*, *b*), see also this Chapter 3. Majorization can handle an entry-weighted objective function and is guaranteed to converge to a stationary point. The rate of convergence is sub-linear.

3.2.3 Geometric programming

The third algorithm that we discuss, is the geometric programming approach of Grubišić & Pietersz (2005), see also Chapter 4. Here, the constraint set is equipped with a differentiable structure. Subsequently geometric programming is applied, which can be seen as Newton-Rhapson or conjugate gradient over curved space. By formulating these algorithms entirely in terms of differential geometric means, a simple expression is obtained for the gradient. The latter allows for an efficient implementation. Another advantage of geometric programming is that it can handle general weights. However, a drawback of the geometric programming approach is that it takes many lines of non-straightforward code to implement, which may hinder its use for non-experts.

3.2.4 Alternating projections without normal correction

Fourth, we consider the alternating projections algorithm of Grubišić (2002) and Morini & Webber (2004). The discussion below of alternating projections applies only to the problem of rank reduction of correlation matrices. The method is based on alternating projections onto the set of $n \times n$ matrices with unit diagonal and onto the set of $n \times n$ matrices of rank d or less. Both these projections can be efficiently calculated. For projection onto the intersection of two convex sets, Dykstra (1983) and Han (1988) have shown that convergence to a minimum can be obtained with alternating projections onto the individual convex sets if a normal vector correction is applied. Their results do not automatically hold for an alternating projections algorithm with normal correction for Problem (4.1)[3], since for $d < n$ the set of $n \times n$ matrices of rank d or less is non-convex. The alternating projections algorithm could in principle be extended to the case with rank restrictions, since we can efficiently calculate the projection onto the set of rank-d matrices. Convergence of the algorithm is however no longer guaranteed by the general results of Dykstra (1983) and Han (1988) because the constraint set $\{\text{rank}(\mathbf{C}) \leq d\}$ is no longer convex for $d < n$. Some preliminary experimentation showed indeed that the extension to the non-convex case did not work generally. Also, Morini & Webber (2004) report that alternating projections with normal correction may fail in solving Problem (4.1). Higham (2002, Section 5, 'Concluding remarks') mentions that he has been investigating alternative algorithms, such as to include rank constraints. The alternating projections algorithm without normal correction stated in Grubišić (2002) and Morini & Webber (2004) however always converges to a feasible point, but not necessarily to a stationary point. In fact, in general, the alternating projections method without normal correction does not converge to a stationary point. The algorithm thus does not minimize the

[3]The algorithm with normal correction for rank reduction has also been studied in Weigel (2004).

objective function in (4.1), it only selects a feasible point satisfying the constraints of (4.1).

3.2.5 Lagrange multipliers

As the fifth algorithm, we mention the Lagrange multiplier technique developed by Zhang & Wu (2003) and Wu (2003). This method lacks guaranteed convergence: Zhang & Wu (2003, Proposition 4.1) and Wu (2003, Theorem 3.4) prove the following result. The Lagrange multiplier algorithm produces a sequence of multipliers for which accumulation points exist. If, for the original matrix plus the Lagrange multipliers of an accumulation point, the d^{th} and $(d+1)^{\text{th}}$ eigenvalues have different absolute values, then the resulting rank-d approximation is a global minimizer of problem (3.4). However, the condition that the d^{th} and $(d+1)^{\text{th}}$ eigenvalues are different has not been guaranteed. In numerical experiments, this equal-eigenvalues phenomenon occurs. Therefore, convergence of the Lagrange multiplier method to a global minimum or even to a stationary point is not guaranteed. It is beyond the scope of this chapter to indicate how often this 'non-convergence' occurs. If the algorithm has not yet converged, then the produced low-rank correlation matrix will not satisfy the diagonal constraint. The appropriate adaptation is to re-scale the associated configuration similarly to the modified PCA approach (3.6). For certain numerical settings, the resulting algorithm has been shown to perform not better and even worse than the geometric programming approach (Grubišić & Pietersz 2005). Another drawback of the Lagrange multiplier algorithm is that only the weighted Frobenius norm can be handled and not general weights.

3.2.6 Parametrization

Sixth, we mention the 'parametrization method' of Rebonato (1999*a*, 1999*b*, 1999*c* (Section 10), 2002 (Section 9), 2004*b* (Sections 20.1–20.4)), Brigo (2002), Brigo & Mercurio (2001, Section 6.9) and Rapisarda, Brigo & Mercurio (2002). The set of correlation matrices of rank d or less $\{\mathbf{Y}\mathbf{Y}^T : \mathbf{Y} \in \mathbb{R}^{n\times d}, \mathbf{Diag}(\mathbf{Y}\mathbf{Y}^T) = \mathbf{I}\}$ is parameterized by trigonometric functions through spherical coordinates $\mathbf{y}_i = \mathbf{y}_i(\boldsymbol{\theta}_i)$ with $\boldsymbol{\theta}_i \in \mathbb{R}^{d-1}$. As a result, the objective value $\varphi(\mathbf{Y})$ becomes a function $\varphi(\mathbf{Y}(\boldsymbol{\Theta}))$ of the angle parameters $\boldsymbol{\Theta}$ that live in $\mathbb{R}^{n\times(d-1)}$. Subsequently, ordinary non-linear optimisation algorithms may be applied to minimize the objective value $\varphi(\mathbf{Y}(\boldsymbol{\Theta}))$ over the angle parameters $\boldsymbol{\Theta}$. In essence, this approach is the same as geometric optimisation, except for the key difference of optimising over $\boldsymbol{\Theta}$ versus over $\mathbf{Y}$. The major benefit of geometric optimisation over the parametrization method is as follows. We consider, for ease of exposition, the case of equal weights. The differential $\varphi_{\mathbf{Y}}$, in terms of $\mathbf{Y}$, is given simply as $2\boldsymbol{\Psi}\mathbf{Y}$, with $\boldsymbol{\Psi} = \mathbf{Y}\mathbf{Y}^T - \mathbf{P}$, see (4.24) below. We note that $\varphi_{\mathbf{Y}} = 2\boldsymbol{\Psi}\mathbf{Y}$ can thus be efficiently calculated. The dif-

ferential $\varphi_{\mathbf{\Theta}}$, in terms of $\mathbf{\Theta}$ however, is $2\mathbf{\Psi Y}$ multiplied by the differential of $\mathbf{Y}$ with respect to $\mathbf{\Theta}$, by the chain rule of differentiation. The latter differential is less efficient to calculate since it involves numerous sums of trigonometric functions. Grubišić & Pietersz (2005, Section 6) have shown empirically for a particular numerical setting with many randomly generated correlation matrices that the parametrization method is numerically less efficient than either the geometric programming approach or the Lagrange multiplier approach. The parametrization approach can handle general weights.

3.2.7 Alternating projections with normal correction ($d = n$)

The seventh important contribution is due to Higham (2002). The algorithm of Higham (2002) is the alternating projection algorithm with normal correction applied to the case $d = n$, i.e., to the problem of finding the nearest (possibly full-rank) correlation matrix. This method can *only* be used when there are *no rank restrictions* ($d := n$) and *only* with the *weighted Frobenius norm*. To understand the methodology, note that minimization Problem (3.4) with equal weights and $d := n$ can be written as $\min\{\|\mathbf{P} - \mathbf{C}\|_F^2;\ \mathbf{C} \succeq 0,\ \mathbf{Diag}(\mathbf{C}) = \mathbf{I}\}$. The two constraint sets $\{\mathbf{C} \succeq 0\}$ and $\{\mathbf{Diag}(\mathbf{C}) = \mathbf{I}\}$ are both convex. The convexity was cleverly exploited by Higham (2002), in which it was shown that the alternating projections algorithm of Dykstra (1983) and Han (1988) could be applied. The same technique has been applied in a different context in Chu, Funderlic & Plemmons (2003), Glunt, Hayden, Hong & Wells (1990), Hayden & Wells (1988) and Suffridge & Hayden (1993). Since the case $d < n$ is the primary interest of this chapter, the method of Higham (2002) will not be considered in the remainder.

3.3 Majorization

In this section, we briefly describe the idea of majorization and apply majorization to the objective function φ of Problem (3.4). The idea of majorization has been described, amongst others, in De Leeuw & Heiser (1977), Kiers & Groenen (1996) and Kiers (2002). We follow here the lines of Borg & Groenen (1997, Section 8.4). The key to majorization is to find a simpler function that has the same function value at a supporting point $\mathbf{x}$ and anywhere else is larger than or equal to the objective function to be minimized. Such a function is called a *majorization function*. By minimizing the majorization function – which is an easier task since this function is 'simpler' – we obtain the next point of the algorithm. This procedure guarantees that the function value never increases along points generated by the algorithm. Moreover, if the objective and majorization functions are once continuously differentiable (which turns out to hold in our case), then the properties above imply that the gradients should match at the supporting point $\mathbf{x}$. As a consequence, from any point where the gradient of the objective function is non-negligible, iterative

majorization will be able to find a next point with a *strictly* smaller objective function value. This generic fact for majorization algorithms has been pointed out in Heiser (1995).

We formalize the procedure somewhat more. Let $\varphi(\cdot)$ denote the function to be minimized. Let for each $\mathbf{x}$ in the domain of φ be given a majorization function $\chi(\cdot, \mathbf{x})$ such that

(i) $\varphi(\mathbf{x}) = \chi(\mathbf{x}, \mathbf{x})$,

(ii) $\varphi(\mathbf{y}) \leq \chi(\mathbf{y}, \mathbf{x})$ for all $\mathbf{y}$, and

(iii) the function $\chi(\cdot, \mathbf{x})$ is 'simple', that is, it is straightforward to calculate the minimum of $\chi(\cdot, \mathbf{x})$.

A majorization algorithm is then given by

(i) Start at $\mathbf{y}^{(0)}$. Set $k := 0$.

(ii) Set $\mathbf{y}^{(k+1)}$ equal to the minimum argument of the function $\chi\big(\cdot, \mathbf{y}^{(k)}\big)$.

(iii) If $\varphi\big(\mathbf{y}^{(k)}\big) - \varphi\big(\mathbf{y}^{(k+1)}\big) < \varepsilon$ then stop with $\mathbf{y} := \mathbf{y}^{(k+1)}$.

(iv) Set $k := k + 1$ and repeat from (ii).

Figure 3.1 illustrates the majorization algorithm.

Below we derive the majorizing function for $\varphi(\cdot)$ in (3.4). The first step is to majorize $\varphi(\mathbf{X})$ as a function of the i^{th} row only and then to repeat this for each row. To formalize the notion of '$\varphi(\mathbf{X})$ as a function of the i^{th} row only' we introduce the notation $\varphi_i(\mathbf{y}; \mathbf{Y})$ to denote the function

$$\varphi_i(\cdot, \mathbf{Y}) : \mathbf{y} \mapsto \varphi\big(\hat{\mathbf{Y}}_i(\mathbf{y})\big),$$

for (column)vectors $\mathbf{y} \in \mathbb{R}^d$ with $\hat{\mathbf{Y}}_i(\mathbf{y})$ denoting the matrix $\mathbf{Y}$ with the i^{th} row replaced by $\mathbf{y}^T$. We interpret $\mathbf{Y}$ as $[\mathbf{y}_1 \cdots \mathbf{y}_n]^T$. We find

$$\begin{aligned}
\varphi(\mathbf{Y}) &= \frac{1}{c} \sum_{j_1 < j_2} w_{j_1 j_2} \big(\rho_{j_1 j_2} - \langle \mathbf{y}_{j_1}, \mathbf{y}_{j_2} \rangle\big)^2 \\
&= \frac{1}{c} \sum_{j_1 < j_2} w_{j_1 j_2} \big(\rho_{j_1 j_2}^2 + (\mathbf{y}_{j_1}^T \mathbf{y}_{j_2})^2 - 2\rho_{j_1 j_2} \mathbf{y}_{j_1}^T \mathbf{y}_{j_2}\big) \\
&= (\text{const in } \mathbf{y}_i) + \frac{1}{c} \Bigg\{ \underbrace{\mathbf{y}_i^T \left[\sum_{j : j \neq i} w_{ij} \mathbf{y}_j \mathbf{y}_j^T \right] \mathbf{y}_i}_{(I)} - \underbrace{2 \mathbf{y}_i^T \left[\sum_{j : j \neq i} w_{ij} \rho_{ij} \mathbf{y}_j \right]}_{(II)} \Bigg\}. \qquad (3.8)
\end{aligned}$$

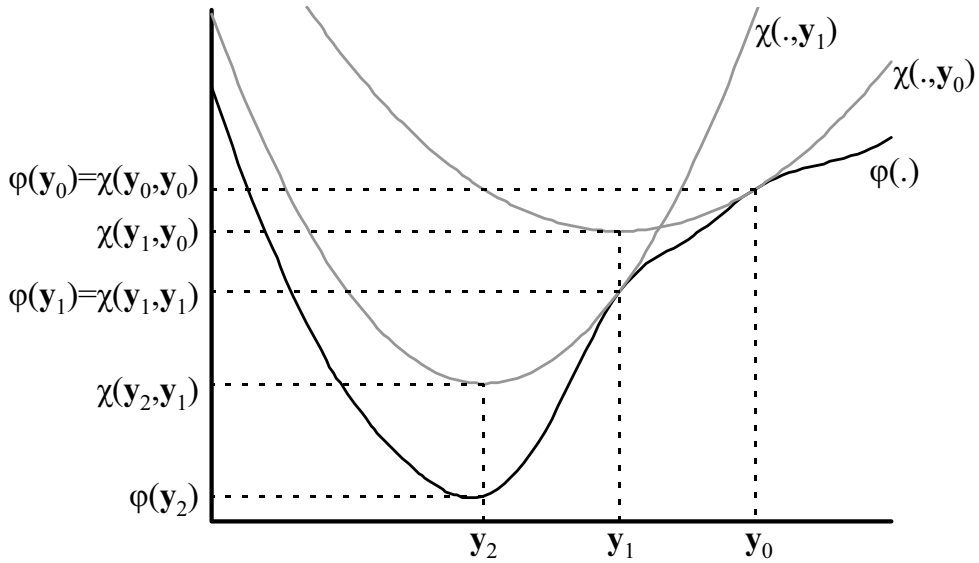

Figure 3.1: The idea of majorization. (Figure adopted from Borg & Groenen (1997, Figure 8.4).) The algorithm sets out at $\mathbf{y}_0$. The majorization function $\chi(\cdot, \mathbf{y}_0)$ is fitted by matching the value and first derivative of $\varphi(\cdot)$ at $\mathbf{y}_0$. Subsequently the function $\chi(\cdot, \mathbf{y}_0)$ is minimized to find the next point $\mathbf{y}_1$. This procedure is repeated to find the point $\mathbf{y}_2$ etc.

Part (I) is quadratic in $\mathbf{y}_i$ whereas part (II) is linear in $\mathbf{y}_i$; the remaining term is constant in $\mathbf{y}_i$. We only have to majorize part (I), as follows. Define

$$\mathbf{B}_i(\mathbf{Y}) := \sum_{j:j\neq i} w_{ij}\ \mathbf{y}_j\ \mathbf{y}_j^T. \tag{3.9}$$

For notational convenience, we shall denote $\mathbf{B}_i(\mathbf{Y})$ by $\mathbf{B}$, the running $\mathbf{y}_i$ by $\mathbf{y}$, and the current $\mathbf{y}_i$, that is, the current i^{th} row vector of $\mathbf{Y}$, is denoted by $\mathbf{x}$. Let λ denote the largest eigenvalue of $\mathbf{B}$. Then, the matrix $\mathbf{B} - \lambda\mathbf{I}$ is negative semidefinite, so that the following inequality holds:

$$(\mathbf{y}-\mathbf{x})^T(\mathbf{B}-\lambda\mathbf{I})(\mathbf{y}-\mathbf{x}) \leq 0,\ \ \forall \mathbf{y},$$

which gives after some manipulations

$$\mathbf{y}^T\mathbf{B}\mathbf{y} \leq 2\lambda - 2\mathbf{y}^T(\lambda\mathbf{x}-\mathbf{B}\mathbf{x}) - \mathbf{x}^T\mathbf{B}\mathbf{x},\ \ \forall \mathbf{y}, \tag{3.10}$$

using the fact that $\mathbf{y}^T\mathbf{y} = \mathbf{x}^T\mathbf{x} = 1$.

Combining (3.8) and (3.10) we obtain the majorizing function of $\varphi_i(\mathbf{y};\mathbf{Y})$, that is,

$$\varphi_i(\mathbf{y};\mathbf{Y}) \leq -\frac{2}{c}\mathbf{y}^T\left(\lambda\mathbf{x}-\mathbf{B}\mathbf{x}+\sum_{j:i\neq j} w_{ij}\rho_{ij}\mathbf{y}_j\right) + (\text{const in } \mathbf{y}) = \chi_i(\mathbf{y};\mathbf{Y}),\ \ \forall \mathbf{y}.$$

The advantage of $\chi_i(\cdot;\mathbf{Y})$ over $\varphi_i(\cdot,\mathbf{Y})$ is that it is linear in $\mathbf{y}$ and that the minimization problem

$$\min\left\{\ \chi_i(\mathbf{y};\mathbf{Y})\ ;\ \|\mathbf{y}\|_2 = 1\ \right\} \tag{3.11}$$

is readily solved by

$$\mathbf{y}^* := \mathbf{z}/\|\mathbf{z}\|_2,\ \ \mathbf{z} := \lambda\mathbf{x}-\mathbf{B}\mathbf{x}+\sum_{j:j\neq i} w_{ij}\rho_{ij}\mathbf{y}_j.$$

If $\mathbf{z} = \mathbf{0}$ then this implies that the gradient is zero, from which it would follow that the current point $\mathbf{x}$ is already a stationary point.

3.4 The algorithm and convergence analysis

Majorization algorithms are known to converge to a point with negligible gradient. This property holds also for the current situation, as will be shown hereafter. As the convergence criterion is defined in terms of the gradient $\mathbf{Grad}\varphi$, an expression for $\mathbf{Grad}\varphi$ is needed. We restrict to the case of all w_{ij} equal. As shown in Grubišić & Pietersz (2005) (see also Section 4.5.3), the gradient is then given by

$$\mathbf{Grad}\varphi = 4c^{-1}\mathbf{\Psi}\mathbf{Y},\ \ \mathbf{\Psi} := \mathbf{Y}\mathbf{Y}^T - \mathbf{P}. \tag{3.12}$$

Algorithm 1 The majorization algorithm for finding a low-rank correlation matrix locally nearest to a given matrix. Here $\mathbf{P}$ denotes the input matrix, $\mathbf{W}$ denotes the weight matrix, n denotes its dimension, d denotes the desired rank, $\varepsilon_{\|\mathbf{Grad}\varphi\|}$ is the convergence criterion for the norm of the gradient and ε_φ is the convergence criterion on the improvement in the function value.

Input: $\mathbf{P}$, $\mathbf{W}$, n, d, $\varepsilon_{\|\mathbf{Grad}\varphi\|}$, ε_φ.

1: Find starting point $\mathbf{Y}$ by means of the modified PCA method (3.6)–(3.7).
2: **for** $k = 0, 1, 2, ...$ **do**
3: **stop** if the norm of the gradient of φ at $\mathbf{X}^{(k)} := \mathbf{X}$ is less than $\varepsilon_{\|\mathbf{Grad}\varphi\|}$ **and** the improvement in the function value $\varphi_{k-1}/\varphi_k - 1$ is less than ε_φ.
4: **for** $i = 1, 2, ..., n$ **do**
5: Set $\mathbf{B} := \sum_{j \neq i} w_{ij} \mathbf{y}_j \mathbf{y}_j^T$.
6: Calculate λ to be the largest eigenvalue of the $d \times d$ matrix $\mathbf{B}$.
7: Set $\mathbf{z} := \lambda \mathbf{y}_i - \mathbf{B}\mathbf{y}_i + \sum_{j \neq i} w_{ij} \rho_{ij} \mathbf{y}_j$.
8: If $\mathbf{z} \neq \mathbf{0}$, then set the i^{th} row $\mathbf{y}_i$ of $\mathbf{Y}$ equal to $\mathbf{z}/\|\mathbf{z}\|_2$.
9: **end for**
10: **end for**

Output: the $n \times n$ matrix $\mathbf{Y}\mathbf{Y}^T$ is the rank-d approximation of $\mathbf{P}$ satisfying the convergence constraints.

An expression for the gradient for the objective function with general weights can be found by straightforward differentiation. The majorization algorithm has been displayed in Algorithm 1.

The row-wise approach of Algorithm 1 makes it dependent of the order of looping through the rows. This order effect will be addressed in Section 3.5.3. In Sections 3.5.4 and 3.5.5 we study different ways of implementing the calculation of the largest eigenvalue of $\mathbf{B}$ in line 6 of Algorithm 1. In particular, we study the use of the power method.

In the remainder of this section the convergence of Algorithm 1 is studied. First, we establish global convergence of the algorithm. Second, we investigate the local rate of convergence.

3.4.1 Global convergence

Zangwill (1969) developed generic sufficient conditions that guarantee convergence of an iterative algorithm. The result is repeated here in a form adapted to the case of majorization. Let M be a compact set. Assume the specification of a subset $S \subset M$ called the *solution set*. A point $\mathbf{Y} \in S$ is deemed a *solution*. An *(autonomous) iterative algorithm* is a map $A : M \to M \cup \{\text{stop}\}$ such that $A^{-1}(\{\text{stop}\}) = S$. The proof of the following theorem is adapted from the proof of Theorem 1 in Zangwill (1969).

Theorem 1 (Global convergence) *Consider finding a local minimum of the objective function $\varphi(\mathbf{Y})$ by use of Algorithm 1. Suppose given a fixed tolerance level ε on the gradient of φ. A point $\mathbf{Y}$ is called a solution if $\|\mathbf{Grad}\varphi(\mathbf{Y})\| < \varepsilon$. Then from any starting point $\mathbf{Y}^{(0)}$, the algorithm either stops at a solution or produces an infinite sequence of points none of which are solutions, for which the limit of any convergent subsequence is a solution point.*

PROOF: Without loss of generality we may assume that the procedure generates an infinite sequence of points $\{\mathbf{Y}^{(k)}\}$ none of which are solutions. It remains to be proven that the limit of any convergent subsequence must be a solution.

First, note that the algorithm $A(\cdot)$ is continuous in $\mathbf{Y}$. Second, note that if $\mathbf{Y}^{(k)}$ is not a solution then

$$\varphi\big(\mathbf{Y}^{(k+1)}\big) = \varphi\Big(A\big(\mathbf{Y}^{(k)}\big)\Big) < \varphi\big(\mathbf{Y}^{(k)}\big).$$

Namely if $\mathbf{Y}^{(k)}$ is not a solution then its gradient is non-negligible. Since the objective and all majorization functions are differentiable, we necessarily have that the gradients agree at $\mathbf{Y}^{(k)}$. Therefore, when minimizing the majorization functions $\chi_i(\cdot, \mathbf{Y})$ there will be at least one i for which we find a strictly smaller objective value. Thus $\mathbf{Y}^{(k+1)} := A(\mathbf{Y}^{(k)})$ has a strictly smaller objective function value than $\mathbf{Y}^{(k)}$. Third, note that the sequence $\{\varphi(\mathbf{Y}^{(k)})\}_{k=0}^{\infty}$ has a limit since it is monotonically decreasing and bounded from below by 0.

Let $\{\mathbf{Y}^{(k_j)}\}_{j=1}^{\infty}$ be any subsequence that converges to $\mathbf{Y}^*$, say. It must be shown that $\mathbf{Y}^*$ is a solution. Assume the contrary. By continuity of the iterative procedure, $A(\mathbf{Y}^{(k_j)}) \to A(\mathbf{Y}^*)$. By the continuity of $\varphi(\cdot)$, we then have

$$\varphi\Big(A\big(\mathbf{Y}^{(k_j)}\big)\Big) \downarrow \varphi\Big(A\big(\mathbf{Y}^*\big)\Big) < \varphi(\mathbf{Y}^*),$$

which is in contradiction with $\varphi(A(\mathbf{Y}^{(k_j)})) \to \varphi(\mathbf{Y}^*)$. □

The algorithm thus converges to a point with vanishing first derivative. We expect such a point to be a local minimum, but, in principle, it may also be a stationary point. In practice, however, we almost always obtain a local minimum, except for very rare degenerate cases. Moreover, global convergence to a point with zero first derivative is the best one may expect from generic optimization algorithms. For example, the globally convergent version of the Newton-Rhapson algorithm may converge to a stationary point, too: Applied to the function $\varphi(x, y) = x^2 - y^2$, it will converge to the stationary point $(0, 0)$ starting from any point on the line $\{y = 0\}$.

3.4.2 Local rate of convergence

The local rate of convergence determines the speed at which an algorithm converges to a solution point in a neighbourhood thereof. Let $\{\mathbf{Y}^{(k)}\}$ be a sequence of points produced

by an algorithm converging to a solution point $\mathbf{Y}^{(\infty)}$. Suppose, for k large enough,

$$\left\|\mathbf{Y}^{(k+1)} - \mathbf{Y}^{(\infty)}\right\| \leq \alpha \left\|\mathbf{Y}^{(k)} - \mathbf{Y}^{(\infty)}\right\|^{\zeta}. \tag{3.13}$$

If $\zeta = 1$ and $\alpha < 1$ or if $\zeta = 2$ the local convergence is called *linear* or *quadratic*, respectively. If the convergence estimate is worse than linear, the convergence is deemed *sub-linear*. For linear convergence, α is called the linear rate of convergence.

When considering several algorithms and indefinite iteration, eventually the algorithm with best rate of convergence will provide the best result. Among the algorithms available in the literature, both the geometric programming and parametrization approach can have a quadratic rate of convergence given that a Newton-Rhapson type algorithm is applied. As the proposition below will show, Algorithm 1 has a sub-linear local rate of convergence, that is, worse than a linear rate of convergence. Thus the majorization algorithm makes no contribution to existing literature for the case of indefinite iteration. However, we did not introduce the majorization algorithm for the purpose of indefinite iteration, but rather for calculating a reasonable answer in limited time, as is the case in practical applications of financial institutions. Given a fixed amount of time, the performance of an algorithm is a trade-off between rate of convergence and computational cost per iterate. Such performance can almost invariably only be measured by empirical investigation, and the results of the next section on numerical experiments indeed show that majorization is the best performing algorithm in a number of financial settings. The strength of majorization lies in the low costs of calculating the next iterate.

The next proposition establishes the local sub-linear rate of convergence.

Proposition 1 (Local rate of convergence) *Algorithm 1 has locally a sub-linear rate of convergence. More specifically, let* $\{\mathbf{Y}^{(k)}\}$ *denote the sequence of points generated by Algorithm 1 converging to the point* $\mathbf{Y}^{(\infty)}$. *Define* $\delta^{(k,i)} = \|\mathbf{y}_i^{(k)} - \mathbf{y}_i^{(\infty)}\|$. *Then*

$$\delta^{(k+1,i)} = \delta^{(k,i)} + \mathcal{O}\Big(\left(\delta^{(k,i)}\right)^2 \Big). \tag{3.14}$$

PROOF: The proof of Equation (3.14) may be found in Appendix 3.A. Equation (3.14) can be written as $\delta^{(k+1,i)} = \alpha(\delta^{(k,i)})\delta^{(k,i)}$ with $\alpha(\delta^{(k,i)}) \to 1$ as $k \to \infty$. It follows that the convergence-type defining Equation (3.13) holds, for Algorithm 1, with $\zeta = 1$, but for $\alpha = 1$ and not for any $\alpha < 1$. We may conclude that the local convergence is worse than linear, thus sub-linear. □

3.5 Numerical results

In this section, we study and assess the performance of the majorization algorithm in practice. First, we numerically compare majorization with other methods in the literature. Second, we present an example with non-constant weights. Third, we explain and

investigate the order effect. Fourth and fifth, we consider and study alternative versions of the majorization algorithm.

Algorithm 1 has been implemented in a MATLAB package called `major`. It can be downloaded from `www.few.eur.nl/few/people/pietersz`. The package consists of the following files: `clamp.m`, `dF.m`, `F.m`, `grad.m`, `guess.m`, `major.m`, `P_tangent.m` and `svdplus.m`. The package can be run by calling `[Yn,fn]=major(P,d,ftol,gradtol)`. Here `P` denotes the input correlation matrix, `d` the desired rank, `Yn` the final configuration matrix, `fn` denotes the final objective function value, `ftol` the convergence tolerance on the improvement of φ, and `gradtol` the convergence tolerance on the norm of the gradient. The aforementioned web-page also contains a package `majorw` that implements non-constant weights for the objective function φ.

3.5.1 Numerical comparison with other methods

The numerical performance of the majorization algorithm was compared to the performance of the Lagrange multiplier method, geometric programming[4] and the parametrization method. Additionally, we considered the function `fmincon` available in the MATLAB optimization toolbox. MATLAB refers to this function as a 'medium-scale constrained nonlinear program'.

We have chosen to benchmark the algorithms by their practical importance, that is the performance under a fixed small amount of computational time. In financial applications, rank reduction algorithms are usually run for a very short time, typically 0.05 to 2 seconds, depending on the size of the correlation matrix. We investigate which method produces, in this limited amount of time, the best fit to the original matrix.

The five algorithms were tested on random 'interest rate' correlation matrices that are generated as follows. A parametric form for correlation matrices is posed in De Jong, Driessen & Pelsser (2004, Equation (8)). We repeat here the parametric form for completeness, that is,

$$\rho_{ij} = \exp\left\{ -\gamma_1|t_i - t_j| - \frac{\gamma_2|t_i - t_j|}{\max(t_i, t_j)^{\gamma_3}} - \gamma_4\left|\sqrt{t_i} - \sqrt{t_j}\right| \right\}, \tag{3.15}$$

with $\gamma_1, \gamma_2, \gamma_4 > 0$ and with t_i denoting the expiry time of rate i. (Our particular choice is $t_i = i$, $i = 1, 2, \dots$) This model was then subsequently estimated with USD historical interest rate data. In Table 3 of De Jong et al. (2004), the estimated γ parameters are listed, along with their standard errors. An excerpt of this table is displayed in Table 3.1. The random financial matrix that we used is obtained by randomizing the γ-parameters

[4]For geometric programming we used the MATLAB package LRCM MIN downloadable from `www.few.eur.nl/few/people/pietersz`. The Riemannian Newton-algorithm was applied.

Table 3.1: Excerpt of Table 3 in De Jong et al. (2004).

	γ_1	γ_2	γ_3	γ_4
estimate	0.000	0.480	1.511	0.186
standard error	-	0.099	0.289	0.127

in (3.15). We assumed the γ-parameters distributed normally with mean and standard errors given by Table 3.1, with $\gamma_1, \gamma_2, \gamma_4$ capped at zero.

Hundred matrices were randomly generated, with n, d, and the computational time t varied as $(n = 10, d = 2, t = 0.05s)$, $(n = 20, d = 4, t = 0.1s)$ and $(n = 80, d = 20, t = 2s)$. Subsequently the five algorithms were applied each with t seconds of computational time and the computational time constraint was the only stopping criterion. The results are presented in the form of performance profiles, as described in Dolan & Moré (2002). The reader is referred there for the merits of using performance profiles. These profiles are an elegant way of presenting performance data across several algorithms, allowing for insight into the results. We briefly describe the workings here. We have 100 test correlation matrices $p = 1, \ldots, 100$ and 5 algorithms $s = 1, \ldots, 5$. The outcome of algorithm s on problem p is denoted by $\mathbf{Y}^{(p,s)}$. The *performance measure* of algorithm s is defined to be $\varphi(\mathbf{Y}^{(p,s)})$. The *performance ratio* $\varrho^{(p,s)}$ is

$$\varrho^{(p,s)} = \frac{\varphi(\mathbf{Y}^{(p,s)})}{\min_s \left\{ \varphi(\mathbf{Y}^{(p,s)}) \right\}}.$$

The cumulative distribution function $\phi^{(s)}$ of the ('random') performance ratio $p \mapsto \rho^{(p,s)}$ is then called the *performance profile*,

$$\phi^{(s)}(\tau) = \frac{1}{100} \# \left\{ \varrho^{(p,s)} \leq \tau;\ p = 1, \ldots, 100 \right\}.$$

A rule of thumb is, that the higher the profile of an algorithm, the better its performance. The quantity $\phi^{(s)}(\tau)$ for $\tau > 1$ is the empirical probability that the achieved performance measure of an algorithm s is less than τ times the performance measure of the algorithm with the smallest (i.e., best) performance measure. The profiles are displayed in Figures 3.2, 3.3 and 3.4. From the performance profiles we may deduce that majorization is the best overall performing algorithm in the numerical cases studied.

The tests were also run with a strict convergence criterion on the norm of the gradient. Because the Lagrange multiplier algorithm has not been guaranteed to converge to a local minimum, we deem an algorithm not to have converged after 30 seconds of CPU time. The majorization algorithm still performs very well, but geometric programming and the

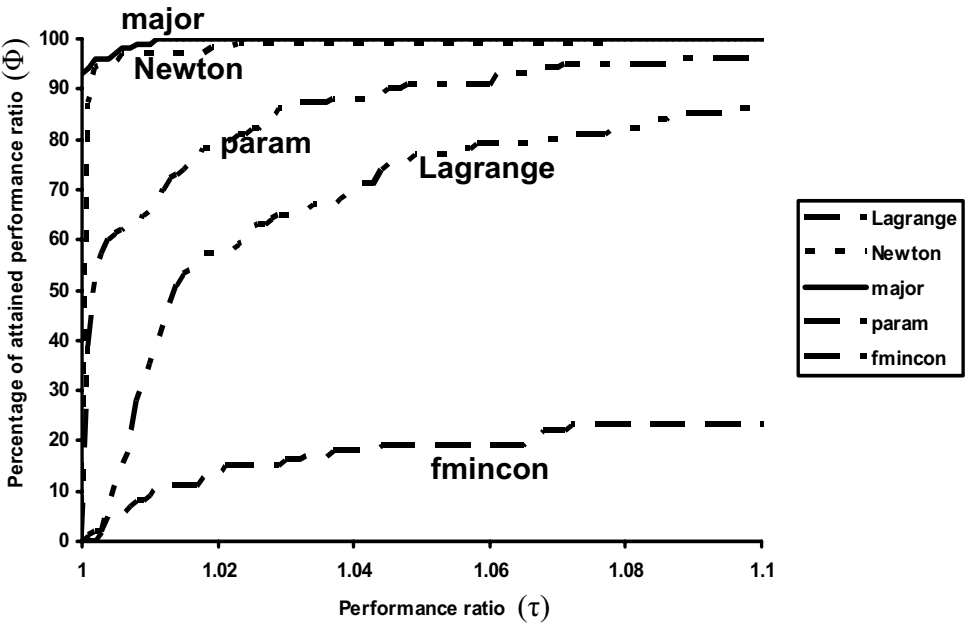

Figure 3.2: Performance profile for $n = 10$, $d = 2$, $t = 0.05s$.

Lagrange multiplier method perform slightly better when running up to convergence. This can be expected from the sub-linear rate of convergence of majorization versus the quadratic rate of convergence of the geometric programming approach. The results have not been displayed since these are not relevant in a finance setting. In financial practice, no additional computational time will be invested to obtain convergence up to machine precision. Having found that majorization is the most efficient algorithm in a finance setting for the numerical cases considered, with the tests of running to convergence we do warn the reader for using Algorithm 1 in applications outside of finance where convergence to machine precision *is* required. For such non-finance applications, we would suggest a mixed approach: use majorization in an initial stage and finish with geometric programming. It is the low cost per iterate that makes majorization so attractive in a finance setting.

To assess the quality of the solutions found in Figures 3.2–3.4, we checked whether the matrices produced by the algorithms were converging to a global minimum. Here, we have the special case (only for equal weights) that we can check for a global minimum,

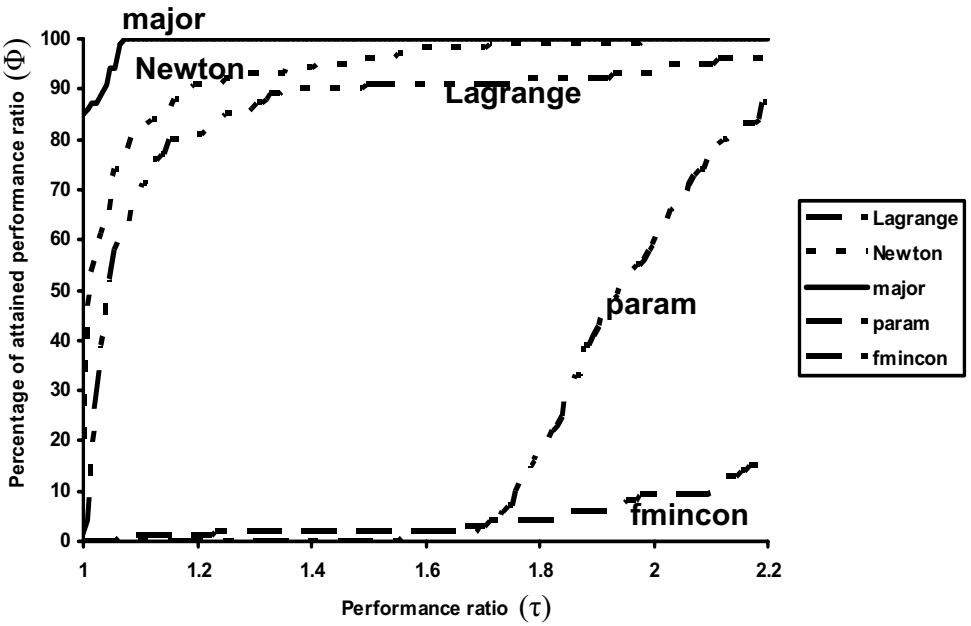

Figure 3.3: Performance profile for $n = 20$, $d = 4$, $t = 0.1s$.

although in other minimization problems it may be difficult to assess whether a minimum is global or not. For clarity, we point out that the majorization algorithm does not have guaranteed convergence to the *global* minimum, nor do any of the other algorithms described in Section 3.2. We only have guaranteed convergence to a point with vanishing first derivative, and in such a point we can *verify* whether that point is a global minimum. If a produced solution satisfied a strict convergence criterion on the norm of the gradient, then it was checked whether such stationary point is a global minimum by inspecting the Lagrange multipliers, see Zhang & Wu (2003), Wu (2003) and Grubišić & Pietersz (2005, Lemma 6.1). The reader is referred to Lemma 1 in Section 4.5.4 for details.

The percentage of matrices that were deemed global minima was between 95% and 100% for both geometric programming and majorization, respectively, for the cases $n = 20$, $d = 4$ and $n = 10$, $d = 2$. The Lagrange multiplier and parametrization methods did not produce any stationary points within 20 seconds of computational time. The percentage of global minima is high since the eigenvalues of financial correlation matrices are rapidly decreasing. In effect, there are large differences between the first 4 or 5

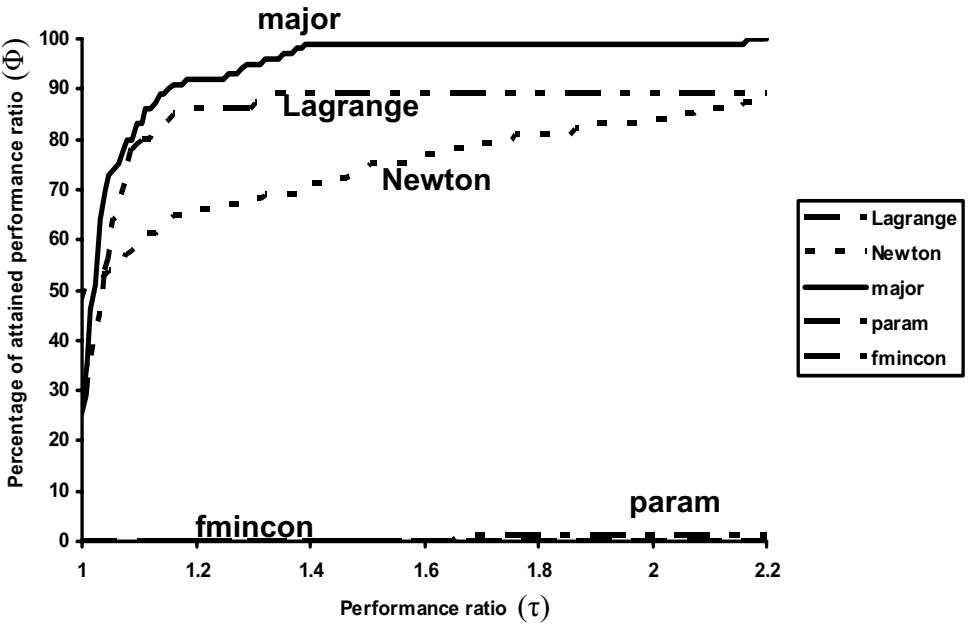

Figure 3.4: Performance profile for $n = 80$, $d = 20$, $t = 2s$.

consecutive eigenvalues. For the case $n = 80$, $d = 20$ it was more difficult to check the global minimum criterion since subsequent eigenvalues are smaller and closer to each other. In contrast, if we apply the methods for all cases to random correlation matrices of Davies & Higham (2000), for which the eigenvalues are all very similar, we find that a much lower percentage of produced stationary points were global minima.

3.5.2 Non-constant weights

We considered the example with non-constant weights described in Rebonato (2002, Section 9.3), in which a functional form for the correlation matrix is specified, that is,

$$\rho_{ij} = \text{LongCorr} + (1 - \text{LongCorr}) \exp\big\{ -\beta|t_i - t_j| \big\}, \quad i, j = 1, \ldots, n.$$

The parameters are set to $n = 10$, LongCorr $= 0.6$, $\beta = 0.1$, $t_i = i$. Subsequently Rebonato presents the rank 2, 3, and 4 matrices found by the parametrization method for the case of equal weights. The majorization algorithm was also applied and its convergence criterion was set to machine precision for the norm of the gradient. Comparative results

Table 3.2: Comparative results of the parametrization and majorization algorithms for the example described in Rebonato (2002, Section 9.3.1).

d	$\|\mathbf{Grad}\varphi\|_F$ major.	φ major.	φ Rebonato	I	II	CPU major.
2	2×10^{-17}	5.131×10^{-04}	5.137×10^{-04}	41×10^{-04}	0.02×10^{-04}	0.4s
3	2×10^{-17}	1.26307×10^{-04}	1.26311×10^{-04}	15×10^{-04}	0.01×10^{-04}	1.0s
4	2×10^{-17}	4.85×10^{-05}	4.86×10^{-05}	70×10^{-04}	0.01×10^{-04}	2.1s

for the parametrization and majorization algorithms are displayed in Table 3.2. Columns I and II denote $\|\mathbf{P}_{\text{Reb}}^{\text{Approx}} - \mathbf{P}_{\text{major}}^{\text{Approx}}\|_F$ and $\|\mathbf{P}_{\text{major, rounded}}^{\text{Approx}} - \mathbf{P}_{\text{major}}^{\text{Approx}}\|_F$, respectively. Here 'Approx' stands for the rank-reduced matrix produced by the algorithm and 'rounded' stands for rounding the matrix after 6 digits, as is the precision displayed in Rebonato (2002). Columns I and II show that the matrices displayed in Rebonato (2002) are not yet fully converged up to machine precision, since the round-off error from displaying only 6 digits is much smaller than the error in obtaining full convergence to the stationary point.

Rebonato proceeds by minimizing φ for rank 3 with two different weights matrices. These weights matrices are chosen by financial arguments specific to a ratchet cap and a trigger swap, which are interest rate derivatives. The weights matrix $\mathbf{W}^{(R)}$ for the ratchet cap is a tridiagonal matrix

$$w_{ij}^{(R)} = 1 \text{ if } j = i-1, i, i+1, \quad w_{ij}^{(R)} = 0, \text{ otherwise}$$

and the weights matrix $\mathbf{W}^{(T)}$ for the trigger swap has ones on the first two rows and columns

$$w_{ij}^{(T)} = 1 \text{ if } i = 1, 2 \text{ or } j = 1, 2, \quad w_{ij}^{(T)} = 0, \text{ otherwise.}$$

Rebonato subsequently presents solution matrices found by the parametrization method. These solutions exhibit a highly accurate yet non-perfect fit to the relevant portions of the correlation matrices. In contrast, majorization finds exact fits. The results are displayed in Table 3.3.

3.5.3 The order effect

The majorization algorithm is based on sequentially looping over the rows of the matrix $\mathbf{Y}$. In Algorithm 1, the row index runs from 1 to n. There is however no distinct reason to start with row 1, then 2, etc. It would be equally reasonable to consider any permutation

Table 3.3: Results for the ratchet cap and trigger swap. Here 'tar.' denotes the target value, 'maj.' and 'Reb.' denote the resulting value obtained by the majorization algorithm and Rebonato (2002, Section 9.3), respectively.

Ratchet cap									
First principal sub-diagonal									
CPU time `major`: 2.8s; obtained $\varphi < 2 \times 10^{-30}$									
tar.	.961935	.961935	.961935	.961935	.961935	.961935	.961935	.961935	.961935
maj.	.961935	.961935	.961935	.961935	.961935	.961935	.961935	.961935	.961935
Reb.	.961928	.961880	.961977	.962015	.962044	.962098	.961961	.961867	.962074
Trigger swap									
First two rows (or equivalently first two columns)									
CPU time `major`: 2.4s; obtained $\varphi < 2 \times 10^{-30}$									
Row 1 (without the unit entry (1,1))									
tar.	.961935	.927492	.896327	.868128	.842612	.819525	.798634	.779732	.762628
maj.	.961935	.927492	.896327	.868128	.842612	.819525	.798634	.779732	.762628
Reb.	.961944	.927513	.896355	.868097	.842637	.819532	.798549	.779730	.762638
Row 2 (without the unit entry (2,2))									
tar.	.961935	.961935	.927492	.896327	.868128	.842612	.819525	.798634	.779732
maj.	.961935	.961935	.927492	.896327	.868128	.842612	.819525	.798634	.779732
Reb.	.961944	.962004	.927565	.896285	.868147	.842650	.819534	.798669	.779705

p of the numbers $\{1,\ldots,n\}$ and then let the row index run as $p(1),p(2),\ldots,p(n)$. A priori, there is nothing to guarantee or prevent that the resulting solution point produced with permutation p would differ from or be equal to the solution point produced by the default loop $1,\ldots,n$. This dependency of the order is termed 'the order effect'. The order effect is a bad feature of Algorithm 1 in general. We show empirically that the solutions produced by the algorithm can differ when using a different permutation. However, we show that this is unlikely to happen for financial correlation matrices. The order effect can have two consequences. First, the produced solution correlation matrix can differ – this generally implies a different objective function value as well. Second, even when the produced solution correlation matrix is equal, the configuration $\mathbf{Y}$ can differ – in this case we have equal objective function values. To see this, consider a $n \times d$ configuration matrix $\mathbf{Y}$ and assume given any orthogonal $d \times d$ matrix $\mathbf{Q}$, that is, $\mathbf{Q}\mathbf{Q}^T = \mathbf{I}$. Then the configuration matrices $\mathbf{Y}$ and $\mathbf{YQ}$ are associated with the same correlation matrices[5]: $\mathbf{YQQ}^T\mathbf{Y} = \mathbf{YY}^T$.

We investigated the order effect for Algorithm 1 numerically, as follows. We generated either a random matrix by (3.15), see Section 3.5.1, or a random correlation matrix in MATLAB by

```
rand('state',0);randn('state',0);n=30;R=gallery('randcorr',n);
```

The random correlation matrix generator `gallery('randcorr',n)` has been described in Davies & Higham (2000). Subsequently we generated 100 random permutations with `p=randperm(n);`. For each of the permutations, Algorithm 1 was applied with $d = 2$ and a high accuracy was demanded: $\varepsilon_{\|\mathbf{Grad}\varphi\|} = \varepsilon_\varphi = 10^{-16}$. The results for the two different correlation matrices are as follows.

(*Random interest rate correlation matrix as in (3.15).*) Only one type of produced solution correlation matrix could be distinguished, which turned out to be a global minimum by inspection of the Lagrange multipliers. We also investigated the orthogonal transformation effect. For $\mathbb{R}^2$, an orthogonal transformation can be characterized by the rotation of the two basis vectors and then by -1 or +1 denoting whether the second basis vector is reflected in the origin or not. All produced matrices $\mathbf{Y}$ were differently rotated, but no reflection occurred. The maximum rotation was equal to 0.8 degrees and the standard deviation of the rotation was 0.2 degrees.

(*Davies & Higham (2000) random correlation matrix.*) Essentially four types of produced solution correlation matrices could be distinguished, which we shall name I, II, III, and IV. The associated objective function values and the frequency at which the types occurred are displayed in Table 3.4. We inspected the Lagrange multipliers to find that

[5]The indeterminacy of the result produced by the algorithm can easily be resolved by either considering only $\mathbf{YY}^T$ or by rotation of $\mathbf{Y}$ into its principal axes. For the latter, let $\mathbf{Y}^T\mathbf{Y} = \mathbf{Q\Lambda Q}^T$ be an eigenvalue decomposition. Then the principal axes representation is given by $\mathbf{YQ}$.

Table 3.4: The order effect. Here $n = 30$, $d = 2$ and 100 random permutations were applied. Four types of produced correlation matrices could be distinguished. The table displays the associated φ and frequency.

type	I	II	III	IV
φ	0.110423	0.110465	0.110630	0.110730
frequency	2%	88%	7%	3%

none of the four types was a global minimum. For type II, the most frequently produced low-rank correlation matrix, we also investigated the orthogonal transformation effect. Out of the 88 produced matrices $\mathbf{Y}$ that could be identified with type II, all were differently rotated, but no reflection occurred. The maximum rotation was equal to 38 degrees and the standard deviation of the rotation was 7 degrees.

From the results above, we conclude that the order effect is not much of an issue for the case of interest rate correlation matrices, at least not for the numerical setting that we investigated.

3.5.4 Majorization equipped with the power method

Line 6 in Algorithm 1 uses the largest eigenvalue of a matrix, which can be implemented in several different ways. For example, our implementation in the MATLAB function `major` implements `lambda=max(eig(B))`, which uses available MATLAB built-in functions. This choice of implementation unnecessarily calculates all eigenvalues whereas only the largest is required. Instead, the algorithm can be accelerated by calculating only the largest eigenvalue, for example with the power method, see Golub & van Loan (1996). We numerically tested the use of the power method versus `lambda=max(eig(B))`, as follows. In Figure 3.5, we display the natural logarithm of the relative residual versus the computational time for the random Davies & Higham (2000) matrix `R` included in the `major` package, for both the power method and `lambda=max(eig(B))`. As can be seen from the figure, the power method causes a significant gain of computational efficiency. The power method is available as `majorpower` at `www.few.eur.nl/few/people/pietersz`.

3.5.5 Using an estimate for the largest eigenvalue

In Algorithm 1, the largest eigenvalue of $\mathbf{B}$ is calculated by an eigenvalue decomposition or by the power method. Such methods may be relatively expensive to apply. Instead of a full calculation, we could consider finding an easy-to-calculate upper bound on the

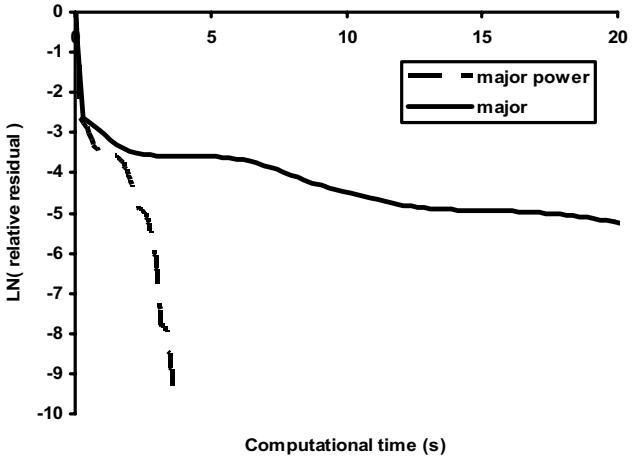

Figure 3.5: Convergence run for the use of the power method versus `lambda=max(eig(B))`. The relative residual is $\|\mathbf{Grad}\varphi(\mathbf{Y}^{(i)})\|_F / \|\mathbf{Grad}\varphi(\mathbf{Y}^{(0)})\|_F$. Here $n = 80$ and $d = 3$.

largest eigenvalue of $\mathbf{B}$. Such upper bound is readily determined as $n-1$ due to the unit length restrictions on the $n-1$ vectors $\mathbf{y}_i$. Replacing λ and its calculation by $n-1$ in Algorithm 1 will result in a reduction of computational time by not having to calculate the eigenvalue decomposition. A disadvantage is however that the resulting fitted majorizing function might be much steeper causing its minimum to be much closer to the point of outset. In other words, the steps taken by the majorization algorithm will be smaller. Whether to use $n-1$ instead of λ is thus a trade-off between computational time for the decomposition and the step-size.

We tested replacing λ by $n-1$ for 100 correlation matrices of dimension 80×80. These matrices were randomly generated with the procedure of Davies & Higham (2000). We allowed both versions of the algorithm a computational time of less than 1 second. We investigated $d = 3$, $d = 6$, $d = 40$ and $d = 70$. For all 400 cases, without a single exception, the version of the algorithm with the full calculation of λ produced a matrix that had a lower value φ than the version with $n-1$. This result suggests that a complete calculation of the largest eigenvalue is most efficient. However, these results could be particular to our numerical setting. The '$n-1$' version of the algorithm remains an interesting alternative and could potentially be beneficial in certain experimental setups.

3.6 Conclusions

We have developed a novel algorithm for finding a low-rank correlation matrix locally nearest to a given matrix. The algorithm is based on iterative majorization and this chapter is the first to apply majorization to the area of derivatives pricing. We showed theoretically that the algorithm converges to a stationary point from any starting point. As an addition to the previously available methods in the literature, majorization was in our simulation setup more efficient than either geometric programming, the Lagrange multiplier technique or the parametrization method. Furthermore, majorization is easier to implement than any method other than modified PCA. The majorization method efficiently and straightforwardly allows for arbitrary weights.

3.A Appendix: Proof of Equation (3.13)

Define the Algorithm 1 mapping $\mathbf{y}_i^{(k+1)} = \mathbf{m}_i(\mathbf{y}_i^{(k)}, \mathbf{Y}^{(k)})$. For ease of exposition we suppress the dependency on the row index i and current state $\mathbf{Y}^{(k)}$, so $\mathbf{y}^{(k+1)} = \mathbf{m}(\mathbf{y}^{(k)})$, with

$$\mathbf{m}(\mathbf{y}) = \frac{\mathbf{z}}{\|\mathbf{z}\|}, \quad \mathbf{z} = (\lambda \mathbf{I} - \mathbf{B})\mathbf{y} + \mathbf{a},$$

where $\mathbf{B}$ depends on $\mathbf{Y}$ according to (3.9), λ is the largest eigenvalue of $\mathbf{B}$ and $\mathbf{a} = \sum_{j:i\neq j} w_{ij}\rho_{ij}\mathbf{y}_j$. We have locally around $\mathbf{y}^{(\infty)}$, by first order Taylor approximation

$$\mathbf{y}^{(k+1)} = \mathbf{y}^{(\infty)} + \mathbf{D}\mathbf{m}(\mathbf{y}^{(\infty)})\Big(\mathbf{y}^{(k)} - \mathbf{y}^{(\infty)}\Big) + \mathcal{O}\Bigg(\Big\|\mathbf{y}^{(k)} - \mathbf{y}^{(\infty)}\Big\|^2 \Bigg).$$

By straightforward calculation, the Jacobian matrix equals

$$\mathbf{D}\mathbf{m}(\mathbf{y}^{(\infty)}) = \Big(\mathbf{I} - \big(\mathbf{y}^{(\infty)}\big)\big(\mathbf{y}^{(\infty)}\big)^T \Big) \frac{1}{\|\mathbf{z}^{(\infty)}\|}(\lambda \mathbf{I} - \mathbf{B}).$$

The matrix $\mathbf{I} - (\mathbf{y}^{(\infty)})(\mathbf{y}^{(\infty)})^T$ is denoted by $\mathbf{P}_{\mathbf{y}^{(\infty)}}$. Then, up to first order in $\delta^{(k)} = \|\mathbf{y}^{(k)} - \mathbf{y}^{(\infty)}\|$,

$$\begin{aligned}
\mathbf{y}^{(k+1)} - \mathbf{y}^{(\infty)} &\approx \mathbf{P}_{\mathbf{y}^{(\infty)}} \frac{1}{\|\mathbf{z}^{(\infty)}\|}(\lambda \mathbf{I} - \mathbf{B})\big(\mathbf{y}^{(k)} - \mathbf{y}^{(\infty)}\big) \\
&= \mathbf{P}_{\mathbf{y}^{(\infty)}} \frac{1}{\|\mathbf{z}^{(\infty)}\|}\Big((\lambda \mathbf{I} - \mathbf{B})\mathbf{y}^{(k)} + \mathbf{a} - \big((\lambda \mathbf{I} - \mathbf{B})\mathbf{y}^{(\infty)} + \mathbf{a}\big) \Big) \\
&= \mathbf{P}_{\mathbf{y}^{(\infty)}} \frac{1}{\|\mathbf{z}^{(\infty)}\|}\big(\mathbf{z}^{(k)} - \mathbf{z}^{(\infty)} \big) \\
&= \frac{\|\mathbf{z}^{(k)}\|}{\|\mathbf{z}^{(\infty)}\|}\mathbf{P}_{\mathbf{y}^{(\infty)}}\big(\mathbf{y}^{(k)} - \mathbf{y}^{(\infty)} \big), \qquad (3.16)
\end{aligned}$$

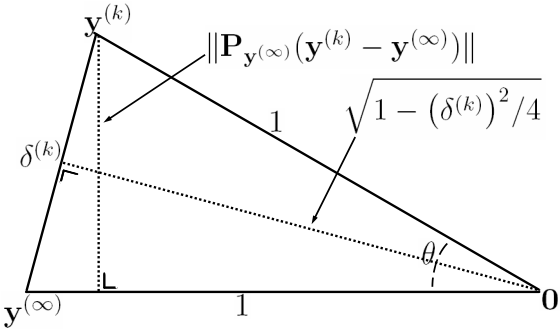

Figure 3.6: The equality $\|\mathbf{P}_{\mathbf{y}^{(\infty)}}(\mathbf{y}^{(k)} - \mathbf{y}^{(\infty)})\| = \delta^{(k)}\sqrt{1 - (\delta^{(k)})^2/4}$.

where in the last equality we have used $\mathbf{P}_{\mathbf{y}^{(\infty)}}\mathbf{y}^{(\infty)} = \mathbf{0}$. We note that, up to first order in $\delta^{(k)}$, $\|\mathbf{z}^{(k)}\|/\|\mathbf{z}^{(\infty)}\| \approx 1$. The term $\|\mathbf{P}_{\mathbf{y}^{(\infty)}}(\mathbf{y}^{(k)} - \mathbf{y}^{(\infty)})\|$ can be calculated by elementary geometry, see Figure 3.6. The projection operator $\mathbf{P}_{\mathbf{y}^{(\infty)}}$ sets any component in the direction of $\mathbf{y}^{(\infty)}$ to zero and leaves any orthogonal component unaltered. The resulting length $\|\mathbf{P}_{\mathbf{y}^{(\infty)}}(\mathbf{y}^{(k)} - \mathbf{y}^{(\infty)})\|$ has been illustrated in Figure 3.6. If we denote this length by μ, then $\mu = \sin(\theta)$, where θ is the angle as denoted in the figure. Also $\sin(\theta/2) = \delta^{(k)}/2$ from which we obtain $\theta = 2\arcsin(\delta^{(k)}/2)$. It follows that

$$\begin{aligned}
\mu &= \sin\left(\, 2\arcsin\left(\delta^{(k)}/2\right)\,\right) \\
&= 2\sin\left(\, \arcsin\left(\delta^{(k)}/2\right)\,\right)\cos\left(\, \arcsin\left(\delta^{(k)}/2\right)\,\right) \\
&= 2\left(\,\frac{\delta^{(k)}}{2}\,\right)\sqrt{1 - \left(\frac{\delta^{(k)}}{2}\right)^2} \\
&= \delta^{(k)}\sqrt{1 - \left(\delta^{(k)}\right)^2/4} = \delta^{(k)} + \mathcal{O}\left(\,\left(\delta^{(k)}\right)^2\,\right). \qquad (3.17)
\end{aligned}$$

The result $\delta^{(k+1)} = \delta^{(k)} + \mathcal{O}((\delta^{(k)})^2)$ follows by combining (3.16) and (3.17). □

Chapter 4

Rank reduction of correlation matrices by geometric programming

Geometric optimisation algorithms are developed that efficiently find the nearest low-rank correlation matrix. We show, in numerical tests, that our methods compare favourably to the existing methods in the literature. The connection with the Lagrange multiplier method is established, along with an identification of whether a local minimum is a global minimum. An additional benefit of the geometric approach is that any weighted norm can be applied. The problem of finding the nearest low-rank correlation matrix occurs as part of the calibration of multi-factor interest rate market models to correlation.

4.1 Introduction

The problem of finding the nearest low-rank correlation matrix occurs in areas such as finance, chemistry, physics and image processing. The mathematical formulation of this problem is stated in (3.4), in terms of the configuration matrix $\mathbf{Y}$. Here, we state the problem in terms of correlation matrices. Let $\mathbb{S}_n$ denote the set of real symmetric $n \times n$ matrices and let $\mathbf{P}$ be a symmetric $n \times n$ matrix with unit diagonal. For $\mathbf{C} \in \mathbb{S}_n$ we denote by $\mathbf{C} \succeq 0$ that $\mathbf{C}$ is positive semidefinite. Let the desired rank $d \in \{1, \ldots, n\}$ be given. The problem is then given by

$$\begin{array}{rl} \textbf{Find} & \mathbf{C} \in \mathbb{S}_n \\ \textbf{to minimize} & \frac{1}{2}\|\mathbf{P} - \mathbf{C}\|^2 \\ \textbf{subject to} & \operatorname{rank}(\mathbf{C}) \leq d;\ \ c_{ii} = 1,\, i = 1, \ldots, n;\ \ \mathbf{C} \succeq 0. \end{array} \tag{4.1}$$

Here $\|\cdot\|$ denotes a semi-norm on $\mathbb{S}_n$. The most important instance is

$$\frac{1}{2}\|\mathbf{P} - \mathbf{C}\|^2 = \frac{1}{2}\sum_{i<j} w_{ij}(\rho_{ij} - c_{ij})^2, \tag{4.2}$$

where $\mathbf{W}$ is a weights matrix consisting of non-negative elements. In words: Find the low-rank correlation matrix $\mathbf{C}$ nearest to the given $n \times n$ matrix $\mathbf{P}$. The choice of the semi-norm will reflect what is meant by nearness of the two matrices. The semi-norm in (4.2) is well known in the literature, and it is called the *Hadamard semi-norm*, see Horn & Johnson (1990). We note that the constraint set is non-convex for $d < n$, which makes it not straightforward to solve Problem (4.1) with standard convex optimization methods.

For concreteness, consider the following example. Suppose $\mathbf{P}$ is

$$\begin{pmatrix} 1.0000 & -0.1980 & -0.3827 \\ -0.1980 & 1.0000 & -0.2416 \\ -0.3827 & -0.2416 & 1.0000 \end{pmatrix},$$

and $\mathbf{W}$ is the full matrix, $w_{ij} = 1$. With the algorithm developed in this chapter, we solve (4.1) with $\mathbf{P}$ as above and $d = 2$. The algorithm takes as initial input a matrix $\mathbf{C}^{(0)}$ of rank 2 or less, for example,

$$\mathbf{C}^{(0)} = \begin{pmatrix} 1.0000 & 0.9782 & 0.8982 \\ 0.9782 & 1.0000 & 0.9699 \\ 0.8982 & 0.9699 & 1.0000 \end{pmatrix},$$

and then produces a sequence of points on the constraint set that converges to the point

$$\mathbf{C}^{*} = \begin{pmatrix} 1.0000 & -0.4068 & -0.6277 \\ -0.4068 & 1.0000 & -0.4559 \\ -0.6277 & -0.4559 & 1.0000 \end{pmatrix}$$

that solves (4.1). The constraint set and the points generated by the algorithm are represented in Figure 4.1. The details of this representation are given in Section 4.5.2. The blue point in the center and the green point represent, respectively, the target matrix $\mathbf{P}$ and the solution point $\mathbf{C}^{*}$. As the figure suggests, the algorithm has fast convergence and the constraint set is a curved space.

This novel technique we propose, is based on geometric optimisation that can locally minimize the objective function in (4.1) and which incorporates the Hadamard semi-norm. In fact, our method can be applied to any sufficiently smooth objective function. Not all other methods available in the literature that aim to solve (4.1) can handle an arbitrary objective function, see the literature review in Section 3.2. We formulate the problem in terms of Riemannian geometry. This approach allows us to use numerical methods on manifolds that are numerically stable and efficient, in particular the Riemannian-Newton method is applied. We show, for the numerical tests we performed, that the numerical efficiency of geometric optimisation compares favourably to the other algorithms available in the literature. The only drawback of the practical use of geometric optimisation is that

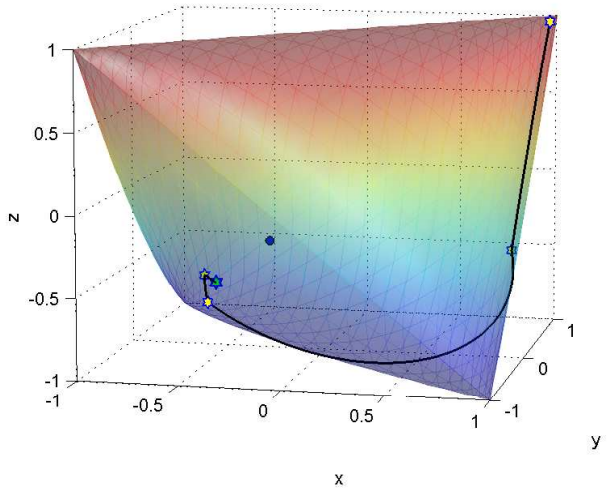

Figure 4.1: The shell represents the set of 3×3 correlation matrices of rank 2 or less. The details of this representation are given in Section 4.5.2.

the implementation is rather involved. To overcome this drawback, we have made available a MATLAB implementation 'LRCM min' (low-rank correlation matrices minimization) at `www.few.eur.nl/few/people/pietersz`.

We develop a technique to instantly check whether an obtained local minimum is a global minimum, by adaptation of Lagrange multiplier results of Zhang & Wu (2003). The novelty consists of an expression for the Lagrange multipliers given the matrix $\mathbf{C}$, whereas until now only the reverse direction (an expression for the matrix $\mathbf{C}$ given the Lagrange multipliers) was known. The fact that one may instantly identify whether a local minimum is a global minimum is very rare for non-convex optimisation problems, and that makes Problem (4.1), which is non-convex for $d < n$, all the more interesting.

Problem (4.1) is important in finance, as it occurs as part of the calibration of the multi-factor LIBOR market model of Brace et al. (1997), Miltersen et al. (1997), Jamshidian (1997) and Musiela & Rutkowski (1997). This model is an interest rate derivatives pricing model, as explained in Section 1.3.2, and it is used in some financial institutions for valuation and risk management of their interest rate derivatives portfolio. The number of stochastic factors needed for the model to fit to the given correlation matrix is equal to the rank of the correlation matrix. This rank can be as high as the number of forward LIBORs in the model, i.e., as high as the dimension of the matrix. The number

of LIBORs in the model can grow large in practical applications, for example, a model with over 80 LIBORs is not uncommon. This implies that the number of factors needed to fit the model to the given correlation matrix can be high, too. There is much empirical evidence that the term structure of interest rates is driven by multiple factors (three, four, or even more), see the review article of Dai & Singleton (2003). Though the number of factors driving the term structure may be four or more, the empirical work shows that it is certainly not as high as, say, 80. This is one reason for using a model with a low number of factors. Another reason is the enhanced efficiency when estimating the model-price of an interest rate derivative through Monte Carlo simulation. First, a lower factor model simply requires drawing less random numbers than a higher factor model. Second, the complexity of calculating LIBOR rates over a single time step in a simulation implementation is of order $n \times d$, with n the number of LIBORs and d the number of factors, see Joshi (2003*b*).

The importance of Problem (4.1) in finance has been recognized by many researchers. In fact, the literature review of Section 3.2 refers to twenty articles or books addressing the problem.

Due to its generality our method finds locally optimal points for a variety of other objective functions subject to the same constraints. One of the most famous problems comes from physics and is called *Thomson's problem*. The Thomson problem is concerned with minimizing the potential energy of n charged particles on the sphere in $\mathbb{R}^3$ ($d = 3$). Geometric optimisation techniques have previously been applied to the Thomson problem by Depczynski & Stöckler (1998), but these authors have only considered conjugate gradient techniques on a 'bigger' manifold, in which the freedom of rotation has not been factored out. In comparison, we stress here that our approach considers a lower dimensional manifold, which allows for Newton's algorithm (the latter not developed in Depczynski & Stöckler (1998)). An implementation of geometric optimisation applied to the Thomson problem has also been included in the 'LRCM min' package.

Finally, for a literature review of interest rate models, the reader is referred to Rebonato (2004*a*).

The chapter is organized as follows. In Section 4.2, the constraints of the problem are formulated in terms of differential geometry. We parameterize the set of correlation matrices of rank at most d with a manifold named the *Cholesky manifold*. This is a canonical space for the optimisation of the arbitrary smooth function subject to the same constraints. In Section 4.3, the Riemannian structure of the Cholesky manifold is introduced. Formulas are given for parallel transport, geodesics, gradient and Hessian. These are needed for the minimization algorithms, which are made explicit. In Section 4.4, we discuss the convergence of the algorithms. In Section 4.5, the application of the algorithms to the problem of finding the nearest low-rank correlation matrix is worked out

in detail. In Section 4.6, we numerically investigate the algorithms in terms of efficiency. Finally, in Section 4.7, we conclude the chapter.

For a literature review on rank reduction methods, the reader is referred to Section 3.2.

4.1.1 Weighted norms

We mention two reasons for assigning *non-constant* or *non-homogeneous* weights in the objective function of (4.2). First, in our setting $\mathbf{P}$ has the interpretation of measured correlation. It can thus be the case that we are more confident of specific entries of the matrix $\mathbf{P}$. Second, the weighted norm of (4.2) has important applications in finance, see, for example, Higham (2002), Rebonato (1999*c*) and Pietersz & Groenen (2004*b*).

The semi-norm in the objective function φ can be (i) a Hadamard semi-norm with arbitrary weights per element of the matrix, as defined in (4.2), or (ii) a weighted Frobenius norm $\|\cdot\|_{F,\mathbf{\Omega}}$ with $\mathbf{\Omega}$ a positive definite matrix. Here $\|\mathbf{X}\|^2_{F,\mathbf{\Omega}} = \mathrm{tr}(\mathbf{X}\mathbf{\Omega}\mathbf{X}^T\mathbf{\Omega})$. The weighted Frobenius norm is, from a practical point of view, by far less transparent than the Hadamard or weights-per-entry semi-norm (4.2). The geometric optimisation theory developed in this chapter, and most of the algorithms mentioned in Section 3.2, can be efficiently applied to both cases. The Lagrange multipliers and alternating projections methods however can only be efficiently extended to the case of the weighted Frobenius norm. The reason is that both these methods need to calculate a projection onto the space of matrices of rank d or less. Such a projection, for the weighted Frobenius norm, can be efficiently found by an eigenvalue decomposition. For the Hadamard semi-norm, such an efficient solution is not available, to our knowledge, and as also mentioned in Higham (2002, page 336).

4.2 Solution methodology with geometric optimisation

We note that Problem (4.1) is a special case of the following more general problem:

$$\begin{array}{rl} \textbf{Find} & \mathbf{C} \in \mathbb{S}_n \\ \textbf{to minimize} & \tilde{\varphi}(\mathbf{C}) \\ \textbf{subject to} & \mathrm{rank}(\mathbf{C}) \leq d;\ \ c_{ii} = 1,\, i = 1, \ldots, n;\ \ \mathbf{C} \succeq 0. \end{array} \tag{4.3}$$

In this chapter methods will be developed to solve Problem (4.3) for the case when $\tilde{\varphi}$ is twice continuously differentiable. In the remainder of the chapter, we assume $d > 1$, since for $d = 1$ the constraint set consists of a finite number (2^{n-1}) of points.

4.2.1 Basic idea

The idea for solving Problem (4.3) is to parameterize the constraint set by a manifold, and subsequently utilize the recently developed algorithms for optimisation over manifolds, such as Newton's algorithm and conjugate gradient algorithms. Such *geometric optimisation* has been developed by Smith (1993).

In Section 4.2.2, the constraint set is equipped with a topology, and we make an identification with a certain quotient space. In Section 4.2.3, it will be shown that the constraint set as such is not a manifold; however a dense subset is shown to be a manifold, namely the set of matrices of rank exactly d. Subsequently, in Section 4.2.4, we will define a larger manifold (named *Cholesky manifold*), of the same dimension as the rank-d manifold, that maps surjectively to the constraint set. We may apply geometric optimisation on the Cholesky manifold. The connection between minima on the Cholesky manifold and on the constraint set will be established.

4.2.2 Topological structure

In this section, the set of $n\times n$ correlation matrices of rank d or less is equipped with the subspace topology from $\mathbb{S}_n$. We subsequently establish a homeomorphism (i.e., a topological isomorphism) between the latter topological space and the quotient space of n products of the $d-1$ sphere over the group of orthogonal transformations of $\mathbb{R}^d$. Intuitively the correspondence is as follows: We can associate with an $n\times n$ correlation matrix of rank d a configuration of n points of unit length in $\mathbb{R}^d$ such that the inner product of points i and j is entry (i,j) of the correlation matrix. Any orthogonal rotation of the configuration does not alter the associated correlation matrix. This idea is developed more rigorously below.

Definition 1 *The set of symmetric $n\times n$ correlation matrices of rank at most d is defined by*

$$C_{n,d} = \big\{\ \mathbf{C} \in \mathbb{S}_n\ ;\ \mathbf{Diag}(\mathbf{C}) = \mathbf{I},\ \ \mathrm{rank}(\mathbf{C}) \le d,\ \ \mathbf{C} \succeq 0\big\}.$$

Here $\mathbf{I}$ denotes the identity matrix and $\mathbf{Diag}$ denotes the map $\mathbb{R}^{n\times n} \to \mathbb{R}^{n\times n}$, $\mathbf{Diag}(\mathbf{C})_{ij} = \delta_{ij}c_{ij}$, where δ_{ij} denotes the Kronecker delta.

The set $C_{n,d}$ is a subset of $\mathbb{S}_n$. The latter space is equipped with the Frobenius norm $\|\cdot\|_F$, which in turn defines a topology. We equip $C_{n,d}$ with the subspace topology.

In the following, the product of n unit spheres S^{d-1} is denoted by $T_{n,d}$. Elements of $T_{n,d}$ are denoted as a matrix $\mathbf{Y} \in \mathbb{R}^{n\times d}$, with each row vector $\mathbf{y}_i$ of unit length. Denote by O_d the group of orthogonal transformations of d-space. Elements of O_d are denoted by a $d\times d$ orthogonal matrix $\mathbf{Q}$.

Definition 2 *We define the following right O_d-action*[1] *on $T_{n,d}$:*

$$T_{n,d} \times O_d \to T_{n,d}, \quad (\mathbf{Y}, \mathbf{Q}) \mapsto \mathbf{YQ}. \tag{4.4}$$

An equivalence class $\{\mathbf{YQ} : \mathbf{Q} \in O_d\}$ associated with $\mathbf{Y} \in T_{n,d}$ is denoted by $[\mathbf{Y}]$ and it is called the orbit of $\mathbf{Y}$. The quotient space $T_{n,d}/O_d$ is denoted by $M_{n,d}$. The canonical projection $T_{n,d} \to T_{n,d}/O_d = M_{n,d}$ is denoted by π. Define the map[2] *$\mathbf{\Psi}$ as*

$$M_{n,d} \xrightarrow{\mathbf{\Psi}} C_{n,d}, \quad \mathbf{\Psi}\big([\mathbf{Y}]\big) = \mathbf{YY}^T.$$

We consider a map $\mathbf{\Phi}$ in the inverse direction of $\mathbf{\Psi}$,

$$C_{n,d} \xrightarrow{\mathbf{\Phi}} M_{n,d},$$

defined as follows: For $\mathbf{C} \in C_{n,d}$ take $\mathbf{Y} \in T_{n,d}$ such that $\mathbf{YY}^T = \mathbf{C}$. Such $\mathbf{Y}$ can always be found as will be shown in Theorem 2 below. Then set $\mathbf{\Phi}(\mathbf{C}) = [\mathbf{Y}]$. It will be shown in Theorem 2 that this map is well defined. Finally, define the map $\mathbf{S} : T_{n,d} \to C_{n,d}$, $\mathbf{S}(\mathbf{Y}) = \mathbf{YY}^T$.

The following theorem relates the spaces $C_{n,d}$ and $M_{n,d}$; the proof has been deferred to Appendix 4.A.1.

Theorem 2 *Consider the following diagram*

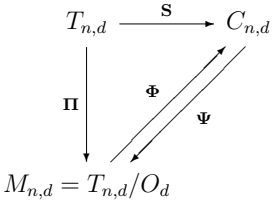

(4.5)

with the objects and maps as in Definitions 1 and 2. We have the following:

(i) The maps $\mathbf{\Psi}$ and $\mathbf{\Phi}$ are well defined.

(ii) The diagram is commutative, i.e., $\mathbf{\Psi} \circ \mathbf{\Pi} = \mathbf{S}$ and $\mathbf{\Phi} \circ \mathbf{S} = \mathbf{\Pi}$.

(iii) The map $\mathbf{\Psi}$ is a homeomorphism with inverse $\mathbf{\Phi}$.

[1] It is trivially verified that the map thus defined is indeed an O_d smooth action: $\mathbf{YI} = \mathbf{Y}$ and $\mathbf{Y}(\mathbf{Q}_1\mathbf{Q}_2)^{-1} = (\mathbf{YQ}_2^{-1})\mathbf{Q}_1{}^{-1}$. Standard matrix multiplication is smooth.

[2] Although rather obvious, it will be shown in Theorem 2 that this map is well defined.

4.2.3 A dense part of $M_{n,d}$ equipped with a differentiable structure

For an exposition on differentiable manifolds, the reader is referred to do Carmo (1992). It turns out that $M_{n,d}$ is not a manifold, but a so-called *stratified space*, see, e.g., Duistermaat & Kolk (2000). However there is a subspace of $M_{n,d}$ that is a manifold, which is the manifold of equivalence classes of matrices of *exactly* rank d. The proof of the following proposition has been deferred to Appendix 4.A.2.

Proposition 2 *Let $T^*_{n,d} \subset T_{n,d}$ be the subspace defined by*

$$T^*_{n,d} = \left\{ \mathbf{Y} \in T_{n,d} \ : \ \mathrm{rank}(\mathbf{Y}) = d \right\}.$$

Then we have the following:

1. *$T^*_{n,d}$ is a sub-manifold of $T_{n,d}$.*
2. *Denote by $M^*_{n,d}$ the quotient space $T^*_{n,d}/O_d$. Then $M^*_{n,d}$ is a manifold of dimension $n(d-1) - d(d-1)/2$.*

As shown in Proposition 2, a subset $M^*_{n,d}$ of $M_{n,d}$ is a manifold. In the following, we will study charts given by sections of the manifold $M^*_{n,d}$ that will ultimately lead to the final manifold over which will be optimized.

A *section* on $M^*_{n,d}$ is a map $\mathbf{\Sigma} : \mathcal{U} \to T^*_{n,d}$, with $\mathcal{U}$ open in $M^*_{n,d}$, such that $\mathbf{\Pi} \circ \mathbf{\Sigma} = \mathbf{id}_{M^*_{n,d}}$. Such a map singles out a unique matrix in each equivalence class. In our case we can explicitly give such a map $\mathbf{\Sigma}$. Let $[\mathbf{Y}]$ in $M^*_{n,d}$, and let I denote a subset of $\{1, \ldots, n\}$ with exactly d elements, such that $\dim(\mathrm{span}(\{\mathbf{y}_i \ : \ i \in I\})) = d$, for $\mathbf{Y} \in [\mathbf{Y}]$. We note that I is well defined since any two $\mathbf{Y}^{(1)}, \mathbf{Y}^{(2)} \in [\mathbf{Y}]$ are coupled by an orthogonal transformation, see the proof of Theorem 2, and orthogonal transformations preserve independence. The collection of all such I is denoted by $\mathcal{I}_{\mathbf{Y}}$. It is readily verified that $\mathcal{I}_{\mathbf{Y}}$ is not empty. Let $\prec$ denote the lexicographical ordering, then $(\mathcal{I}_{\mathbf{Y}}, \prec)$ is a well-ordered set. Thus we can choose the smallest element, denoted by $J(\mathbf{Y}) = (j_1, \ldots, j_d)$. Define $\tilde{\mathbf{Y}} \in \mathbb{R}^{d \times d}$ by taking the rows of $\mathbf{Y}$ from $J_{\mathbf{Y}}$, thus $\tilde{\mathbf{y}}_i = \mathbf{y}_{j_i}$. Define $\tilde{\mathbf{C}} = \tilde{\mathbf{Y}}\tilde{\mathbf{Y}}^T$. Since $\tilde{\mathbf{C}}$ is positive definite, Cholesky decomposition can be applied to $\tilde{\mathbf{C}}$, see for example Golub & van Loan (1996, Theorem 4.2.5), to obtain a unique lower-triangular matrix $\bar{\mathbf{Y}}$ such that $\bar{\mathbf{Y}}\bar{\mathbf{Y}}^T = \tilde{\mathbf{C}}$ and $\bar{\mathbf{y}}_{ii} > 0$. By Theorem 2, there exists a unique orthogonal matrix $\mathbf{Q} \in O_d$ such that $\bar{\mathbf{Y}} = \tilde{\mathbf{Y}}\mathbf{Q}$. Define $\mathbf{Y}^* = \mathbf{YQ}$. We note that $\mathbf{Y}^*$ is lower-triangular, since for $i \notin J_{\mathbf{Y}}$, let p be the largest integer such that $i > j_p$, then $\mathbf{Y}^*_i$ is dependent on $\mathbf{y}^*_1, \ldots, \mathbf{y}^*_{j_p}$, as $J_{\mathbf{Y}}$ is the smallest element from $\mathcal{I}_{\mathbf{Y}}$, which implies a lower-triangular form for $\mathbf{Y}^*$. Then define $\mathcal{U}_{\mathbf{Y}} = \{[\mathbf{Z}] \ : \ J(\mathbf{Y}) \in \mathcal{I}_{\mathbf{Z}}\} \subset M^*_{n,d}$. It is obvious that $\mathcal{U}_{\mathbf{Y}}$ and $\mathbf{\Pi}^{-1}(\mathcal{U}_{\mathbf{Y}})$ are open in the corresponding topologies. Then

$$\mathbf{\Sigma}_Y : \mathcal{U}_Y \to \mathbf{\Pi}^{-1}(\mathcal{U}_{\mathbf{Y}}), \ \ [\mathbf{Z}] \mapsto \mathbf{Z}^*, \tag{4.6}$$

is a section of $\mathcal{U}_{\mathbf{Y}}$ at $\mathbf{Y}$. The following proposition shows that the sections are the charts of the manifold $M^*_{n,d}$. The proof has been deferred to Appendix 4.A.3.

Proposition 3 *The differentiable structure on $M^*_{n,d}$ is the one which makes $\Sigma_{\mathbf{Y}} : \mathcal{U}_{\mathbf{Y}} \to \Sigma(\mathcal{U}_{\mathbf{Y}})$ into a diffeomorphism.*

4.2.4 The Cholesky manifold

In this section, we will show that, for the purpose of optimisation, it is sufficient to perform the optimisation on a compact manifold that contains one of the sections. For simplicity we choose the section $\mathbf{\Sigma_Y}$ where $J(\mathbf{Y}) = \{1, \ldots, d\}$. The image $\mathbf{\Sigma_Y}(\mathcal{U}_{\mathbf{Y}})$ is a smooth sub-manifold of $T_{n,d}$ with the following representation in $\mathbb{R}^{n\times d}$

$$\Big\{ \begin{pmatrix} \mathbf{y}_1^T & \ldots & \mathbf{y}_n^T \end{pmatrix}^T \; : \; \mathbf{y}_1 = (1, 0, \ldots, 0);\ \mathbf{y}_i \in S_+^{i-1},\ i = 2, \ldots, d; \\ \mathbf{y}_i \in S^{d-1},\ i = d+1, \ldots, n \Big\},$$

with S_+^{i-1} embedded in $\mathbb{R}^d$ by the first i coordinates such that coordinate i is bigger than 0 and with the remaining coordinates set to zero. Also, S^{d-1} is similarly embedded in $\mathbb{R}^d$. We can consider the map $\mathbf{S} : T_{n,d} \to C_{n,d}$ restricted to $\mathbf{\Sigma_Y}(\mathcal{U}_{\mathbf{Y}})$, which is differentiable since $\mathbf{\Sigma_Y}(\mathcal{U}_{\mathbf{Y}})$ is a sub-manifold of $T_{n,d}$. The map $\mathbf{S}|_{\mathbf{\Sigma_Y}(\mathcal{U}_{\mathbf{Y}})}$ is a homeomorphism, in virtue of Theorem 2.

For the purpose of optimisation, we need a compact manifold which is surjective with $C_{n,d}$. Define the following sub-manifold of $T_{n,d}$ of dimension $n(d-1) - d(d-1)/2$,

$$\mathrm{Chol}_{n,d} \;=\; \Big\{ \mathbf{Y} \in \mathbb{R}^{n\times d} \; : \; \mathbf{y}_1 = (1, 0, \ldots, 0); \\ \mathbf{y}_i \in S^{i-1},\ i = 2, \ldots, d;\ \mathbf{y}_i \in S^{d-1}, i = d+1, \ldots, n \Big\},$$

which we call the Cholesky manifold. The Cholesky parametrization has been considered before by Rapisarda et al. (2002), but these authors do not consider non-Euclidean geometric optimisation. The map $\mathbf{S}|_{\mathrm{Chol}_{n,d}}$ is surjective, in virtue of the following theorem, the proof of which has been relegated to Appendix 4.A.4.

Theorem 3 *If $\mathbf{C} \in C_{n,d}$, then there exists a $\mathbf{Y} \in \mathrm{Chol}_{n,d}$ such that $\mathbf{Y}\mathbf{Y}^T = \mathbf{C}$.*

A function $\tilde{\varphi}$ on $C_{n,d}$ can be considered on $\mathrm{Chol}_{n,d}$, too, via the composition

$$\mathrm{Chol}_{n,d} \xrightarrow{\mathbf{S}} C_{n,d} \xrightarrow{\tilde{\varphi}} \mathbb{R}, \quad \mathbf{Y} \mapsto \mathbf{Y}\mathbf{Y}^T \mapsto \tilde{\varphi}(\mathbf{Y}\mathbf{Y}^T).$$

From here on, we will write $\varphi(\mathbf{Y}) := \tilde{\varphi}(\mathbf{Y}\mathbf{Y}^T)$ viewed as a function on $\mathrm{Chol}_{n,d}$.

For a *global* minimum $\varphi(\mathbf{Y})$ on $\mathrm{Chol}_{n,d}$, we have that $\mathbf{Y}\mathbf{Y}^T$ attains a global minimum of $\tilde{\varphi}$ on $C_{n,d}$, since the map $\mathbf{S} : \mathrm{Chol}_{n,d} \to C_{n,d}$ is surjective. For a *local* minimum, we have the following theorem. The proof has been deferred to Appendix 4.A.5.

Theorem 4 *The point* $\mathbf{Y}$ *attains a local minimum of* φ *on* $\mathrm{Chol}_{n,d}$ *if and only if* $\mathbf{Y}\mathbf{Y}^T$ *attains a local minimum of* $\tilde{\varphi}$ *on* $C_{n,d}$.

These considerations on global and local minima on $\mathrm{Chol}_{n,d}$ show that, to optimize $\tilde{\varphi}$ over $C_{n,d}$, we might as well optimize φ over the manifold $\mathrm{Chol}_{n,d}$. For the optimisation of $\tilde{\varphi}$ over $C_{n,d}$, there is no straightforward way to use numerical methods such as Newton and conjugate gradient, since they require a notion of differentiability, but for optimisation of φ on $\mathrm{Chol}_{n,d}$, we can use such numerical methods.

4.2.5 Choice of representation

In principle, we could elect another manifold $\tilde{M}$ and a surjective open map $\tilde{M} \to C_{n,d}$. We insist however on explicit knowledge of the geodesics and parallel transport, for this is essential to obtaining an efficient algorithm. We found that if we choose the Cholesky manifold then convenient expressions for geodesics, etc., are obtained. Moreover, the Cholesky manifold has the minimal dimension, i.e., $\dim(\mathrm{Chol}_{n,d}) = \dim(M^*_{n,d})$.

In the next section, the geometric optimisation tools are developed for the Cholesky manifold.

4.3 Optimisation over the Cholesky manifold

For the development of minimization algorithms on a manifold, certain objects of the manifold need to calculated explicitly, such as geodesics, parallel transport, etc. In this section, these objects are introduced and made explicit for $\mathrm{Chol}_{n,d}$.

From a theoretical point of view, it does not matter which coordinates we choose to derive the geometrical properties of a manifold. For the numerical computations however this choice is essential because the simplicity of formulas for the geodesics and parallel transport depends on the chosen coordinates. We found that simple expressions are obtained when $\mathrm{Chol}_{n,d}$ is viewed as a sub-manifold of $T_{n,d}$, which, in turn, is viewed as a subset of the *ambient space* $\mathbb{R}^{n\times d}$. This representation reveals that, to calculate geodesics and parallel transport on $\mathrm{Chol}_{n,d}$, it is sufficient to calculate these on a single sphere.

The tangent space of the manifold $\mathrm{Chol}_{n,d}$ at a point $\mathbf{Y} \in \mathrm{Chol}_{n,d}$ is denoted by $T_{\mathbf{Y}}\mathrm{Chol}_{n,d}$. A tangent vector at a point $\mathbf{Y}$ is an element of $T_{\mathbf{Y}}\mathrm{Chol}_{n,d}$ and is denoted by $\mathbf{\Delta}$.

4.3.1 Riemannian structure

We start with a review of basic concepts of Riemannian geometry. Our exposition follows do Carmo (1992). Let M be an m-dimensional differentiable manifold. A *Riemannian*

structure on M is a smooth map $\mathbf{Y} \mapsto \langle \cdot, \cdot \rangle_{\mathbf{Y}}$, which for every $\mathbf{Y} \in M$ assigns an inner product $\langle \cdot, \cdot \rangle_{\mathbf{Y}}$ on $T_{\mathbf{Y}}M$, the tangent space at point $\mathbf{Y}$. *A Riemannian manifold* is a differentiable manifold with a Riemannian structure.

Let φ be a smooth function on a Riemannian manifold M. Denote the *differential* of φ at a point $\mathbf{Y}$ by $\varphi_{\mathbf{Y}}$. Then $\varphi_{\mathbf{Y}}$ is a linear functional on $T_{\mathbf{Y}}M$. In particular, let $\mathbf{\Upsilon}(t)$, $t \in (-\varepsilon, \varepsilon)$, be a smooth curve on M such that $\mathbf{\Upsilon}(0) = \mathbf{Y}$ and $\dot{\mathbf{\Gamma}}(0)$ expressed in a coordinate chart $(\mathcal{U}, x_1, \ldots, x_m)$ is equal to $\mathbf{\Delta}$, then $\varphi_{\mathbf{Y}}(\mathbf{\Delta})$ can be expressed in this coordinate chart by

$$\varphi_{\mathbf{Y}}(\mathbf{\Delta}) = \sum_{i=1}^{m} \frac{\partial}{\partial x^i}(\varphi \circ x_i^{-1})(\mathbf{\Upsilon})\Big|_{t=0} \tag{4.7}$$

The linear space of linear functionals on $T_{\mathbf{Y}}M$ (the dual space) is denoted by $(T_{\mathbf{Y}}M)^*$. A *vector field* is a map on M that selects a tangent $\mathbf{\Delta} \in T_{\mathbf{Y}}M$ at each point $\mathbf{Y} \in M$. The Riemannian structure induces an isomorphism between $T_{\mathbf{Y}}M$ and $(T_{\mathbf{Y}}M)^*$, which guarantees the existence of a unique vector field on M, denoted by $\mathbf{Grad}\varphi$, such that

$$\varphi_{\mathbf{Y}}(\mathbf{\Delta}) = \langle \mathbf{Grad}\varphi, \mathbf{X} \rangle_{\mathbf{Y}} \quad \text{for all } \mathbf{X} \in T_{\mathbf{Y}}M. \tag{4.8}$$

This vector field is called the *gradient* of φ. Also, for Newton and conjugate gradient methods, we have to use second order derivatives. In particular, we need to be able to differentiate vector fields. To do this on a general manifold, we need to equip the manifold with additional structure, namely the *connection*. A connection on a manifold M is a rule $\boldsymbol{\nabla}_{\cdot}\cdot$ which assigns to each two vector fields $\mathbf{Y}_1, \mathbf{Y}_2$ on M a vector field $\boldsymbol{\nabla}_{\mathbf{Y}_1}\mathbf{Y}_2$ on M, satisfying the following two conditions:

$$\boldsymbol{\nabla}_{\varphi\mathbf{Y}_1+\chi\mathbf{Y}_2}\mathbf{Y}_3 = \varphi\boldsymbol{\nabla}_{\mathbf{Y}_1}\mathbf{Y}_3 + \chi\boldsymbol{\nabla}_{\mathbf{Y}_2}\mathbf{Y}_3, \quad \boldsymbol{\nabla}_{\mathbf{Y}_1}(\varphi\mathbf{Y}_2) = \varphi\boldsymbol{\nabla}_{\mathbf{Y}_1}(\mathbf{Y}_2) + (\mathbf{Y}_1\varphi)\mathbf{Y}_2, \tag{4.9}$$

for φ, χ smooth functions on M and $\mathbf{Y}_1, \mathbf{Y}_2, \mathbf{Y}_3$ vector fields on M.

Let $\mathbf{\Upsilon}(t)$ be a smooth curve on M with tangent vector $\mathbf{Y}_1(t) = \dot{\mathbf{\Upsilon}}(t)$. A given family $\mathbf{Y}_2(t)$ of tangent vectors at the points $\mathbf{\Upsilon}(t)$ is said to be *parallel transported* along $\mathbf{\Upsilon}$ if

$$\boldsymbol{\nabla}_{\mathbf{Y}_1}\mathbf{Y}_2 = 0 \quad \text{on } \mathbf{\Upsilon}(t), \tag{4.10}$$

where $\mathbf{Y}_1, \mathbf{Y}_2$ are vector fields that coincide with $\mathbf{Y}_1(t)$ and $\mathbf{Y}_2(t)$, respectively, on $\mathbf{\Upsilon}(t)$. If the tangent vector $\mathbf{Y}_1(t)$ itself is parallel transported along $\mathbf{\Upsilon}(t)$ then the curve $\mathbf{\Upsilon}(t)$ is called a *geodesic*. In particular, if $(\mathcal{U}, x_1, \ldots, x_m)$ is a coordinate chart on M and $\{\mathbf{X}_1, \ldots, \mathbf{X}_m\}$ the corresponding vector fields then the affine connection $\boldsymbol{\nabla}$ on $\mathcal{U}$ can be expressed by

$$\boldsymbol{\nabla}_{\mathbf{X}_i}\mathbf{X}_j = \sum_{k=1}^{m} \gamma_{i,j}^k \mathbf{X}_k. \tag{4.11}$$

The functions $\gamma_{i,j}^k$ are smooth functions, called the *Christoffel symbols* for the connection. In components, the geodesic equation becomes

$$\ddot{x}_k + \sum_{i,j=1}^{m} \gamma_{i,j}^k \dot{x}_i \dot{x}_j = 0, \tag{4.12}$$

where x_k are the coordinates of $\boldsymbol{\Upsilon}(t)$. On a Riemannian manifold there is a unique torsion free connection compatible with the metric, called the *Levi-Civita* connection. This means that Christoffel symbols can be expressed as functions of a metric on M. We note that (4.12) implies as well that, once we have determined the equation for the geodesic, we can simply read off Christoffel symbols. With respect to an induced metric the geodesic is the curve of shortest length between two points on a manifold. For a manifold embedded in Euclidean space an equivalent characterization of a geodesic is that the acceleration vector at each point along a geodesic is normal to the manifold so long as the curve is traced with uniform speed.

We start by defining Riemannian structures for $T_{n,d}$ and for the Cholesky manifold $\mathrm{Chol}_{n,d}$. We use the Levi-Civita connection, associated to the metric defined as follows on the tangent spaces. Both tangent spaces are identified with suitable subspaces of the ambient space $\mathbb{R}^{n\times d}$, and subsequently the inner product for two tangents $\boldsymbol{\Delta}_1$, $\boldsymbol{\Delta}_2$ is defined as

$$\langle \boldsymbol{\Delta}_1, \boldsymbol{\Delta}_2 \rangle = \mathrm{tr} \boldsymbol{\Delta}_1 \boldsymbol{\Delta}_2^T, \tag{4.13}$$

which is the Frobenius inner product for $n \times d$ matrices. We note that, in our special case, the inner product $\langle \cdot, \cdot \rangle_{\mathbf{Y}}$ is independent of the point $\mathbf{Y}$; therefore we suppress the dependency on $\mathbf{Y}$.

4.3.2 Normal and tangent spaces

An equation determining tangents to $T_{n,d}$ at a point $\mathbf{Y}$ can be obtained by differentiating $\mathbf{Diag}(\mathbf{Y}\mathbf{Y}^T) = \mathbf{I}$ yielding $\mathbf{Diag}(\mathbf{Y}\boldsymbol{\Delta}^T + \boldsymbol{\Delta}\mathbf{Y}^T) = 0$, i.e., $\mathbf{Diag}(\boldsymbol{\Delta}\mathbf{Y}^T) = 0$. The dimension of the tangent space is $n(d-1)$. The *normal space* at the point $\mathbf{Y}$ is defined to be the orthogonal complement of the tangent space at the point $\mathbf{Y}$, i.e., it consists of the matrices $\mathbf{N}$, for which $\mathrm{tr}\boldsymbol{\Delta}\mathbf{N}^T = 0$ for all $\boldsymbol{\Delta}$ in the tangent space. It follows that the normal space is n dimensional. It is straightforward to verify that if $\mathbf{N} = \mathbf{D}\mathbf{Y}$, where $\mathbf{D}$ is $n \times n$ diagonal, then $\mathbf{N}$ is in the normal space. Since the dimension of the space of such matrices is n, we see that the normal space $N_{\mathbf{Y}}T_{n,d}$ at $\mathbf{Y} \in T_{n,d}$ is given by

$$N_{\mathbf{Y}}T_{n,d} = \left\{ \mathbf{D}\mathbf{Y} \ ; \ \mathbf{D} \in \mathbb{R}^{n\times n} \ \text{ diagonal } \right\}.$$

The projections $\boldsymbol{\Pi}_{N_{\mathbf{Y}}T_{n,d}}$ and $\boldsymbol{\Pi}_{T_{\mathbf{Y}}T_{n,d}}$ onto the normal and tangent spaces of $T_{n,d}$ are given by

$$\boldsymbol{\Pi}_{N_{\mathbf{Y}}T_{n,d}}(\boldsymbol{\Delta}) = \mathbf{Diag}(\boldsymbol{\Delta}\mathbf{Y}^T)\mathbf{Y} \ \text{ and } \ \boldsymbol{\Pi}_{T_{\mathbf{Y}}T_{n,d}}(\boldsymbol{\Delta}) = \boldsymbol{\Delta} - \mathbf{Diag}(\boldsymbol{\Delta}\mathbf{Y}^T)\mathbf{Y},$$

respectively. The projection $\mathbf{\Pi}_{T_{\mathbf{Y}}\mathrm{Chol}_{n,d}}$ onto the tangent space of $\mathrm{Chol}_{n,d}$ is given by

$$\mathbf{\Pi}_{T_{\mathbf{Y}}\mathrm{Chol}_{n,d}}(\mathbf{\Delta}) = \mathbf{Z}\big(\ \mathbf{\Pi}_{T_{\mathbf{Y}}T_{n,d}}(\mathbf{\Delta})\ \big),$$

with $\mathbf{Z}(\mathbf{\Delta})$ defined by

$$z_{ij}(\mathbf{\Delta}) = \begin{cases} 0 & \text{for } j > i \text{ or } i = j = 1, \\ \delta_{ij} & \text{otherwise.} \end{cases}$$

4.3.3 Geodesics

It is convenient to work with the coordinates of the ambient space $\mathbb{R}^{n\times d}$. In this coordinate system, geodesics on $T_{n,d}$ with respect to the Levi-Civita connection obey the second order differential equation

$$\ddot{\mathbf{Y}} + \mathbf{\Gamma}_{\mathbf{Y}}(\dot{\mathbf{Y}}, \dot{\mathbf{Y}}) = 0, \quad \text{with } \mathbf{\Gamma}_{\mathbf{Y}}(\mathbf{\Delta}_1, \mathbf{\Delta}_2) := \mathbf{Diag}(\mathbf{\Delta}_1\mathbf{\Delta}_2^T)\mathbf{Y}. \tag{4.14}$$

To see this, we begin with the condition that $\mathbf{Y}(t)$ remains on $T_{n,d}$,

$$\mathbf{Diag}(\mathbf{Y}\mathbf{Y}^T) = \mathbf{I}. \tag{4.15}$$

Differentiating this equation twice, we obtain,

$$\mathbf{Diag}(\ddot{\mathbf{Y}}\mathbf{Y}^T + 2\dot{\mathbf{Y}}\dot{\mathbf{Y}}^T + \mathbf{Y}\ddot{\mathbf{Y}}^T) = 0. \tag{4.16}$$

In order for $\mathbf{Y}(\cdot)$ to be a geodesic, $\ddot{\mathbf{Y}}(t)$ must be in the normal space at $\mathbf{Y}(t)$, i.e.,

$$\ddot{\mathbf{Y}}(t) = \mathbf{D}(t)\mathbf{Y}(t) \tag{4.17}$$

for some diagonal matrix $\mathbf{D}(t)$. To obtain an expression for $\mathbf{D}$, substitute (4.17) into (4.16), which yields (4.14).

The function $\mathbf{\Gamma}_{\mathbf{Y}}$ is the matrix notation of the Christoffel symbols, γ_{ij}^k, with respect to $\mathbf{E}_1, \ldots, \mathbf{E}_{nd}$, the standard basis vectors of $\mathbb{R}^{n\times d}$. More precisely, $\mathbf{\nabla}_{\mathbf{E}_i}\mathbf{E}_j = \sum_{k=1}^{nd}\gamma_{ij}^k\mathbf{E}_k$ with γ_{ij}^k defined by

$$\langle \mathbf{\Gamma}_{\mathbf{Y}}(\mathbf{X}_1, \mathbf{X}_2), \mathbf{E}_k\rangle = \sum_{i,j=1}^{nd}\gamma_{ij}^k(\mathbf{X}_1)_i(\mathbf{X}_2)_j.$$

The geodesic at $\mathbf{Y}(0) \in T_{n,d}$ in the direction $\mathbf{\Delta} \in T_{\mathbf{Y}(0)}T_{n,d}$ is given by,

$$\mathbf{Y}_i(t) = \cos(\ \|\mathbf{\Delta}_i\|t\ )\ \mathbf{Y}_i(0) + \frac{1}{\|\mathbf{\Delta}_i\|}\sin\big(\ \|\mathbf{\Delta}_i\|t\ \big)\ \mathbf{\Delta}_i. \tag{4.18}$$

for $i = 1, \ldots, n$, per component on the sphere. By differentiating, we obtain an expression for the evolution of the tangent along the geodesic:

$$\dot{\mathbf{Y}}_i(t) = -\|\mathbf{\Delta}_i\|\sin\big(\ \|\mathbf{\Delta}_i\|t\ \big)\ \mathbf{Y}_i(0) + \cos\big(\ \|\mathbf{\Delta}_i\|t\ \big)\ \mathbf{\Delta}_i. \tag{4.19}$$

Since $\mathrm{Chol}_{n,d}$ is a Riemannian sub-manifold of $T_{n,d}$ it has the same geodesics.

4.3.4 Parallel transport along a geodesic

We consider this problem per component on the sphere. If $\mathbf{\Delta}^{(2)} \in T_{\mathbf{Y}^{(1)}}T_{n,d}$ is parallel transported along a geodesic starting from $\mathbf{Y}^{(1)}$ in the direction of $\mathbf{\Delta}^{(1)} \in T_{\mathbf{Y}^{(1)}}T_{n,d}$, then decompose $\mathbf{\Delta}^{(2)}$ in terms of $\mathbf{\Delta}^{(1)}$,

$$\mathbf{\Delta}_i^{(2)}(t) = \langle \mathbf{\Delta}_i^{(1)}(0), \mathbf{\Delta}_i^{(2)}(0)\rangle \mathbf{\Delta}_i^{(1)}(t) + \mathbf{R}_i, \;\; \mathbf{R}_i \perp \mathbf{\Delta}_i^{(1)}(0).$$

Then $\mathbf{\Delta}_i^{(1)}(t)$ changes according to (4.19) and $\mathbf{R}_i$ remains unchanged. Parallel transport from $\mathbf{Y}^{(1)}$ to $\mathbf{Y}^{(2)}$ defines an isometry $\mathbf{T}(\mathbf{Y}^{(1)}, \mathbf{Y}^{(2)}) : T_{\mathbf{Y}^{(1)}}T_{n,d} \rightarrow T_{\mathbf{Y}^{(2)}}T_{n,d}$. When it is clear in between which two points is transported, then parallel transport is denoted simply by $\mathbf{T}$. Since $\mathrm{Chol}_{n,d}$ is a Riemannian sub-manifold of $T_{n,d}$ it has the same equations for parallel transport.

4.3.5 The gradient

Since $\mathrm{Chol}_{n,d}$ is a sub-manifold of $\mathbb{R}^{n\times d}$ we can use coordinates of $\mathbb{R}^{n\times d}$ to express the differential $\varphi_{\mathbf{Y}}$ of φ at the point $\mathbf{Y}$, namely $(\varphi_{\mathbf{Y}})_{ij} = \frac{\partial F}{\partial Y_{ij}}$. The gradient $\mathbf{Grad}\varphi$ of a function φ on $\mathrm{Chol}_{n,d}$ can be determined by (4.8). It follows that,

$$\mathbf{Grad}\varphi \;\; = \;\; \mathbf{\Pi}_{T_{\mathbf{Y}}\mathrm{Chol}_{n,d}}(\varphi_{\mathbf{Y}}) = \mathbf{Z}\big(\, \varphi_{\mathbf{Y}} - \mathbf{Diag}(\varphi_{\mathbf{Y}}\mathbf{Y}^T)\mathbf{Y} \,\big). \tag{4.20}$$

4.3.6 Hessian

The Hessian $\mathbf{Hess}\varphi$ of a function φ is a second covariant derivative of φ. More precisely, let $\mathbf{\Delta}_1, \mathbf{\Delta}_2$ be two vector fields, then

$$\mathbf{Hess}\varphi(\mathbf{\Delta}_1, \mathbf{\Delta}_2) = \langle \mathbf{\nabla}_{\mathbf{\Delta}_1}\mathbf{Grad}\varphi, \mathbf{\Delta}_2\rangle$$

In local coordinates of $\mathbb{R}^{n\times d}$

$$\mathbf{Hess}\varphi(\mathbf{\Delta}_1, \mathbf{\Delta}_2) = \varphi_{\mathbf{YY}}(\mathbf{\Delta}_1, \mathbf{\Delta}_2) - \langle \varphi_{\mathbf{Y}}, \Gamma_{\mathbf{Y}}(\mathbf{\Delta}_1, \mathbf{\Delta}_2)\rangle, \tag{4.21}$$

where

$$\varphi_{\mathbf{YY}}(\mathbf{\Delta}_1, \mathbf{\Delta}_2) = \frac{\mathrm{d}}{\mathrm{d}t}\frac{\mathrm{d}}{\mathrm{d}s}\bigg|_{t=s=0} \varphi(\mathbf{Y}(t,s)), \text{ with } \frac{\mathrm{d}}{\mathrm{d}t}\bigg|_{t=0} \mathbf{Y} = \mathbf{\Delta}_1, \;\; \frac{\mathrm{d}}{\mathrm{d}s}\bigg|_{s=0} \mathbf{Y} = \mathbf{\Delta}_2.$$

Newton's method requires inverting the Hessian at minus the gradient, therefore we need to find the tangent $\mathbf{\Delta}$ to $\mathrm{Chol}_{n,d}$ such that

$$\mathbf{Hess}\varphi(\mathbf{\Delta}, \mathbf{X}) = \langle -\mathbf{Grad}\varphi, \mathbf{X}\rangle, \text{ for all tangents } \mathbf{X} \text{ to } \mathrm{Chol}_{n,d}. \tag{4.22}$$

To solve (4.22), it is convenient to calculate the unique tangent vector $\mathbf{H} = \mathbf{H}(\boldsymbol{\Delta})$ satisfying

$$\mathbf{Hess}\varphi(\boldsymbol{\Delta}, \mathbf{X}) = \langle \mathbf{H}, \mathbf{X} \rangle, \text{ for all tangents } \mathbf{X} \text{ to } \mathrm{Chol}_{n,d},$$

since then the Newton Equation (4.22) becomes $\mathbf{H}(\boldsymbol{\Delta}) = -\mathbf{Grad}\varphi$. From (4.14) and (4.21), we obtain

$$\mathbf{H}(\boldsymbol{\Delta}) = \boldsymbol{\Pi}_{T_{\mathbf{Y}}\mathrm{Chol}_{n,d}}(\varphi_{\mathbf{YY}}(\boldsymbol{\Delta})) - \mathbf{Diag}(\varphi_{\mathbf{Y}}\mathbf{Y}^T)\boldsymbol{\Delta}, \tag{4.23}$$

where the notation $\varphi_{\mathbf{YY}}(\boldsymbol{\Delta})$ means the tangent vector satisfying

$$\varphi_{\mathbf{YY}}(\boldsymbol{\Delta}) = \frac{\mathrm{d}}{\mathrm{d}t}\bigg|_{t=0} \varphi_{\mathbf{Y}}(\mathbf{Y}(t)), \quad \dot{\mathbf{Y}}(0) = \boldsymbol{\Delta}.$$

4.3.7 Algorithms

We are now in a position to state the conjugate gradient algorithm, given as Algorithm 2, and the Newton algorithm, given as Algorithm 3, for optimisation over the Cholesky manifold. These algorithms are instances of the geometric programs presented in Smith (1993), for the particular case of the Cholesky manifold.

4.4 Discussion of convergence properties

In this section, we discuss convergence properties of the geometric programs: global convergence and the local rate of convergence.

4.4.1 Global convergence

First, we discuss global convergence for the Riemannian-Newton algorithm. It is well known that the Newton algorithm, as displayed in Algorithm 3, is not globally convergent to a local minimum. Moreover, the steps in Algorithm 3 may even not be well defined, because the Hessian mapping could be singular. The standard way to resolve these issues, is to introduce jointly a steepest descent algorithm. So Algorithm 3 is adjusted in the following way. When the new search direction $\boldsymbol{\Delta}^{(k)}$ has been calculated, then we also consider the steepest descent search direction $\boldsymbol{\Delta}^{(k)}_{\mathrm{Steep}} = -\mathbf{Grad}\varphi(\mathbf{Y}^{(k)})$. Subsequently, a line minimization of the objective value is performed in both directions, $\boldsymbol{\Delta}^{(k)}$ and $\boldsymbol{\Delta}^{(k)}_{\mathrm{Steep}}$. We then take as the next point of the algorithm whichever search direction finds the point with lowest objective value. Such a steepest descent method with line minimization is well known to have guaranteed convergence to a local minimum.

Second, we discuss global convergence for conjugate gradient algorithms. For the Riemannian case, we have not seen any global convergence results for conjugate gradient

Algorithm 2 Conjugate gradient for minimizing $\varphi(\mathbf{Y})$ on $\mathrm{Chol}_{n,d}$

Input: $\mathbf{Y}^{(0)}, \varphi(\cdot)$.

Require: $\mathbf{Y}^{(0)}$ such that $\mathbf{Y}^{(0)}(\mathbf{Y}^{(0)})^T = \mathbf{I}$.

Compute $\mathbf{G}^{(0)} = \mathbf{Grad}\varphi(\mathbf{Y}^{(0)}) = \mathbf{Z}(\varphi_{\mathbf{Y}} - \mathbf{Diag}(\varphi_{\mathbf{Y}}(\mathbf{Y}^{(0)})^T)\mathbf{Y}^{(0)})$ and set $\mathbf{J}^{(0)} = -\mathbf{G}^{(0)}$.

for $k = 0, 1, 2, \ldots$ **do**

Minimize $\varphi\big(\mathbf{Y}^{(k)}(t)\big)$ over t where $\mathbf{Y}^{(k)}(t)$ is a geodesic on $\mathrm{Chol}_{n,d}$ starting from $\mathbf{Y}^{(k)}$ in the direction of $\mathbf{J}^{(k)}$.

Set $t_k = t_{\min}$ and $\mathbf{Y}^{(k+1)} = \mathbf{Y}^{(k)}(t_k)$.

Compute $\mathbf{G}^{(k+1)} = \mathbf{Grad}\varphi(\mathbf{Y}^{(k+1)}) = \mathbf{Z}\big(\ \varphi_{\mathbf{Y}} - \mathbf{Diag}(\varphi_{\mathbf{Y}}(\mathbf{Y}^{(k+1)})^T)\mathbf{Y}^{(k+1)}\ \big)$.

Parallel transport tangent vectors $\mathbf{J}^{(k)}$ and $\mathbf{G}^{(k)}$ to the point $\mathbf{Y}^{(k+1)}$.

Compute the new search direction

$$\mathbf{J}^{(k+1)} = -\mathbf{G}^{(k+1)} + \gamma_k \mathbf{T}\mathbf{J}^{(k)} \quad \text{where} \quad \begin{cases} \gamma_k = \frac{\langle \mathbf{G}^{(k+1)} - \mathbf{T}\mathbf{G}^{(k)}, \mathbf{G}^{(k+1)} \rangle}{\langle \mathbf{G}^{(k)}, \mathbf{G}^{(k)} \rangle}, & \text{Polak-Ribière,} \\ \gamma_k = \frac{||\mathbf{G}^{(k+1)}||^2}{||\mathbf{G}^{(k)}||^2}, & \text{Fletcher-Reeves.} \end{cases}$$

Reset $\mathbf{J}^{(k+1)} = -\mathbf{G}^{(k+1)}$ if $k + 1 \equiv 0 \mod n(d-1) - \frac{1}{2}d(d-1)$.

end for

Algorithm 3 Newton's method for minimizing $\varphi(\mathbf{Y})$ on $\mathrm{Chol}_{n,d}$.

Input: $\mathbf{Y}^{(0)}, \varphi(\cdot)$.

Require: $\mathbf{Y}^{(0)}$ such that $\mathbf{Diag}(\mathbf{Y}^{(0)}(\mathbf{Y}^{(0)})^T) = \mathbf{I}$.

for $k = 0, 1, 2, \ldots$ **do**

Compute $\mathbf{G}^{(k)} = \mathbf{Grad}\varphi(\mathbf{Y}^{(k)}) = \mathbf{Z}\big(\ \varphi_{\mathbf{Y}} - \mathbf{Diag}(\varphi_{\mathbf{Y}}\mathbf{Y}^T)\mathbf{Y}\ \big)$.

Compute $\boldsymbol{\Delta}^{(k)} = -\mathbf{H}^{-1}\mathbf{G}^{(k)}$, i.e. $\boldsymbol{\Delta}^{(k)} \in T_{\mathbf{Y}}\mathrm{Chol}_{n,d}$ and

$$\mathbf{Z}\Big(\ \varphi_{\mathbf{YY}}(\boldsymbol{\Delta}^{(k)}) - \mathbf{Diag}\big(\ \varphi_{\mathbf{YY}}(\boldsymbol{\Delta}^{(k)})(\mathbf{Y}^{(k)})^T\ \big)\mathbf{Y}^{(k)}\ \Big) - \mathbf{Diag}(\varphi_{\mathbf{Y}}(\mathbf{Y}^{(k)})^T)\boldsymbol{\Delta}^{(k)} = -\mathbf{G}^{(k)}.$$

Move from $\mathbf{Y}^{(k)}$ in direction $\boldsymbol{\Delta}^{(k)}$ to $\mathbf{Y}^{(k)}(1)$ along the geodesic.

Set $\mathbf{Y}^{(k+1)} = \mathbf{Y}^{(k)}(1)$.

end for

algorithms in the literature. Therefore we focus on the results obtained for the flat-Euclidean case. Zoutendijk (1970) and Al-Baali (1985) establish global convergence of the Fletcher & Reeves (1964) conjugate gradient method with line minimization. Gilbert & Nocedal (1992) establish alternative line search minimizations that guarantee global convergence of the Polak & Ribière (1969) conjugate gradient method.

4.4.2 Local rate of convergence

Local rates of convergence for geometric optimisation algorithms are established in Smith (1993), Edelman, Arias & Smith (1999) and Dedieu, Priouret & Malajovich (2003).

In Theorem 3.3 of Smith (1993), the following result is established for the Riemannian-Newton method. If $\hat{\mathbf{Y}}$ is a non-degenerate stationary point, then there exists an open set $\mathcal{U}$ containing $\hat{\mathbf{Y}}$, such that starting from any $\mathbf{Y}^{(0)}$ in $\mathcal{U}$, the sequence of points produced by Algorithm 3 converges quadratically to $\hat{\mathbf{Y}}$.

In Theorem 4.3 of Smith (1993), the following result is stated for the Riemannian Fletcher & Reeves (1964) and Polak & Ribière (1969) conjugate gradient methods. Suppose $\hat{\mathbf{Y}}$ is a non-degenerate stationary point such that the Hessian at $\hat{\mathbf{Y}}$ is positive definite. Suppose $\{\mathbf{Y}^{(j)}\}_{j=0}^{\infty}$ is a sequence of points, generated by Algorithm 2, converging to $\hat{\mathbf{Y}}$. Then, for sufficiently large j, the sequence $\{\mathbf{Y}^{(j)}\}_{j=0}^{\infty}$ has $\dim(\mathrm{Chol}_{n,d})$-steps quadratic convergence to $\hat{\mathbf{Y}}$.

As a numerical illustration, convergence runs are displayed in Figure 4.2, for reducing a 10×10 correlation matrix to rank 3. The following algorithms are compared:

1. Steepest descent, for which the search direction $\mathbf{J}^{(k+1)}$ in Algorithm 2 is equal to $-\mathbf{G}^{(k+1)}$, i.e., to minus the gradient. The steepest descent method has a linear local rate of convergence, see Smith (1993, Theorem 2.3).

2. PRCG, Polak-Ribière conjugate gradient.

3. FRCG, Fletcher-Reeves conjugate gradient.

4. Newton.

5. Lev.-Mar., the Levenberg (1944) & Marquardt (1963) method, which is a Newton-type method.

The code that is used for this test is the package 'LRCM min', to be discussed in Section 4.6. This package also contains the correlation matrix used for the convergence run test. Figure 4.2 clearly illustrates the convergence properties of the various geometric programs. The efficiency of the algorithms is studied in Section 4.6 below.

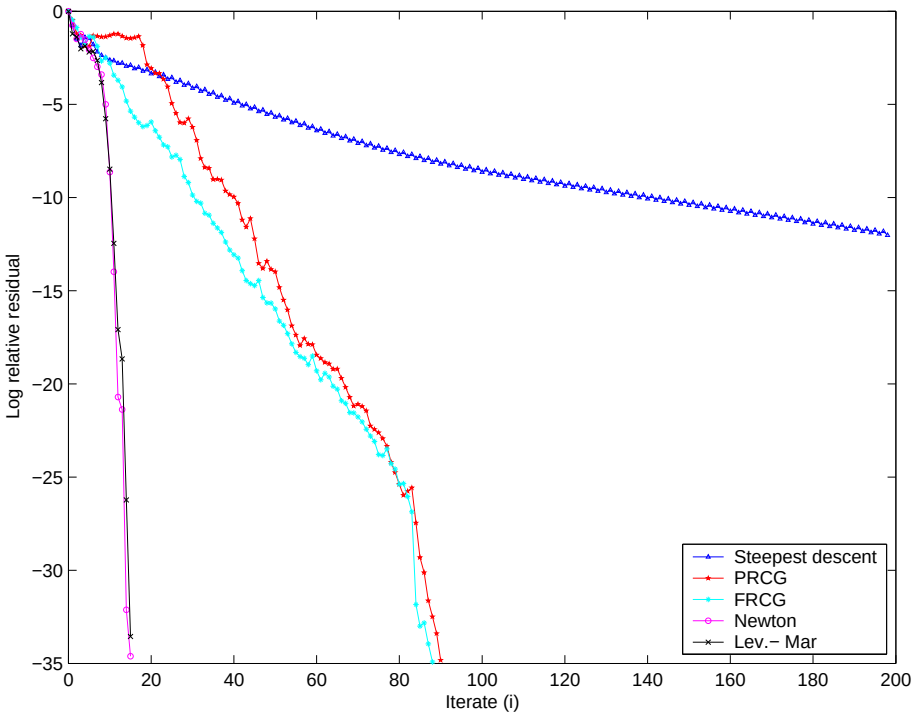

Figure 4.2: Convergence runs: log relative residual $ln(\|\mathbf{Grad}\varphi(\mathbf{Y}^{(i)})\|/\|\mathbf{Grad}\varphi(\mathbf{Y}^{(0)})\|)$ versus the iterate i.

4.5 A special case: Distance minimization

In this section, the primary concern of this chapter to minimize the objective function of (4.2) is studied. The outline of this section is as follows. First, some particular choices for n and d are examined. Second, the differential and Hessian of φ are calculated. Third, the connection with Lagrange multipliers is stated; in particular, this will lead to an identification method of whether a local minimum is a global minimum. Fourth, we discuss the PCA with re-scaling method for obtaining an initial feasible point.

4.5.1 The case of $d = n$

The case that $\mathbf{P}$ is a symmetric matrix and the closest positive semidefinite matrix $\mathbf{C}$ is to be found allows a successive projection solution, which was shown by Higham (2002).

4.5.2 The case of $d = 2$, $n = 3$

A 3×3 symmetric matrix with ones on the diagonals is denoted by

$$\begin{pmatrix} 1 & x & y \\ x & 1 & z \\ y & z & 1 \end{pmatrix}.$$

Its determinant is given by

$$\det = -\left\{ x^2 + y^2 + z^2 \right\} + 2xyz + 1.$$

By straightforward calculations it can be shown that $\det = 0$ implies that all eigenvalues are nonnegative. The set of 3 by 3 correlation matrices of rank 2 may thus be represented by the set $\{\det = 0\}$. To get an intuitive understanding of the complexity of the problem, the feasible region has been displayed in Figure 4.1.

4.5.3 Formula for the differential of φ

We consider the specific case of the weighted Hadamard semi-norm of (4.2). This semi-norm can be represented by a Frobenius norm by introducing the Hadamard product $\circ$. The Hadamard product denotes entry-by-entry multiplication. Formally, for two matrices $\mathbf{A}$ and $\mathbf{B}$ of equal dimensions, the Hadamard product $\mathbf{A} \circ \mathbf{B}$ is defined by $(\mathbf{A} \circ \mathbf{B})_{ij} = a_{ij} b_{ij}$. The objective function (4.2) can then be written as

$$\varphi(\mathbf{Y}) = \frac{1}{2} \sum_{i<j} w_{ij} (\rho_{ij} - \mathbf{y}_i \mathbf{y}_j^T)^2 = \frac{1}{2} \|\mathbf{W}^{\circ 1/2} \circ \mathbf{\Psi}\|_\varphi^2 = \frac{1}{2} \langle \mathbf{W}^{\circ 1/2} \circ \mathbf{\Psi}, \mathbf{W}^{\circ 1/2} \circ \mathbf{\Psi} \rangle,$$

with $\mathbf{\Psi} := \mathbf{Y}\mathbf{Y}^T - \mathbf{P}$ and with $(\mathbf{W}^{\circ 1/2})_{ij} = \sqrt{w_{ij}}$. Then

$$\begin{aligned}\frac{\mathrm{d}}{\mathrm{d}t}\varphi(\mathbf{Y}(t)) &= \langle \mathbf{W}^{\circ 1/2} \circ \dot{\mathbf{\Psi}}, \mathbf{W}^{\circ 1/2} \circ \mathbf{\Psi}\rangle = \langle \dot{\mathbf{\Psi}}, \mathbf{W} \circ \mathbf{\Psi}\rangle \\ &= \langle \mathbf{\Delta}\mathbf{Y}^T + \mathbf{Y}\mathbf{\Delta}^T, \mathbf{W} \circ \mathbf{\Psi}\rangle \\ &= \langle \mathbf{\Delta}\mathbf{Y}^T, \mathbf{W} \circ \mathbf{\Psi}\rangle + \langle \mathbf{Y}\mathbf{\Delta}^T, \mathbf{W} \circ \mathbf{\Psi}\rangle \\ &= \langle \mathbf{\Delta}, 2(\mathbf{W} \circ \mathbf{\Psi})\mathbf{Y}\rangle \;=\; \langle \mathbf{\Delta}, \varphi_{\mathbf{Y}}\rangle, \;\; \forall \mathbf{\Delta}.\end{aligned}$$

Thus from (4.7) we have

$$\varphi_{\mathbf{Y}} = 2(\mathbf{W} \circ \mathbf{\Psi})\mathbf{Y}. \tag{4.24}$$

Similarly, we may compute the second derivative

$$\varphi_{\mathbf{Y}\mathbf{Y}}(\mathbf{\Delta}) = \frac{\mathrm{d}}{\mathrm{d}t}\Big|_{t=0} \varphi_{\mathbf{Y}}(\mathbf{Y}(t)) = 2\Big((\mathbf{W} \circ \mathbf{\Psi})\mathbf{\Delta} + \big(\mathbf{W} \circ (\mathbf{\Delta}\mathbf{Y}^T + \mathbf{Y}\mathbf{\Delta}^T)\big)\mathbf{Y}\Big),$$

with $\mathbf{Y}(\cdot)$ any curve starting from $\mathbf{Y}$ in the direction of $\mathbf{\Delta}$.

4.5.4 Connection normal with Lagrange multipliers

The following lemma provides the basis for the connection of the normal vector at $\mathbf{Y}$ versus the Lagrange multipliers of the algorithm of Zhang & Wu (2003) and Wu (2003). The result is novel since previously only an expression was known for the matrix $\mathbf{Y}$ given the Lagrange multipliers. The result below establishes the reverse direction. This Lagrange result will allow us to identify whether a local minimum is also a global minimum. That we are able to efficiently determine whether a local minimum is a global minimum, is a very rare phenomenon in non-convex optimisation, and makes the rank reduction problem (non-convex for $d < n$) all the more interesting.

We note that the Lagrange theory is based on an efficient expression of the low-rank projection by an eigenvalue decomposition. Therefore the theory below can be extended efficiently only for the Hadamard norm with equal weights and for the weighted Frobenius norm, see also the discussion in Section 4.1.1. The proof of the following lemma has been deferred to Appendix 4.A.6.

Lemma 1 *Let $\mathbf{Y} \in T_{n,d}$ be such that $\mathbf{Grad}\varphi(\mathbf{Y}) = 0$. Here, $\mathbf{Grad}\varphi$ is the gradient of φ on $T_{n,d}$, $\mathbf{Grad}\varphi(\mathbf{Y}) = \mathbf{\Pi}_{T_{\mathbf{Y}}T_{n,d}}(\varphi_{\mathbf{Y}}) = \varphi_{\mathbf{Y}} - \mathbf{Diag}(\varphi_{\mathbf{Y}}\mathbf{Y}^T)\mathbf{Y}$, with $\varphi_{\mathbf{Y}}$ in (4.24). Define*

$$\boldsymbol{\lambda} := \frac{1}{2}\,\mathbf{diag}\big(\,\varphi_{\mathbf{Y}}\mathbf{Y}^T\,\big)$$

and define $\mathbf{P}(\boldsymbol{\lambda}) := \mathbf{P} + \mathbf{Diag}(\boldsymbol{\lambda})$. Then there exist a joint eigenvalue decomposition

$$\mathbf{P}(\boldsymbol{\lambda}) = \mathbf{Q}\mathbf{D}\mathbf{Q}^T, \;\; \mathbf{Y}\mathbf{Y}^T = \mathbf{Q}\mathbf{D}^*\mathbf{Q}^T$$

where $\mathbf{D}^*$ can be obtained by selecting at most d nonnegative entries from $\mathbf{D}$ (here if an entry is selected it retains the corresponding position in the matrix).

The characterization of the global minimum for Problem (4.1) was first achieved in Zhang & Wu (2003) and Wu (2003), which we repeat here: Denote by $\{\mathbf{C}\}_d$ a matrix obtained by eigenvalue decomposition of $\mathbf{C}$ together with leaving in only the d largest eigenvalues (in absolute value). Denote for $\boldsymbol{\lambda} \in \mathbb{R}^n$: $\mathbf{P}(\boldsymbol{\lambda}) = \mathbf{P} + \mathbf{Diag}(\boldsymbol{\lambda})$. The proof of the following theorem has been repeated for clarity in Appendix 4.A.7.

Theorem 5 (Characterization of the global minimum of Problem (4.1), see Zhang & Wu (2003) and Wu (2003)) *Let* $\mathbf{P}$ *be a symmetric matrix. Let* $\boldsymbol{\lambda}^*$ *be such that there exists* $\{\mathbf{P} + \mathbf{Diag}(\boldsymbol{\lambda}^*)\}_d \in C_{n,d}$ *with*

$$\mathbf{Diag}\big(\{\mathbf{P} + \mathbf{Diag}(\boldsymbol{\lambda}^*)\}_d \big) = \mathbf{Diag}(\mathbf{P}). \tag{4.25}$$

Then $\{\mathbf{P} + \mathbf{Diag}(\boldsymbol{\lambda}^*)\}_d$ *is a global minimizer of Problem (4.1).*

This brings us in a position to identify whether a local minimum is a global minimum:

Theorem 6 *Let* $\mathbf{Y} \in T_{n,d}$ *be such that* $\mathbf{Grad}\varphi(\mathbf{Y}) = 0$ *on* $T_{n,d}$*. Let* $\boldsymbol{\lambda}$ *and* $\mathbf{P}(\boldsymbol{\lambda})$ *be defined as in Lemma 1. If* $\mathbf{YY}^T$ *has the d largest eigenvalues from* $\mathbf{P}(\boldsymbol{\lambda})$ *(in absolute value) then* $\mathbf{YY}^T$ *is a global minimizer to the Problem (4.1).*

PROOF: Apply Lemma 1 and Theorem 5. □

4.5.5 Initial feasible point

To obtain an initial feasible point $\mathbf{Y} \in T_{n,d}$ we use the modified PCA method described in Section 3.2.1. To obtain an initial feasible point in $\text{Chol}_{n,d}$, we perform a Cholesky decomposition as in the proof of Theorem 3.

We note that the condition in Section 3.2.1 of decreasing norm of the eigenvalues is thus key to ensure that the initial point is close to the global minimum, see the result of Theorem 6.

4.6 Numerical results

There are many different algorithms available in the literature, as detailed in Section 3.2. Some of these have an efficient implementation, i.e., the cost of a single iteration is low. Some algorithms have fast convergence, for example, the Newton method has quadratic convergence. Algorithms with fast convergence usually require less iterations to attain a predefined convergence criterion. Thus, the real-world performance of an algorithm is a trade-off between cost-per-iterate and number of iterations required. A priori, it is not clear which algorithm will perform best. Therefore, in this section, the numerical performance of geometric optimisation is compared to other methods available in the literature.

4.6.1 Acknowledgement

Our implementation of geometric optimisation over low-rank correlation matrices 'LRCM min'[3] is an adoption of the 'SG min' template of Edelman & Lippert (2000) (written in MATLAB) for optimisation over the Stiefel and Grassmann manifolds. This template contains four distinct well-known non-linear optimisation algorithms adapted for geometric optimisation over Riemannian manifolds: Newton algorithm; dogleg step or Levenberg (1944) and Marquardt (1963) algorithm; Polak & Ribière (1969) conjugate gradient; and Fletcher & Reeves (1964) conjugate gradient.

4.6.2 Numerical comparison

The performances of the following seven algorithms, all of these described in Sections 4.3 and 3.2, except for item 7 (`fmincon`), are compared:

1. Geometric optimisation, Newton (Newton).
2. Geometric optimisation, Fletcher-Reeves conjugate gradient (FRCG).
3. Majorization, e.g., Pietersz & Groenen (2004*b*) (Chapter 3) (Major.).
4. Parametrization, e.g., Rebonato (1999*b*) (Param.).
5. Alternating projections without normal vector correction, e.g., Grubišić (2002) (Alt. Proj.).
6. Lagrange multipliers, e.g., Zhang & Wu (2003) (Lagrange).
7. `fmincon`, a MATLAB built-in medium-scale constrained nonlinear program (fmincon).

We note that the first two algorithms in this list have been developed in this chapter. The algorithms are tested on a large number (one hundred) of randomly generated correlation matrices. The benefit of testing on many correlation matrices is, that the overall and generic performance of the algorithms may be assessed. The random financial correlation matrices are generated as described in Section 3.5.1.

As the benchmark criterion for the performance of an algorithm, we take its obtained accuracy of fit given a fixed amount of computational time. Such a criterion corresponds to financial practice, since decisions based on derivative valuation calculations often need to be made within seconds. To display the comparison results, we use the state-of-the-art and convenient *performance profiles*; see Dolan & Moré (2002). The reader is referred

[3]LRCM min can be downloaded from `www.few.eur.nl/few/people/pietersz`.

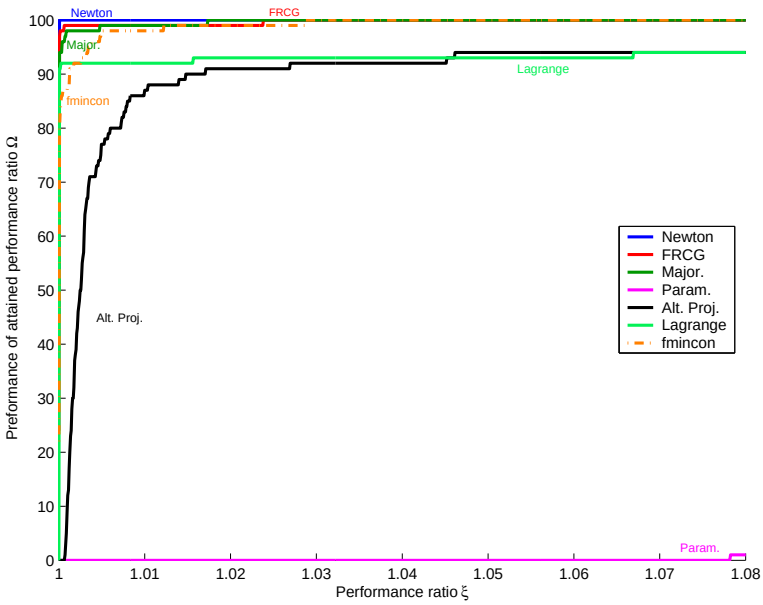

Figure 4.3: Performance profile with $n = 30$, $d = 3$, 2 seconds of computational time, Hadamard norm with equal weights. A rule of thumb is, that the higher the graph of an algorithm, the better its performance.

there for details, but the idea is described briefly in Section 3.5.1. A rule of thumb is, that the higher the profile of an algorithm, the better its performance. The performance profiles are displayed in Figures 4.3–4.6, for various choices of n, d, and computational times. Each performance profile represents a benchmark on 100 different test interest rate correlation matrices. For Figures 4.3–4.5, an objective function with equal weights is used. For Figure 4.6, we use a Hadamard semi-norm with non-constant weights. These weights are chosen so as to reflect the importance of the correlation entries for a specific trigger swap, as outlined in, e.g., Rebonato (2004*b*, Section 20.4.3). For this specific trigger swap, the first three rows and columns are important. Therefore the weights matrix $\mathbf{W}$ takes the form

$$w_{ij} = \begin{cases} 1 & \text{if } i \leq 3 \text{ or } j \leq 3, \\ 0 & \text{otherwise.} \end{cases}$$

From Figures 4.3–4.6 it becomes clear that geometric optimisation compares favourably to the other methods available in the literature, with respect to obtaining the best fit to the original correlation matrix within a limited computational time.

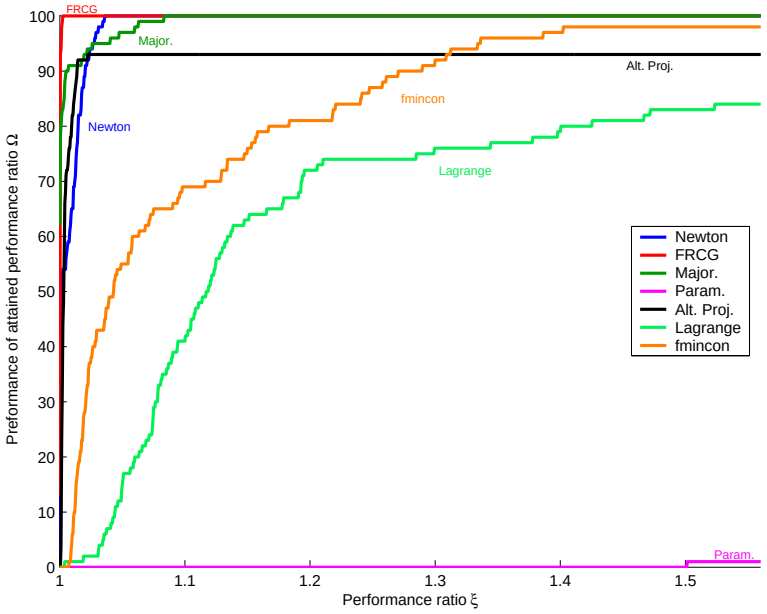

Figure 4.4: Performance profile with $n = 50$, $d = 4$, 1 second of computational time, Hadamard norm with equal weights.

4.7 Conclusions

We applied geometric optimisation tools for finding the nearest low-rank correlation matrix. The differential geometric machinery provided us with an algorithm more efficient than any existing algorithm in the literature, at least for the numerical cases considered. The geometric approach also allows for insight and more intuition into the problem. We established a technique that allows one to straightforwardly identify whether a local minimum is a global minimum.

4.A Appendix: Proofs

4.A.1 Proof of Theorem 2

PROOF *of (i). The maps* $\mathbf{\Psi}$ *and* $\mathbf{\Phi}$ *are well defined:* To show that $\mathbf{\Psi}$ is well defined, we need to show that if $\mathbf{Y}_2 \in [\mathbf{Y}_1]$, then $\mathbf{Y}_2\mathbf{Y}_2^T = \mathbf{Y}_1\mathbf{Y}_1^T$. From the assumption, we have

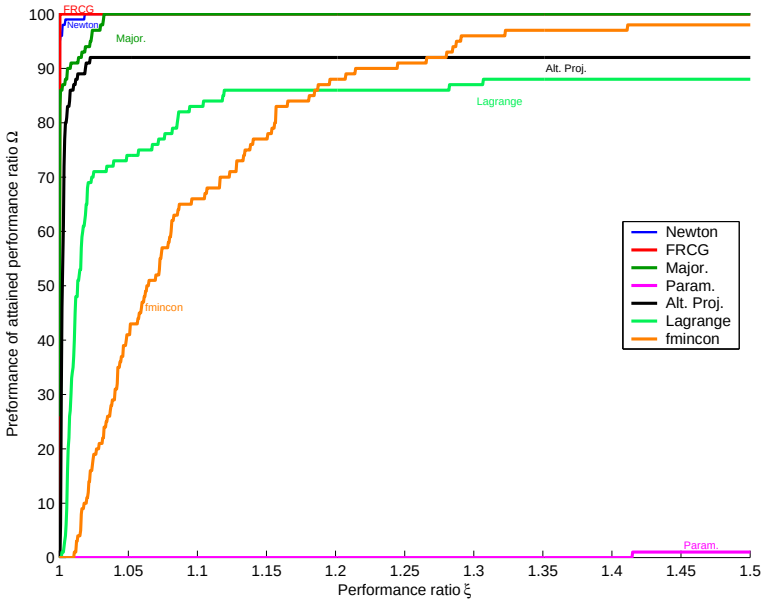

Figure 4.5: Performance profile with $n = 60$, $d = 5$, 3 seconds of computational time, Hadamard norm with equal weights.

that $\exists \mathbf{Q} \in O_d : \ \mathbf{Y}_2 = \mathbf{Y}_1\mathbf{Q}$. If follows that

$$\mathbf{Y}_2\mathbf{Y}_2^T = (\mathbf{Y}_1\mathbf{Q})(\mathbf{Y}_1\mathbf{Q})^T = \mathbf{Y}_1\mathbf{Q}\mathbf{Q}^T Y_1^T = \mathbf{Y}_1\mathbf{Y}_1^T,$$

which was to be shown.

To show that $\mathbf{\Phi}$ is well defined, we need to show:

(A) If $\mathbf{C} \in C_{n,d}$ then there exists $\mathbf{Y} \in T_{n,d}$ such that $\mathbf{C} = \mathbf{Y}\mathbf{Y}^T$.

(B) If $\mathbf{X}, \mathbf{Y} \in T_{n,d}$, with $\mathbf{X}\mathbf{X}^T = \mathbf{Y}\mathbf{Y}^T =: \mathbf{C}$ then there exists $\mathbf{Q} \in O_d$ such that $\mathbf{X} = \mathbf{Y}\mathbf{Q}$.

Ad (A): Let

$$\mathbf{C} = \mathbf{Q}\mathbf{D}\mathbf{Q}^T, \ \ \mathbf{Q} \in O_n, \ \ \mathbf{D} = \mathbf{Diag}(\mathbf{D}),$$

be an eigenvalue decomposition with $d_{ii} = 0$ for $i = d+1, \ldots, n$. We note that such a decomposition of the specified form is possible because of the restriction $\mathbf{C} \in C_{n,d}$. Then note that

$$\mathbf{Q}\sqrt{\mathbf{D}} = \left(\ (\mathbf{Q}\sqrt{\mathbf{D}})(:, 1:d) \ \middle| \ 0 \ \right).$$

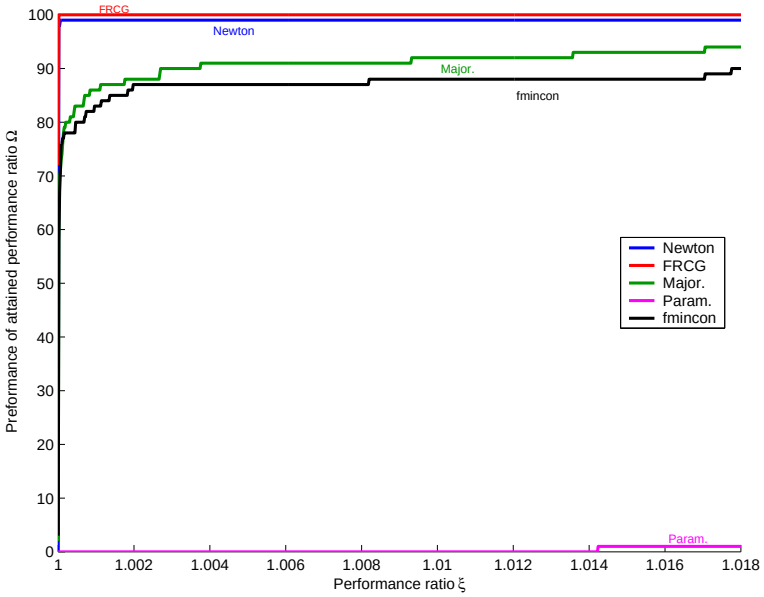

Figure 4.6: Performance profile with $n = 15$, $d = 3$, 1 second of computational time, trigger swap Hadamard semi-norm.

Thus if we set $\mathbf{Y} = (\mathbf{Q}\sqrt{\mathbf{D}})(:, 1:d)$ then $\mathbf{Y}\mathbf{Y}^T = \mathbf{C}$ and $\mathbf{Y} \in T_{n,d}$, which was to be shown.

Ad (B): Let $\operatorname{rank}(\mathbf{X}) = \operatorname{rank}(\mathbf{Y}) = \operatorname{rank}(\mathbf{C}) = k \leq d$. Without loss of generality, we may assume that the first k rows of $\mathbf{X}$ and $\mathbf{Y}$ are independent. We extend the set of k row vectors $\{\mathbf{x}_1, \ldots, \mathbf{x}_k\}$ to a set of d row vectors $\{\mathbf{x}_1, \ldots, \mathbf{x}_k, \tilde{\mathbf{x}}_{k+1}, \ldots, \tilde{\mathbf{x}}_d\}$, such that the latter forms a basis of $\mathbb{R}^d$. Similarly, we obtain a basis $\{\mathbf{y}_1, \ldots, \mathbf{y}_k, \tilde{\mathbf{y}}_{k+1}, \ldots, \tilde{\mathbf{y}}_d\}$ of $\mathbb{R}^d$. It follows that there exists an orthogonal rotation $\mathbf{Q}$, $\mathbf{Q}\mathbf{Q}^T = \mathbf{I}$, such that $\mathbf{Q}\mathbf{x}_i = \mathbf{y}_i$ $(i = 1, \ldots, k)$, $\mathbf{Q}\tilde{\mathbf{x}}_i = \tilde{\mathbf{y}}_i$ $(i = k+1, \ldots, d)$. We note that then also $\mathbf{Q}\mathbf{x}_i = \mathbf{y}_i$ for $i = k+1, \ldots, n$, by linearity of $\mathbf{Q}$ and since the last $n - k$ row vectors are linearly dependent on the first k row vectors by assumption. It follows that $\mathbf{X}\mathbf{Q} = \mathbf{Y}$, which was to be shown. □

PROOF *of (ii). Diagram (4.5) is commutative:* To show $\boldsymbol{\Psi} \circ \boldsymbol{\Pi} = \mathbf{S}$: Let $\mathbf{Y} \in T_{n,d}$, then $\boldsymbol{\Pi}(\mathbf{Y}) = [\mathbf{Y}]$ and $\boldsymbol{\Psi}([\mathbf{Y}]) = \mathbf{Y}\mathbf{Y}^T$ and also $\mathbf{S}(\mathbf{Y}) = \mathbf{Y}\mathbf{Y}^T$. To show that $\boldsymbol{\Phi} \circ \mathbf{S} = \boldsymbol{\Pi}$: Let $\mathbf{Y} \in T_{n,d}$, then $\mathbf{S}(\mathbf{Y}) = \mathbf{Y}\mathbf{Y}^T$ and $\boldsymbol{\Phi}(\mathbf{Y}\mathbf{Y}^T) = [\mathbf{Y}]$ and also $\boldsymbol{\Pi}(\mathbf{Y}) = [\mathbf{Y}]$. □

PROOF *of (iii). The map $\boldsymbol{\Psi}$ is a homeomorphism with inverse $\boldsymbol{\Phi}$:* It is straightforward to verify that $\boldsymbol{\Phi} \circ \boldsymbol{\Psi}$ and $\boldsymbol{\Psi} \circ \boldsymbol{\Phi}$ are both the identity maps. The map $\boldsymbol{\Psi}$ is thus

bijective with inverse $\mathbf{\Phi}$. To show that $\mathbf{\Psi}$ is continuous, note that for quotient spaces we have: The map $\mathbf{\Psi}$ is continuous if and only if $\mathbf{\Psi} \circ \mathbf{\Pi}$ is continuous (see for example Abraham, Marsden & Ratiu (1988), Proposition 1.4.8). In our case, $\mathbf{\Psi} \circ \mathbf{\Pi} = \mathbf{S}$ with $\mathbf{S}(\mathbf{Y}) = \mathbf{Y}\mathbf{Y}^T$ is continuous. The proof now follows from a well-known lemma from topology: A continuous bijection from a compact space into a Hausdorff space is a homeomorphism (see for example Munkres (1975), Theorem 5.6). □

4.A.2 Proof of Proposition 2

1. It is sufficient to show that $\{\mathbf{Y} \in \mathbb{R}^{n\times d} : \text{rank}(\mathbf{Y}) = d\}$ is open in $\mathbb{R}^{n\times d}$, since $T^*_{n,d}$ is open in $T_{n,d}$ if and only if $\{\mathbf{Y} \in \mathbb{R}^{n\times d} : \text{rank}(\mathbf{Y}) = d\}$ is open in $\mathbb{R}^{n\times d}$. Since the rank of a symmetric matrix is a locally constant function, it follows that $\{\mathbf{Y} \in \mathbb{R}^{n\times d} : \text{rank}(\mathbf{Y}) = d\} = \mathbf{S}^{-1}(\text{rank}^{-1}(d))$ is an open subset of $\mathbb{R}^{n\times d}$, with $\mathbf{S}(\mathbf{Y}) = \mathbf{Y}\mathbf{Y}^T$ as in Definition 2. □

2. This part is a corollary of Theorem 1.11.4 of Duistermaat & Kolk (2000). This theorem essentially states that for a smooth action of a Lie group on a manifold the quotient is a manifold if the action is proper and free. First, we show that the action of O_d on $T^*_{n,d}$ is proper[4]. Let

$$\mathbf{\Xi} : T^*_{n,d} \times O_d \to T^*_{n,d} \times T^*_{n,d}, \;\; (\mathbf{Y}, \mathbf{Q}) \mapsto (\mathbf{YQ}, \mathbf{Y})$$

and K a compact subset of $T^*_{n,d} \times T^*_{n,d}$. We have to show that $\mathbf{\Xi}^{-1}(K)$ is compact. By continuity of $\mathbf{\Xi}$, $\mathbf{\Xi}^{-1}(K)$ is closed in $T^*_{n,d} \times O_d$. Because $T^*_{n,d} \times O_d$ is bounded it follows that $\mathbf{\Xi}^{-1}(K)$ is compact.

Second, we show that the O_d-action on $T^*_{n,d}$ is free. Let $\mathbf{Y} \in T^*_{n,d}$ and $\mathbf{Q} \in O_d$ such that $\mathbf{YQ} = \mathbf{Y}$. Since $\text{rank}(\mathbf{Y}) = d$, it follows from the proof of Theorem 2 (i) that there exists precisely one $\mathbf{Q} \in O_d$ such that $\mathbf{YQ} = \mathbf{Y}$. Thus, this $\mathbf{Q}$ must be the identity matrix.

The dimension of $M^*_{n,d} = \dim(T^*_{n,d}) - \dim(O_d) = n(d-1) - \frac{1}{2}d(d-1)$. □

4.A.3 Proof of Proposition 3

This part is a corollary of Theorem 1.11.4 of Duistermaat & Kolk (2000). This theorem states that there is only one differentiable structure on the orbit space which satisfies the following: Suppose that, for every $[\mathbf{Y}] \in M^*_{n,d}$, we have an open neighbourhood $\mathcal{U} \subseteq M^*_{n,d}$ and a bijective map:

$$\mathbf{U} : \mathbf{\Pi}^{-1}(\mathcal{U}) \to \mathcal{U} \times O_d, \;\; \mathbf{Y} \mapsto (\mathbf{\Pi}(\mathbf{Y}), \mathbf{V}(\mathbf{Y})),$$

[4]For a definition, see Duistermaat & Kolk (2000, page 53).

such that, for every $\mathbf{Y} \in \mathbf{\Pi}^{-1}(\mathcal{U})$, $\mathbf{Q} \in O_d$, $\mathbf{U}(\mathbf{YQ}) = (\mathbf{\Pi}(\mathbf{Y}), \mathbf{V}(\mathbf{Y})\mathbf{Q})$. The differentiable structure on $M^*_{n,d}$ is the one which makes $\mathbf{U}$ into a diffeomorphism. The topology of $M^*_{n,d}$ obtained in this manner is equal to the quotient topology.

Let $\mathbf{Y} \in T^*_{n,d}$ and $\mathbf{\Sigma_Y}$ be a section over $\mathcal{U}_\mathbf{Y}$ defined in (4.6). We define $\mathbf{U_Y} : \mathbf{\Pi}^{-1}(\mathcal{U}_\mathbf{Y}) \to \mathcal{U}_\mathbf{Y} \times O_d$ as follows. For $\mathbf{Z} \in \mathbf{\Pi}^{-1}([\mathbf{Z}])$, $[\mathbf{Z}] \in \mathcal{U}_\mathbf{Y}$, there is a unique element $\mathbf{Q_Z} \in O_d$ such that $\mathbf{Z} = \mathbf{\Sigma_Y}([\mathbf{Z}])\mathbf{Q_Z}$. Then we define $\mathbf{U_Y}$ by $\mathbf{U_Y}(\mathbf{Z}) = ([\mathbf{Z}], \mathbf{Q_Z})$. By definition, we have that $\mathbf{U}_\mathbf{Y}^{-1}([\mathbf{Z}], \mathbf{Q}) = \mathbf{\Sigma_Y}([\mathbf{Z}])\mathbf{Q}$. Since $\mathbf{U}_\mathbf{Y}^{-1} : \mathbf{\Pi}^{-1}(\mathcal{U}_\mathbf{Y}) \to \mathcal{U}_\mathbf{Y} \times O_d$ is a bijective map, we have that $\mathbf{U_Y}$ is bijective, too. It can be easily verified that $\mathbf{U_Y}$ satisfies the condition $\mathbf{U_Y}(\mathbf{YQ}) = ([\mathbf{Y}], \mathbf{Q_Y Q})$ of Theorem 1.11.4 of Duistermaat & Kolk (2000) stated above. It follows that $\mathbf{U_Y}$ is a diffeomorphism if and only if $\mathbf{\Sigma_Y} : \mathcal{U} \to \mathbf{\Sigma_Y}(\mathcal{U})$ is a diffeomorphism. Thus, the differentiable structure on $M^*_{n,d}$ is the one which makes $\mathbf{\Sigma_Y} : \mathcal{U}_\mathbf{Y} \to \mathbf{\Sigma}(\mathcal{U}_\mathbf{Y})$ into a diffeomorphism. □

4.A.4 Proof of Theorem 3

Let $\mathbf{C} \in C_{n,d}$ and suppose that $\operatorname{rank}(\mathbf{C}) = k \leq d$. Then there is a $\mathbf{Y} \in T_{n,k}$ such that $\mathbf{YY}^T = \mathbf{C}$, by Theorem 2. Apply to $\mathbf{Y}$ the procedure[5] outlined in Section 4.2.3, to obtain a lower-triangular matrix $\mathbf{Y}^* \in T_{n,k}$, such that $\mathbf{Y}^*(\mathbf{Y}^*)^T = \mathbf{C}$. A lower-triangular matrix $\bar{\mathbf{Y}} \in \operatorname{Chol}_{n,d}$ that satisfies $\bar{\mathbf{Y}}\bar{\mathbf{Y}}^T = \mathbf{C}$ can now easily be obtained by setting

$$\bar{\mathbf{Y}} = \begin{pmatrix} \mathbf{Y}^* & \underbrace{\mathbf{0}}_{n \times (d-k)} \end{pmatrix},$$

which was to be shown. □

4.A.5 Proof of Theorem 4

First, we prove the 'only if' part. We note that it is sufficient to show that the map $\mathbf{S} : \operatorname{Chol}_{n,d} \to C_{n,d}$ is *open*. For then if $\mathbf{Y}$ attains a local minimum of φ on the open neighbourhood $\mathcal{U} \subset \operatorname{Chol}_{n,d}$, then $\mathbf{S}(\mathbf{Y}) = \mathbf{YY}^T$ attains a local minimum of $\tilde{\varphi}$ on the open neighbourhood $\mathbf{S}(\mathcal{U})$ of $\mathbf{YY}^T$, since for any $\mathbf{C}' = \mathbf{Y}'\mathbf{Y}'^T \in \mathbf{S}(\mathcal{U})$, $\tilde{\varphi}(\mathbf{C}') = \tilde{\varphi}(\mathbf{Y}'\mathbf{Y}'^T) = \varphi(\mathbf{Y}') \geq \varphi(\mathbf{Y}) = \tilde{\varphi}(\mathbf{YY}^T)$.

To show that $\mathbf{S} : \operatorname{Chol}_{n,d} \to C_{n,d}$ is open, note that it is sufficient to show that $\mathbf{\Pi} : \operatorname{Chol}_{n,d} \to M_{n,d}$ is open, since $\mathbf{\Psi} : M_{n,d} \to C_{n,d}$ is a homeomorphism (see Proposition 2, item 3) and $\mathbf{S} = \mathbf{\Psi} \circ \mathbf{\Pi}$.

Suppose, then, that $\mathcal{U}$ is open in $\operatorname{Chol}_{n,d}$. We have to show that $\mathbf{\Pi}^{-1}(\mathbf{\Pi}(\mathcal{U}))$ is open in $T_{n,d}$, by definition of the quotient topology of $M_{n,d}$. We have

$$\mathbf{\Pi}^{-1}\big(\ \mathbf{\Pi}(\mathcal{U})\ \big) = \big\{\ \mathbf{YQ}\ :\ \mathbf{Y} \in \mathcal{U},\ \mathbf{Q} \in O_d\ \big\}.$$

[5] The procedure in Section 4.2.3 is stated in terms of d, but k should be read there in this case.

It is sufficient to show that the complement $(\mathbf{\Pi}^{-1}(\mathbf{\Pi}(\mathcal{U})))^c$ is closed. Let $\{\mathbf{Y}^{(i)}\}$ be a sequence in $(\mathbf{\Pi}^{-1}(\mathbf{\Pi}(\mathcal{U})))^c$ converging to $\mathbf{Y}$, i.e. $\lim_{i\to\infty}\|\mathbf{Y}^{(i)}-\mathbf{Y}\|=0$. We can write $\mathbf{Y}^{(i)}=\mathbf{Z}^{(i)}\mathbf{Q}^{(i)}$ with $\mathbf{Z}^{(i)}\in\mathcal{U}^c$ and $\mathbf{Q}^{(i)}\in O_d$. Then,

$$\lim_{i\to\infty}\|\mathbf{Y}^{(i)}-\mathbf{Y}\|=\lim_{i\to\infty}\|\mathbf{Z}^{(i)}\mathbf{Q}^{(i)}-\mathbf{Y}\|=\lim_{i\to\infty}\|\mathbf{Z}^{(i)}-\mathbf{Y}(\mathbf{Q}^{(i)})^T\|=0. \tag{4.26}$$

Since $\mathcal{U}^c\times O_d$ is compact, there exists a convergent subsequence $\{(\mathbf{Z}^{(i_j)},\mathbf{Q}^{(i_j)})\}$, with $\mathbf{Z}^{(i_j)}\to\mathbf{Z}^*\in\mathcal{U}^c$ and $\mathbf{Q}^{(i_j)}\to\mathbf{Q}^*$, say. From (4.26) it follows that $\mathbf{Z}^*=\mathbf{Y}(\mathbf{Q}^*)^T\in\mathcal{U}^c$, which implies $\mathbf{Y}\in(\mathbf{\Pi}^{-1}(\mathbf{\Pi}(\mathcal{U})))^c$.

The reverse direction is obvious since the map $\mathbf{S}:\mathrm{Chol}_{n,d}\to C_{n,d}$ is continuous. □

4.A.6 Proof of Lemma 1

It is recalled from matrix analysis that $\mathbf{C}_1$ and $\mathbf{C}_2$ admit a joint eigenvalue decomposition if and only if their Lie bracket $[\mathbf{C}_1,\mathbf{C}_2]=\mathbf{C}_1\mathbf{C}_2-\mathbf{C}_2\mathbf{C}_1$ equals zero. Define $\bar{\mathbf{P}}(\boldsymbol{\lambda}):=-\mathbf{\Psi}+\mathbf{Diag}(\boldsymbol{\lambda})$. We note that $2\mathbf{Diag}(\boldsymbol{\lambda})\mathbf{Y}$ is the projection $\mathbf{\Pi}_{N_{\mathbf{Y}}T_{n,d}}(\varphi_{\mathbf{Y}})$ of $\varphi_{\mathbf{Y}}$ onto the normal space at $\mathbf{Y}$. We note also that

$$\mathbf{Y}\mathbf{Y}^T+\bar{\mathbf{P}}(\boldsymbol{\lambda})=\mathbf{P}(\boldsymbol{\lambda}). \tag{4.27}$$

We calculate

$$\bar{\mathbf{P}}(\boldsymbol{\lambda})\mathbf{Y}=\big\{-\mathbf{\Psi}+\mathbf{Diag}(\boldsymbol{\lambda})\big\}\mathbf{Y}=-\frac{1}{2}\varphi_{\mathbf{Y}}+\frac{1}{2}\mathbf{\Pi}_{N_{\mathbf{Y}}T_{n,d}}\big(\varphi_{\mathbf{Y}}\big)=0. \tag{4.28}$$

The last equality follows from the assumption that $\mathbf{Grad}\varphi(\mathbf{Y})=0$, i.e. the differential $\varphi_{\mathbf{Y}}$ is normal at $\mathbf{Y}$. (Here, $\mathbf{Grad}\varphi(\mathbf{Y})$ denotes the gradient on $T_{n,d}$.) It follows from (4.28) and from the symmetry of $\bar{\mathbf{P}}(\boldsymbol{\lambda})$ that

(i) $\mathbf{Y}\mathbf{Y}^T\bar{\mathbf{P}}(\boldsymbol{\lambda})=0$ and also,

(ii) $[\mathbf{Y}\mathbf{Y}^T,\bar{\mathbf{P}}(\boldsymbol{\lambda})]=0$.

From (ii), $\mathbf{Y}\mathbf{Y}^T$ and $\bar{\mathbf{P}}(\boldsymbol{\lambda})$ admit a joint eigenvalue decomposition, but then also jointly with $\mathbf{P}(\boldsymbol{\lambda})$ because of (4.27). Suppose $\bar{\mathbf{P}}(\boldsymbol{\lambda})=\mathbf{Q}\bar{\mathbf{D}}\mathbf{Q}^T$. From (i) we then have that d^*_{ii} and $\bar{d}_{ii}$ cannot both be non-zero. The result now follows since $\mathbf{Y}\mathbf{Y}^T$ is positive semidefinite and has rank less than or equal to d. □

4.A.7 Proof of Theorem 5

Define the Lagrangian

$$\ell(\mathbf{C},\boldsymbol{\lambda}):=-\|\mathbf{P}-\mathbf{C}\|^2_{\varphi}-2\boldsymbol{\lambda}^T\mathbf{diag}(\mathbf{P}-\mathbf{C}),\quad\text{and}$$

$$v(\boldsymbol{\lambda}) := \min \left\{ \ \ell(\mathbf{C}, \boldsymbol{\lambda}) \ : \ \mathrm{rank}(\mathbf{C}) = d \ \right\}. \tag{4.29}$$

We note that the minimization problem in (4.29) is attained by any $\{\mathbf{P}(\boldsymbol{\lambda})\}_d$ (see e.g., Equation (30) of Wu (2003)). For any $\mathbf{C} \in C_{n,d}$,

$$\|\mathbf{P} - \mathbf{C}\|_F^2 \overset{(a)}{=} -\ell(\mathbf{C}, \boldsymbol{\lambda}^*) \overset{(b)}{\geq} -v(\boldsymbol{\lambda}^*) \overset{(c)}{=} \|\mathbf{P} - \{\mathbf{P}(\boldsymbol{\lambda})\}_d\|_F^2.$$

(This is the equation at the end of the proof of Theorem 4.4 of Zhang & Wu (2003).) Here (in-)equality

(a) is obtained from the property that $\mathbf{C} \in C_{n,d}$,

(b) is by definition of v, and

(c) is by assumption of (4.25). □

Chapter 5

Fast drift-approximated pricing in the BGM model

[1] It is demonstrated that the forward rates process discretized by a single time step together with a separability assumption on the volatility function allows for representation by a low-dimensional Markov process. This in turn leads to efficient pricing by, for example, finite differences. We then develop a discretization based on the Brownian bridge that is especially designed to have high accuracy for single time stepping. The scheme is proven to converge weakly with order one. We compare the single time step method for pricing on a grid with multi-step Monte Carlo simulation for a Bermudan swaption, reporting a computational speed increase by a factor 10, yet maintaining sufficiently accurate pricing.

5.1 Introduction

The BGM framework, developed by Brace et al. (1997), Miltersen et al. (1997) and Jamshidian (1997), is now one of the most popular models for pricing interest rate derivatives. In the BGM framework almost all prices are computed using Monte Carlo simulation. An advantage of Monte Carlo is its applicability to almost any product. However, it has the drawback of being computationally rather slow. In an attempt to limit the computational time, Hunter et al. (2001), Jäckel (2002, Section 12.5) and Kurbanmuradov, Sabelfeld & Schoenmakers (2002) introduced predictor-corrector drift approximations, which reduce the Monte Carlo stage to single time-step simulation.

[1] This chapter has been published in different form as Pietersz, R., Pelsser, A. A. J. & van Regenmortel, M. (2004), 'Fast drift-approximated pricing in the BGM model', *Journal of Computational Finance* **8**(1), 93–124. An extended abstract of this chapter appeared as Pietersz, R., Pelsser, A. A. J. & van Regenmortel, M. (2005), 'Bridging Brownian LIBOR', *Wilmott Magazine* **18**, 98–103.

This chapter presents a significant addition to the single time step pricing method. We show that much more efficient numerical methods (either numerical integration or finite differences) may be used at the cost of a minor additional assumption, *separability*. The latter is a non-restrictive requirement on the form of the volatility function. The single time step together with separability renders the state of the BGM model completely determined by a low-dimensional Markov process. This enables efficient implementation.

We give an example of the fast single time step pricing framework for Bermudan swaptions. A comparison is made with prices obtained by least-squares multi-time step Monte Carlo simulation in the BGM model. This includes the use of the Longstaff & Schwartz (2001) method.

The computational speed increase achieved with the use of finite differences for BGM single time step pricing is the main result. This chapter also contains two other results:

- The first result is a new time discretization using a Brownian bridge, as introduced in Section 5.3, which is proven to have least-squares error in a certain sense (to be defined) for single time step discretizations. In Section 5.5 it is shown numerically that the Brownian bridge scheme outperforms (in the case of single time steps) various other discretizations for the LIBOR-in-arrears density test. In the first part of Section 5.6, we prove theoretically that the Brownian bridge scheme converges weakly with order one when used for multi-time step Monte Carlo. In the second part of Section 5.6, we compare the Brownian bridge scheme numerically with other discretizations for multi-time steps.

- The second result is a method for measuring the accuracy of single time stepping. This is the timing inconsistency test as outlined in Section 5.9.

A further application of the Brownian bridge drift approximation is its use in the likelihood ratio method. This method, introduced by Broadie & Glasserman (1996), efficiently estimates risk sensitivities for Monte Carlo pricing. The particular application of the likelihood ratio method to the LIBOR market model has been developed by Glasserman & Zhao (1999), who proposed the use of drift approximations.

The outline of this chapter is as follows. After setting out some basic notation and the most important formulas for the BGM model, the single time step pricing framework is developed, various discretization schemes are discussed and the Brownian bridge scheme is introduced. The Brownian bridge scheme is then investigated theoretically and numerically for both single and multi-time steps, respectively. Next, the proposed framework is worked out for the one-factor case. This is followed by an example of the pricing of Bermudan swaptions, both for a one- and a two-factor model. A test is then developed to assess the quality of single time steps. Finally, conclusions are drawn.

5.2 Notation for BGM model

In this section our notation of the BGM model is introduced.

We consider a BGM model, $\mathcal{M}$[2] Such a model features n forward rates, f_i, $i = 1, \ldots, n$, where forward i accrues from time t_i to time t_{i+1}, $0 < t_1 < \cdots < t_{n+1}$. Denote by α_i the accrual factor over the period $[t_i, t_{i+1}]$. Denote by $b_i(t)$ the time-t price of a discount bond that expires at time t_i. Bond prices and forward rates are linked by the relation

$$1 + \alpha_i f_i(t) = \frac{b_i(t)}{b_{i+1}(t)}.$$

Each forward rate is driven by a d-dimensional Brownian motion (where d is the number of stochastic factors in the BGM model), $\mathbf{w}$, as follows:

$$\frac{\mathrm{d}f_i(t)}{f_i(t)} = \tilde{\mu}_i(t)\mathrm{d}t + \boldsymbol{\sigma}_i(t) \cdot \mathrm{d}\mathbf{w}(t). \tag{5.1}$$

Here $\boldsymbol{\sigma}_i$ is the d-dimensional volatility vector, and $\tilde{\mu}_i$ is the drift term, whose form will in general depend on the choice of probability measure. Throughout this chapter, we use the numeraire probability measure associated with the bond maturing at time t_{n+1}, the so called *terminal measure*. There is a specific reason why we use the terminal measure, and this is explained in Remark 2 of Section 5.3. For the terminal measure, the drift term will have the following form for $i < n$:

$$\tilde{\mu}_i(t, f_{i+1}, \ldots, f_n) = -\sum_{k=i+1}^{n} \frac{\alpha_k f_k \boldsymbol{\sigma}_k(t) \cdot \boldsymbol{\sigma}_i(t)}{1 + \alpha_k f_k}. \tag{5.2}$$

For $i = n$ the drift term is zero. This simply expresses the well-known fact that a forward rate is a martingale under its associated forward measure.

For the remainder of this chapter it will be useful to have stochastic differential equation (SDE) (5.1) in logarithmic form:

$$\begin{aligned} \mathrm{d}\log f_i(t) &= \mu_i(t)\mathrm{d}t + \boldsymbol{\sigma}_i(t) \cdot \mathrm{d}\mathbf{w}^{(n+1)}(t), \\ \mu_i(t) &= \tilde{\mu}_i(t) - \frac{1}{2}\|\boldsymbol{\sigma}_i(t)\|^2. \end{aligned} \tag{5.3}$$

Last, we introduce the notion of all available forward rates at a given point in time. Define $i(t)$ to be the smallest integer i such that $t \leq t_i$. Define $\mathbf{f}$ to consist of all forward rates that have not yet expired at time t, i.e.,

$$\mathbf{f}(t) = \big(f_{i(t)}(t), \ldots, f_n(t)\big). \tag{5.4}$$

[2]The construction of such a model may be found in, e.g., Musiela & Rutkowski (1997), Pelsser (2000) or Brigo & Mercurio (2001).

5.3 Single time step method for pricing on a grid

The two key elements in the development of a method to price interest rate derivatives in the BGM model by low-dimensional finite differences are:

- the forward rates process should be discretized by a single time step scheme; and
- the volatility structure should be separable, which permits the dynamics of the single time step forward rates process to be represented by a low-dimensional Markov process.

5.3.1 Justification of the above assumptions

Because the forward rates are approximated by a single-step scheme, the model will in general no longer be arbitrage-free. This timing inconsistency is addressed in Section 5.9, where it is shown that its impact is negligible for most cases. The single-step approximation is accurate enough for the pricing of derivatives, as shown numerically in Section 5.8. At the end of this section we introduce a novel discretization scheme based on the Brownian bridge that is especially designed for single time stepping. Its superiority (for single time steps only) over other discretizations is established in Section 5.5.

We proceed by first introducing notation for the single step-approximated forward rates process. This is followed by a statement of the separability assumption, after which we establish the low-dimensional Markov representation result. Single time step discretizations are then discussed, and we end by considering methods for pricing American style options with Monte Carlo methods.

5.3.2 Notation

We assume as given a time discretization $\tau_0 < \cdots < \tau_m$, $m \geq 1$. A *single time step discretization* is a discretization with $m = 1$. Define $z_i(u,v) = \int_u^v \boldsymbol{\sigma}_i(t) \cdot \mathrm{d}\mathbf{w}^{(n+1)}(t)$. Given a scheme for the log rates

$$\log f_i(\tau_{j+1}) = \log f_i(\tau_j) + \mu_i\big(\tau_j, \tau_{j+1}, \mathbf{f}(\tau_j), \mathbf{z}(\tau_j, \tau_{j+1})\big) + z_i(\tau_j, \tau_{j+1}) \tag{5.5}$$

then denote by

$$f_i^A(t) = f_i(0) \exp\left\{\mu_i\big(0, t, \mathbf{f}(0), \mathbf{z}(0,t)\big) + z_i(0,t)\right\}$$

its single time step-approximated equivalent. Here μ is the "drift approximation" and it is determined by the scheme applied, which may be the Euler, the predictor-corrector or the Brownian bridge scheme. These schemes will be elaborated on in Section 5.4. The A in f^A stands for "approximated". The vector $\mathbf{z}$ is defined by analogy with $\mathbf{f}$ in (5.4).

5.3.3 Separability

Definition 3 (Separability) *A collection of volatility functions* $\boldsymbol{\sigma}_i : [0, t_i] \to \mathbb{R}^d$, $i = 1, \ldots, n$, *is called "separable" if there exists a vector-valued function* $\boldsymbol{\sigma} : [0, t_n] \to \mathbb{R}^d$ *and vectors* $\mathbf{v}_i \in \mathbb{R}^d$, $i = 1, \ldots, n$, *such that*

$$\boldsymbol{\sigma}_i(t) = \mathbf{v}_i \boldsymbol{\sigma}(t) \tag{5.6}$$

(no vector product; entry-by-entry multiplication) for $0 \leq t \leq t_i$, $i = 1, \ldots, n$.

Separability appears regularly in the context of requiring a process to be Markov. We mention three examples. First, we mention Ritchken & Sankarasubramanian (1995, Proposition 2.1). Working in the HJM model (Heath, Jarrow & Morton 1992), they show that separability is a necessary and sufficient condition on the volatility structure such that the dynamics of the term structure may be represented by a two-dimensional Markov process. Second, we mention the Wiener chaos expansion framework of Hughston & Rafailidis (2005). In this framework any interest rate model is completely characterized by its so-called Wiener chaos expansion. The nth chaos expansion is represented by a function $\phi_n : \mathbb{R}_+^n \to \mathbb{R}$ that satisfies certain integrability conditions. If all ϕ_n are separable, the resulting interest rate model turns out to be Markov. Third, we mention the finite-dimensional Markov realizations for stochastic volatility forward rate models (see Björk, Landén & Svensson (2004)). Here a necessary condition for a stochastic volatility model to have a finite-dimensional Markov realization is that the drift term and each component of the volatility term in the Stratonovich representation of the short rate SDE should be a sum of functions that are separable in time to expiry and the stochastic volatility driver.

We give an example of a separable volatility function in the case of a one-factor model ($d = 1$).

Example 1 (mean-reversion) *Following De Jong et al. (2004), the instantaneous volatility may be specified as*

$$\sigma_i(t) = \gamma_i e^{-\kappa(t_i - t)}. \tag{5.7}$$

The constant κ is usually referred to as the *mean-reversion parameter*.

5.3.4 Single time step method

The following proposition shows that a single time step plus separability yields low-dimensional representability.

Proposition 4 *Suppose that* $\mathcal{M}$ *is a d-factor BGM model, for which the instantaneous volatility structure is separable. Then the single time step discretized forward rates process may be represented by a d-dimensional Markov process.*

PROOF: Define the Markov process $\mathbf{x} : [0, t_n] \to \mathbb{R}^d$ by

$$\mathbf{x}(t) = \int_0^t \boldsymbol{\sigma}(s) \mathrm{d}\mathbf{w}^{(n+1)}(s),$$

(entry-by-entry multiplication) where $\boldsymbol{\sigma}$ is as in Definition 3. Then the single time step process $\mathbf{f}^A : [0, t_n] \to (0, \infty)^{n-i(t)+1}$ at time t satisfies

$$f_i^A(t) = f_i(0) \exp\left\{ \mu_i\big(0, t, \mathbf{f}(0), \mathbf{v}\mathbf{x}(t)\big) + \mathbf{v}_i \cdot \mathbf{x}(t) \right\}. \tag{5.8}$$

Here μ_i is defined implicitly in (5.5) and $\mathbf{v}$ is a matrix of which row i is $\mathbf{v}_i$. The claim follows, bar a clarifying remark:

The second term in the exponent of (5.8) is exactly equal to the stochastic part occurring in the BGM SDE (5.1), in virtue of the separability of the volatility structure:

$$\begin{aligned} \int_0^t \boldsymbol{\sigma}_i(s) \cdot \mathrm{d}\mathbf{w}(s) &= \int_0^t \left(\mathbf{v}_i \, \boldsymbol{\sigma}(s) \right) \cdot \mathrm{d}\mathbf{w}^{(n+1)}(s) \\ &= \mathbf{v}_i \cdot \mathbf{x}(t), \end{aligned}$$

where the notation of Definition 3 has been used. □

Remark 1 *The vector of single time-stepped rates may be considered (if separability holds) to be a time-dependent function of the Markov process* $\mathbf{x}$*, i.e.,*

$$\mathbf{f}^A(t) = \mathbf{f}\big(t, \mathbf{x}(t)\big),$$

for some function $\mathbf{f}$*. Hunt et al. (2000, Theorem 1) showed that this is impossible to achieve for the true BGM forward rates themselves in the case when* $\mathbf{x}$ *is one-dimensional and under some technical restrictions.*

Another essential building block for the fast single time step pricing framework is use of the terminal measure. This is explained in the following remark.

Remark 2 (Choice of numeraire) *For the workings of the fast single time step pricing algorithm it is essential that the terminal measure be used. This is explained as follows. As proven in Proposition 4, the time-*t *single time-stepped forward rates are fully determined by* $\mathbf{x}(t)$*. This result holds for any choice of measure or numeraire. However, for the terminal numeraire, the value of the numeraire at time* t *is fully determined by the forward rate values at time* t*, but this does not hold in the case of, for example, the spot numeraire, in that the latter is generally determined by bond values observed at earlier times. The spot numeraire* b_0 *rolls its holdings over by the spot LIBOR account. Its time-*t_i *value is*

$$b_0(t_i) = \frac{1}{\prod_{j=1}^i b_j(t_{j-1})}, \quad t_0 := 0.$$

Put in another way, the value of the spot numeraire is path-dependent, whereas that of the terminal numeraire is not. For pricing on a grid it is essential that the numeraire value is known given the value of $\mathbf{x}(t)$*. Therefore the fast single time step framework requires the use of the terminal numeraire.*

5.3.5 Valuation of interest rate derivatives with the single time step method

Interest rate derivatives with mild path-dependency may be valued by numerical integration, by a lattice/tree or by finite differences, provided that the single time-stepped rates are used and the separability assumption holds. The derivatives that may be valued include, but are not restricted to: caps, floors, European and Bermudan swaptions, trigger swaps and discrete barrier caps.

5.4 Discretizations

We discuss four time-discrete approximation schemes of the log BGM SDE (5.3):

- Euler;
- predictor-corrector;
- Milstein second-order scheme; and
- Brownian bridge.

The notation (Equation (5.5)) for a discretization of SDE (5.3) is recalled here:

$$\log f_i(\tau_{j+1}) = \log f_i(\tau_j) + \mu_i\big(\tau_j, \tau_{j+1}, \mathbf{f}(\tau_j), \mathbf{z}(\tau_j, \tau_{j+1})\big) + z_i(\tau_j, \tau_{j+1})$$

We implicitly define $\tilde{\mu}$ by

$$\mu_i\big(\tau_j, \tau_{j+1}, \mathbf{f}(\tau_j), \mathbf{z}(\tau_j, \tau_{j+1})\big) = \tilde{\mu}_i\big(\tau_j, \tau_{j+1}, \mathbf{f}(\tau_j), \mathbf{z}(\tau_j, \tau_{j+1})\big) - \frac{1}{2}\int_{\tau_j}^{\tau_{j+1}} \|\boldsymbol{\sigma}_i(s)\|^2 \mathrm{d}s,$$

so as to remove the term common to the Euler, predictor-corrector and Brownian bridge discretizations.

5.4.1 Euler discretization

The Euler discretization (see, for example, Kloeden & Platen (1999, Equation (9.3.1)) sets

$$\tilde{\mu}_i\big(\tau_j, \tau_{j+1}, \mathbf{f}(\tau_j), \mathbf{z}(\tau_j, \tau_{j+1})\big) = -\left\{\sum_{k=i+1}^{n} \frac{\alpha_k f_k(\tau_j)\boldsymbol{\sigma}_k(\tau_j)\cdot\boldsymbol{\sigma}_i(\tau_j)}{1+\alpha_k f_k(\tau_j)}\right\}(\tau_{j+1}-\tau_j).$$

5.4.2 Predictor-corrector discretization

The predictor-corrector discretization was introduced to the setting of LIBOR market models by Hunter et al. (2001). The key idea is to use predicted information to more accurately estimate the contribution of the drift to the increment of the log rate. For the terminal measure, an iterative procedure may be applied that loops from the terminal forward rate, n, to the spot LIBOR rate, $i(t)$. Initially, we set $\tilde{\mu}_n(\tau_j, \tau_{j+1}, \mathbf{f}(\tau_j), \mathbf{z}(\tau_j, \tau_{j+1})) = 0$. Then, for $i = n-1, \ldots, i(t)$,

$$\begin{aligned}\tilde{\mu}_i\big(\tau_j, \tau_{j+1}, \mathbf{f}(\tau_j), \mathbf{z}(\tau_j, \tau_{j+1})\big) &= -\Bigg\{\frac{1}{2}\sum_{k=i+1}^{n}\frac{\alpha_k f_k(\tau_j)\boldsymbol{\sigma}_k(\tau_j)\cdot\boldsymbol{\sigma}_i(\tau_j)}{1+\alpha_k f_k(\tau_j)} \\ &\quad + \frac{1}{2}\sum_{k=i+1}^{n}\frac{\alpha_k f_k(\tau_{j+1})\boldsymbol{\sigma}_k(\tau_{j+1})\cdot\boldsymbol{\sigma}_i(\tau_{j+1})}{1+\alpha_k f_k(\tau_{j+1})}\Bigg\}(\tau_{j+1}-\tau_j),\end{aligned}$$

with $f_k(\tau_{j+1})$ dependent on $f_m(\tau_j)$ and $z_m(\tau_j, \tau_{j+1})$, $m = k+1, \ldots, n$.

5.4.3 Milstein discretization

The second-order Milstein scheme (see, for example, Kloeden & Platen (1999, Equation (14.2.1)) was introduced to the setting of LIBOR market models in the series of papers by Glasserman & Merener (2003*a*, *b* and 2004). Moreover, these papers extended the convergence results to the case of jumpdiffusion with thinning, which is key to the development of the jumpdiffusion LIBOR market model. Also, these papers considered discretizations in various different sets of state variables, such as forward rates, log-forward rates, relative discount bond prices and log-relative discount bond prices. In Glasserman & Merener (2003*b*, 2004) it is shown numerically that the time-discretization bias of the log-Euler scheme is less than the bias of other discretizations, for example, in terms of the bonds. The results of Glasserman and Merener thus justify the log-type discretization (5.5) used in the present work.

The Milstein scheme can indeed be used to obtain a single time step discretization of the forward rates process - and hence it may be applied to the single time step pricing framework - but it is not particularly suited to single large time steps, as shown in the numerical comparisons for single time step accuracy in Section 5.5. Therefore we omit here the exact form of the scheme.

5.4.4 Brownian bridge discretization

Here we develop a novel discretization for the drift term. The idea is to calculate the expectation of the drift integral given the (time-changed) Wiener increment.

$$\tilde{\mu}_i\big(\tau_j, \tau_{j+1}, \mathbf{f}(\tau_j), \mathbf{z}(\tau_j, \tau_{j+1})\big) = \\ -\mathbb{E}^{(n+1)}\left[\int_{\tau_j}^{\tau_{j+1}} \sum_{k=i+1}^{n} \frac{\alpha_k f_k(s)\boldsymbol{\sigma}_k(s)\cdot\boldsymbol{\sigma}_i(s)}{1+\alpha_k f_k(s)}\mathrm{d}s \middle| \mathcal{F}(\tau_j), \mathbf{z}(\tau_j, \tau_{j+1})\right]. \tag{5.9}$$

The Brownian bridge scheme uses information present in the Wiener increment $\mathbf{z}(\tau_j, \tau_{j+1})$ to approximately determine the most likely value for the stochastic drift term. The Brownian bridge scheme thus takes into account the specific form of drift terms for LIBOR market model forward rates, whereby it can outperform general discretization schemes.

The Brownian bridge discretization is superior when a single time step is applied. This is shown theoretically and numerically in Section 5.5. Viewed as a numerical scheme for multi-step discretizations, it converges weakly with order one, as will be shown in the first part of Section 5.6. In the multi-step Monte Carlo numerical experiments of the second part of Section 5.6, we show that the bias is significantly less than for the Euler discretization.

In the remainder of this section, we show how expression (5.9) can be calculated in practice. In Section 5.5.1, we establish that the Brownian bridge scheme has least-squares error (in a yet to be defined sense).

In practice, expression (5.9) can be approximated with high accuracy. The calculation proceeds in four steps (it is indicated when a step contains an approximation):

Step 1 To calculate expression (5.9), the first step is to note that the order of the expectation and integral may be interchanged.

$$-\mathbb{E}^{(n+1)}\left[\int_{\tau_j}^{\tau_{j+1}} \sum_{k=i+1}^{n} \frac{\alpha_k f_k(s)\boldsymbol{\sigma}_k(s)\cdot\boldsymbol{\sigma}_i(s)}{1+\alpha_k f_k(s)}\mathrm{d}s \middle| \mathcal{F}(\tau_j), \mathbf{z}(\tau_j, \tau_{j+1})\right] = \\ -\int_{\tau_j}^{\tau_{j+1}} \mathbb{E}^{(n+1)}\left[\sum_{k=i+1}^{n} \frac{\alpha_k f_k(s)\boldsymbol{\sigma}_k(s)\cdot\boldsymbol{\sigma}_i(s)}{1+\alpha_k f_k(s)} \middle| \mathcal{F}(\tau_j), \mathbf{z}(\tau_j, \tau_{j+1})\right]\mathrm{d}s. \tag{5.10}$$

This is a straightforward application of Fubini's theorem (see, for example, Williams (1991, Section 8.2)).

Step 2 (approximation) For the purposes of calculating the conditional expected value of expressions of the form $f/(1+\alpha f)$, the forward rates are approximated with a single-step Euler discretization. We note that once this assumption has been made, the drift no longer affects the calculation. This stems from a property of

the Brownian bridge: a Wiener process with deterministic drift conditioned to pass through a given point at some future time is always a Brownian bridge, independently of its drift prior to conditioning. Thus the estimation of the drift integral (5.9) is the same whether it is assumed that the forward rates are driftless or whether these follow a single time step Euler approximation.

$$\begin{aligned} &-\int_{\tau_j}^{\tau_{j+1}} \mathbb{E}^{(n+1)}\left[\sum_{k=i+1}^{n} \frac{\alpha_k f_k \boldsymbol{\sigma}_k \cdot \boldsymbol{\sigma}_i}{1+\alpha_k f_k}\middle| \mathcal{F}(\tau_j), \mathbf{z}(\tau_j,\tau_{j+1})\right] \mathrm{d}s \approx \\ &\quad -\int_{\tau_j}^{\tau_{j+1}} \mathbb{E}^{(n+1)}\left[\sum_{k=i+1}^{n} \frac{\alpha_k f_k^{\mathrm{BB}} \boldsymbol{\sigma}_k \cdot \boldsymbol{\sigma}_i}{1+\alpha_k f_k^{\mathrm{BB}}}\middle| \mathcal{F}(\tau_j), \mathbf{z}(\tau_j,\tau_{j+1})\right] \mathrm{d}s, \end{aligned} \tag{5.11}$$

where BB indicates the use of the Brownian bridge, and where we have suppressed the dependence of time s. Formula (5.11) is thus obtained by approximating (5.10) by using single step Euler dynamics for the forward rates instead of the true LIBOR market model dynamics. Single step Euler dynamics imply Brownian bridge dynamics, since we condition on time-τ_{j+1} values.

We note that the assumption of singe-step Euler discretization for the calculation of expression (5.9) renders this calculation an approximation. In principle, the approximation could affect the quality of the discretization. We show numerically that this is not the case in the LIBOR-in-arrears case considered in Section 5.5.

Step 3 The conditional mean and conditional variance of the log forward rates are calculated. See Appendix 5.A for details.

Step 4 (approximation) The drift expression (5.9) may be approximated by a single numerical integration over time; the expectation term is approximated by inserting the conditional mean of the forward rates process:[3]

$$\begin{aligned} &-\int_{\tau_j}^{\tau_{j+1}} \mathbb{E}^{(n+1)}\left[\sum_{k=i+1}^{n} \frac{\alpha_k f_k^{\mathrm{BB}} \boldsymbol{\sigma}_k \cdot \boldsymbol{\sigma}_i}{1+\alpha_k f_k^{\mathrm{BB}}}\middle| \mathcal{F}(\tau_j), \mathbf{z}(\tau_j,\tau_{j+1})\right] \mathrm{d}s \approx \\ &\quad -\int_{\tau_j}^{\tau_{j+1}} \sum_{k=i+1}^{n} \frac{\alpha_k \mathbb{E}^{(n+1)}[f_k^{\mathrm{BB}}|\mathcal{F}(\tau_j), \mathbf{z}(\tau_j,\tau_{j+1})] \boldsymbol{\sigma}_k \cdot \boldsymbol{\sigma}_i}{1+\alpha_k \mathbb{E}^{(n+1)}[f_k^{\mathrm{BB}}|\mathcal{F}(\tau_j), \mathbf{z}(\tau_j,\tau_{j+1})]} \mathrm{d}s. \end{aligned}$$

Remark 3 *If a two-point trapezoidal rule (i.e., the average of the begin and end points) is used to evaluate the time integral in expression (5.9), the Brownian bridge reduces to*

[3] Alternatively, the expectation term could be evaluated by numerical integration as well, but this is computationally expensive. The full numerical integration ("BB alternative") has been compared numerically in Section 5.5 with the mean-insertion approximation ("BB"); the loss in accuracy is negligible on an absolute level. A theoretical error analysis of the mean-insertion approximation is given in Appendix 5.B.

the predictor-corrector scheme. In this sense, the predictor-corrector scheme is a special case of the Brownian bridge scheme.

For illustration, MATLAB code is given in Appendix 5.C, implementing the Brownian bridge scheme. The code implements a single time-step in a single-factor model with constant volatility. These simplifications are for clarity of exposition only and are, of course, *not* a restriction imposed by the Brownian bridge scheme.

We end this section with a discussion of the method used in this chapter for pricing American-style options with Monte Carlo. The method used is the regression-based method of Longstaff & Schwartz (2001), which is a method of stochastic mesh type (see Broadie & Glasserman (2004)). Convergence of the method to the correct price follows generically from the asymptotic convergence property of stochastic mesh methods, as shown by Avramidis & Matzinger (2004).

5.5 The Brownian bridge scheme for single time steps

In this section, we establish theoretically and numerically that the Brownian bridge scheme has superior accuracy for single time steps.

5.5.1 Theoretical result

Consider a stochastic differential equation of the form

$$\mathrm{d}\mathbf{x}(t) = \boldsymbol{\mu}\big(t, \mathbf{x}(t)\big)\mathrm{d}t + \boldsymbol{\Sigma}(t)\mathrm{d}\mathbf{w}(t). \tag{5.12}$$

We note that the BGM log SDE (5.3) is of the above form. We consider a certain class of discretizations:

Definition 4 *Let the function $\bar{\boldsymbol{\mu}}(\cdot,\cdot,\cdot)$ denote a single time step discretization of SDE (5.12) with the following form:*

$$\mathbf{y}(\tau_{j+1}) = \mathbf{y}(\tau_j) + \bar{\boldsymbol{\mu}}\big(\tau_j, \mathbf{y}(\tau_j), \mathbf{z}(\tau_j, \tau_{j+1})\big) + \mathbf{z}(\tau_j, \tau_{j+1}). \tag{5.13}$$

Here $\mathbf{z}(\tau_j, \tau_{j+1}) = \int_{\tau_j}^{\tau_{j+1}} \boldsymbol{\sigma}(s)\mathrm{d}\mathbf{w}(s)$. Any such discretization is said to use information about the Gaussian increment to estimate the drift term.

We note that Euler, predictor-corrector and Brownian bridge are such schemes. The next theorem states that, for the BGM setting, the Brownian bridge scheme (5.9) has least-squares error for a single time step over all discretizations that use information about the Gaussian increment for the drift term.

Lemma 2 *Let $\{\mathbf{y}\}$ be a single time step discretization of SDE (5.12) that uses information about the Gaussian increment for the drift term. Consider the discretization expected squared error*

$$s^2\big(\{\mathbf{y}\}\big) := \mathbb{E}\Big[\big\|\mathbf{y}(\tau_{j+1}) - \mathbf{x}_{\{\tau_j,\mathbf{y}(\tau_j)\}}(\tau_{j+1})\big\|^2\Big|\mathcal{F}(\tau_j)\Big].$$

Here $\mathbf{x}_{\{t,\mathbf{y}\}}$ denotes the solution of SDE (5.12) starting from $(t,\mathbf{y})$. Then the discretization $\{\mathbf{y}^*\}$ that yields least squared error, s^2, over all possible discretizations that use information about the Gaussian increment to estimate the drift term is defined by

$$\bar{\boldsymbol{\mu}}^*\big(\tau_j,\mathbf{y}(\tau_j),\mathbf{z}(\tau_j,\tau_{j+1})\big) = \mathbb{E}\bigg[\int_{\tau_j}^{\tau_{j+1}} \boldsymbol{\mu}\Big(s,\mathbf{x}_{\{\tau_j,\mathbf{y}(\tau_j)\}}(s)\Big)\mathrm{d}s\bigg|\mathcal{F}(\tau_j),\mathbf{z}(\tau_j,\tau_{j+1})\bigg]. \tag{5.14}$$

PROOF: Define

$$\mathbf{i} := \int_{\tau_j}^{\tau_{j+1}} \boldsymbol{\mu}\Big(s,\mathbf{x}_{\{\tau_j,\mathbf{y}(\tau_j)\}}(s)\Big)\mathrm{d}s.$$

For ease of exposition we write $\mathbf{z} = \mathbf{z}(\tau_j,\tau_{j+1})$ and $\bar{\boldsymbol{\mu}} = \bar{\boldsymbol{\mu}}(\tau_j,\mathbf{y}(\tau_j),\mathbf{z})$, but we keep in mind that $\bar{\boldsymbol{\mu}}$ is $\{\mathcal{F}(\tau_j),\mathbf{z}\}$-measurable. Also write $\mathbb{E}_t[\cdot] := \mathbb{E}[\cdot|\mathcal{F}(t)]$. Then let $\{\mathbf{y}'\}$ with drift term $\bar{\boldsymbol{\mu}}'$ be a discretization of the form of Definition 4. First, we condition on $\mathbf{z}$:

$$\mathbb{E}_{\tau_j}\big[\|\bar{\boldsymbol{\mu}}' - \mathbf{i}\|^2\big|\mathbf{z}\big] \geq \mathbb{E}_{\tau_j}\big[\|\mathbb{E}_{\tau_j}[\mathbf{i}|\mathbf{z}] - \mathbf{i}\|^2\big|\mathbf{z}\big] = \mathbb{E}_{\tau_j}\big[\|\bar{\boldsymbol{\mu}}^* - \mathbf{i}\|^2\big|\mathbf{z}\big].$$

The inequality holds since expectation equals projection, and the latter has, by definition, least squared error over all possible $\{\mathcal{F}(\tau_j),\mathbf{z}\}$-measurable drift terms. Continuing, we find

$$s^2\big(\{\mathbf{y}'\}\big) = \mathbb{E}_{\tau_j}\big[\|\bar{\boldsymbol{\mu}}' - \mathbf{i}\|^2\big] = \mathbb{E}_{\tau_j}\Big[\mathbb{E}_{\tau_j}\big[\|\bar{\boldsymbol{\mu}}' - \mathbf{i}\|^2\big|\mathbf{z}\big]\Big] \geq \mathbb{E}_{\tau_j}\Big[\mathbb{E}_{\tau_j}\big[\|\bar{\boldsymbol{\mu}}^* - \mathbf{i}\|^2\big|\mathbf{z}\big]\Big] = s^2\big(\{\mathbf{y}^*\}\big),$$

i.e., $\mathbf{y}^*$ has less squared error than $\mathbf{y}'$. As $\mathbf{y}'$ was an arbitrary discretization of the form of Definition 4, the result follows. □

5.5.2 LIBOR-in-arrears case

We estimate numerically the accuracy in the LIBOR-in-arrears test of the various schemes of Section 5.4. We extend here the LIBOR-in-arrears test of Hunter et al. (2001) by including the Milstein and Brownian bridge schemes. The test is designed to measure the accuracy of a single time step discretization. The idea of the test is briefly described here; for details the reader is referred to Hunter et al. (2001).

We consider the distribution of a forward rate under the measure associated with the numeraire of a discount bond maturing at the *fixing* time of the forward. We note that the forward rate is not a martingale under such a measure as the natural payment time of the forward is not the same as its fixing time. An analytical formula for the associated density, however, is known. We can thus compare the density obtained from

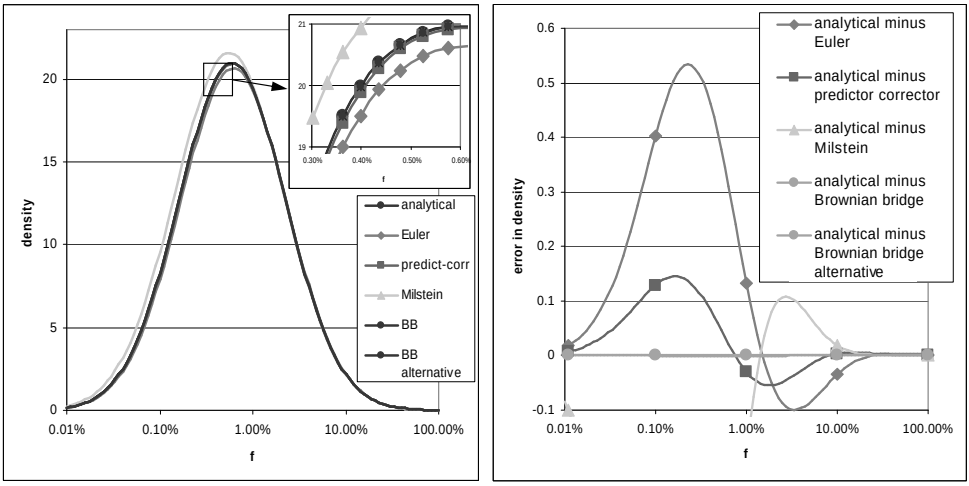

Figure 5.1: Plots of the estimated densities and absolute errors in densities of various single time step discretizations. The deal set-up is the same as in Hunter et al. (2001); the three-month forward rate fixing 30 years from today is set initially to 8% and its volatility to 24%. The legend key "BB" denotes Brownian bridge and "BB alternative" denotes full numerical integration of the expectation term. We note that three densities have been added to the above figures compared with Figure 1 of Hunter et al. (2001): Milstein and the two Brownian bridge schemes. On both figures, however, the differences between the analytical and Brownian bridge densities are indiscernible to the eye. The most notable addition is the Milstein density. Outside of the error graph, the Milstein scheme reaches a maximum absolute error that is around twice the maximum absolute error for the Euler scheme. The maximum absolute error in the density for the Brownian bridge and its alternative are 10^{-3} and 6×10^{-4}, respectively. In this particular test the Brownian bridge scheme thus achieves a reduction by a factor 100 in the maximum absolute error over the predictor-corrector scheme, the latter being the second best scheme.

a single time step discretization with the analytical formula for the density. The results of this test are displayed in Figure 5.1. It is shown (for the particular set-up) that the Brownian bridge scheme reduces the maximum error in the density by a factor 100 over the predictor-corrector scheme.

5.6 The Brownian bridge scheme for multi-time step Monte Carlo

This section consists of two parts. First, we show theoretically that the Brownian bridge scheme converges weakly with order one. Second, we estimate numerically the convergence behavior of the various schemes of Section 5.4.

5.6.1 Weak convergence of the Brownian bridge scheme

In a financial context, the interest lies in calculating the prices of derivatives, which are in certain cases expectations of payoff functions. Therefore we are interested mainly in *weak convergence* of Monte Carlo simulations. The definition is recalled here and may be found in, for example, Kloeden & Platen (1999, Section 9.7).

Definition 5 (Weak convergence) *A scheme* $\{\mathbf{y}^{\varepsilon}(\tau_j)\}$ *with maximum step size* ε *is said to convergence weakly with order* β *to* $\mathbf{x}$ *if, for each function* g *with* $2(\beta+1)$ *polynomially bounded derivatives, there exists a constant* c *such that, for sufficiently small* ε*,*

$$\left|\mathbb{E}\big[g\big(\mathbf{x}(t)\big)\big] - \mathbb{E}\big[g\big(\mathbf{y}^{\varepsilon}(t)\big)\big]\right| \leq c \cdot \varepsilon^{\beta}. \tag{5.15}$$

A criterion that is easier to verify than the above definition is the concept of *weak consistency*, and under quite natural conditions it follows that weak consistency implies weak convergence. The definition of weak consistency is recalled here, and may be found for example on page 327 of Kloeden & Platen (1999). Here we develop the remainder of the theory in terms of approximating an autonomous SDE, say,

$$\mathrm{d}\mathbf{x}(t) = \boldsymbol{\mu}\big(\mathbf{x}(t)\big)\mathrm{d}t + \boldsymbol{\Sigma}\big(\mathbf{x}(t)\big)\mathrm{d}\mathbf{w}(t), \quad \mathbf{x}(0) \text{ deterministic.} \tag{5.16}$$

However, the theory holds in more general cases too.

Definition 6 (Weak consistency) *A scheme* $\{\mathbf{y}^{\varepsilon}(\tau_j)\}$ *with maximum step size* ε *is weakly consistent if there exists a function* $c = c(\varepsilon)$ *with*

$$\lim_{\varepsilon \downarrow 0} c(\varepsilon) = 0 \tag{5.17}$$

such that

$$\mathbb{E}\left[\left\|\mathbb{E}\left[\frac{\mathbf{y}^{\varepsilon}(\tau_{j+1}) - \mathbf{y}^{\varepsilon}(\tau_j)}{\Delta\tau_j}\middle|\mathcal{F}(\tau_j)\right] - \boldsymbol{\mu}\big(\mathbf{y}^{\varepsilon}(\tau_j)\big)\right\|^2\right] \leq c(\varepsilon) \tag{5.18}$$

and

$$\begin{aligned}\mathbb{E}\Bigg[\Bigg\|\mathbb{E}\Big[\tfrac{1}{\Delta\tau_j}\big\{\mathbf{y}^{\varepsilon}(\tau_{j+1}) - \mathbf{y}^{\varepsilon}(\tau_j)\big\}\big\{\mathbf{y}^{\varepsilon}(\tau_{j+1}) - \mathbf{y}^{\varepsilon}(\tau_j)\big\}^{\top}\Big|\mathcal{F}(\tau_j)\Big] \\ -\boldsymbol{\Sigma}\big(\mathbf{y}^{\varepsilon}(\tau_j)\big)\boldsymbol{\Sigma}^{\top}\big(\mathbf{y}^{\varepsilon}(\tau_j)\big)\Bigg\|^2\Bigg] \leq c(\varepsilon).\end{aligned} \tag{5.19}$$

Here $\{\mathcal{F}(t)\}$ is the filtration generated by the Brownian motion driving SDE (5.16).

Kloeden and Platen prove the following theorem (see Theorem 9.7.4 of Kloeden & Platen (1999)) linking weak consistency to weak convergence.

Theorem 7 (Linking weak consistency to weak convergence) *Suppose that $\boldsymbol{\mu}$ and $\boldsymbol{\Sigma}$ in (5.16) are four times continuously differentiable with polynomial growth and uniformly bounded derivatives. Let $\{\mathbf{y}^{\varepsilon}(\tau_j)\}$ be a weakly consistent scheme with equitemporal steps $\Delta\tau_j = \varepsilon$ and initial value $\mathbf{y}^{\varepsilon}(0) = \mathbf{x}(0)$ which satisfies the moment bounds*

$$\mathbb{E}\left[\max_j |\mathbf{y}^{\varepsilon}(\tau_j)|^{2q}\right] \leq k\big(1 + |\mathbf{x}(0)|^{2q}\big), \quad q = 1, 2, \ldots \text{ and}$$

$$\mathbb{E}\left[\frac{1}{\varepsilon}\big|\mathbf{y}^{\varepsilon}(\tau_{j+1}) - \mathbf{y}^{\varepsilon}(\tau_j)\big|^6\right] \leq c(\varepsilon), \tag{5.20}$$

where $c(\varepsilon)$ is as in Definition 6. Then $\mathbf{y}^{\varepsilon}$ converges weakly to $\mathbf{x}$.

In the proposition below we show that the Brownian bridge scheme with the proposed calculation method is weakly consistent. The above theorem then allows us to deduce that the Brownian bridge scheme converges weakly.

Proposition 5 (Brownian bridge scheme is weakly consistent) *Assume that the volatility functions $\boldsymbol{\sigma}_i(\cdot)$ are piece-wise analytical on the model horizon $[0, t_n]$. Then the Brownian bridge scheme defined by (5.9) and by the four-step calculation method described in Section 5.4 is weakly consistent with the forward rates process defined in (5.3).*

PROOF: Without loss of generality, we may assume that the volatility functions are analytical. Otherwise, due to the piecewise property of the volatility functions, we can break up the problem into sub-problems for which each has analytical volatility functions. We note as well that all derivatives of the volatility functions are bounded because the interval $[0, t_n]$ is compact.

We need only verify the consistency Equation (5.18) for the drift term. To achieve this, define for i and for all $\tau \in [0, t_n]$ and for all $\mathbf{f}$ the function $g_{\{i,\tau,\mathbf{f}\}} : [0, t_n - \tau] \to \mathbb{R}$,

$$g_{\{i,\tau,\mathbf{f}\}}(t) = -\sum_{k=i+1}^{n} \frac{\alpha_k f_k}{1 + \alpha_k f_k} \int_0^t \boldsymbol{\sigma}_k(\tau + s) \cdot \boldsymbol{\sigma}_i(\tau + s) \mathrm{d}s.$$

Due to the assumption that the volatility functions are analytical, it follows that the function $g_{\{i,\tau,\mathbf{f}\}}$ is analytical in t. Taylor's formula states that there exists an error term $e_{\{i,\tau,\mathbf{f}\}}(\cdot)$ depending on i, τ and $\mathbf{f}$ such that

$$g_{\{i,\tau,\mathbf{f}\}}(t) = g_{\{i,\tau,\mathbf{f}\}}(0) + t\, \frac{\partial g_{\{i,\tau,\mathbf{f}\}}}{\partial t}(0) + e_{\{i,\tau,\mathbf{f}\}}(t) \tag{5.21}$$

with

$$\lim_{t\downarrow 0} \frac{\left|e_{\{i,\tau,\mathbf{f}\}}(t)\right|}{t^2} < \infty. \tag{5.22}$$

Due to the analyticity, bounded-ness and limiting behaviour of the function $h(x) = x/(1+x)$, namely $h \uparrow 1$ ($h \downarrow 0$) as $x \to \infty$ ($x \to -\infty$, respectively), we have that all its derivatives are bounded. Viewed as a function $[0, t_n] \times [0, t_n] \times \mathbb{R}^n \to \mathbb{R}$,

$$(t, \tau, \mathbf{f}) \mapsto g_{\{i,\tau,\mathbf{f}\}}(t),$$

we can thus find a bound on the second derivative $\partial^2 g_{\{i,\tau,\mathbf{f}\}}/\partial t^2$, independent of $(\tau, \mathbf{f})$. Theorem 7.7 of Apostol (1967) then states that the error term in (5.21) may be chosen independently of τ and $\mathbf{f}$. Hence we find that

$$g_{\{i,\tau,\mathbf{f}\}}(t) = t\left\{ -\sum_{k=i+1}^{n} \boldsymbol{\sigma}_k(\tau)\cdot\boldsymbol{\sigma}_i(\tau)\frac{\alpha_k f_k}{1+\alpha_k f_k}\right\} + e(t),$$

with e satisfying the second-order Equation (5.22). Here we have used

$$g_{\{i,\tau,\mathbf{f}\}}(0) = 0 \quad \text{and}$$

$$\left.\frac{\partial g_{\{i,\tau,\mathbf{f}\}}}{\partial t}\right|_{t=0} = \left\{ -\sum_{k=i+1}^{n} \boldsymbol{\sigma}_k(\tau)\cdot\boldsymbol{\sigma}_i(\tau)\frac{\alpha_k f_k}{1+\alpha_k f_k}\right\}.$$

If $\mathbf{Y}^\varepsilon$ denotes the Brownian bridge scheme, then

$$\begin{aligned}\mathbb{E}\big[y_i^\varepsilon(\tau_{j+1}) - y_i^\varepsilon(\tau_j)\big|\mathcal{F}(\tau_j)\big] &= g_{\{i,\tau_j,\mathbf{Y}^\varepsilon(\tau_j)\}}(\varepsilon)\\ &= \varepsilon\left\{ -\sum_{k=i+1}^{n} \frac{\alpha_k y_k^\varepsilon(\tau_j)\boldsymbol{\sigma}_k(\tau_j)\cdot\boldsymbol{\sigma}_i(\tau_j)}{1+\alpha_k y_k^\varepsilon(\tau_j)}\right\} + e(\varepsilon).\end{aligned}$$

We note that the term within braces is exactly drift term i evaluated at $(\tau_j, \mathbf{Y}^\varepsilon(\tau_j))$. It follows that consistency Equation (5.18) holds with $c(\varepsilon)$ equal to $(e(\varepsilon)/\varepsilon)^2$. The function $c(\cdot)$ is then quadratic in ε. □

Corollary 1 (Brownian bridge scheme converges weakly with order one) *Under the assumptions of Proposition 5, the Brownian bridge scheme defined by (5.9) and by the four-step calculation method described in Section 5.4 converges weakly to the forward rates process defined in (5.3). It has order of convergence one.*

PROOF: We only need verify the claim with regards to the order of convergence. In the proof of Theorem 7 in Kloeden & Platen (1999), it is shown that the error term in the weak convergence criterion (5.15) is less than $\sqrt{c(\varepsilon)}$, with $c(\cdot)$ satisfying the requirements (5.17), (5.18), (5.19) and (5.20). All these requirements can be met for the Brownian bridge scheme with a quadratic function c. Taking the square root then yields first-order weak convergence for the Brownian bridge scheme. □

5.6.2 Numerical results

We now turn to the second part of Section 5.6, in which the various discretization schemes are compared numerically. A floating leg and a cap were valued with 10 million simulation paths. This large number of paths was used because the time discretization bias for the log rates is small compared to the standard error often observed with 10,000 paths. For example, the Euler one-step-per-accrual discretization relative bias for the floating leg and the cap was estimated at 0.02% and 0.003%, whereas twice the standard error at 10,000 paths is 0.07% and 0.01%, respectively.

To obtain a bias-estimate with minimal standard error, we jointly simulate the values of individual payments in the floating leg and cap under their respective forward measures. Such procedure filters out the discretization bias from the random noise in the simulation. We note that, under the forward measure, there is no drift term and therefore the associated payoff is an unbiased estimator of the value of the contract. If we denote by π_{terminal} and π_{fwd} the numeraire-deflated contract payoff in the terminal and forward measure, respectively, then an unbiased estimator of the bias is $\pi_{\text{terminal}} - \pi_{\text{fwd}}$. Alternatively, we can benchmark against the analytical value $\pi_{\text{analytical}}$ of the floating leg or cap, which yields the unbiased estimator of the bias $\pi_{\text{terminal}} - \pi_{\text{analytical}}$. The variances of the two estimators are

$$\text{Var}\big[\pi_{\text{terminal}} - \pi_{\text{fwd}}\big] = \text{Var}\big[\pi_{\text{terminal}}\big] + \text{Var}\big[\pi_{\text{fwd}}\big] - 2\text{Cov}\big[\pi_{\text{terminal}}, \pi_{\text{fwd}}\big] \tag{5.23}$$

$$\text{Var}\big[\pi_{\text{terminal}} - \pi_{\text{analytical}}\big] = \text{Var}\big[\pi_{\text{terminal}}\big] \tag{5.24}$$

If we assume $\text{Var}\big[\pi_{\text{terminal}}\big] \approx \text{Var}\big[\pi_{\text{fwd}}\big]$, then (5.23) becomes

$$\text{Var}\big[\pi_{\text{terminal}} - \pi_{\text{fwd}}\big] \approx 2\Big(1 - \rho\big[\pi_{\text{terminal}}, \pi_{\text{fwd}}\big]\Big)\text{Var}\big[\pi_{\text{terminal}}\big] \tag{5.25}$$

Therefore, if the correlation term $\rho[\pi_{\text{terminal}}, \pi_{\text{fwd}}]$ is larger than $\frac{1}{2}$, we have variance reduction. In our numerical LIBOR tests we found $\rho \approx 0.999$, which means that the variance is reduced by a factor of 500. The benchmark against the forward measure payoff is thus also a useful tool when validating an implementation of a LIBOR market model, since a bias that stems from an implementation error is more easily filtered out from the random noise of the MC simulation.

The results are presented in Figure 5.2. They show that the predictor-corrector, Milstein and Brownian bridge schemes have a time discretization bias that is hardly distinguishable from the standard error of the estimate. The Euler scheme, however, has a clear time discretization bias for larger time steps. We classify the schemes from best suited to worst suited (for the particular numerical cases under consideration) using the criterion of the minimal computational time required to achieve a bias that is indistinguishable

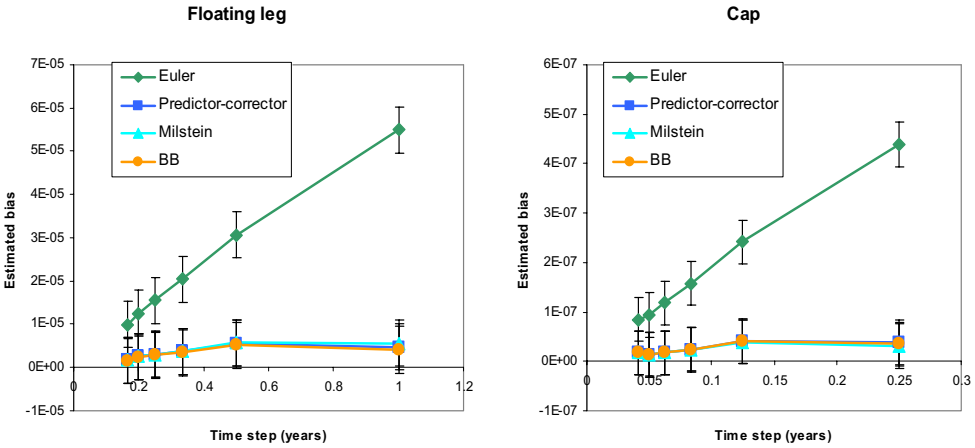

Figure 5.2: Plots of the estimated biases for a floating leg and a cap for the Euler, predictor-corrector, Milstein and Brownian bridge schemes. A single-factor model was applied. The floating leg is a six-year deal, with the fixings at $1, \ldots, 5$ years, and payments of annual LIBOR at $2, \ldots, 6$ years. The cap is a 1.5-year deal, with the fixings at $0.25, 0.5, \ldots, 1.25$ years, and payments of quarterly LIBOR above 5% (if at all) at $0.5, 0.75, \ldots, 1.5$ years. The market conditions are the same for both deals: all initial forward rates are 6%, and all volatility is constant at 20%. The net present values of the floating leg and cap are 0.24 and 0.013, respectively, on a notional of one unit of currency. The error bars denote a 95% confidence bound based on twice the sample standard error.

from the standard error at 10,000,000 paths. As Milstein is slightly faster than predictor-corrector, which in turn is faster than the Brownian bridge, we obtain: first, Milstein; second, predictor-corrector; third, Brownian bridge; and fourth, Euler. We stress here that this classification might be particular to the numerical cases that we considered. We also stress that the strength of the Brownian bridge lies in single time steps rather than in multi-time steps.

5.7 An example: one-factor BGM framework with drift approximations

This section illustrates the framework for fast single time step pricing in BGM by setting it up in the special case of a one-factor model with a volatility structure as in Example

1. This structure may be written as follows:

$$\sigma_i(t) = \tilde{\gamma}_i e^{\kappa t},$$

for certain constants $\tilde{\gamma}_i$. The corresponding Markov factor, x, is then defined as and characterized by

$$x(t) = \int_0^t e^{\kappa s} \mathrm{d}w(s), \quad x(t) \sim \mathcal{N}\big(0, v(t)\big), \quad \text{where}$$

$$v(t) = \int_0^t e^{2\kappa s} \mathrm{d}s = \begin{cases} \frac{e^{2\kappa t}-1}{2\kappa}, & \kappa \neq 0, \\ t, & \kappa = 0. \end{cases}$$

Prices may now be computed by either numerical integration or finite differences. In the case of numerical integration, if $\pi(t, x)$ denotes the numeraire-deflated value of the contingent claim, we have

$$\pi\big(0, x(0)\big) = \int_{-\infty}^{\infty} \pi(t, x) p\big(x; 0, v(t)\big) \mathrm{d}x$$

where t denotes the expiry of the contingent claim and $p(\cdot; \mu, v)$ denotes the Gaussian density with mean μ and standard deviation $\sqrt{v}$. In case of finite differences, Feynman-Kac yields the following PDE for the price relative to the terminal bond:

$$\frac{\partial \pi}{\partial t} + \frac{1}{2} e^{2\kappa t} \frac{\partial^2 \pi}{\partial x^2} = 0, \tag{5.26}$$

with use of appropriate boundary conditions. For example, for a Bermudan payer swaption we have $\pi(\cdot, -\infty) \equiv 0$, zero convexity $\partial^2 \pi / \partial x^2 \equiv 0$ at $x = \infty$, and exercise boundary conditions at the exercise times.

5.7.1 A simple numerical example

We will evolve five annual ($\alpha_i = 1$) forward rates over a one-year period. Forward rate i accrues from year i until year $i + 1$, $i = 1, \ldots, 5$. Take $f_i(0) = 7\%$, $\tilde{\gamma}_i = 25\%$ and $\kappa = 15\%$; then $v(1) \approx 1.166196$. Suppose that, after one year, the process x jumps to 1; thus $x(1) = 1$. All computations are displayed in Table 5.1. Column (II) is determined by (5.2). To evaluate the effect of the Brownian bridge scheme over the Euler scheme, the "drift-frozen" forward rates (where the drift is evaluated at time zero) are displayed in column (V), using the equation (V) = (I) exp ((II) + (III) + (IV)). Then, we start with computing the Brownian bridge scheme forward rate 5 and work back to forward rate 1. Forward rate 5 is easily computed as no drift terms are involved. To compute the drift term integral at time 1 for forward rate 4, we compute the drift term integral of

Table 5.1: A simple numerical example.

	(I)	(II)	(III)	(IV)	(V)	(VI)	(VII)
i	$f_i(0)$	$\mu_i(0)$	$-\frac{1}{2}\tilde{\gamma}_i^2 v(1)$	$\tilde{\gamma}_i x(1)$	Drift frozen $f_i(1)$	Equation $(5.9)_{i-1}$ $-(5.9)_i$	Brownian bridge $f_i(1)$
5	7.00%	0.00000	−0.03644	0.25	8.67%	−0.00569	8.67%
4	7.00%	−0.00409	−0.03644	0.25	8.63%	−0.00567	8.62%
3	7.00%	−0.00818	−0.03644	0.25	8.60%	−0.00564	8.57%
2	7.00%	−0.01227	−0.03644	0.25	8.56%	−0.00562	8.53%
1	7.00%	−0.01636	−0.03644	0.25	8.53%		8.47%

(5.9) for forward rate 5. The result is displayed in column (VI). This we may then use to compute the Brownian bridge scheme forward rate 4 (see column (VII)), where we use the equation $(\text{VII})_i = (\text{I})\exp(\{\sum_{j=i+1}^{n}(\text{VI})_j\} + (\text{III}) + (\text{IV}))$. Continuing, we compute the drift for forward rate 3 using only the Brownian bridge forward rates 4 and 5. And so on until all forward rates have been computed.

5.8 Example: Bermudan swaption

As an example of the single time step pricing framework, an analysis is made for Bermudan swaptions in comparison with a BGM model combined with the least-squares Monte Carlo method introduced by Longstaff & Schwartz (2001). The one-factor set-up introduced in the previous section was used with zero mean-reversion.

Callable Bermudan and European payer swaptions were priced in a one-factor BGM model for various tenors and non-call periods. The zero rates were taken to be flat at 5%, and the volatility of the forwards was set flat at 15%. The Bermudans were priced on a grid, the Europeans through numerical integration. The PDE was solved using an explicit finite-difference scheme. The explanatory variable in the least-squares Monte Carlo was taken to be the net present value (NPV) of the underlying swap. This was regressed on to a constant and a linear term. These two basis functions yield sufficiently accurate results because the value of a Bermudan swaption increases almost linearly with the value of the underlying swap.

Problems may possibly occur for American-style derivatives in the single time step framework. Since the framework is not arbitrage-free, spurious early or delayed exercise may take place to collect the arbitrage opportunity. The effects of these phenomena have been analyzed by comparing the exercise boundaries[4] and risk sensitivities of Longstaff-Schwartz and single time step BGM. In both models the exercise rule turned out to be of the following form: exercise whenever the NPV of the underlying swap, s, is larger than a certain value s^*, which is then defined to be the *exercise boundary*.

For a full description of the deal see Table 5.2. Results have been summarized in Table 5.3. Computational times may be found in Table 5.4. Exercise boundaries for the 8 year deal are displayed in Figure 5.3, including confidence bounds on the Longstaff-Schwartz

[4]In the Longstaff-Schwartz case, the future discounted cashflows are regressed against the NPV of the underlying swap with a constant and linear term – say, with coefficients a and b. So the option is exercised whenever $s > a + bs \Leftrightarrow s > a/(1-b) =: s^*$, where it is assumed that $b < 1$, which turns out to hold in practice. Hence the exercise boundary s^* may be computed from the regression coefficients by the above formula.

Table 5.2: Specification of the Bermudan swaption comparison deal.

Callable Bermudan swaption	
Market data	
Zero rates	Flat at 5%
Volatility	Flat at 15%
Product specification	
Tenor	Variable (2-8 years)
Non-call period	Variable
Call dates	Semi-annual
Pay/receive	Pay fixed
Fixed leg properties	
Frequency	Semi-annual
Date roll	None
Day count	Half year = 0.5
Fixed rate	5.06978% (ATM)
Floating leg properties	
Frequency	Semi-annual
Date roll	None
Day count	Half year = 0.5
Margin	0%
Numerics	
Simulation paths	10,000
Finite-difference scheme	Explicit
Longstaff-Schwartz	
Explanatory variable	Swap NPV
Basis function type	Monomials
No. of basis functions	2 (constant and linear)

Table 5.3: Results of the Bermudan swaption comparison deal. The notation xNCy in the first column denotes an x-year underlying swap with a non-call period of y years. In case of a European swaption, it means that the swaption is exercisable after y years exactly. All prices and standard errors are in basis points.

	Bermudan			**European**		
	Drift-approx. BGM	Longstaff-Schwartz	Standard error	Drift-Approx. BGM	Monte Carlo BGM	Standard error
2NC1	29.40	28.85	0.42	27.36	26.88	0.43
3NC1	64.33	62.78	0.83	53.78	52.92	0.83
4NC1	101.66	101.51	1.29	78.04	78.77	1.24
4NC3	44.09	43.59	0.70	42.93	42.55	0.71
5NC1	141.22	137.95	1.68	100.85	99.31	1.55
5NC3	89.25	86.75	1.34	83.08	80.83	1.36
6NC1	182.16	179.48	2.22	122.27	123.36	1.92
6NC3	134.88	136.43	2.01	120.60	123.06	2.03
6NC5	50.93	50.79	0.86	50.07	50.09	0.87
7NC1	224.40	221.38	2.61	142.93	140.66	2.19
7NC3	181.20	177.11	2.53	156.15	153.71	2.53
7NC5	101.84	100.59	1.64	97.28	96.57	1.65
8NC1	266.63	266.35	3.15	159.38	161.00	2.50
8NC3	226.55	226.94	3.14	185.20	190.98	3.08
8NC5	151.23	151.13	2.38	137.73	140.95	2.41
8NC7	54.20	53.70	0.96	52.38	53.12	0.96

Table 5.4: Computational times for the Bermudan swaption comparison deal for a computer with a 700 MHz processor. The notation xNCy in the first column denotes an x-year underlying swap with a non-call period of y years. In the single time step framework Bermudans are priced on a grid and Europeans are priced through numerical integration. All computational times are in seconds.

	Bermudan		**European**	
	Drift-approximated BGM	Longstaff Schwartz	Drift-approximated BGM	Monte Carlo BGM
2NC1	0.4	3.0	0.0	1.9
3NC1	0.4	6.6	0.1	3.7
4NC1	0.7	11.1	0.2	6.1
4NC3	0.2	4.5	0.1	3.4
5NC1	1.4	17.3	0.6	9.1
5NC3	0.3	9.0	0.1	6.2
6NC1	2.4	24.5	0.6	12.8
6NC3	0.7	14.6	0.2	9.8
6NC5	0.2	5.8	0.0	4.8
7NC1	4.0	33.1	0.8	16.8
7NC3	1.4	21.2	0.4	13.5
7NC5	0.3	11.4	0.2	8.6
8NC1	5.6	45.9	1.2	23.9
8NC3	2.2	30.2	0.6	18.8
8NC5	0.6	18.4	0.2	13.5
8NC7	0.1	7.4	0.0	7.8

boundaries.[5] We looked at exercise boundaries for other deals as well and these revealed a similar picture. Risk sensitivities for the various deals are displayed in Figure 5.4.

[5]The empirical covariance matrix of the regression-estimated coefficients a and b may be used to obtain the empirical variance of s^*. Denote random errors in a and b by ϵa and ϵb, respectively. If it is assumed that these errors are relatively small, a Taylor expansion yields (ignoring second-order terms)

$$s^* \approx \frac{a}{1-b}\Big(1 + \frac{\epsilon_a}{a} + \frac{\epsilon_b}{1-b}\Big).$$

We thus obtain the empirical variance of s^* (as well as its standard error). Assuming that s^* is normally distributed, a 95% confidence interval is given by plus and minus twice the standard error.

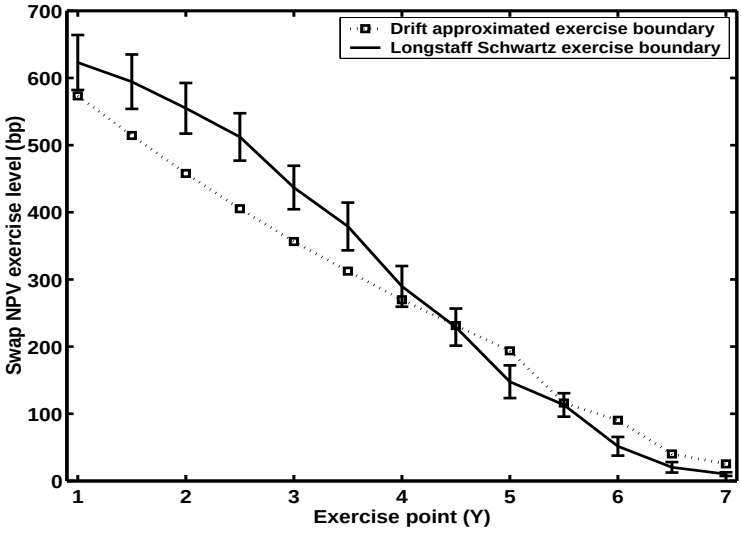

Figure 5.3: Exercise boundaries for the eight-year deal.

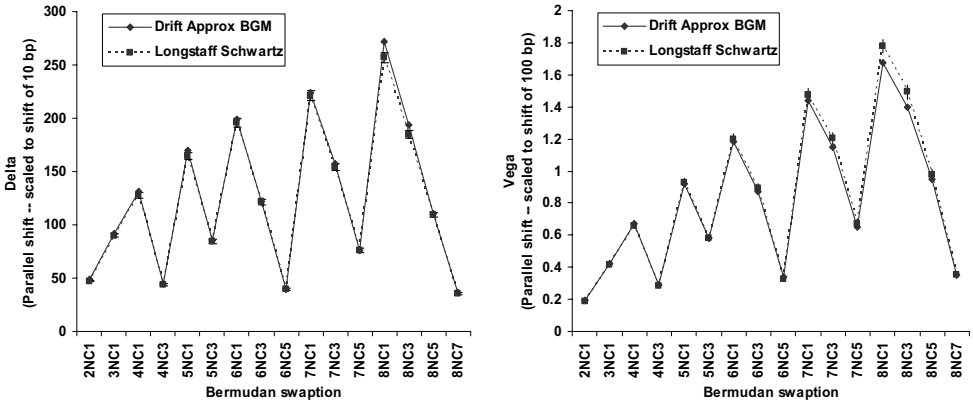

Figure 5.4: Risk sensitivities: deltas and vegas with respect to a parallel shift in the zero rates and caplet volatilities, respectively. The error bars for the Longstaff-Schwartz prices represent a 95% confidence bound based on twice the empirical standard error.

Table 5.5: BGM pricing simulation re-run for 500,000 paths using pre-computed exercise boundaries. The standard errors for both prices were virtually the same in all cases, therefore only a single standard error is reported. All prices and standard errors are in basis points.

BGM simulation price			
	LS pre-computed exercise boundaries	DA pre-computed exercise boundaries	Standard error
2NC1	28.63	28.62	0.06
3NC1	62.80	62.77	0.12
4NC1	99.51	99.58	0.18
5NC1	138.38	138.55	0.24
6NC1	178.08	179.41	0.30
7NC1	221.51	222.49	0.36
8NC1	263.05	265.27	0.42

The results show that the single time step BGM pricing framework indeed prices the Bermudan swaptions close to Longstaff-Schwartz, including correct estimates of risk sensitivities for shorter-maturity deals. In all cases the price difference is within twice the standard error of the simulation. Moreover, the computational time involved is less by a factor 10. We note that the exercise boundary is calculated slightly differently by the Longstaff-Schwartz and drift-approximated (DA) approach. Also, risk sensitivities for longer-maturity deals (seven to eight years) can be outside of the two-standard-error confidence bound. The Brownian bridge drift approximation thus becomes worse for longer-maturity deals, as also explained in Section 5.9. To determine which approach computed the best exercise boundaries, the BGM pricing simulation was re-run for 500,000 paths using the pre-computed exercise boundaries. The results, given in Table 5.5, show that the drift-approximated exercise boundaries are not worse than their Longstaff-Schwartz counterparts and are even slightly better.[6] Hence there is no problem with the spurious early exercise opportunities arising from the absence of no-arbitrage in the fast single time step framework. The non-arbitrage-free issue is investigated further in the next section. This section ends with the results for a two-factor model.

[6]This does not necessarily mean that the DA framework outperforms Longstaff-Schwartz because we only regress on the NPV of the underlying swap. Longstaff-Schwartz may possibly yield better exercise boundaries when it is regressed on to more explanatory variables.

Table 5.6: Two-factor model comparison. 50,000 paths were used for the Longstaff-Schwartz simulation. "Swap NPV only" and "All forward rates" indicate that Longstaff-Schwartz regressed on only the NPV of the swap and on all forward swap rates, respectively. All prices and standard errors are in basis points.

	Fast drift approximation	Longstaff-Schwartz Swap NPV only	Longstaff-Schwartz All forward rates (benchmark)	Standard error
2NC1	25.45	23.27	24.64	0.2
3NC1	59.22	55.79	58.08	0.3
4NC1	94.67	89.54	93.00	0.5
5NC1	132.35	124.79	129.42	0.7
6NC1	171.41	162.89	169.76	0.9
7NC1	212.15	202.97	210.89	1.1
8NC1	252.49	242.59	251.88	1.3
9NC1	292.62	283.89	294.68	1.5

5.8.1 Two-factor model

We consider a two-factor model with the same set-up as above with the exception of the volatility structure, which we now take to be

$$\frac{\mathrm{d}f_i(t)}{f_i(t)} = v_{i,1}\mathrm{d}w_1^{(i+1)}(t) + v_{i,2}\mathrm{d}w_2^{(i+1)}(t).$$

Here $|\mathbf{v}_i| = 15\%$. For a model with forward expiry structure $t_1 < \cdots < t_n$, we take the $\mathbf{v}_i \in \mathbb{R}^2$ to be

$$\mathbf{v}_i = (15\%)\left(a_i, \sqrt{1-a_i^2}\right), \quad a_i = \frac{t_i - t_1}{t_n - t_1}.$$

This instantaneous volatility structure is purely hypothetical. It has the property that correlation steadily drops between more separated forward rates. To solve the two-dimensional PDE version of (5.26) we used the hopscotch method (see paragraph 48.5 of Wilmott (1998)). Results for the two-factor model are displayed in Table 5.6. In a two-factor model (with de-correlation) the exercise decision no longer depends only on the NPV of the underlying swap but also on all forward swap rates. We therefore take the results with regression on all forward swap rates to be the benchmark. Indeed, the drift-approximated prices agree more with the benchmark than with prices obtained when Longstaff-Schwartz regresses on the NPV of a single swap. The computational time for

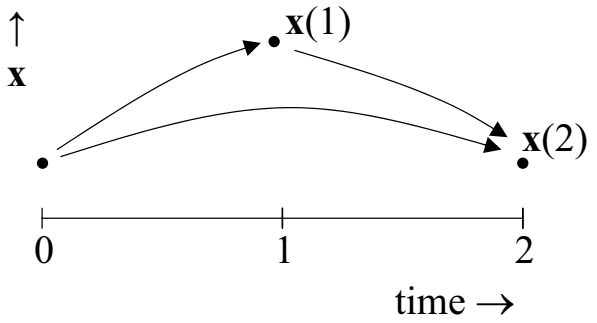

Figure 5.5: Timing inconsistency in the single time step framework for BGM.

the fast drift-approximated pricing two-dimensional grid was, on average, only a quarter of the computational time for Monte Carlo.

5.9 Test of accuracy of drift approximation

Besides the approximation of the drift, the framework (Proposition 4) contains a timing inconsistency. The inconsistency is best described by an example (see Figure 5.5). Suppose that the underlying Markov process $\mathbf{x}$ jumps to $\mathbf{x}(2)$, say, in two years. We consider computing the value of the forwards at year 2. We could jump immediately to year 2 and calculate the forwards there. Alternatively, we could consider first calculating the forwards at time 1 (under the assumption that $\mathbf{x}$ jumps to some value $\mathbf{x}(1)$) and from this point calculate the forwards at time 2 (assuming that $\mathbf{x}$ then jumps to the very same $\mathbf{x}(2)$). In general, the so computed forwards at time 2 will be different.

In a way, any low-dimensional approximation of BGM will exhibit this timing inconsistency. Consider the following. Given the value of $\mathbf{x}(t)$, we cannot determine all time-t forward rates. We do, however, know the value of $f_n(t)$ because f_n has zero drift under the terminal measure $n+1$. The value of any other forward rate $f_i(t)$ does not depend solely on the value of $\mathbf{x}(t)$ but is dependent on the whole path that $\mathbf{x}$ traversed on the interval $[0,t]$. The framework for fast single time step pricing simply calculates the most likely value of $f_i(t)$ given the value of $\mathbf{x}(t)$. If we start from a different initial model state (for example, if we start from the state determined by $\mathbf{x}(1)$), then almost surely our guess for the most likely value of $f_i(t)$ will be different. In this way, it is not really fair to consider this timing inconsistency, but we will nonetheless investigate it. In the following, a test will be proposed to evaluate the size of the inconsistency error.

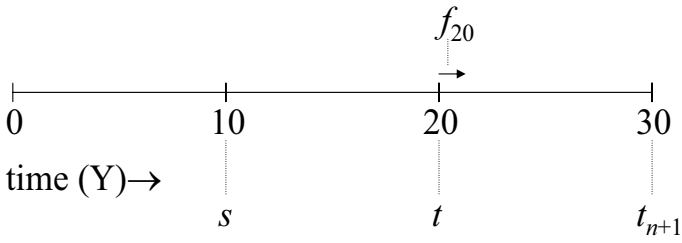

Figure 5.6: Set-up for inconsistency test.

5.9.1 Test of accuracy of drift approximations based on no-arbitrage

The accuracy test is described by an example. We consider some time t at which forwards $i, \ldots, n$ have not yet expired. The framework for fast drift-approximated pricing yields time-t forward rates as a function of $\mathbf{x}(t)$. Under the assumptions that the model state is determined by the Markov process $\mathbf{x}$, and that the framework is arbitrage-free, the fundamental arbitrage-free pricing formula will yield values of forward rates at time $s < t$ *as a function of* $\mathbf{x}(s)$ given by the following formula:[7]

$$f_i^{\mathrm{AF}}(s,\mathbf{x}) = \frac{1}{\alpha_i}\left\{\frac{b_i^{\mathrm{AF}}(s)/b_{n+1}^{\mathrm{AF}}(s)}{b_{i+1}^{\mathrm{AF}}(s)/b_{n+1}^{\mathrm{AF}}(s)} - 1\right\} = \frac{1}{\alpha_i}\left\{\frac{\mathbb{E}^{(n+1)}\left[\frac{b_i^{\mathrm{DA}}(t)}{b_{n+1}^{\mathrm{DA}}(t)}\middle|\mathbf{x}(s)=\mathbf{x}\right]}{\mathbb{E}^{(n+1)}\left[\frac{b_{i+1}^{\mathrm{DA}}(t)}{b_{n+1}^{\mathrm{DA}}(t)}\middle|\mathbf{x}(s)=\mathbf{x}\right]} - 1\right\} \tag{5.27}$$

where each of the above-stated t random variables should be evaluated at $(t, \mathbf{x}(t))$. The second equality follows from $b_i^{\mathrm{AF}}/b_{n+1}^{\mathrm{AF}}$ being a martingale by the assumption of no arbitrage. The "arbitrage-free" forward rates $f_i^{\mathrm{AF}}(s,\mathbf{x})$ obtained in this way may then be compared with forward rates $f_i^{\mathrm{DA}}(s,\mathbf{x})$ obtained by single time stepping.

5.9.2 Numerical results for single time step test

The inconsistency test was performed under the following set-up. Ten annual forward rates were considered where forward rate i accrued from year i to $i+1$, for $i = 20, \ldots, 29$. Under the notation of the previous section, s was taken to be 10 years, t was taken to be 20 years and t_{n+1} was taken to be 30 years. See also Figure 5.6. $f_i(0)$ was taken to be 5%, and mean-reversion, κ, was varied at 0%, 5% and 10%. The $\tilde{\gamma}_i$ were chosen such that the volatility of the corresponding caplet was equal to some general volatility level v, which was varied at 10%, 15% and 20%. Let sd denote the standard deviation of $x(10)$. $x(10)$

[7]Here the notations "AF" and "DA" indicate "arbitrage-free" and "drift-approximated", respectively.

Table 5.7: Quality of drift approximations: comparison of $f_{20}^{\mathrm{AF}}(10)$ and $f_{20}^{\mathrm{DA}}(10)$ under different $x(10)$ moves for the volatility/mean-reversion scenario 15%/10%. sd denotes the standard deviation of $x(10)$. All variables are evaluated at time t=10.

Brownian Bridge				**Predictor-corrector**			
$x(10)$	f_{20}^{AF} (%)	f_{20}^{DA} (%)	$f_{20}^{\mathrm{DA}} - f_{20}^{\mathrm{AF}}$ (bp)	$x(10)$	f_{20}^{AF} (%)	f_{20}^{DA} (%)	$f_{20}^{\mathrm{DA}} - f_{20}^{\mathrm{AF}}$ (bp)
$-$sd	3.75	3.81	5.11	$-$sd	3.74	3.81	7.17
$-$sd/2	4.23	4.27	4.03	$-$sd/2	4.19	4.27	7.94
0	4.77	4.79	2.37	0	4.70	4.79	8.81
+sd/2	5.38	5.38	-0.05	+sd/2	5.28	5.38	9.79
+sd	6.07	6.03	-3.47	+sd	5.92	6.03	10.91

Table 5.8: Quality of drift approximations: Maximum of $|f_{20}^{\mathrm{AF}}(10) - f_{20}^{\mathrm{DA}}(10)|$ over $x(10)$ moves $0, \pm\mathrm{sd}/2, \pm\mathrm{sd}$ for different volatility/mean-reversion scenarios. sd denotes the standard deviation of $x(10)$. Differences are denoted in basis points.

	Brownian Bridge				**Predictor-corrector**		
Mean-reversion	Volatility level (v) 10%	15%	20%	Mean-reversion	Volatility level (v) 10%	15%	20%
0%	2.97	9.34	28.73	0%	2.86	8.60	37.45
5%	2.56	8.21	19.46	5%	2.32	12.29	53.85
10%	1.46	5.11	12.56	10%	1.69	10.91	44.59

moves were considered for $0, \pm\mathrm{sd}/2$, and $\pm\mathrm{sd}$. Results for the volatility/mean-reversion scenario 15%/10% are given in Table 5.7. The comparison is only reported for f_{20} because this forward rate contains the most drift terms, and therefore its corresponding error is the largest among $i = 20, \ldots, 29$. We note that the error for f_{29} is always zero as it is fully determined by x. In Table 5.8 the maximum error (over the five considered $x(10)$ moves) between $f_{20}^{\mathrm{AF}}(10)$ and $f_{20}^{\mathrm{DA}}(10)$ is reported.

The test was performed for both the Brownian bridge and predictor-corrector schemes. The results show that the former outperforms the latter in the timing inconsistency test.

The inconsistency test results show that, for less volatile market scenarios, the single time step framework performs very accurately, with errors only up to a few basis points.

For more volatile market scenarios the approximation deteriorates. But for realistic yield curve and forward volatility scenarios there are no problems with respect to pricing (see Section 5.8). The worsening of the approximation for more volatile scenarios is what may be expected from the nature of the drift approximations: as the model dimensions increase, the single time step approximation will break up. By "model dimensions" we mean the volatility level, the tenor of the deal, the difference between the forward index i and n, or time zero forward rates, etc. Care should be taken in applying the single time step framework for BGM that the market scenario does not violate the realm where the single time step approximation is reasonably valid.

5.10 Conclusions

We have introduced a fast approximate pricing framework as an addition to the predictor-corrector drift approximation developed by Hunter et al. (2001). These authors used the drift approximation only to speed up their Monte Carlo by reducing it to single time step simulation. We have shown that, at a slight cost, much faster computational methods may be used, such as numerical integration or finite differences. The additional cost is a non-restrictive assumption, namely, separability of the volatility function. The proposed drift approximation framework was applied to the pricing of Bermudan swaptions, for which it yielded very accurate prices with much lower computation times.

5.A Appendix: Mean of geometric Brownian bridge

In this appendix, the time-t mean of the process f_k defined in (5.9) is determined. Equivalently, we may determine the time-t mean of the process y, given by

$$\frac{\mathrm{d}y(t)}{y(t)} = \boldsymbol{\sigma}(t) \cdot \mathrm{d}\mathbf{w}(t), \quad y(0) = y_0, \quad y(t^*) = y^*.$$

(Compare with (5.9).) The solution of y (unconditional of time-t^*) is given by

$$y(t) = y_0 e^{x(t) - \frac{1}{2}v(t)},$$

where

$$x(t) := \int_0^t \boldsymbol{\sigma}(s) \cdot \mathrm{d}\mathbf{w}(s), \quad v(t) := \int_0^t \|\boldsymbol{\sigma}(s)\|^2 \mathrm{d}s.$$

We note that

$$\big\{\omega \in \Omega; y(t^*) = y^*\big\} = \big\{\omega \in \Omega; x(t^*) = \log(y^*/y_0) + \frac{1}{2}v(t^*) =: x^*\big\}.$$

According to the martingale time change theorem (for example Theorem 4.6 of Karatzas & Shreve (1991)), we have that $x(\tau(\cdot))$ is a Brownian motion, where the time change τ is defined by

$$\tau(t) = \inf\{s \geq 0;\ v(t) > s\}.$$

Working in the time-changed time coordinates, $x(\cdot)|x(\tau^*) = x^*$ is a standard Brownian bridge, and so, according to Section 5.6.B of Karatzas & Shreve (1991),

$$\big(x(\tau)\big|x(\tau^*) = x^*\big) \sim \mathcal{N}\left(\frac{\tau}{\tau^*}x^*, \tau - \frac{\tau^2}{\tau^*}\right).$$

Back in the original time coordinates, this translates to

$$\big(x(t)\big|x(t^*) = x^*\big) \sim \mathcal{N}\left(\frac{v(t)}{v(t^*)}x^*, v(t) - \frac{\big(v(t)\big)^2}{v(t^*)}\right).$$

With this, we may evaluate the mean of $(y(t)|y(t^*) = y^*)$ to be

$$\mathbb{E}\big[y(t)\big|y(t^*) = y^*\big] = y_0\left(\frac{y^*}{y_0}\right)^{\frac{v(t)}{v(t^*)}} \exp\left\{\frac{1}{2}\frac{v(t)}{v(t^*)}\big(v(t^*) - v(t)\big)\right\}, \tag{5.28}$$

where the following simple rule has been used: $\mathbb{E}[e^z] = e^{\beta+\tau^2/2}$ whenever z is normally distributed, $z \sim \mathcal{N}(\beta, \tau^2)$.

5.B Appendix: Approximation of substituting the mean in the expectation of expression (5.9)

In Section 5.3 a four-step method for the calculation of expression (5.9) is described. An approximating fourth step is proposed that evaluates the expectation of the BGM drift inserting the mean. In this appendix an error bound for this approximation is derived, and it is shown that the approximation is of order two in volatility in the neighbourhood of zero.

The expectation term can always be rewritten as

$$g(\mu, \sigma) = \mathbb{E}\left[\frac{\exp\{\mu + \sigma z\}}{1 + \exp\{\mu + \sigma z\}}\right],$$

where z is distributed standard normally. It is straightforward to verify that the above function $g : \mathbb{R}^2 \to \mathbb{R}$ is infinitely differentiable at every point of the whole real plane. We note that approximating the above expectation at the mean signifies that the above function is approximated as

$$g(\mu, \sigma) \approx g(\mu, 0) = \frac{\exp\{\mu\}}{1 + \exp\{\mu\}}.$$

Fix μ and calculate the derivative of g with respect to σ. The interchange of differentiation and expectation is a subtle argument that may, for example, be found in Williams (1991, paragraph A.16.1). We carefully verified that in the above case all the requirements for interchange are satisfied. We then find

$$\frac{\partial g}{\partial \sigma}(\mu, \sigma) = \mathbb{E}\left[z \frac{\exp\{\mu + \sigma z\}}{\left(1 + \exp\{\mu + \sigma z\}\right)^2} \right].$$

Due to the odd nature of the above integrand at the point $\sigma = 0$, we find that

$$\frac{\partial g}{\partial \sigma}(\mu, 0) = 0.$$

Taylor's formula then states that there exists $c \geq 0$ (possibly depending on μ) such that

$$\left| g(\mu, \sigma) - \frac{\exp\{\mu\}}{1 + \exp\{\mu\}} \right| \leq c\sigma^2.$$

Because a bound on the second derivative of $\sigma \mapsto g(\mu, \sigma)$ may be found independently of μ on some interval $[0, \bar{\sigma}]$, it follows from Theorem 7.7 of Apostol (1967) that the constant c may then be chosen independently of μ for all $\sigma \in [0, \bar{\sigma}]$.

5.C Appendix: MATLAB code for Brownian bridge scheme

MATLAB code illustrating the Brownian bridge scheme and the four-steps calculation method in Section 5.4, is displayed below.

```
function result = fBB(n,f0,a,vol,t,z)
% Calculates forward LIBOR rates in one-factor model with Brownian bridge
% drift approximation & single time step, given the normal increment z.

% n, no. of forward LIBORs, a positive integer
% f0, array with n elements, time zero forward LIBORs
% a, array with n elements, day count fractions
% vol, array with n elements, vol[i] = volatility of forward LIBOR i
% t, time (scalar)
% z, Gaussian increment ~N(0,1), scalar

% f is used to store result
f=zeros(n,1); % creates zero array with n entries
```

```
% First do ultimate forward LIBOR => martingale!
f(n)=f0(n)*exp(-0.5*vol(n)^2*t+vol(n)*sqrt(t)*z);
% Loop from penultimate LIBOR down to first LIBOR.
run_drift=0.0; % used for efficient calculation of drift
for i=n-1:-1:1
    zt=log(f(i+1)/f0(i+1))+0.5*vol(i+1)^2*t; % Needed for driftBB.
    % quad is a standard integration routine in MATLAB.
    % quad(@f,a,b,tol,trace,p1,p2,...) integrates the function
    % f(s,p1,p2,...) over s from a to b with convergence criteria tol and
    % trace.
    % For definitions of tol and trace we refer to MATLAB documentation.
    % Of course, one can use any integration routine instead of quad.
    % Adjusting the convergence criterion of the numerical integrator
    % allows for a trade-off between accuracy and computational speed.
    % For example, the predictor-corrector scheme is a special case of
    % the Brownian bridge scheme if the crudest integrator (two-point
    % trapezoid) is used.
    run_drift=run_drift ...
      -quad(@driftBB,0.0,t,1.0e-6,0,f0(i+1),a(i+1),vol(i+1),t,zt);
    % Equation (5.3) in exp form
    f(i)=f0(i)*exp((run_drift*vol(i)-0.5*vol(i)^2*t)+vol(i)*sqrt(t)*z);
end

result = f; % return result f

function result = driftBB(s,f0,a,vol,t,zt)
% Calculates drift term evaluated at the mean of the Brownian bridge.
% This function will be integrated over time.

% s, scalar, current (intermediate) time
% f0, scalar, time zero forward LIBOR
% a, scalar, day count fraction
% vol, scalar, volatility of forward LIBOR
% t, scalar, time (at which forward LIBOR has already been predicted)
% zt, scalar, help variable associated with LIBOR predicted at time t

% Mean of Brownian bridge, Equation (5.26) in log-form:
m=s./t.*zt-0.5.*vol.^2.*s.*s./t+log(f0)+log(a);
```

```
% Essential form of BGM drift in terms of log rates:exp(.)/(1+exp(.)):
result=vol*exp(m)./(1.0+exp(m));
```

Chapter 6

A comparison of single factor Markov-functional and multi factor market models

We compare single factor Markov-functional and multi factor market models for hedging performance of Bermudan swaptions. We show that hedging performance of both models is comparable, thereby supporting the claim that Bermudan swaptions can be adequately risk-managed with single factor models. Moreover, we show that the impact of smile can be much larger than the impact of correlation. We propose a new method for calculating risk sensitivities of callable products in market models, which is a modification of the least-squares Monte Carlo method. The hedge results show that this new method enables proper functioning of market models as risk-management tools.

6.1 Introduction

Bermudan swaptions form a popular class of interest rate derivatives. The underlying is a plain-vanilla interest rate swap, in which periodic fixed payments are exchanged for floating LIBOR payments. Institutional debt issuers use interest rate swaps to revert from floating to fixed interest rate payments, and vice versa. Often the issuers want to reserve the right to cancel the swap. A cancellable swap can be valued by the following parity relation. A cancellable interest rate swap is equal to a plain-vanilla interest rate swap plus a callable interest rate swap with reversed cash flows. Thus a cancellable swap can be valued when the callable swap can be valued. Such callable swap options are referred to as Bermudan swaptions. *Bermudan* means that the exercise opportunities are at a discrete set of time points. A *European* swaption is an option to enter into a swap at only a single exercise date.

In this chapter, we will study the pricing and hedging performance of two popular models for Bermudan swaptions. Many models have been proposed in the literature for valuation and risk management of Bermudan swaptions. We distinguish three categories: short-rate models, Markov-functional models and market models.

Short-rate models model the dynamics of the term structure of interest rates by specifying the dynamics of a single rate (the short rate) from which the whole term structure at any point in time can be calculated. Examples of short-rate models include the models of Vasicek (1977), Cox et al. (1985), Dothan (1978), Black et al. (1990), Ho & Lee (1986) and Hull & White (1990).

The Markov-functional model of Hunt et al. (2000) assumes that the discount factors are a function of some underlying Markov process. The model is then fully determined by no-arbitrage arguments and by requiring a fit to the initial yield curve and interest rate option volatility.

Market models were introduced by Brace et al. (1997), Miltersen et al. (1997) and Jamshidian (1997). The name 'market model' refers to the modelling of market observable variables such as LIBOR rates and swap rates. The explicit modelling of market rates allows for natural formulas for interest rate option volatility, that are consistent with the market practice of using the formula of Black (1976) for caps (options on LIBOR) and swaptions (options on swap rates).

Short-rate and Markov-functional models are usually[1] implemented as models with a single stochastic process driving the term structure of interest rates. A disadvantage is then that the instantaneous correlation between interest rates can only be 1. Market models however efficiently allow for any number of stochastic variables to be used, so that any instantaneous correlation structure can be captured. There is substantial evidence that the term structure of interest rates is driven by multiple factors (three, four, or even more), see the review article of Dai & Singleton (2003). A more realistic description of reality may thus be expected from multi factor models, which points to possibly better hedge performance. The question addressed in this chapter is whether the increase in hedge performance due to use of a multi factor model is significant. To those that a priori dismiss the use of single factor models due to their economic irrelevance by failure in capturing the multi factor dynamics of the term structure of interest rates, we say: Models that are best for managing an interest rate derivatives book are not necessarily models that are most realistic, rather they are models that most reduce variance of profit and loss (P&L), thereby preserving wealth in the most stable manner. We mention four articles that compare single and multi factor models.

First, in favour of multi factor models, Longstaff et al. (2001) claim that short-rate models, because of supposedly misspecified dynamics, lead to suboptimal exercise strate-

[1] Two factor short rate models exist too, see for example Ritchken & Sankarasubramanian (1995).

gies. This claim is supported by empirical evidence performed with the short-rate models of Black et al. (1990) and Black & Karasinski (1991). The authors then conclude that the costs to Wall Street firms of following single factor exercise strategies could be several billion dollars. The argument of Andersen & Andreasen (2001), and also ours, against the claim of Longstaff et al. (2001), is that their choice of calibration does not correspond to market practice and leads to models that are poorly fitted to market.

Second, in favour of single factor models, Andersen & Andreasen (2001) claim that the exercise strategy obtained from a properly calibrated single factor model only leads to insignificant losses when applied in a two factor model.

Third, Driessen, Klaassen & Melenberg (2003) are the first to investigate hedge performance. These authors investigate two types of delta hedge instruments, (i) a number of delta hedge securities, i.e. discount bonds, equal to the number of factors, and (ii) a large set of discount bonds, one for each security spanning the yield curve. They show that if the number of hedge instruments is equal to the number of factors, then multi factor models outperform single factor models. If, however, the large set of hedging instruments is used, which is the case in practice, then single factor models perform as well as multi factor models in terms of delta hedging of European swaptions.

Fourth, Fan, Gupta & Ritchken (2003) show, for the case of the number of hedge instruments equal to the number of factors, that higher factor models perform better than lower factor models in terms of delta hedging of European swaptions and European swaption straddles[2]. The results of Fan et al. (2003) are thus consistent with the findings of Driessen et al. (2003).

Relative to Driessen et al. (2003) and Fan et al. (2003), we make the contribution of also considering *vega* hedging and *Bermudan*-style swaptions rather than only delta hedging and only European-style swaptions. A European product depends solely on the marginal distributions of the swap rates, whereas a Bermudan product depends on the joint distribution, too. Moreover, we fit the models exactly to a subset of European swaptions particular to a Bermudan swaption rather than attempting to fit to the whole swaption volatility surface, as Driessen et al. (2003) and Fan et al. (2003). The two practices of (i) fitting to an appropriate set of swaptions, and (ii) vega hedging, are probably more close in spirit to financial practice. In fact, we show that the variance of P&L is significantly reduced when a vega hedge has been set up additional to a delta hedge.

There is one drawback of using high factor models however, which is lesser tractability than low (one or two) factor models. For valuation in high factor models, we must resort to Monte Carlo (MC) simulation. Valuation by MC is not a problem, but the estimation

[2]A *European swaption straddle* consists of a position of long a payer swaption and long an otherwise identical receiver swaption.

of sensitivities (*Greeks*) can be less efficient. This is not due to the choice of calibration, as can sometimes be the case as shown by Pietersz & Pelsser (2004*a*) (see Chapter 2), since in this chapter the safe option of time-constant volatility (but dependent on the forward rates) is used. The less efficient estimation of sensitivities occurs if the payoff along the path can change discontinuously as dependent on initial parameters, see, for example, Glasserman (2004, Section 7.1). We show that such discontinuity appears in the Longstaff & Schwartz (2001) algorithm for valuation of Bermudan-style options. We consider two methods to improve the efficiency of sensitivity estimates. The comparison of hedge performance of single and multi factor models thus entails a trade-off between more realistic modelling and tractability.

For the Markov-functional model, the failure of not capturing a realistic instantaneous correlation structure can be remedied, in some sense, for Bermudan swaptions and perhaps for other derivatives, too, as follows. In theory the price of a co-terminal Bermudan swaption is dependent of and fully determined by the joint distribution of the forward co-terminal swap rates at each of the exercise dates. In effect there are thus $n(n+1)/2$ stochastic variables that determine the price. In this chapter, we use the observation that the price of a Bermudan swaption is, up to first order approximation, determined by the joint distribution of only the underlying spot co-terminal swap rates at the exercise dates, see, e.g., Piterbarg (2004, page 67). There are only n such spot co-terminal swap rates. The marginal distributions of these swap rates are governed by the associated European swaption volatility quoted in the market, whereby, in a log-normal model, we only need to specify correlation. We will call their correlation the *terminal correlation*. A novel approximating formula is derived for the terminal correlation in the Markov-functional model. The accuracy of the new formula is tested numerically. The novel formula allows the Markov-functional model to be calibrated to terminal correlation. We then equip a full factor swap market model with a parameterized instantaneous correlation matrix, calculate the resulting terminal correlation and fit the Markov-functional model to this terminal correlation. Thus, although the Markov-functional model fails to capture instantaneous correlation, it can be tweaked such that it is fitted to product specific terminal correlation. Since such correct correlation specification more or less determines the price of the Bermudan swaption, it then no longer matters for pricing Bermudan swaptions whether the single factor Markov-functional model is a realistic or unrealistic model of other parts of reality in the interest rate market, outside of the volatilities and correlations of the relevant swap rates. Essentially, we have projected all relevant parts of reality correctly onto the single factor Markov-functional model. With the thus fitted Markov-functional model, and also with swap and LIBOR market models, we subsequently compare hedge performance of Bermudan swaptions with real market data over a 1 year period.

The research in this chapter is not aimed at comparing the model generated Bermudan swaption prices to real-life market quoted prices. Rather, the hypothetical viewpoint is taken that swaps and European swaptions are liquidly traded in the market, and Bermudan swaptions are less liquidly traded. The model is then used as an extrapolation tool to determine a Bermudan swaption price consistent with swap and European swaption prices, and such that the risk sensitivities provide a hedge of the former in terms of the latter securities. In any case, the study in this chapter is relevant for non-standard Bermudan swaptions, for which the underlying has more exotic coupon payments. Examples of such exotic coupon payments are *capped floater* ($\min(\ell f, k)$ for some cap rate k and leverage ℓ), *inverse floater* ($\max(k - \ell f, 0)$) and *range accrual* (ϱf, with ϱ the fraction for which LIBOR within the accrual period is within a certain range). These non-standard Bermudan swaptions are called *callable LIBOR exotics*. The results of this chapter may apply to many types of callable LIBOR exotics, but further research will have to provide a definitive answer. Nonetheless, the results of this chapter are interesting for the study of callable LIBOR exotics, since these have evolved from standard Bermudan swaptions.

For both the swap market model and the Markov-functional model we initially use the basic well-known non-smile versions. Smile is the phenomenon that for European options different Black-implied volatility is quoted for different strikes of the option. As mentioned in Hunt et al. (2000, last paragraph of Section 3.2), the Markov-functional model can be fitted to smile. We provide details, also for the swap market model, and show that the resulting smile-fitting procedure is numerically efficient and straightforward to implement. The smile Markov-functional model and smile swap market model are subsequently fitted to USD swaption smile data. We then compare empirically the impact of smile versus the impact of correlation.

The LIBOR Markov-functional model has been compared with the LIBOR market model before by Bennett & Kennedy (2004). These authors show that the one factor LIBOR Markov-functional model with mean reversion and the one factor separable LIBOR market model are largely similar in terms of dynamics and pricing. They also show this for an approximated version of the LIBOR market model by drift approximations, as introduced by Pietersz et al. (2004) (see also Chapter 5) and Hunter et al. (2001). Relative to Bennett & Kennedy (2004) this chapter makes the contribution of also comparing multi factor models with the Markov-functional model. Moreover, we show how multi factor models can a priori be compared to the Markov-functional model which is not a straightforward extension from the one-dimensional case.

The remainder of the chapter is organized as follows. First, we outline the comparison methodology for the two models. The LIBOR and swap market models and Markov-functional model are discussed, as well as the two Greeks calculation methods for market models. Second, the data is described. Third, we numerically test the accuracy of an approximating formula for the terminal correlation in the Markov-functional

model. Fourth, empirical comparison results are presented. Fifth, the impact of smile is investigated. Sixth, we conclude.

6.2 Methodology

In this section, we first introduce some notation. Second, we set up the framework that enables a comparison between multi factor and single factor models.

The type of Bermudan swaption that is considered here is the *co-terminal* version, as opposed to, for example, the *fixed maturity* version. A co-terminal Bermudan swaption is an option to enter into an underlying swap at several exercise opportunities, where each swap ends at the same contractually determined end date. The maturity of the swap entered into thus becomes smaller as the option is exercised later. In contrast, for a fixed maturity Bermudan swaption, each swap that can be entered into has the same contractually specified maturity and the respective end dates then differ. We consider a Bermudan swaption on an underlying swap with n payments and a fixed rate k. Associated with this swap is a tenor structure $0 < t_1 < \cdots < t_{n+1}$. The underlying swap makes a payment π_i at time t_{i+1} depending on the LIBOR rate $f(t_i)$ fixed at time t_i for $i = 1, \ldots, n$. Denote the notional amount by q and the day count fraction for accrual period $[t_i, t_{i+1}]$ by α_i. Introduce the variable $\eta \in \{-1, 1\}$ by $\eta = 1$ for a pay fixed swap and $\eta = -1$ for a receive fixed swap. The payment π_i is then $\eta\alpha_i(f(t_i) - k)q$. The holder of the Bermudan swaption has the right to enter into the swap at the dates $t_1, \ldots, t_n$. If the holder exercises the option at time t_i, then he or she will receive the payments $\pi_i, \ldots, \pi_n$. Alternatively, in the market the holder could have entered into an otherwise equal swap but with fixed rate equal to the swap rate $s_{i:n+1}(t_i)$. Here $s_{i:j}$ denotes the forward swap rate for a swap that start at t_i and ends at t_{j+1}. The holder will thus only exercise the Bermudan at time t_i if $\eta(s_{i:n+1}(t_i) - k) > 0$. But even when the immediate exercise value is positive, the holder can nonetheless decide to hold on to the option in view of a more favourable forward swap rate $s_{j:n+1}(t_i)$, $j > i$. It follows that the price of a Bermudan swaption is dependent of and fully determined by the joint distribution of the variables $\{s_{j:n+1}(t_i)\ ;\ j = i, \ldots, n,\ i = 1, \ldots, n\}$. The forward swap rates $\{s_{1:n+1}, \ldots, s_{n:n+1}\}$ are called *co-terminal* since they all co-end at the same termination date.

We contend that the main driver for the price of Bermudan swaptions is the joint distribution of the realizations of the co-terminal swap rates $\{s_{i:n+1}(t_i)\ ;\ i = 1, \ldots, n\}$. Ostrovsky (2002) calls this the *diagonal process*. The economic argument is that prima facta, the holder of the option has to choose between receiving the payoffs of entering into the swaps starting at $t_1, t_2, \ldots, t_n$ and the associated payoffs are determined fully by $s_{1:n+1}(t_1), s_{2:n+1}(t_2), \ldots, s_{n:n+1}(t_n)$.

As is common in financial practice, we calibrate models to only those sections of the market that are relevant to the product, rather than attempting to fit the models to all available market data. We assume that any valuation model for the Bermudan swaption is calibrated to the so-called *diagonal* of European swaptions that start at t_i and end at t_{n+1}, $i = 1, \ldots, n$. This means that the variance of the variables $\{s_{1:n+1}(t_1), \ldots, s_{n:n+1}(t_n)\}$ is already fully determined. Thus the diagonal process is fully determined (given a normal or log-normal distribution) if we specify the correlation matrix for the variables $\{s_{i:n+1}(t_i)\ ;\ i = 1, \ldots, n\}$. This correlation matrix will be called the *terminal correlation*. In the next three sections, we discuss the LIBOR and swap market models and the Markov-functional model, respectively. We show how the terminal correlation can approximately be calculated in the swap market model and the Markov-functional model. For the Markov-functional model we show how the model can be calibrated to the terminal correlation.

The idea of terminal correlation is not new to finance. For example, Rebonato (2002, Section 7.1.2) shows that it is the terminal and not the instantaneous correlation that directly affects the price of swaptions. The terminal correlation itself is determined both by the instantaneous correlation and the term structure of instantaneous volatility. In Rebonato (1999*c*, Section 11.4) it is shown that the terminal correlation is influenced just as much, and even more, by the instantaneous volatility than by the instantaneous correlation.

6.2.1 The LIBOR and swap market models

Within the swap market model, n forward swap rates are modelled as log-normal processes under their respective forward measure, with forward swap rate $s_{i:n+1}$ satisfying,

$$\frac{\mathrm{d}s_{i:n+1}(t)}{s_{i:n+1}(t)} = \boldsymbol{\sigma}_{i:n+1}(t) \cdot \mathrm{d}\mathbf{w}^{(i:n+1)}(t), \quad \left\langle \mathrm{d}\mathbf{w}^{(i:n+1)}(t), \mathrm{d}\mathbf{w}^{(j:n+1)}(t) \right\rangle = \rho_{i:n+1,j:n+1}(t)\mathrm{d}t.$$

Here $\boldsymbol{\sigma}_{i:n+1}(\cdot)$ denotes the instantaneous volatility function and $\mathbf{w}^{(i:n+1)}$ denotes a Brownian motion under the i^{th} forward swap measure. The latter measure is associated with a portfolio of discount bonds, weighted by the respective day count fractions, with maturity times corresponding to the payment times of the swap. The value of such a portfolio of discount bonds is named the *present value of a basis point (PVBP)*.

Within the LIBOR market model, n forward LIBORs are modelled as log-normal processes under their respective forward measure, with forward LIBOR f_i satisfying,

$$\frac{\mathrm{d}f_i(t)}{f_i(t)} = \boldsymbol{\sigma}_i(t) \cdot \mathrm{d}\mathbf{w}^{(i+1)}(t), \quad \left\langle \mathrm{d}\mathbf{w}^{(i+1)}(t), \mathrm{d}\mathbf{w}^{(j+1)}(t) \right\rangle = \rho_{ij}(t)\mathrm{d}t.$$

Here $\boldsymbol{\sigma}_i(\cdot)$ denotes the instantaneous volatility function and $\mathbf{w}^{(i+1)}$ denotes a Brownian motion under the i^{th} forward measure. The latter measure is associated with a discount

bond that matures at t_{i+1}, the payment time of the i^{th} LIBOR deposit. The LIBOR market model is calibrated approximately to swaption volatility, via an approximation of swaption volatility in terms of LIBOR volatility, see, e.g., Hull & White (2000). By assumption of constant volatility and constant correlation (see below), the resulting calibration algorithm reduces to a simple bootstrap algorithm for determining the LIBOR volatility levels.

Within both market models, we set the instantaneous volatility and correlation constant over time, i.e., $\boldsymbol{\sigma}_{i:n+1}(t) = \boldsymbol{\sigma}_{i:n+1}$ and $\rho_{i:n+1,j:n+1}(t) = \rho_{i:n+1,j:n+1}$ for the swap model, and $\boldsymbol{\sigma}_i(t) = \boldsymbol{\sigma}_i$ and $\rho_{ij}(t) = \rho_{ij}$ for the LIBOR model. These choices, relative to the time-homogeneous case, will not, or only favourably, impact the results, as explained by the following two arguments. First, a constant instantaneous volatility assumption leads to efficiently estimated risk sensitivities, whereas certain specific time-homogeneous specifications may not, as shown by Pietersz & Pelsser (2004*a*), see also Chapter 2. Second, our choice of parametrization of the correlation matrix is both a constant and time-homogeneous parametrization.

The rank of the correlation matrix $\mathbf{P} = (\rho_{ij})_{i,j=1}^{n}$ determines the number of Brownian motions (*number of factors*) driving the model. When an arbitrary correlation matrix has been specified, generally such matrix has full rank n, but then if a number of factors $d < n$ be required, we are led to solve a rank reduction problem[3]. To test the two extreme cases, we consider only either rank 1 or full-rank correlation matrices, allowing respectively correlation constant at 1 or a full fit to any correlation matrix.

We parameterize the instantaneous correlation matrix by, for $i < j$,

$$\rho_{ij}(a) = \sqrt{\frac{(e^{2at_i} - 1)/t_i}{(e^{2at_j} - 1)/t_j}} \quad \text{for} \quad a > 0, \quad \text{and} \quad \rho_{ij}(a) \equiv 1, \quad \text{for} \quad a = 0. \tag{6.1}$$

This parametrization of instantaneous correlation allows for a simple calibration of the Markov-functional model to the terminal correlation of the swap market model. In fact, parametrization (6.1) has been chosen such that the resulting terminal correlation of the swap market model exactly matches the terminal correlation of a Markov-functional model with mean reversion parameter a. The correlation structure (6.1) is nonetheless a good choice, since we will show that, for a suitable choice of a, (6.1) corresponds to a form that is often quoted in the literature, see, for example, Rebonato (1998, Equation (4.5), page 83),

$$\rho_{ij}(\beta) = \exp\big(-\beta|t_i - t_j| \big), \quad \text{for some} \quad \beta \geq 0. \tag{6.2}$$

We numerically fitted the form of (6.1) to (6.2), for 10×10 correlation matrices, where $n = 10$ corresponds to the setting in the forthcoming hedge tests. In other words, fix β,

[3]For solving such rank reduction problems the reader is referred to Pietersz & Groenen (2004*a*, *b*) (see Chapter 3), Grubišić & Pietersz (2005) (see Chapter 4), Wu (2003), Rebonato (2002, Section 9) or Brigo (2002).

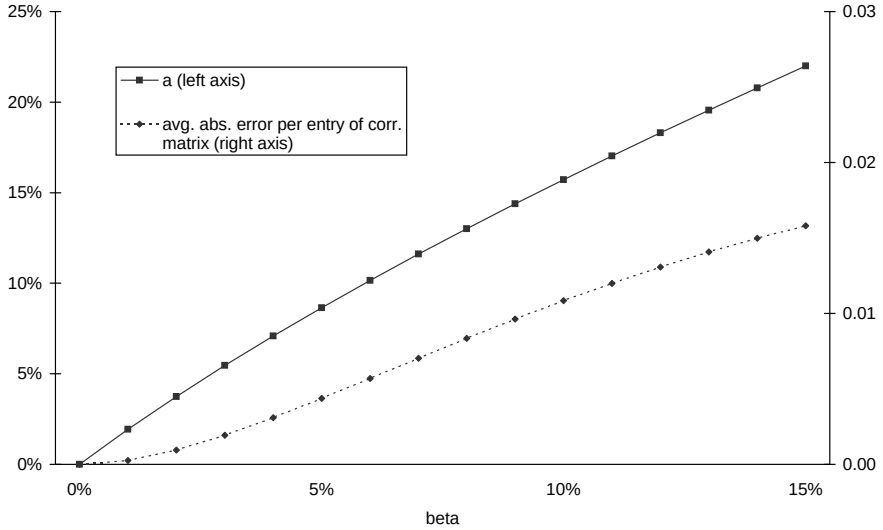

Figure 6.1: Fitted a-parameter of parametrization (6.1) (left axis) and fit error (right axis) versus the β-parameter of the Rebonato (1998) parametrization (6.2). The fit error is the average absolute error over the entries.

and then find a that solves

$$\min_{a \geq 0} \sum_{i=1}^{n} \sum_{j=1}^{n} \left| \, \rho_{ij}(a) - \rho_{ij}(\beta) \, \right|.$$

The relationship between the fitted a as dependent on β is displayed in Figure 6.1. As can be seen from the figure, the fit is of good quality, obtaining an average absolute error over the entries in the correlation matrix that is less than 0.02 for typical values of β and a.

6.2.2 The Markov-functional model

We consider the *swap* variant of the Markov-functional model, see Hunt et al. (2000, Section 3.4) for details on this variant. Within the (swap) Markov-functional model, any model variable is a function of an underlying Markov process x. For example, for a forward swap rate we have $s_{i:n+1}(t_j) = s_{i:n+1}(t_j, x(t_j))$. We assume that the driving Markov process of the model is a deterministically time-changed Brownian motion, satisfying

$$\mathrm{d}x(t) = \tau(t)\mathrm{d}w(t).$$

Here $\tau(\cdot)$ denotes a deterministic function (that can be chosen piece-wise constant) and w denotes a Brownian motion.

We now present an approximate formula for the terminal correlation. An argument explaining the formula is given, and in a later section we investigate the accuracy of the approximating formula. By a Taylor expansion, we have $\ln s_{i:n+1}(t_i, x) \approx s^{(0)}_{i:n+1}(t_i) + s^{(1)}_{i:n+1}(t_i)x$. Since correlation is unaltered by a linear transformation, the terminal correlation of the swap rates is thus approximately equal to the terminal correlation of the underlying Markov process,

$$\rho\big(\ \ln s_{i:n+1}(t_i), \ln s_{j:n+1}(t_j)\ \big) \approx \rho\big(\ x(t_i), x(t_j)\ \big). \tag{6.3}$$

By straightforward calculation, for $i < j$,

$$\rho\big(\ x(t_i), x(t_j)\ \big) = \frac{\mathrm{Cov}(x(t_i), x(t_j))}{\sqrt{\mathrm{Var}(x(t_i))\mathrm{Var}(x(t_j))}} = \sqrt{\frac{\int_0^{t_i} \tau^2(t)\mathrm{d}t}{\int_0^{t_j} \tau^2(t)\mathrm{d}t}}. \tag{6.4}$$

In fact, any functional of the Markov process can be linearized by a Taylor expansion and, according to the argument above, would exhibit the same approximate terminal correlation (6.4). The above theoretical argument is therefore not very strong. The approximation however turns out to be accurate, as will be shown numerically in Section 6.4.

In principle, the Markov-functional model can thus be approximately fitted to the terminal correlation by minimization of the fitting error given a market-implied or historically estimated terminal correlation matrix. The parameters for this minimization problem are for example the n parameters governing the piece-wise constant function $\tau(\cdot)$. For ease of exposition we will however restrict our attention to the case of mean reversion, i.e. $\tau(t) = \exp(at)$, with a denoting the mean reversion parameter, see Section 4 of Hunt et al. (2000). In this case we have, for $i < j$,

$$\rho\big(\ x(t_i), x(t_j)\ \big) = \sqrt{\frac{e^{2at_i} - 1}{e^{2at_j} - 1}}. \tag{6.5}$$

To verify that the Markov-functional model is properly calibrated to terminal correlation, in the swap market model this correlation is approximately calculated to be, from (6.1), for $i < j$,

$$\frac{\int_0^{t_i} \sigma_{i:n+1}(t)\sigma_{j:n+1}(t)\rho_{ij}(t)\mathrm{d}t}{\sqrt{\int_0^{t_i} \sigma^2_{i:n+1}(t)\mathrm{d}t \int_0^{t_j} \sigma^2_{j:n+1}(t)\mathrm{d}t}} = \frac{\sigma_{i:n+1}\sigma_{j:n+1}\rho_{ij}t_i}{\sqrt{\sigma^2_{i:n+1}t_i\sigma^2_{j:n+1}t_j}} = \rho_{ij}\sqrt{\frac{t_i}{t_j}} = \sqrt{\frac{e^{2at_i} - 1}{e^{2at_j} - 1}}. \tag{6.6}$$

The specification (6.1) of the instantaneous correlation of the swap market model was constructed such that the (approximate) terminal correlation (6.5) of the Markov-functional

model with mean reversion parameter a is equal to the (approximate) terminal correlation (6.6) in the swap market model with parameter a. We note that this correspondence does not necessarily hold for the LIBOR market model, though we nonetheless employ it in the comparison tests.

6.2.3 Estimating Greeks for callable products in market models

The algorithm of Longstaff & Schwartz (2001) (LS) renders the numeraire relative payoff along a simulated path discontinuously dependent on initial input. The discontinuity in the LS algorithm stems from the estimated optimal exercise index chosen from a discrete set of possible exercise opportunities. Such a discrete choice is inherently discontinuously dependent on initial input. Any discontinuity in a simulation may cause finite difference estimates of sensitivities to be less efficient, see Glasserman (2004, Section 7.1). We describe two methods that enhance the efficiency of finite difference estimates, the second of which is novel. These are:

(i) Finite differences with optimal perturbation size.

(ii) Constant exercise decision heuristic.

The two methods are discussed below in more detail. We denote by v the *base value* of the derivative, i.e., the value of the derivative in the unperturbed model.

Method (i), the finite differences method is best described as the *bump-and-revalue* approach. Initial market data is perturbed by amount ε, the model is re-calibrated and subsequently priced at $v(\varepsilon)$. The finite difference estimate of the Greek is then $(v(\varepsilon) - v)/\varepsilon$. The mean square error (MSE) of the finite difference estimator is dependent on the chosen perturbation size ε. If the numeraire relative payoff along the path is continuously dependent on initial input, then least MSE is obtained when ε is selected as small as possible (though larger than machine precision), see Glasserman (2004). If the payoff is discontinuous however, then there is a trade-off between increasing and decreasing ε, leading to an optimal ('large' and positive) choice of ε that attains least MSE, see Glasserman (2004). After some preliminary testing, we found perturbation sizes of roughly 1 basis point (bp, 0.01%) for delta and 5 bp for vega.

Method (ii) that we propose, is named the constant exercise decision method. Here, for the base valuation we record per path when the exercise decision takes place. In the perturbed model, we no longer perform LS least-squares Monte Carlo, but rather use the very same exercise strategy as in the base valuation case. The constant exercise boundary method is a heuristic, since its estimate is stable but biased. The bias stems from not taking into account the change in value of the derivative as a result of a change in the (approximate) exercise decision. The bias is likely to be small, because the exercise decision is close to optimal by construction. Therefore, the change in value due to a change

in exercise decision is likely to be small. Though the method is biased, we nevertheless consider it in our tests. In finance, the importance is not bias, rather it is reduction of variance of P&L. Moreover, the method is straightforward to implement, and more efficient, since in re-valuations linear regressions for the LS algorithm are no longer required. We note that the constant exercise method renders a re-valuation continuously dependent on initial market data, provided the underlying swap payoff is continuous, which is the case for the Bermudan swaption studied in this chapter. From the discussion on perturbation sizes for method (i), it then follows that a least-MSE finite difference estimate of sensitivities is obtained by employing perturbation sizes that are as small as possible. We use 10^{-5} bp for both delta and vega.

We end this section by a brief discussion of other methods for calculation of Greeks available in the literature. These methods could not straightforwardly be extended to the situation of our investigations. Discussed are the path-wise method (Glasserman & Zhao 1999), the likelihood ratio method (Glasserman & Zhao 1999), the Malliavin calculus approach (Fournié, Lasry, Lebuchoux, Lions & Touzi 1999) and the utility minimization approach (Avellaneda & Gamba 2001). The path-wise method cannot handle discontinuous payoffs. The likelihood ratio and Malliavin calculus method both require that the matrix of instantaneous volatility be invertible. For the market model setting, we have an $n \times d$ matrix with n the number of forward rates and d the number of stochastic factors. Usually $d < n$ and most often $d \ll n$, which rules out inverting the instantaneous volatility matrix. Glasserman & Zhao (1999, Section 4.2) have resolved the non-invertibility issue only for a particular case, that does not apply to our case: When the payoff is dependent only on the rates at their fixing times, $\{s_{1:n+1}(t_1), s_{2:n+1}(t_2), \ldots, s_{n:n+1}(t_n)\}$. Finally, the utility minimization approach simply calculates a different sort of risk sensitivity and is thus altogether biased.

6.3 Data

We describe the data used in the empirical comparison and smile-impact tests. All market data was kindly provided by ABN AMRO Bank.

First, we describe the data used in the comparison test. For the comparison test, we use an arbitrarily chosen time-span, 16 June 2003–2004, of USD data of mid-quotes for deposit rates, swap rates and at-the-money (ATM) swaption volatility. We use the 1 and 12 months deposit rates and the 2Y, 3Y, 4Y, 5Y, 7Y, 10Y and 15Y swap rates. The discount factors are bootstrapped from market data. Any discount factors required at dates not available from the bootstrap are calculated by means of linear interpolation on zero rates. A statistical description of the swaption volatility data is displayed in Table 6.1. For each available tenor and expiry (Exp.), the associated column with four entries

Table 6.1: Statistical description of the swaption volatility data.

	Tenor (Years)								
Exp.	1	2	3	4	5	7	10	15	30
1M	46.3	51.7	45.9	40.6	37.8	32.1	27.5	22.9	19.0
	(6.2)	(6.4)	(6.2)	(5.0)	(4.7)	(3.8)	(3.5)	(3.0)	(2.7)
	[34.3,	[34.0,	[30.3,	[27.8,	[26.2,	[22.8,	[19.6,	[16.6,	[13.6,
	65.8]	68.3]	62.1]	53.1]	48.7]	42.1]	37.4]	33.0]	27.6]
2M	45.8	50.6	44.9	40.0	37.3	31.9	27.4	22.9	19.0
	(4.8)	(5.5)	(5.3)	(4.3)	(4.1)	(3.2)	(2.9)	(2.5)	(2.2)
	[36.0,	[34.0,	[30.3,	[27.8,	[26.2,	[23.0,	[19.9,	[16.9,	[13.8,
	61.0]	63.5]	57.0]	50.1]	47.2]	39.4]	35.0]	30.9]	25.7]
3M	45.4	49.4	44.0	39.5	36.9	31.7	27.3	22.9	18.9
	(3.9)	(4.9)	(4.5)	(3.9)	(3.6)	(2.8)	(2.5)	(2.1)	(1.8)
	[36.0,	[34.0,	[30.0,	[27.6,	[26.0,	[23.0,	[19.8,	[16.9,	[13.7,
	57.7]	60.3]	54.1]	49.3]	46.3]	37.8]	32.6]	28.8]	23.8]
6M	48.0	46.5	41.2	37.2	34.9	30.4	26.6	22.3	18.6
	(4.3)	(4.6)	(4.1)	(3.6)	(3.4)	(2.6)	(2.1)	(1.6)	(1.3)
	[34.9,	[33.1,	[29.3,	[27.1,	[25.4,	[22.7,	[20.0,	[17.1,	[14.1,
	56.9]	56.8]	52.7]	47.6]	44.5]	37.0]	31.3]	25.5]	20.9]
1Y	46.0	41.0	36.5	33.5	31.7	28.3	25.1	21.4	17.9
	(5.0)	(4.7)	(3.9)	(3.4)	(3.2)	(2.5)	(2.0)	(1.5)	(1.2)
	[32.1,	[29.4,	[27.0,	[25.2,	[23.7,	[21.6,	[19.5,	[16.7,	[14.2,
	55.5]	55.5]	48.2]	43.3]	40.6]	34.8]	30.0]	24.4]	20.3]
2Y	36.7	33.0	30.3	28.5	27.1	25.0	22.6	19.6	16.8
	(4.3)	(3.7)	(3.1)	(2.8)	(2.6)	(2.2)	(1.8)	(1.5)	(1.2)
	[26.9,	[24.7,	[23.2,	[22.1,	[21.1,	[19.7,	[17.9,	[15.6,	[13.5,
	50.4]	44.3]	39.4]	36.5]	34.5]	30.8]	27.1]	22.7]	19.5]
3Y	29.9	27.8	26.3	25.0	24.0	22.4	20.5	18.0	15.5
	(3.1)	(2.7)	(2.4)	(2.2)	(2.1)	(1.8)	(1.6)	(1.3)	(1.1)
	[23.2,	[21.7,	[20.7,	[20.0,	[19.3,	[18.1,	[16.6,	[14.6,	[12.7,
	38.6]	34.9]	32.6]	30.9]	29.7]	27.1]	24.2]	20.6]	18.1]
4Y	25.7	24.5	23.4	22.5	21.7	20.4	18.8	16.6	14.3
	(2.2)	(2.1)	(1.9)	(1.8)	(1.7)	(1.5)	(1.3)	(1.1)	(1.0)
	[20.8,	[19.8,	[19.1,	[18.4,	[17.9,	[16.9,	[15.6,	[13.7,	[11.9,
	31.0]	29.6]	28.2]	27.2]	26.4]	24.4]	22.0]	19.0]	16.9]
5Y	23.2	22.3	21.4	20.7	19.9	18.8	17.4	15.5	13.4
	(1.8)	(1.7)	(1.6)	(1.6)	(1.5)	(1.3)	(1.2)	(1.0)	(1.0)
	[19.1,	[18.4,	[17.8,	[17.2,	[16.7,	[15.8,	[14.7,	[12.9,	[11.2,
	28.0]	26.7]	25.7]	24.8]	24.0]	22.3]	20.2]	17.7]	15.8]

Table 6.2: Discount factors for the USD data of 21 February 2003.

1Y	2Y	3Y	4Y	5Y	6Y
0.98585	0.96223	0.92697	0.88571	0.84286	0.79986

Table 6.3: Swaption volatility, in percentages, against strike and expiry for the USD data of 21 February 2003. All displayed swaptions co-terminate 6 years from today. Here 'Exp.' denotes Expiry.

	Strike, in offset in basis points from the ATM forward swap rate								
Exp.	-300	-200	-100	-50	0	50	100	200	300
1Y	58.78	45.41	37.34	35.19	33.15	32.55	31.99	31.32	31.21
2Y	43.65	38.62	32.57	30.82	29.13	28.59	28.10	27.46	27.30
3Y	40.72	35.12	30.01	28.46	26.95	26.12	25.31	25.03	24.75
4Y	38.65	32.41	27.96	26.59	25.23	24.75	24.31	23.72	23.52
5Y	37.17	30.92	26.66	25.36	24.08	23.63	23.20	22.63	22.43

reports, respectively, the mean, the standard deviation (in parentheses), the minimum (in [·, form) and the maximum (in ·] form). Any volatility required at expiries and tenors not available from Table 6.1 are calculated by means of linear surface interpolation.

Second, we describe the data used in the smile-impact test, in which we will consider a 6 year deal. We use USD data for 21 February 2003. The discount factors are displayed in Table 6.2. The swaption volatility against strike and expiry is displayed in Table 6.3.

6.4 Accuracy of the terminal correlation formula

The terminal correlation in the Markov-functional model is estimated via the terminal covariance. We have, for $i < j$, for any measure,

$$\mathbb{E}\big[\ln s_{i:n+1}(t_i)\ln s_{j:n+1}(t_j)\big] = \mathbb{E}\Big[\ \ln s_{i:n+1}(t_i)\mathbb{E}\big[\ln s_{j:n+1}(t_j)\big|\mathcal{F}(t_i)\big]\ \Big]. \tag{6.7}$$

The above equality follows from the $\mathcal{F}(t_i)$-measurability of $\ln s_{i:n+1}(t_i)$. Expression (6.7) can be calculated on a lattice. We estimate (6.7) by calculating for each grid point at time t_i the conditional expectation $\mathbb{E}[\ln s_{j:n+1}(t_j)\big|\mathcal{F}(t_i)]$, subsequently we integrate the result multiplied by $\ln s_{i:n+1}(t_i)$ to obtain the required expectation.

Table 6.4: Error analysis of the terminal correlation measured in the Markov-functional model versus given by the approximate formula (6.3), for a 40 years annual-paying deal, thus for a 40×40 correlation matrix. Abbreviations used are *m.r.* for *mean reversion*, *max.* for *maximum*, *abs.* for *absolute*, *err.* for *error*, *rel.* for *relative*, and *avg.* for *average*.

M.r.	Max. abs. err.	Max. rel. err.	Avg. abs. err.	Avg. rel. err.
0%	1.6×10^{-4}	0.0190%	4.5×10^{-5}	0.0076%
5%	5.0×10^{-5}	0.0072%	1.2×10^{-5}	0.0030%
10%	2.1×10^{-5}	0.0032%	3.0×10^{-6}	0.0012%
15%	1.0×10^{-5}	0.0018%	9.8×10^{-7}	0.0006%
20%	5.7×10^{-6}	0.0011%	4.0×10^{-7}	0.0003%

The accuracy of the approximate formula (6.3) is tested for a 40 years deal, with EUR market data of 8 February 1999, for which the swaption volatility level is on average 14%. The test is performed at various mean reversion levels, 0%, 5%, 10%, 15%, and 20%. The terminal correlation matrix within the Markov-functional model is calculated numerically on a lattice under the terminal measure and subsequently compared to the correlation matrix given by the approximate formula (6.3). We note that the comparison contains two sources of error: First, the approximation (6.3), and, second, the numerical error inherent in the lattice calculation. In Table 6.4, various descriptive data for the comparison test are displayed. Reported are, over the entries in the matrix, the maximum absolute and relative errors, and the average absolute and relative errors. As can be seen from Table 6.4, these errors are quite small, especially considered over a 40 years horizon.

6.5 Empirical comparison results

In this section, we report the results of our empirical comparison. The deal description is given in Table 6.5. For market models we use the terminal measure, 10,000 simulation paths (5,000 plus 5,000 antithetic) and 10 stochastic factors (a full factor model), bar when $a = 0\%$, we use a single factor model. To determine the exercise boundary in market models, we use the least-squares Monte Carlo algorithm of Longstaff & Schwartz (2001), with all forward rates as explanatory variables, i.e., all available LIBOR rates for the LIBOR market model and all available swap rates for the swap market model. The reason for using all available rates as explanatory variables is that the multi factor nature of the market models needs be retained (if at all present; for $a = 0\%$ a single factor model must be used). As basis functions we use a constant and one linear term

Table 6.5: The Bermudan swaption deal used in the comparison.

Trade:	Bermudan Swaption
Trade Type:	Receive Fixed
Notional:	USD 100m
Start Date:	16-Jun-2004
End Date:	16-Jun-2014
Fixed Rate:	3.2%
Index Coupon:	Per Annum
Index Basis:	ACT/365
Roll Type:	Modified Following
Callable:	At Fixing Dates

per explanatory variable, $\{1, x_1, \ldots, x_m\}$, where m denotes the number of explanatory variables. The NPVs, deltas and vegas of the deal are calculated at each trade date from 16 June 2003 till 15 June 2004, inclusive, for the mean reversion levels 0%, 5% and 10%. A price comparison is displayed in Figure 6.2. As can be seen from the figure, the Markov-functional and market models are similar in terms of NPV, and prices co-move and stay together over time.

The models are, more importantly, compared in terms of hedge performance. With respect to hedging, we use so-called *bucket* hedging rather than *factor* hedging. With factor hedging, the number of hedge instruments equals the number of factors in the model. Risk sensitivities are calculated by perturbing only the model intrinsic factors. With bucket hedging, the number of hedge instruments equals the number of market traded instruments to which the model has been calibrated to. Risk sensitivities are calculated by perturbing the value of a market traded asset, and then by re-valuation of the derivative in a model re-calibrated to the perturbed market data. The reasons that we employ bucket hedging rather than factor hedging are twofold. First, Driessen et al. (2003, Section VII.C) show that bucket hedging outperforms factor hedging for caps and European swaptions (for delta hedging). Second, bucket hedging corresponds to financial practice.

Two types of hedges are considered:

(i) Delta hedging only.

(ii) Delta and vega hedging.

The delta hedge is set up in terms of discount bonds, one discount bond for each tenor time associated with the deal. In the case of the deal of Table 6.5, there are 11 such

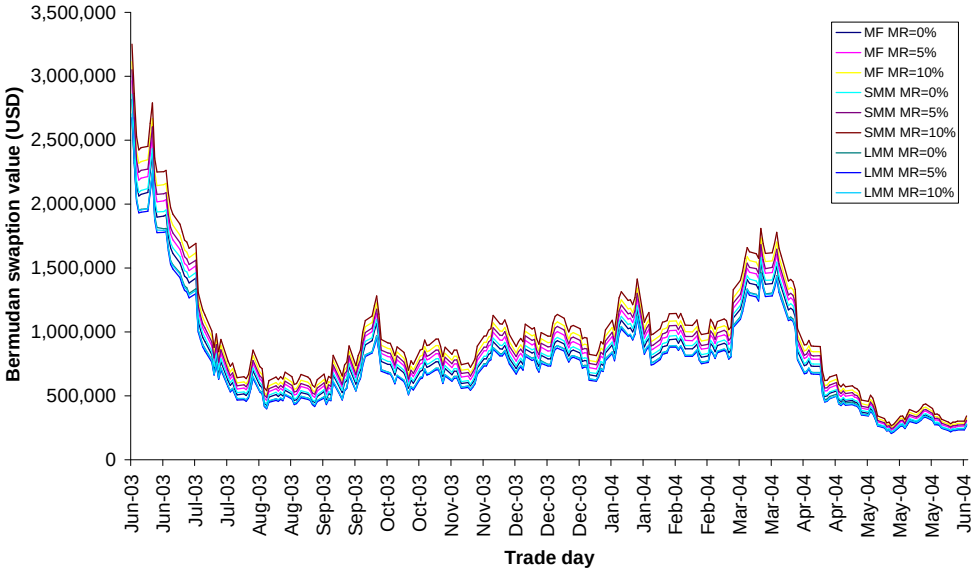

Figure 6.2: Bermudan swaption values per trade date, for various models and correlation specifications.

discount bonds. To set up a joint delta and vega hedge, we proceed in the following four steps. First, we calculate the vegas of the 10 underlying European swaptions. Second, we calculate the amount of each of the European swaptions needed to have zero portfolio vega for all underlying volatilities. Third, the aggregate delta position, of the Bermudan and European swaptions, is calculated. Fourth, discount bonds are acquired to obtain zero delta exposure for all 11 delta buckets.

The risk sensitivities are calculated in two ways, as detailed in Section 6.2.3, (i) finite differences with perturbation sizes 1 bp for delta and 5 bp for vega (referred to as 'large' perturbation sizes), and, (ii) constant exercise decision method, with perturbation sizes 10^{-5} bp for both delta and vega (referred to as 'small' perturbation sizes).

We note here that the computational time of calculating the NPV, the 11 deltas and the 10 vegas, at any particular trade date, is around 92 seconds for market models[4] with ordinary LS, around 42 seconds for market models with constant exercise decision method, versus 3 seconds for the Markov-functional model. This difference of compu-

[4]There are fast algorithms for implementation of market models with Monte Carlo, see Joshi (2003*b*) for LIBOR models, and Pietersz & van Regenmortel (2005, Section 5) (see also Section 7.5 in this thesis) for swap models. Needless to say, we used these fast algorithms.

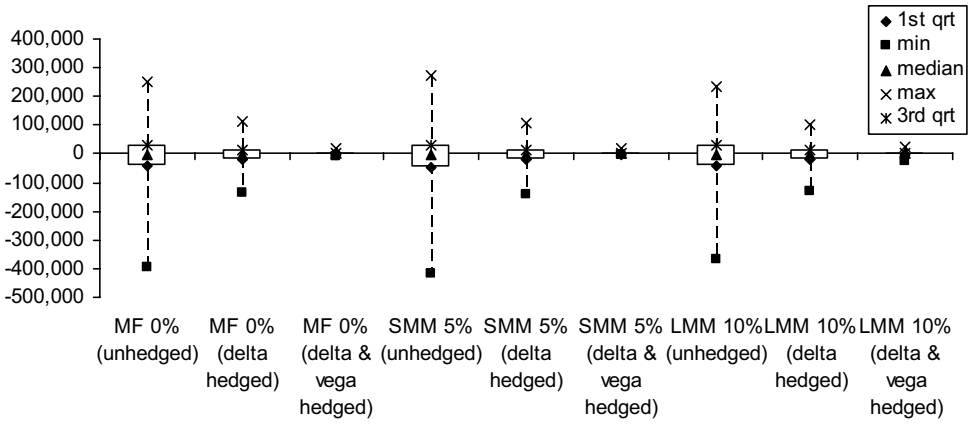

Figure 6.3: Comparison of delta versus delta and vega hedging. Box-whisker plots for the change in value (in USD) of the hedged portfolio. The percentages denote the mean reversion level (MF) or correlation parametrization parameter (LMM and SMM). For market models, we use the constant exercise decision method, with 'small' perturbation sizes.

tational time is inherent to the (least squares) Monte Carlo implementation of market models versus the lattice implementation of Markov-functional models. Of course, such lattice implementation is allowed only because of the mild path-dependency of Bermudan swaptions.

The hedge portfolios are set up at each trade day and the change in portfolio value on the next trade day is recorded. The hedge test results are ordered in three subsections.

6.5.1 Delta hedging versus delta and vega hedging

The performance of delta hedging versus delta and vega hedging is compared. Box-whisker plots, for the change in hedge portfolio value, are displayed in Figure 6.3, for various models and mean reversion or correlation parametrization parameters. Here, MF, LMM, and SMM denote respectively, Markov-functional model, LIBOR market model and swap market model. Box-whisker plots provide a convenient representation of a distribution, by displaying five of its key characteristics: the minimum, median, and maximum values, and the first and third quartiles.

We draw the following conclusions from the box-whisker plots in Figure 6.3:

1. Delta hedging significantly decreases variance of P&L.

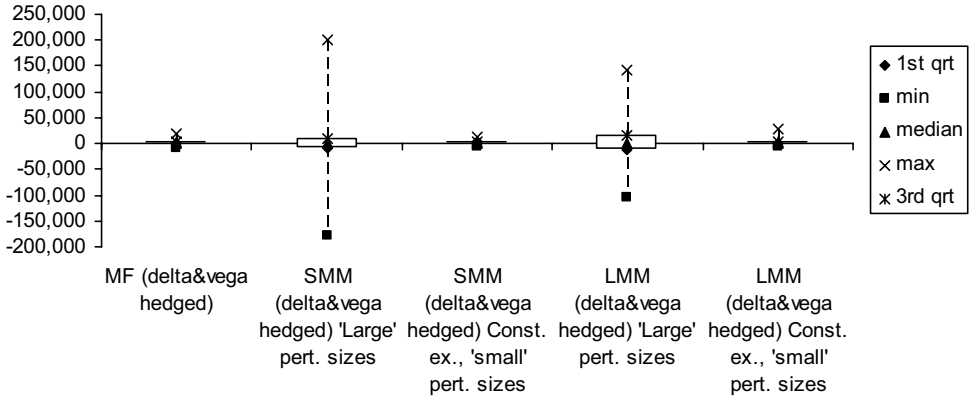

Figure 6.4: 'Large' perturbation sizes versus constant exercise decision method with 'small' perturbation sizes. Box-whisker plots for the change in value (in USD) of the hedged portfolio. Mean reversion or correlation parameter of 0%.

2. Vega hedging additional to delta hedging significantly further decreases variance of P&L.

It is clear that a joint delta and vega hedge by far outperforms a delta hedge. Therefore we omit, in the remainder of the chapter, further study of delta hedges without a vega hedge.

6.5.2 'Large' perturbation sizes versus constant exercise decision method with 'small' perturbation sizes

The performance of joint delta-vega hedging is compared as dependent on the method used to calculate risk sensitivities. Box-whisker plots for the change in value of the delta-vega hedged portfolios, with a mean reversion of 0% or a correlation parameter of 0%, are displayed in Figure 6.4. Here, 'const. ex.' and 'pert.' denote 'constant exercise decision method' and 'perturbation', respectively. The analogous box-whisker plots for mean reversion or correlation parameters 5% and 10% are similar. We draw the following conclusions from the box-whisker plots in Figure 6.4.

1. The estimation of sensitivities by finite differences over MC with 'large' perturbation sizes adversely affects the variance of P&L for hedging in market models.

2. The best performing Greek calculation method, for delta-vega hedging, is the constant exercise decision method, for which we approximately obtain similar results as with the Markov-functional model.

3. The use of the constant exercise decision method enables proper functioning of market models as risk management tools, for callable products on underlying assets that are continuously dependent on initial market data.

It is clear that the constant exercise decision method with 'small' perturbation sizes by far outperforms ordinary LS with 'large' perturbation sizes. The theoretical explanation of this out-performance is related to two issues. First, the classical LS algorithm causes a discontinuity in the numeraire relative payoff along the path, which renders finite difference estimates of sensitivities to be less efficient. Second, 'larger' perturbation sizes cause more variance in the finite difference estimate of a sensitivity, since the correlation between the payoff in the original and perturbed models becomes smaller. These two effects lead to more Monte Carlo caused randomness in the contents of the hedge portfolio, which ultimately leads to increased variance of P&L, as can be seen in Figure 6.4.

We omit, in the remainder of the chapter, further study of ordinary LS with 'large' perturbation sizes.

6.5.3 Delta-vega hedge results

The performance of joint delta-vega hedging is compared across models and mean reversion or correlation specifications. For the market models, we use the constant exercise decision method with 'small' perturbation sizes. Box-whisker plots for the change in value of the delta-vega hedged portfolios are displayed in Figure 6.5. We draw the following conclusions from the box-whisker plots in Figure 6.5.

1. The impact of mean reversion or correlation parameter specification on hedge performance is not very large.

2. The hedge performance for all three models is very similar.

6.6 The impact of smile

In this section, we provide details on how the Markov-functional and swap market models can be fitted to smile and investigate the impact of smile relative to the impact of correlation cq. mean reversion on the prices of Bermudan swaptions. As a concrete example, the displaced diffusion smile dynamics of Rubinstein (1983) are considered. In a displaced

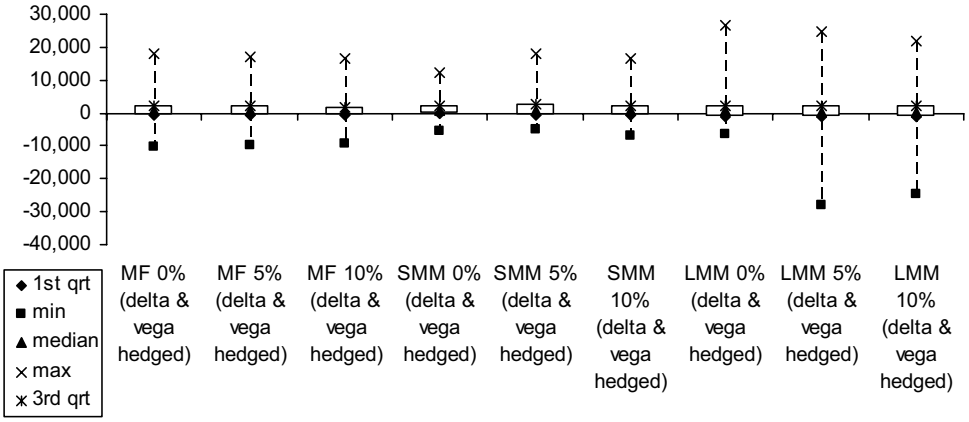

Figure 6.5: Delta-vega hedge results. Box-whisker plots for the change in value (in USD) of the hedged portfolio. The percentages denote the mean reversion level (MF) or correlation parametrization parameter (LMM and SMM). For market models, we use the constant exercise decision method, with 'small' perturbation sizes.

diffusion setting, the forward swap rate is modelled as

$$s_{i:n+1}(t) = \tilde{s}_{i:n+1}(t) - r_i, \quad \frac{\mathrm{d}\tilde{s}_{i:n+1}(t)}{\tilde{s}_{i:n+1}(t)} = \sigma_{i:n+1}\mathrm{d}w^{(i:n+1)}(t), \tag{6.8}$$

with r_i the displacement parameter and $w^{(i:n+1)}$ a Brownian motion under the forward swap measure associated with $s_{i:n+1}$. The solution to stochastic differential equation (SDE) (6.8) is

$$s_{i:n+1}(t) = -r_i + \big(s_{i:n+1}(0) + r_i\big) \exp\left\{ \sigma_{i:n+1} w^{(i:n+1)}(t) - \frac{1}{2}\sigma_{i:n+1}^2 t \right\}. \tag{6.9}$$

The displaced diffusion extension is first discussed for the Markov-functional model and second for the swap market model. The Markov-functional model is fitted to volatility by fitting the digital swaptions. The value $v^{(i)}$ of the digital swaption on swap rate $s_{i:n+1}(t_i)$ with strike k is given by the familiar formula in the Black world

$$v^{(i)} = p_{i:n+1}(0)\phi\Big(d_2^{(i)}\Big), \quad d_2^{(i)} = \frac{\log\big(k/s_{i:n+1}(0)\big) - \frac{1}{2}\sigma_{i:n+1}^2 t_i}{\sigma_{i:n+1}\sqrt{t_i}} \tag{6.10}$$

where $\phi(\cdot)$ denotes the cumulative normal distribution function and where $p_{i:n+1}$ denotes the *present value of a basis point*, $p_{i:n+1} = \sum_{k=i}^{n} \alpha_i b_{i+1}(t)$. Here α_i denotes the day count fraction for period $[t_i, t_{i+1}]$ and $b_i(t)$ denotes the time-t value of a discount bond

for payment of one unit of currency at time t_i. In the displaced diffusion world, the value $\tilde{v}^{(i)}$ of the digital swaption is given by a displaced forward swap rate and strike

$$\tilde{v}^{(i)} = p_{i:n+1}(0)\phi\Big(\tilde{d}_2^{(i)}\Big), \quad \tilde{d}_2^{(i)} = \frac{\log\Big(\frac{s_{i:n+1}(0)+r_i}{k+r_i}\Big) - \frac{1}{2}\sigma_{i:n+1}^2 t_i}{\sigma_{i:n+1}\sqrt{t_i}}. \tag{6.11}$$

The implementation of a non-smile Markov-functional model has to be changed only in two places to incorporate displaced diffusion smile dynamics. First, the functional form of the terminal discount bond b_{n+1} at time t_n is determined, using the equation

$$b_{n+1}(t_n) = \frac{1}{1+\alpha_n s_{n:n+1}(t_n)}. \tag{6.12}$$

In a non-smile Markov-functional model, we then have

$$b_{n+1}(t_n, x(t_n)) = \frac{1}{1+\alpha_n s_{n:n+1}(0)\exp\Big\{-\frac{1}{2}\sigma_{n:n+1}^2 t_n + \frac{\sigma_{n:n+1}}{e^{2at_n}-1}x(t_n)\Big\}}, \tag{6.13}$$

this is exactly the penultimate equation on page 399 of Hunt et al. (2000). In a displaced diffusion setting, we substitute (6.9) into (6.12) and then (6.13) becomes

$$\tilde{b}_{n+1}(t_n, x(t_n)) = \frac{1}{1+\alpha_n\Big[-r_i + \big(s_{n:n+1}(0)+r_i\big)\exp\Big\{-\frac{1}{2}\sigma_{n:n+1}^2 t_n + \frac{\sigma_{n:n+1}}{e^{2at_n}-1}x(t_n)\Big\}\Big]},$$

Second, the functional forms of the swap rates $s_{i:n+1}(t_i, \cdot)$, $i = 1, \ldots, n-1$ are determined, by inverting the value of the digital swaption against strike. In a non-smile Markov-functional model, we invert (6.10) and obtain

$$s_{i:n+1}(t_i, x(t_i)) = s_{i:n+1}(0)\exp\left\{-\frac{1}{2}\sigma_{i:n+1}^2 t_i - \sigma_{i:n+1}\sqrt{t_i}\phi^{-1}\left(\frac{j^{(i)}(x(t_i))}{p_{i:n+1}(0)}\right)\right\},$$

with $j^{(i)}(x)$ denoting the value of a digital swaption with strike x in the model, calculated by induction from $i = n-1, \ldots, 1$. In a displaced diffusion setting, we invert (6.11) to obtain

$$s_{i:n+1}(t_i, x(t_i)) = -r_i + \big(s_{i:n+1}(0)+r_i\big)\exp\left\{-\frac{1}{2}\sigma_{i:n+1}^2 t_i - \sigma_{i:n+1}\sqrt{t_i}\phi^{-1}\left(\frac{j^{(i)}(x(t_i))}{p_{i:n+1}(0)}\right)\right\}.$$

Next, the displaced diffusion swap market model is made reference to. The dynamics of the forward swap rates under the terminal measure in general smile models can be found in Jamshidian (1997, Equation (6), page 320).

We fit the displaced diffusion model to the market data of Table 6.3 and find the volatility parameters $\sigma_{i:n+1}$ and displacement parameters r_i as listed in Table 6.6. The fitted volatility and fit errors are displayed in Table 6.7. As can be seen from the table,

Table 6.6: Displaced diffusion parameters fitted to the USD market data of 21 February 2003 of Table 6.3.

i	1	2	3	4	5
Expiry	1Y	2Y	3Y	4Y	5Y
Tenor	5Y	4Y	3Y	2Y	1Y
$\sigma_{i:n+1}$	28.29%	21.76%	18.28%	16.08%	14.62%
r_i	0.71%	1.55%	2.33%	2.89%	3.39%

Table 6.7: Fitted swaption volatility and fit errors with the displaced diffusion model, in percentages, against strike and expiry for the USD data of 21 February 2003. All displayed swaptions co-terminate 6 years from today. Here 'Exp.' denotes Expiry.

	Fitted swaption volatility								
	Strike, in offset in basis points from the ATM forward swap rate								
Exp.	-300	-200	-100	-50	0	50	100	200	300
1Y	37.82	35.11	33.88	33.48	33.15	32.89	32.66	32.30	32.03
2Y	34.32	31.57	30.07	29.54	29.11	28.74	28.43	27.92	27.51
3Y	32.23	29.58	28.02	27.45	26.98	26.57	26.21	25.63	25.16
4Y	30.34	27.83	26.29	25.72	25.23	24.82	24.46	23.85	23.37
5Y	29.17	26.74	25.21	24.63	24.14	23.72	23.35	22.73	22.23
	Absolute fit errors, model volatility minus market volatility								
	Strike, in offset in basis points from the ATM forward swap rate								
Exp.	-300	-200	-100	-50	0	50	100	200	300
1Y	-20.96	-10.29	-3.46	-1.71	0.00	0.34	0.67	0.98	0.82
2Y	-9.33	-7.05	-2.50	-1.28	-0.02	0.15	0.33	0.45	0.21
3Y	-8.49	-5.54	-1.99	-1.01	0.02	0.44	0.90	0.60	0.41
4Y	-8.31	-4.58	-1.67	-0.87	0.00	0.06	0.14	0.13	-0.15
5Y	-8.00	-4.18	-1.45	-0.73	0.06	0.09	0.14	0.10	-0.20

the displaced diffusion model fits the market well for ATM and out-of-the-money (OTM) options (fit error less than a percent), but not so well for in-the-money (ITM) options, for which the model underfits the market up to 21%. We note here that the disability of obtaining a perfect fit to the smile volatility data is due solely to the displaced diffusion model, and not to the Markov-functional or market models. An exact fit to the swaption smile surface can be obtained, for example, with the relative-entropy minimization framework of Avellaneda, Holmes, Friedman & Samperi (1997). To benchmark the implementation of the displaced diffusion Markov-functional and swap market models, European swaptions are valued in (i) a constant volatility model with the volatility associated with the expiry and strike of the swaption and (ii) the smile model. The results of this test for the Markov-functional model have been displayed in Table 6.8. The benchmark is of high quality, though there are some slight differences due to numerical errors in the grid calculation. The benchmark results for the swap market model are of similar good quality.

Subsequently, Bermudan swaptions are priced with varying strikes and otherwise specified in Table 6.9. The Bermudan swaptions are priced in the Markov-functional and SMM models, and in their displaced diffusion counterparts, at various mean reversion or correlation parameter levels. In the non-smile models, there are two possibilities for choosing the volatilities. First, the volatilities can be used that correspond to the strike of the Bermudan swaption. Second, the ATM volatilities can be used, regardless of the strike of the Bermudan swaption. The calculated prices are displayed in Table 6.10. The results in the table show that the impact of correlation is significant, since a 10% change in mean reversion can cause a change in value equal to a parallel volatility shift of 1%. The impact of correlation is comparable to that reported by Choy, Dun & Schlögl (2004, Table 11), though the latter authors name this impact 'non-substantial'. The impact of smile is, for the deal considered, much larger than the impact of correlation and mean reversion, since 10% mean reversion is usually a high level when observed in the market. In terms of vega, the smile impact can be as large as a parallel shift in volatility of -8% to 1%, for per-strike volatilities, and -1% to 6%, for ATM volatilities. Furthermore, the displaced diffusion smile model underfitted the volatility smile observed in the market. Since increasing the volatility usually leads to a higher value for Bermudan swaptions[5], the impact of smile can thus be even higher, when ATM volatilities are used.

[5]Pietersz & Pelsser (2004*a*, Appendix) (see also Appendix 2.A) explain that Bermudan swaptions can in certain particular circumstances have negative vega.

Table 6.8: Benchmark results for the displaced diffusion Markov-functional model: European swaption prices in a constant volatility model versus a smile model. The notional is USD 100 million. All displayed swaptions co-terminate 6 years from today. Here 'Exp.' denotes Expiry.

	Strike, in offset in basis points from the ATM forward swap rate								
	-300	-200	-100	-50	0	50	100	200	300
Exp.	Constant volatility Markov-functional model								
1Y	328	52,561	606,777	1,304,851	2,340,174	3,689,485	5,298,889	9,053,757	13,203,090
2Y	24,540	249,639	1,018,213	1,683,785	2,542,759	3,580,442	4,773,685	7,521,975	10,595,480
3Y	84,026	391,072	1,098,965	1,629,508	2,276,285	3,030,862	3,881,504	5,818,070	7,984,799
4Y	106,959	367,457	878,156	1,237,121	1,663,274	2,151,967	2,697,073	3,928,998	5,305,394
5Y	82,725	235,077	504,020	684,928	895,662	1,134,225	1,398,093	1,990,497	2,650,706
	Displaced diffusion Markov-functional model								
1Y	322	52,255	605,446	1,303,083	2,338,220	3,687,599	5,297,237	9,052,727	13,202,556
2Y	24,201	248,060	1,015,124	1,680,221	2,538,993	3,576,743	4,770,238	7,519,330	10,593,675
3Y	83,169	388,983	1,095,781	1,626,018	2,272,668	3,027,290	3,878,101	5,815,249	7,982,667
4Y	105,990	365,588	875,586	1,234,362	1,660,433	2,149,153	2,694,366	3,926,683	5,303,550
5Y	82,154	234,125	502,792	683,627	894,329	1,132,903	1,396,815	1,989,378	2,649,787

Table 6.9: The Bermudan swaption deal used in the test of impact of smile.

Trade:	Bermudan Swaption
Trade Type:	Receive Fixed
Notional:	USD 100m
Valuation Date:	21-Feb-2003
Start Date:	21-Feb-2004
End Date:	21-Feb-2009
Index Coupon:	Per Annum
Index Basis:	ACT/365
Roll Type:	Modified Following
Callable:	At Fixing Dates

6.7 Conclusions

We investigated the impact of correlation on the pricing and hedge performance of Bermudan swaptions for various models. We showed how the Markov-functional model can approximately be fitted to terminal correlation, by developing a novel approximate formula for terminal correlation. The approximate formula was shown to be of high quality in a numerical test. Empirically, the impact of terminal correlation was shown to be somewhat significant for pricing of Bermudan swaptions in market models, and the same effect can be attained in the single-factor Markov-functional model by calibration to terminal correlation. We showed empirically by comparison with multi factor market models that hedge performance for Bermudan swaptions is, for practical purposes, almost identical, regardless of the model, number of factors, or correlation specification. Our results show that the need of modelling correlation can already be adequately met by a single factor model. Whether these results extend beyond the asset class of Bermudan swaptions, is an interesting question that we leave to answer in future research. With respect to hedge portfolios, we showed (i) that delta hedging significantly reduces variance of P&L in both Markov-functional and market models, (ii) that vega hedging additional to delta hedging significantly further reduces variance of P&L in both Markov-functional and market models, (iii) that estimation of Greeks by finite differences over Monte Carlo for callable products with the regular LS algorithm and 'large' perturbation sizes adversely affects the delta-vega hedge performance of market models. We showed that our proposal of the constant exercise decision method with 'small' perturbation sizes enables proper functioning of market models as risk management tools, for callable products on underlying assets that are continuously dependent on initial market data. Moreover, we investigated

Table 6.10: Prices of Bermudan swaptions in smile versus non-smile models with various correlation/mean reversion assumptions. Here 'MF', 'MR', 'a' and 'SE' denote 'Markov-functional model', 'mean reversion', 'the correlation parameter a of (6.1)' and the 'standard error', respectively. Any difference ('Diff.') is with respect to a price at zero mean reversion or at zero a. The non-smile models use per-strike volatilities, except where indicated that ATM volatilities are used.

	Strike				
	2%	3%	4%	5%	6%
MF-MR=0%	420,954	1,072,043	2,452,060	5,047,951	8,573,535
Vega 1% MF	34,609	68,118	96,242	93,513	68,477
SMM-a=0%	407,667	1,053,210	2,443,332	5,065,794	8,605,508
SMM SE-a=0%	7,551	12,964	17,204	16,032	10,625
Vega 1% SMM	33,105	66,154	97,141	91,850	67,194
MF-MR=5%	436,518	1,103,269	2,495,689	5,090,486	8,606,769
Diff. in vega	0.4	0.5	0.5	0.5	0.5
SMM-a=5%	407,922	1,060,731	2,461,625	5,101,071	8,657,349
SMM SE-a=5%	7,386	12,764	17,228	16,244	11,243
Diff. in vega	0.0	0.1	0.2	0.4	0.8
MF-MR=10%	452,417	1,135,155	2,540,694	5,135,323	8,642,685
Diff. in vega	0.9	0.9	0.9	0.9	1.0
SMM-a=10%	405,819	1,062,986	2,485,969	5,142,268	8,708,570
SMM SE-a=10%	7,202	12,488	17,090	16,359	11,873
Diff. in vega	-0.1	0.1	0.4	0.8	1.5
Smile MF	148,130	747,270	2,347,664	5,074,574	8,623,356
Diff. in vega	-7.9	-4.8	-1.1	0.3	0.7
Smile SMM	146,223	756,925	2,373,545	5,094,288	8,642,666
Smile SMM SE	4,710	11,138	16,781	14,437	9,801
Diff. in vega	-8.3	-4.8	-0.8	0.5	1.0
ATM volatilities					
MF-MR=0%	67,210	650,483	2,328,235	5,124,154	8,691,466
Vega 1% MF	14,997	60,797	95,139	93,681	72,106
Smile MF	148,130	747,270	2,347,664	5,074,574	8,623,356
Diff. in vega	5.4	1.6	0.2	-0.5	-0.9
SMM-a=0%	61,944	610,939	2,286,869	5,139,345	8,731,084
SMM SE-a=0%	2,626	10,114	16,763	16,122	11,628
Vega 1% SMM	13,915	59,861	94,495	91,859	77,375
Smile SMM	146,223	756,925	2,373,545	5,094,288	8,642,666
Diff. in vega	6.1	2.4	0.9	-0.5	-1.1

the impact of smile via displaced diffusion versions of the Markov-functional and swap market models. For a particular deal and USD market data, we showed that the impact of smile is much larger that the impact of correlation.

Chapter 7

Generic market models

Currently, there are two market models for valuation and risk management of interest rate derivatives, the LIBOR and swap market models of Brace et al. (1997), Jamshidian (1997), Musiela & Rutkowski (1997) and Miltersen et al. (1997). In this chapter, we introduce arbitrage-free constant maturity swap (CMS) market models and generic market models featuring forward rates that span periods other than the classical LIBOR and swap periods. The generic market model generalizes the LIBOR and swap market models. We derive necessary and sufficient conditions for the structure of the forward rates to span an arbitrage-free economy in terms of relative discount bond prices, at all times. We develop generic expressions for the drift terms occurring in the stochastic differential equation driving the forward rates under a single pricing measure. The generic market model is particularly apt for pricing of Bermudan CMS swaptions, fixed-maturity Bermudan swaptions, and callable hybrid coupon swaps. We show how the instantaneous correlation of the generic forward rates can be calculated from the single instantaneous correlation matrix of forward LIBOR rates. These results are sufficient for implementation of calibration and pricing algorithms for generic market models.

7.1 Introduction

Generic market models are specifically designed for the pricing of certain types of swaps. In particular, we will consider constant maturity swaps (CMS) and hybrid coupon swaps. An interest rate swap is an agreement to exchange, over a specified period, interest rate payments, at a specified frequency, over a specified underlying notional that is not exchanged. In a plain-vanilla swap, the floating interest rate is the LIBOR rate. A *constant maturity swap* pays not the LIBOR rate but instead a swap rate with specified tenor, fixed for all payments in the CMS swap. The payment frequency remains unchanged however. A *hybrid coupon swap* is a swap that features a floating payment schedule, designating the

nature of each of the floating payments. The nature of the floating payment can be that it is determined by either a LIBOR rate with varying maturity or a swap rate with varying tenor. An example of such a payment schedule has been given in Table 7.1. Additionally, the function that transforms the LIBOR or swap rate into a cash flow may even be not entirely linear, for example, capped, floored or inverse.

The above swaps may have the feature that the swaps can be cancelled. Such versions are deemed *cancellable swaps*. To hold a cancellable swap is equal to holding a swap and an option to enter into the very same swap but with reversed cash flows[1]. The latter option is called a *callable swap*. In this chapter we will also be concerned with the pricing of callable and cancellable CMS and hybrid coupon swaps. There are two types of callable swaptions: *fixed-maturity* or *co-terminal*. A co-terminal option allows to enter into an underlying swap at several exercise opportunities, where each swap ends at the same contractually determined end date. The swap maturity becomes shorter as exercise is delayed. In contrast, for the fixed-maturity version, each underlying swap has the same contractually specified maturity and the respective end dates then differ.

The main outset of the chapter is that a model is deemed to be proper for valuing a certain callable or cancellable swap, if the volatility of a rate that appears in the contract payoff has been calibrated correctly to the market volatility. The concept is best illustrated by example. In the case of the hybrid coupon swap of Table 7.1 at the valuation date 11 June 2004, we would want to calibrate exactly to the volatilities of the $1Y \times 2Y$ swaption, $2Y \times 4Y$ swaption, $3Y$ caplet, $4Y \times 2Y$ swaption and $5Y$ caplet. In contrast, for a cap one would calibrate to the volatilities of the $1Y$, $2Y$, $3Y$, $4Y$ and $5Y$ caplets. For a co-terminal Bermudan swaption, to the volatilities of the $1Y \times 5Y$, $2Y \times 4Y$, $3Y \times 3Y$, $4Y \times 2Y$ and $5Y \times 1Y$ swaptions. When employing a LIBOR market model to value a cap, the model would feature the following $1Y$ forward LIBOR rates: $1Y$, $2Y$, $3Y$, $4Y$ and $5Y$. If a swap market model would be used to value the Bermudan swaption, it would feature the $1Y \times 5Y$, $2Y \times 4Y$, $3Y \times 3Y$, $4Y \times 2Y$ and $5Y \times 1Y$ forward swap rates. For both LIBOR and swap market models, the canonical interest rates are simply equipped with the corresponding canonical volatilities, allowing for an efficient and straightforward calibration. Obviously, to straightforwardly calibrate a market model for the hybrid coupon swap of Table 7.1, and callable or cancellable versions thereof, the model would have to feature the forward swap rates $1Y \times 2Y$, $2Y \times 4Y$, $4Y \times 2Y$, and the $1Y$ forward LIBOR rates at $3Y$ and $5Y$. Up to now, whether a model containing such rates would be arbitrage-free is not well-known. To our knowledge, generic methods for deriving the arbitrage-free drift terms for the SDE driving the various forward rates have not been developed yet. In this chapter, we develop such generic theory.

[1]Some readers might not be familiar with 'callable' and 'cancellable' swaps and might prefer to think of swaps and options thereon.

Table 7.1: Example of a hybrid coupon swap payment structure for the floating side. Date roll is modified following and day count is actual over 365.

Fixing date	Day count fraction	Payment date	Rate
11-Jun-04	1.005479	13-Jun-05	1Y LIBOR
13-Jun-05	0.997260	12-Jun-06	2Y swap rate
12-Jun-06	0.997260	11-Jun-07	4Y swap rate
11-Jun-07	1.002740	11-Jun-08	1Y LIBOR
11-Jun-08	1.000000	11-Jun-09	2Y swap rate
11-Jun-09	1.000000	11-Jun-10	1Y LIBOR

In terms of practical relevance, the generic market model technology is valuable to financial institutions that aim to trade in CMS Bermudan swaptions or callable hybrid coupon swaps. As such, their costumers might require any sequence of various maturity LIBOR or swap rate payments in the tailored exotic derivatives that they demand for their business. In this chapter, we show that a generic implementation of the resulting drift terms is feasible in practice, thereby enabling proper pricing and hedging of such hybrid coupon swaps.

A further motivation for the theory in this chapter is that the idea of generic market models is not new to the finance literature, since it has already been suggested by Galluccio, Huang, Ly & Scaillet (2004). These authors discuss what they call the *co-sliding* (commonly referred to as 'LIBOR') and *co-terminal* (commonly referred to as 'swap') market models. The class of co-sliding market models corresponds to our class of CMS market models, but ours is defined differently. Galluccio et al. (2004) show that the only admissible co-sliding model is the LIBOR market model. Interestingly, we show that there are n arbitrage-free CMS market models associated with a tenor structure with n fixings, and the LIBOR and swap models are two special cases of these CMS models. In addition to the n CMS models, we introduce generic market models, extending the number of arbitrage-free market models to $n!$. Also, Galluccio et al. (2004) discuss the *co-initial* market model, but this model does not fit into our dynamic market model framework. Moreover, in contrast to Galluccio et al. (2004), we derive generic expressions for the drift terms of the forward rates, for all $n!$ models (thus for LIBOR, swap, CMS and generic models).

An alternative way of calibrating a model to the relevant volatility levels, is to take a LIBOR market model, and derive generic approximate expressions for the volatility of various forward rates. Such a procedure, for the specific case of calibration of the LIBOR model to swaption volatility, has been investigated in Jäckel & Rebonato (2003), Joshi & Theis (2002), Hull & White (2000) and Pietersz & Pelsser (2004*a*) (Chapter 2). The advantage of the generic market model specification is that the relevant volatility functions can be directly specified. Moreover, the development of the theory of generic market models is justified already by the additional insight into the workings of LIBOR and swap market models. Also, Pietersz & Pelsser (2005*a*) (see also Chapter 6) provide an empirical price and hedge comparison for Bermudan swaptions with either (i) the LIBOR model calibrated to swaption volatility via the approximate formula, or (ii) the swap model equipped with its canonical swaption volatility. Prices turn out to be largely similar, while hedge performance seems to be slightly better for the canonical models, see Figures 2 and 5, respectively, of Pietersz & Pelsser (2005*a*) (see Figures 6.2 and 6.5 of this thesis). These results are thus slightly in favour of CMS and generic market models, rather than the use of approximate swaption volatility with the LIBOR model.

We mention three areas of market model theory to which the generic market model approach extends. First, generic models may also be used in multi-currency market models, see Schlögl (2002). Second, a numerical implementation of a generic model may utilize drift approximations, see, for example, Hunter et al. (2001) and Pietersz et al. (2004, 2005) (see also Chapter 5). Third, generic models may be equipped with smile dynamics. The volatility smile is the phenomenon that for European options different Black (1976) implied volatilities are quoted in the market when the strike of the option is varied. The derivation of generic market models in this chapter does not make any assumptions on the instantaneous volatility. As a result, smile-incorporating models, such as the displaced diffusion (Rubinstein 1983), and constant elasticity of variance (CEV) (Cox & Ross 1976) models, can be readily applied to the generic market model framework. An application of the CEV specification to the LIBOR market model can be found in Andersen & Andreasen (2000).

Finally, for an in-depth overview of pricing models for interest rate derivatives, the reader is referred to Rebonato (2004*a*).

An outline of the chapter is as follows. First, preliminaries are introduced. Second, necessary and sufficient no-arbitrage conditions on the structure and values of the forward rates are derived. Third, generic arbitrage-free drift terms for the forward rates are derived under a change of measure in a market model setting. Fourth, the numeric efficiency of the generic drift term calculations is discussed. Fifth, the issue of calibrating generic market models to correlation is addressed. Sixth, we end with conclusions.

7.2 Preliminaries

We consider *tenor times* or a *tenor structure* $0 =: t_1 < \cdots < t_{n+1}$ and *day count fractions* α_i, over the period $[t_i, t_{i+1}]$, for $i = 1, \ldots, n$. Suppose traded in the market is a set of m forward LIBOR or swap rate agreements that are associated with that tenor structure[2]. Initially, m may be different from n, but in Theorem 8 we show that it makes sense, from an economic point of view, to consider only $m = n$. The set of associated forward swap agreements is administered by a set of pairs

$$\mathcal{E} = \Big\{ \epsilon_j = \big(s(j), e(j)\big) \ ; \ j = 1, \ldots, m \ ; \ s(j), e(j) \text{ integers } 1 \leq s(j) < e(j) \leq n+1 \Big\}. \tag{7.1}$$

Here $s(j)$ and $e(j)$ denote *start* and *end* of the forward swap agreement. The above set expression for $\mathcal{E}$ simply designates that there are m associated forward swap agreements, that each forward swap agreement starts and ends on one of the tenor times and that a

[2]The frequency of the floating payments is restricted to one payment per fixed-payment period, but this is only for ease of exposition. In practice, this assumption may be relaxed and the theory follows through unchanged for any positive whole number of floating payments per fixed-payment period.

start is strictly before an end. If the start s and end e of two forward swap agreements $\epsilon^{(1)}$, $\epsilon^{(2)}$ are equal, then $\epsilon^{(1)}$ and $\epsilon^{(2)}$ are considered equal, thereby a priori excluding the possibility of different forward rates for the same forward swap agreement. We note also that different payment frequencies for a given swap period are not allowed. The value of the forward rate associated with ϵ_j is denoted by f_j. Forward rate f_j may, and shall, in the course of our chapter, depend on time, $f_j = f_j(t)$. The associated forward swap agreement is defined as follows. At times $t_{s(j)}$ and $t_{e(j)}$ the agreement starts and ends, respectively. The agreement is partitioned by a number of $e(j) - s(j)$ accrual periods $[t_{s(j)}, t_{s(j)+1}]$, $\ldots$, $[t_{e(j)-1}, t_{e(j)}]$. The LIBOR rate is recorded at the start of each accrual period. If the accrual periods are indexed by $i = s(j), \ldots, e(j) - 1$, then the LIBOR-observation time is t_i, the maturity of the LIBOR deposit is $t_{i+1} - t_i$, and the observed LIBOR rate is denoted by $\ell(t_i)$. If forward swap agreement j has been entered into at time t^* at rate $f_j(t^*)$, then the fixed and floating payments are $\alpha_i f_j(t^*)$ and $\alpha_i \ell(t_i)$, respectively. We assume liquid trading in the market at times $t^* = t_1, \ldots, t_n$ of those forward swap agreements $\epsilon \in \mathcal{E}$ for which $t_{s(j)} \geq t^*$. In other words, there is trading in a forward swap agreement if the agreement has not yet started or is about to start. We assume the cost of entering into any forward swap agreement at any tenor time to be zero.

The forward swap agreement structures of the LIBOR and swap market models fit into the framework of (7.1). For the LIBOR market model (LMM), $\mathcal{E}_{\text{LMM}} = \{(1,2), (2,3), \ldots, (n, n+1)\}$. For the swap market model (SMM), $\mathcal{E}_{\text{SMM}} = \{(1, n+1), (2, n+1), \ldots, (n, n+1)\}$. We introduce here a third kind of market model, associated with the q-period CMS rates. We name it the *CMS(q) market model*, for $q = 1, \ldots, n$, and it is defined by $\mathcal{E}_{\text{CMS}(q)} = \{(1, 1+q), (2, 2+q), \ldots, (n-q+1, n+1), (n-q+2, n+1), \ldots, (n, n+1)\}$. We note that for $q = 1$ and $q = n$ we retain the LIBOR and swap market models, respectively.

The structure of these market models can be specified equivalently as follows, too. There exists an enumeration $\epsilon_j = (s(j), e(j))$, such that, for the LIBOR model, $s(j) = j$, $e(j) = j+1$. For the swap model, $s(j) = j$, $e(j) = n+1$. For the CMS(q) model, $s(j) = j$,

$$e(j) = j + q \ \ (j = 1, \ldots, n - q + 1), \ \ e(j) = n + 1 \ \ (j = n - q + 2, \ldots, n). \tag{7.2}$$

7.2.1 Absence of arbitrage

Associated with the tenor structure we also consider *discount bonds*. A discount bond is a hypothetical security that pays one unit of currency at its maturity. The price at time t of a discount bond maturing at time t_i is denoted by $b_i(t)$. We note that there are $n+1$ discount bonds and that we necessarily have $b_i(t_i) = 1$ for $i = 1, \ldots, n+1$. The latter is just saying that the cost of immediately receiving one unit of currency is one unit of currency. The time-t_1 discount bond prices are sometimes simply denoted by b_i rather than by $b_i(t_1)$.

In terms of price consistency among the discount bonds, forward swap agreements, and LIBOR deposits, we require some form of absence of arbitrage. We follow Musiela & Rutkowski (1997), in which two forms of no-arbitrage are introduced. First, a weaker notion of no-arbitrage is the usual no-arbitrage condition in a *pure bond market*. Second, a stronger notion of no-arbitrage assumes, in addition, that *cash* is also available in the market, which means that money, not stored in a money market account, can be carried over at zero cost. The stronger form of no-arbitrage excludes a number of situations allowed by the weaker form. For example, discount bond prices greater than 1 (negative interest rates) are excluded by the strong form, but not by the weak form. More generally, the discount bond prices are required, by the strong form, but not by the weak form, to not increase with increasing maturity, as shown by Musiela & Rutkowski (1997, page 267, below Equation (13)). In the next section, it will be shown that the generic market models guarantee the weak form of no-arbitrage. Conditions guaranteeing the stronger form of no-arbitrage are more difficult to derive. Therefore, hereafter we only consider the weak form of no-arbitrage, and any mentioning of 'no-arbitrage' will refer to the weak form. We note that the weak form of absence of arbitrage is guaranteed when all discount bond prices are positive, since a set of positive future cash flows implies a portfolio that holds non-negative amounts of discount bonds, of which at least one position is positive. Since all discount bond prices are positive by assumption, we have that the price of such a portfolio is positive, thereby excluding arbitrage.

Valuation of non-European interest rate derivatives requires a dynamic model, that is, a model that generates unique arbitrage-free discount bond prices at all future time points. Examples of such dynamic models are the LIBOR and swap market models. An example of a non-dynamic model is the co-initial market model, as defined by Galluccio & Hunter (2004). The co-initial model features forward swap rates that span the periods $(1,2)$,$(1,3)$,$\ldots$,$(1,n+1)$, that is, all swap rates start at time t_1 but end consecutively at times $t_2,\ldots,t_{n+1}$. The co-initial specification is non-dynamic since at time t_2, all forward swap agreements have expired. From a practical point of view, non-dynamic models are less useful than dynamic models, since non-dynamic models can only be used for European-style options. For the dynamic case, arbitrary specification of forward rates at not only t_1, but at all time points $t_1,\ldots,t_n$, is required to lead to unique discount bond prices.

Given an arbitrary set $\mathcal{E}$ of forward rates and their values $\{f_j(t_i)\}_{i,j}$, there are two mutually exclusive possibilities, that are given in the following definition.

Definition 7

- Condition A. *At each of the times $t_1,\ldots,t_n$, there is a unique system of prices for the discount bonds, such that the resulting aggregate trade system of discount bonds, forward swap agreements, and LIBOR deposits, is arbitrage-free.*

- Condition B. *At least at one of the times $t_1, \ldots, t_n$, either there exists no system or there are more than one different systems of prices for the discount bonds, such that the resulting aggregate trade system of discount bonds, forward swap agreements, and LIBOR deposits, is arbitrage-free.*

Obviously, we would want condition A to hold in financial models, and, in particular, in generic market models. In this chapter, we will derive necessary and sufficient conditions on $\mathcal{E}$ and the values $\{f_j(t_i)\}$, for condition A to hold. In particular, given a number of $n+1$ tenor times, we will show that there are exactly $n!$ possibilities of choosing $\mathcal{E}$. The CMS market model (with LIBOR and swap market models as special cases) only accounts for n of these possibilities. An example for $n = 6$ with market models of LIBOR, CMS(3), swap, co-initial, and the hybrid swap of Table 7.1 (viewed from the valuation date 11 June 2003), is given in Figures 7.1 and 7.2.

Remark 4 (*Forward LIBOR versus swaption frequencies*) In this remark we point out a silent assumption that is sometimes made when calibrating a market model to parts of the swaption volatility matrix. For concreteness, we consider the EUR market, for which market traded swaps have annual fixed payments and semi-annual floating LIBOR payments. If a market model with semi-annual fixed payments is calibrated to a swaption volatility, then silently it has been assumed that there is no significant difference between semi-annual fixed versus semi-annual floating swaption volatility and annual fixed versus semi-annual floating swaption volatility.

7.3 Necessary and sufficient conditions on the forward swap agreements structure for guaranteed no-arbitrage

In this section we derive the necessary and sufficient conditions for a set of forward rates to specify unique arbitrage-free discount bond prices. The program to achieve that goal is as follows. First, we value the forward swap agreements in terms of discount bond prices. Second, the conditions on the forward swap agreements are translated into conditions on the discount bond prices.

A forward swap agreement is valued by valuation of its floating and fixed payments in turn. The collections of floating and fixed payments of a forward swap agreement are called *floating* and *fixed legs*, respectively. The value $\pi_{\text{flt}}(\epsilon)$ of the floating leg of a forward swap agreement $\epsilon = (s, e)$ is[3]

$$\pi_{\text{flt}}(\epsilon) = b_s - b_e.$$

[3]Here we assume equality of the forecast and discount curves and of the payment and index day count fractions.

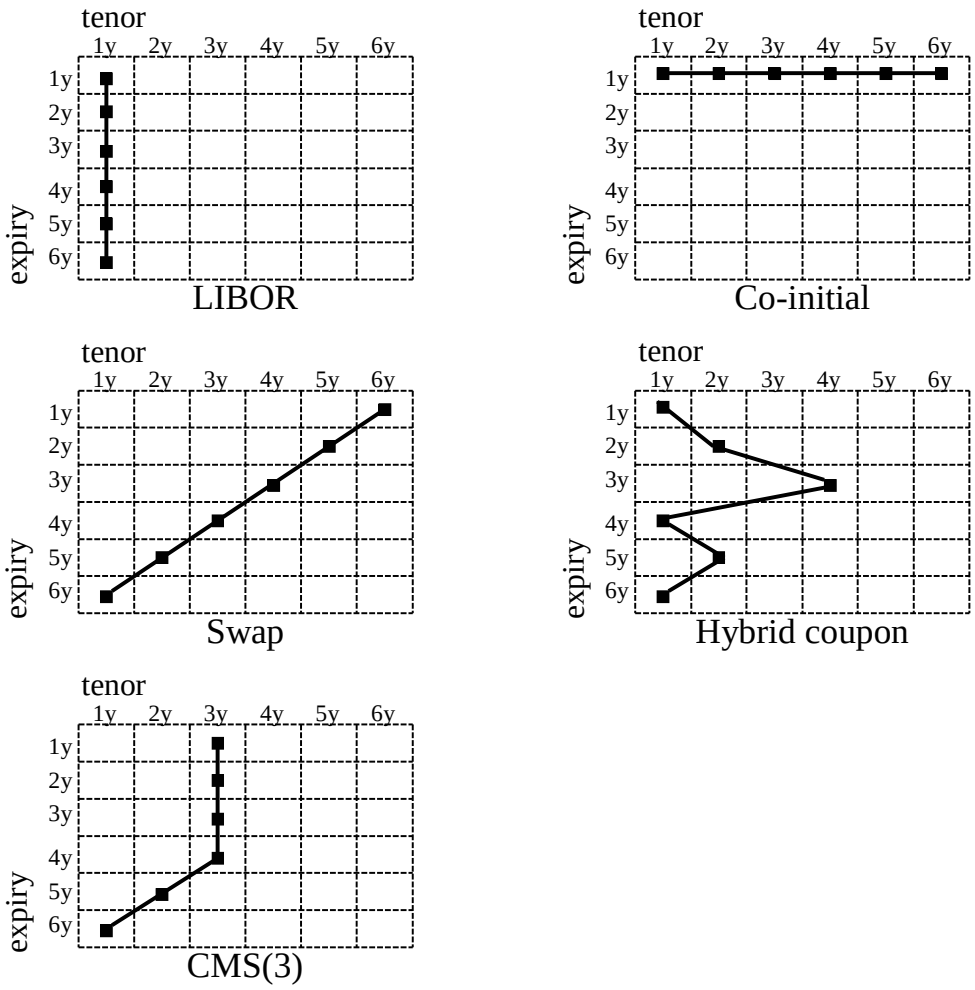

Figure 7.1: The swaptions from the swaption matrix to which various market models are calibrated.

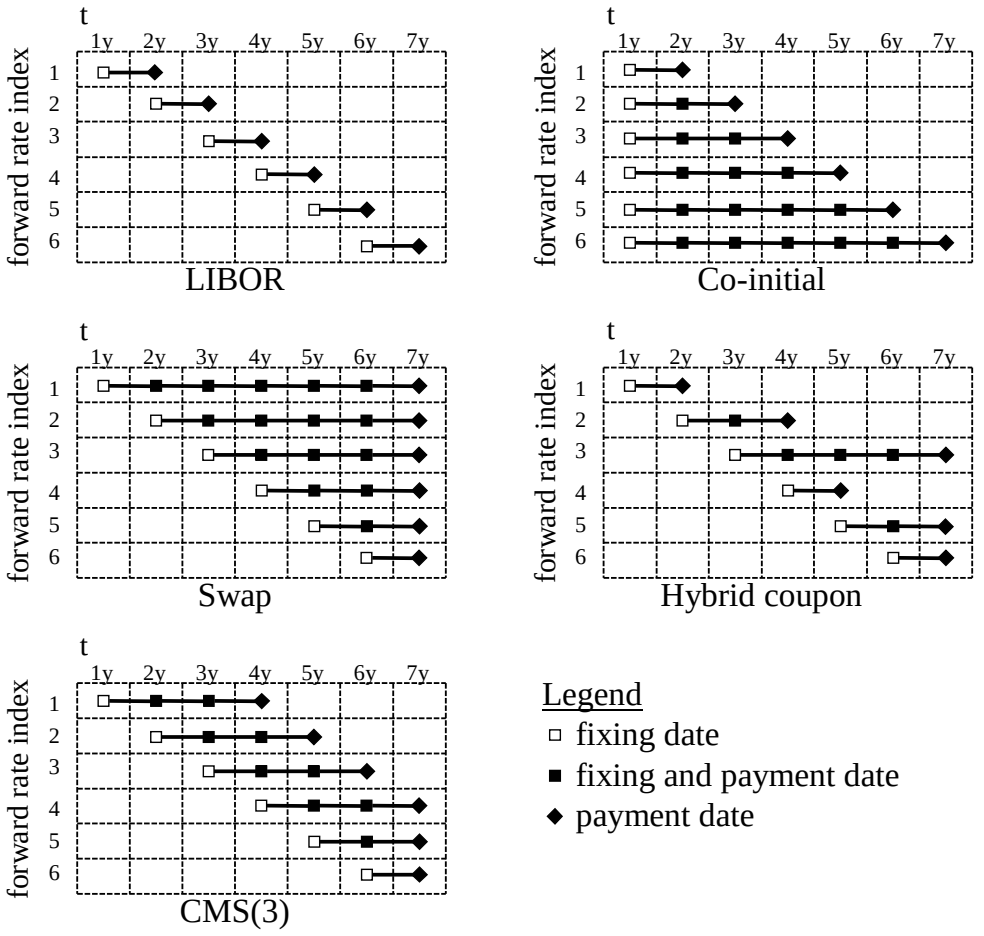

Figure 7.2: An overview of the forward swap agreements for various market models.

This equation can be seen to hold by considering a portfolio in the discount bonds that will have the exact same cash flows as the floating leg, to wit, long a discount bond maturing at time t_s and short a bond maturing at time t_e. At time t_s, we invest the proceeds of the long position in the discount bond into the LIBOR deposit. At each LIBOR payment, we re-invest the notional into the LIBOR deposit. At the end of the floating leg, the notional cancels against the short position in the discount bond. It is not hard to see that such procedure provides the exact same cash flows as a floating leg.

The value $\pi_{\text{fxd}}(\epsilon, f)$ of a fixed leg with forward rate f can be obtained by simply discounting back the known future cash flows[4],

$$\pi_{\text{fxd}}(\epsilon, f) = f \underbrace{\sum_{i=s}^{e-1} \alpha_i b_{i+1}}\,.$$

The under-braced expression is also called *present value of a basis point* (*PVBP* in short), and is denoted by $p_{s:e}$.

The conditions on the forward rates are governed by the forward swap agreements to have zero value, that is, $\pi_{\text{flt}}(\epsilon) - \pi_{\text{fxd}}(\epsilon, f) = 0$. In fact, there exists a unique system of prices for the discount bonds consistent with the forward rates if and only if the system of m linear equations in the n unknown variables $b_2, \ldots, b_{n+1}$ given by

$$\left\{ b_{s(j)} - b_{e(j)} - \sum_{i=s(j)}^{e(j)-1} f_j \alpha_i b_{i+1} = 0 \right\}_{j=1}^{m}, \tag{7.3}$$

with $b_1 = 1$, has a unique solution. The latter is already a precisely specified and tractable necessary and sufficient condition for existence of unique discount bond prices that are consistent with the forward rates. This condition can be validated by numerically checking invertibility of linear equation (7.3). In the sequel, we will develop conditions and implications that are more straightforward to verify and that a priori guarantee invertibility of (7.3), and we will sketch scenarios in which these implications will hold. It will be shown that invertibility of (7.3) is guaranteed in typical finance scenarios, and that invertibility can be violated only under extreme situations, that are fully irrelevant to a finance setting.

If $m < n$ then if a solution exists, it is bound to exhibit non-uniqueness. If $m > n$, then the system is in general over-determined. Only for a very particular choice of forward rates f_j, the system could then be degenerate, thereby still allowing for a unique solution. Given arbitrarily specified forward rates however, the degeneracy will occur, if at all, only occasionally. Generally specified forward rates span a non-degenerate set of equations,

[4]We assume, for notational simplicity only, that the fixed payment frequency equals the floating payment frequency.

thereby implying that, when $m > n$, in most cases the model does not have unique discount bond prices. In other words, two different subsets of n forward rates determine, via (7.3), two sets of discount bond prices that are different and thus inconsistent with each other. The model should have the property that there exist unique discount bond prices regardless of how the forward rates are specified. The possibility of degeneracy is excluded by the following assumption on the values that the forward rates can attain.

Assumption 1 *A forward rate f can only attain any non-negative value, that is, we must have*

$$f \geq 0. \tag{7.4}$$

Assumption 1 will be satisfied almost always in any interest rate market. Only in very rare occasions have negative interest rates been observed. An example of negative interest rates in Japan at the start of November 1998 is given in Ostrom (1998). These interest rates reached -3 to -6 basis points (bp) (-.03% to -.06%). Moreover, the popular displaced diffusion smile model of Rubinstein (1983) can generate negative forward rates with positive probability, if the displacement parameter is negative. However, violation of Assumption 1 does not necessarily imply that the system of forward rates admits arbitrage of the weak form. In fact, we make plausible that slightly negative interest rates still allow for unique discount bond prices that are arbitrage-free in the weak sense, by considering a simple numerical example. We consider a single forward rate, two tenor times $\{t_1 = 0, t_2\}$ market model. The price of the discount bond for maturity at time t_2 is given by $1/(1 + \alpha f)$. The rate f should thus satisfy $f > -1/\alpha$, to ensure a positive and finite price for the discount bond. For annual payments, for which $\alpha \approx 1$, we have $-1/\alpha \approx -100\%$. In fact, for more frequent payments than annual, the arbitrage-defying rate is even more negative than -100%. These considerations lead us to conclude that arbitrage of the weak form in a forward swap agreement market can occur only in situations that are considered financially extreme. Essential to no-arbitrage is thus the structure of the forward swap agreements.

7.3.1 Main result

The main result can now be formulated. The theorem below states that, for dynamic market models, (i) if a tenor structure has n fixing times $t_1, \ldots, t_n$, then we require n forward swap agreements, and (ii) for each fixing time t_i, there is exactly one forward swap agreement that starts at that fixing time t_i, $i = 1, \ldots, n$. We note that the co-initial model does not fit the requirements below, though it is a perfectly sensible arbitrage-free model. The reason that the co-initial model is not incorporated is the requirement that a model be *dynamic*, see the discussion in Section 7.2.1.

Algorithm 4 Back substitution.

Input: n, $\mathbf{U}$ ($(n+1) \times (n+1)$ unit upper-triangular), $\mathbf{c} \in \mathbb{R}^{n+1}$.
Output: $\hat{\mathbf{b}} = \mathbf{U}^{-1}\mathbf{c} \in \mathbb{R}^{n+1}$.

1: Set $\hat{b}_{n+1} \Leftarrow c_{n+1}$.
2: **for** $i = n, \ldots, 1$ **do**
3: $\quad \hat{b}_i \Leftarrow c_i - \sum_{j=i+1}^{n+1} u_{ij}\hat{b}_j$.
4: **end for**

Theorem 8 *Let $\{t_1, \ldots, t_{n+1}\}$ be a set of tenor times. Let $\mathcal{E} = \{\epsilon_j\}_{j=1}^m$ and f_j be a set of forward swap agreements and forward rates, respectively, associated with the tenor times. Then, at each of the times $t_1, \ldots, t_n$, for all forward rates $\{f_j\}_{j=1}^m$ satisfying Assumption 1, there exists a unique weak-form arbitrage-free solution to the system of linear equations (7.3) in the discount bond prices, if and only if $m = n$ and there exists an ordering of the n forward swap agreements $\epsilon_j = (s(j), e(j))$, $j = 1, \ldots, m$ such that $s(j) = j$.*

PROOF: The proof is split into two parts. First, we prove that the described structure of forward rates leads to arbitrage-free invertibility of system (7.3) for all forward rates satisfying Assumption 1. Second, the reverse implication is proven.

Suppose that the structure $\mathcal{E}$ of forward swap agreements is such that $m = n$ and that there exists an ordering of the n forward swap agreements $\epsilon_j = (s(j), e(j))$, $j = 1, \ldots, m$ such that $s(j) = j$. The existence of unique arbitrage-free discount bond prices is guaranteed if we show there exists unique discount bond prices that are all positive. To that order, consider system (7.3) in terms of the deflated discount bond prices, $\hat{b}_i \equiv b_i/b_{n+1}$, and substitute $s(j) = j$,

$$\left\{ \hat{b}_j - \hat{b}_{e(j)} - \sum_{i=j}^{e(j)-1} f_j \alpha_i \hat{b}_{i+1} = 0 \right\}_{j=1}^{n}, \ \{\hat{b}_{n+1} = 1\}. \tag{7.5}$$

We note that the $(n+1) \times (n+1)$ matrix $\mathbf{U} = \mathbf{U}(\mathbf{f})$ associated with this system is unit upper-triangular, which means that the diagonal contains ones and that the lower-triangular part of the matrix contains zeros. It follows that this matrix is invertible. We thus have

$$\mathbf{U}(\mathbf{f})\hat{\mathbf{b}} = \mathbf{c}, \ \ \hat{\mathbf{b}} = \mathbf{U}(\mathbf{f})^{-1}\mathbf{c}, \ \ \mathbf{c} = (0 \ \cdots \ 0 \ 1)^T \in \mathbb{R}^{n+1}.$$

An efficient method for calculating the inverse of a unit upper-triangular matrix is *back substitution*, see for example Golub & van Loan (1996, Algorithm 3.1.2). Back substitution will aid in the proof, therefore it has been displayed in Algorithm 4. We show by induction for $i = n+1, n, \ldots, 1$ that $\hat{b}_i \geq 1$. For $i = n+1$, $\hat{b}_i = \hat{b}_{n+1} = 1$, by line 1 of Algorithm 4, which states that $\hat{b}_{n+1} = c_{n+1} = 1$. Suppose, then, that $\hat{b}_j \geq 1$ for $j = i+1, \ldots, n+1$.

We have, by line 3 of Algorithm 4, that $\hat{b}_i = c_i - \sum_{j=i+1}^{n+1} u_{ij}\hat{b}_j = -\sum_{j=i+1}^{n+1} u_{ij}\hat{b}_j$. We note that, for $j > i$, u_{ij} is either $-\alpha_j f_i$, $-1-\alpha_j f_i$, or 0. It follows that

$$\hat{b}_i = \underbrace{f_i \sum_{j=i}^{e(i)-1} \alpha_j \hat{b}_{j+1}}_{\geq 0} + \underbrace{\hat{b}_{e(i)}}_{\geq 1} \geq 1,$$

which concludes the induction proof. The unique solution for the *un*deflated discount bond prices at tenor point t_1 is then given by $b_i \equiv \hat{b}_i/\hat{b}_1$, which is defined and positive since $\hat{\mathbf{b}} = (\hat{b}_1, \ldots, \hat{b}_{n+1}) \geq 1$.

We note that the above proof is independent of the number of tenor times. Therefore the forward swap agreements structure $n = m$ and $\{s(j) = j\}$ guarantees existence of unique arbitrage-free discount bond prices for *all* forward rates satisfying Assumption 1 at all tenor times $t_1, \ldots, t_n$, which was to be shown.

The reverse implication is proven by induction on n. For $n = 1$, the result is immediate. Now, assume the result is true for $i = 1$ to $n-1$. We want to prove it is true for n. The model viewed from t_2 has n tenor points, so by the induction hypothesis we must have that: (i) $m \geq n-1$, (ii) there are exactly $n-1$ forward swap agreements that start at t_2 or later, (iii) for these $n-1$ forward swap agreements, there is an enumeration $j = 2, \ldots, n$, such that $s(j) = j$. There are three possibilities: $m = n-1$, $m > n$ or $m = n$. We show that the cases $m = n-1$ and $m > n$ lead to non-uniqueness or non-invertibility of (7.3) for some of the forward rates f that satisfy Assumption 1.

If $m = n-1$, there are less equations than unknown variables in (7.3), and it follows that, if there is a solution at all, it will be non-unique.

If $m > n$, then we may form a sub-model with n forward swap agreements such that $s(j) = j$ for $j = 1, \ldots, n$. We have already proven that such a structure with n forward rates leads to unique positive discount bond prices. For a left out forward swap agreement, say $\epsilon = (s, e)$, the associated forward rate f should then satisfy

$$f = \frac{b_s - b_e}{\sum_{i=s}^{e-1} \alpha_i b_{i+1}}. \tag{7.6}$$

We conclude then that there are forward rates satisfying Assumption 1 for which there do not exist discount bond prices.

Thus we must have $m = n$ and for remaining forward swap agreement 1 we have $s(1) = 1$ from which the result follows. □

As a corollary, we can count the dynamic market model structures given the number of tenor times $n+1$. For forward rate 1, we can chose from n end times $t_2, \ldots, t_{n+1}$, for forward rate 2, from $n-1$ end times $t_3, \ldots, t_{n+1}$, etcetera.

Corollary 2 (Counting dynamic market model structures) *Consider market models with $n+1$ tenor times. Then there are $n!$ ways of selecting forward swap agreements such that, for all forward rates satisfying Assumption 1, and at all tenor times $t_1, \ldots, t_n$, there exist unique weak-form arbitrage-free discount bond prices satisfying (7.3).*

We note that Theorem 8 rules out the applicability of generic market models to Bermudan-callable spread options, in the sense that we cannot define two rates, fixing at the same time, as state variables.

7.4 Generic expressions for no-arbitrage drift terms

In this section, generic expressions are derived for the arbitrage-free drift terms of generic market models, that are so characteristic for the LIBOR and swap market models. We assume given a dynamic market model, therefore the forward swap agreements are of the form $\epsilon_i = (i, e(i))$. If dependency of the end index is clear we simply write $e(i)$ as e. The forward rate $f_{i:e}$ has start date t_i and end date t_e. Forward rate $f_{i:e}$ is modelled under its forward measure, which is associated with the p $p_{i:e}$ as numeraire. Forward rate $f_{i:e}$ is modelled as

$$\frac{\mathrm{d}f_{i:e}(t)}{f_{i:e}(t)} = \boldsymbol{\sigma}_{i:e}(t) \cdot \mathrm{d}\mathbf{w}^{(i:e)}(t), \tag{7.7}$$

with $\boldsymbol{\sigma}_{i:e}$ denoting a d-dimensional volatility vector, and with $\mathbf{w}^{(i:e)}$ a d-dimensional Brownian motion under the forward measure $\mathbb{Q}_{i:e}$ associated with $p_{i:e}$ as numeraire. The positive integer d is deemed the *number of factors* of the model. The volatility vector $\boldsymbol{\sigma}_{i:e}(t) = \boldsymbol{\sigma}_{i:e}(t, \omega)$ can be state dependent to allow for smile modelling.

For pricing of non-standard interest rate derivatives, it is necessary to jointly implement the above scheme (7.7) for all forward rates simultaneously. Therefore we must work out the SDE for the forward rates under a single pricing measure. We can work either with the terminal or spot measure. Each is treated below consecutively.

7.4.1 Terminal measure

In this subsection, we work with the terminal measure $\mathbb{Q}_{n+1}$, that is the measure associated with the terminal discount bond b_{n+1} as numeraire.

Without loss of generality, the presentation is given as if all forward rates have not yet expired. We work with the numeraire-deflated discount bond prices. The quantity $\hat{p}_{i:e}$ denotes the deflated p, $\hat{p}_{i:e} \equiv p_{i:e}/b_{n+1}$. The deflated ps can be calculated, in turn, when the deflated discount bond prices $\hat{b}_i \equiv b_i/b_{n+1}$ are known. The deflated discount bond prices are given by (7.5). Recall that (7.5) can be written in matrix form as $\mathbf{U}\hat{\mathbf{b}} = \mathbf{c}$, with

$\mathbf{c} = (0\ \cdots\ 0\ 1)^T$, and $\mathbf{U} = \mathbf{U}(\mathbf{f})$ an $(n+1)\times(n+1)$ unit upper-triangular matrix, given by

$$u_{ij} = \begin{cases} 0 & \text{if } i > j \text{ or } (i < j \text{ and } j > e(i)), \\ 1 & \text{if } i = j, \\ -\alpha_{j-1} f_{i:e(i)} & \text{if } i < j \text{ and } j < e(i), \\ -\alpha_{j-1} f_{i:e(i)} - 1 & \text{if } i < j \text{ and } j = e(i). \end{cases}$$

Thus $\hat{\mathbf{b}} = \mathbf{U}(\mathbf{f})^{-1}\mathbf{c}$. We may write $\hat{\mathbf{p}}$ as a function of the forward rates, $\hat{\mathbf{p}} = \hat{\mathbf{p}}(\mathbf{f})$. In fact,

$$\hat{\mathbf{p}} = \mathbf{A}\hat{\mathbf{b}}, \quad \mathbf{A} \equiv \begin{pmatrix} 0 & (\alpha_1\ \cdots\ \alpha_{e(1)-1}\ 0\ \cdots\ 0) \\ 0 & 0 \quad (\alpha_2\ \cdots\ \alpha_{e(2)-1}\ 0\ \cdots\ 0) \\ 0 & \vdots \quad \ddots \quad \ddots \quad \vdots \\ 0 & 0 \quad \cdots \quad 0 \quad (\alpha_n) \end{pmatrix},$$

for the $n\times(n+1)$ matrix $\mathbf{A}$. Thus, $\hat{\mathbf{p}} = \mathbf{A}\mathbf{U}(\mathbf{f})^{-1}\mathbf{c}$. Subsequently, we define the Radon-Nikodým density

$$z_{i:e,n+1}(t) \equiv \frac{p_{i:e}(t)/b_{n+1}(t)}{p_{i:e}(0)/b_{n+1}(0)} = \frac{\hat{p}_{i:e}(t)}{\hat{p}_{i:e}(0)}. \tag{7.8}$$

We note that $z_{i:e,n+1}(t)$ is a martingale under the terminal measure $\mathbb{Q}_{n+1}$. This implies that

$$\frac{\mathrm{d}z_{i:e,n+1}(t)}{z_{i:e,n+1}(t)} = \frac{\mathrm{d}\hat{p}_{i:e}(t)}{\hat{p}_{i:e}(t)} = \boldsymbol{\theta}_{i:e,n+1}(t)\cdot\mathbf{w}^{(n+1)}(t), \tag{7.9}$$

with the d-dimensional vector $\boldsymbol{\theta}$ given by

$$\boldsymbol{\theta}_{i:e,n+1}(t) = \frac{1}{\hat{p}_{i:e}(t)}\sum_{k=i+1}^{n}\frac{\partial\hat{p}_{i:e}}{\partial f_{k:e(k)}}(t) f_{k:e(k)}(t)\boldsymbol{\sigma}_{k:e(k)}(t). \tag{7.10}$$

The summation is required only from $i+1$ to n since $\hat{p}_{i:e}$ is dependent on $f_{k:e(k)}$ only for $k > i$. Finally we apply Girsanov's theorem to obtain the required expression for $\mathrm{d}\mathbf{w}^{(i:e)}(t) - \mathrm{d}\mathbf{w}^{(n+1)}(t)$,

$$\mathrm{d}\mathbf{w}^{(i:e)}(t) - \mathrm{d}\mathbf{w}^{(n+1)}(t) = -\boldsymbol{\theta}_{i:e,n+1}(t)\mathrm{d}t. \tag{7.11}$$

Thus,

$$\begin{aligned}\frac{\mathrm{d}f_{i:e}(t)}{f_{i:e}(t)} &= -\frac{1}{\hat{p}_{i:e}(t)}\sum_{k=i+1}^{n}\frac{\partial\hat{p}_{i:e}}{\partial f_{k:e(k)}}(t) f_{k:e(k)}(t)|\boldsymbol{\sigma}_{k:e(k)}(t)||\boldsymbol{\sigma}_{i:e}(t)|\rho_{k:e(k),i:e}(t)\mathrm{d}t \\ &\qquad + \boldsymbol{\sigma}_{i:e}(t)\cdot\mathrm{d}\mathbf{w}^{(n+1)}(t),\end{aligned}$$

where the scalar $\rho_{k:e(k),i:e}$ has been defined as

$$\rho_{k:e(k),i:e}(t) = \frac{\boldsymbol{\sigma}_{k:e(k)}(t)\cdot\boldsymbol{\sigma}_{i:e}(t)}{|\boldsymbol{\sigma}_{k:e(k)}(t)||\boldsymbol{\sigma}_{i:e}(t)|},$$

and has the interpretation of instantaneous correlation.

An expression is given for $\partial\hat{\mathbf{p}}/\partial f_{k:e(k)}$. We note that $\partial\mathbf{U}/\partial f_{k:e(k)}$ is a matrix that is zero bar a single row, the k^{th} row, and that the derivative is independent of f, since all f terms occur linearly in the matrix $\mathbf{U}$. The k^{th} row is filled, from entry $(k, k+1)$, with the row vector $(-\alpha_k \ \cdots \ -\alpha_{e(k)-1} \ 0 \ \cdots \ 0)$. We have that

$$\frac{\partial\hat{\mathbf{p}}}{\partial f_{k:e(k)}} = -\mathbf{A}\mathbf{U}^{-1}\frac{\partial\mathbf{U}}{\partial f_{k:e(k)}}\mathbf{U}^{-1}\mathbf{c} = -\mathbf{A}\mathbf{U}^{-1}\frac{\partial\mathbf{U}}{\partial f_{k:e(k)}}\hat{\mathbf{b}} = \mathbf{A}\mathbf{U}^{-1}\mathbf{c}_k\hat{p}_{k:e(k)}, \tag{7.12}$$

where $\mathbf{c}_k \in \mathbb{R}^{n+1}$ denotes the standard basis vector with unit k^{th} coordinate, and zero coordinates otherwise. We define $\tilde{b}_i^{(k)}$ by

$$\tilde{b}_i^{(k)} = (\mathbf{U}^{-1}\mathbf{c}_k)_i, \quad i = 1, \ldots, n, \quad k = 1, \ldots, n. \tag{7.13}$$

Substituting (7.13) into (7.12) yields

$$\frac{\partial\hat{p}_{i:e}}{\partial f_{k:e(k)}} = 1_{\{k\geq i+1\}}\hat{p}_{k:e(k)}\left(\sum_{j=i}^{\min(e(i)-1,k-1)}\alpha_j\tilde{b}_{j+1}^{(k)}\right). \tag{7.14}$$

Define $\mu(i,k) \equiv \min\big(e(i)-1, k-1\big)$. Substituting (7.14) into (7.12), suppressing the dependency of time, and using $\hat{p}_{k:e(k)}f_{k:e(k)} = \hat{b}_k - \hat{b}_{e(k)}$, we obtain the generic market model SDE under the terminal measure:

$$\frac{\mathrm{d}f_{i:e}}{f_{i:e}} = -\frac{1}{\hat{p}_{i:e}}\sum_{k=i+1}^{n}\big(\hat{b}_k - \hat{b}_{e(k)}\big)\left(\sum_{j=i}^{\mu(i,k)}\alpha_j\tilde{b}_{j+1}^{(k)}\right)\boldsymbol{\sigma}_{k:e(k)}\cdot\boldsymbol{\sigma}_{i:e}\mathrm{d}t + \boldsymbol{\sigma}_{i:e}\cdot\mathrm{d}\mathbf{w}^{(n+1)}. \tag{7.15}$$

7.4.2 Spot measure

In this subsection, we work with the spot measure $\mathbb{Q}_{\text{Spot}}$, that is the measure associated with the spot LIBOR numeraire, defined as follows. The account starts out with one unit of currency. Subsequently, this amount is invested in the spot LIBOR account. After the first accrual period, the proceeds are re-invested in the then spot LIBOR account. This procedure is repeated. For the spot measure it is convenient to define the *spot index* $i(t)$, defined by $i(t) = \min\{\text{integer} \ \ i \ ; \ t < t_i\}$.

For the spot measure, we work with discount bond prices, deflated by the spot discount bond $b_{i(t)}$. The quantities $\bar{\mathbf{p}}$ and $\bar{\mathbf{b}}$ denote the vectors of $b_{i(t)}$-deflated PVBPs and discount bond prices, respectively. We have $\bar{\mathbf{p}} = \mathbf{A}\bar{\mathbf{b}}$ and

$$\bar{\mathbf{b}} = \frac{1}{\hat{b}_{i(t)}}\hat{\mathbf{b}} = \frac{1}{(\mathbf{U}^{-1}\mathbf{c})_{i(t)}}\mathbf{U}^{-1}\mathbf{c}.$$

The Radon-Nikodým density $z_{i:e,i(t)}(t)$ is defined similarly to (7.8). A martingale SDE for the Radon-Nikodým density holds,

$$\frac{\mathrm{d}z_{i:e,i(t)}(t)}{z_{i:e,i(t)}(t)} = \frac{\mathrm{d}\bar{p}_{i:e,i(t)}(t)}{\bar{p}_{i:e,i(t)}(t)} = \boldsymbol{\theta}_{i:e,i(t)}(t) \cdot \mathrm{d}\mathbf{w}^{(i(t))},$$

similar to (7.9), with d-dimensional volatility vector equal to

$$\boldsymbol{\theta}_{i:e,i(t)}(t) = \frac{1}{\bar{p}_{i:e}(t)} \sum_{k=i(t)}^{n} \frac{\partial \bar{p}_{i:e}}{\partial f_{k:e(k)}}(t) f_{k:e(k)}(t) \boldsymbol{\sigma}_{k:e(k)}(t). \tag{7.16}$$

If we compare (7.16) to (7.10), we find that, for the spot measure, we sum over all available forward rates from $i(t)$ to n, since $\bar{p}_{i:e}$ might depend on all those forward rates. Recall that, for the terminal measure, we need only sum from $i+1$ to n.

Similar to (7.11), we have $\mathrm{d}\mathbf{w}^{(i:e)} - \mathrm{d}\mathbf{w}^{(i(t))} = -\boldsymbol{\theta}_{i:e,i(t)}\mathrm{d}t$. Thus we obtain the equivalent of (7.12),

$$\begin{aligned} \frac{\mathrm{d}f_{i:e}(t)}{f_{i:e}(t)} &= -\frac{1}{\bar{p}_{i:e}(t)} \sum_{k=i(t)}^{n} \frac{\partial \bar{p}_{i:e}}{\partial f_{k:e(k)}}(t) f_{k:e(k)}(t) |\boldsymbol{\sigma}_{k:e(k)}(t)| |\boldsymbol{\sigma}_{i:e}(t)| \rho_{k:e(k),i:e}(t) \mathrm{d}t \\ &\quad + \boldsymbol{\sigma}_{i:e}(t) \cdot \mathrm{d}\mathbf{w}^{(i(t))}(t). \end{aligned} \tag{7.17}$$

An expression for $\partial \bar{\mathbf{p}} / \partial f_{k:e(k)}$ is given by

$$\frac{\partial \bar{\mathbf{p}}}{\partial f_{k:e(k)}} = \frac{1}{\hat{b}_{i(t)}} \frac{\partial \hat{\mathbf{p}}}{\partial f_{k:e(k)}} + \frac{1}{\hat{b}_{i(t)}} \underbrace{\left(\mathbf{U}^{-1} \frac{\partial \mathbf{U}}{\partial f_{k:e(k)}} \mathbf{U}^{-1} \mathbf{c} \right)_{i(t)}}_{= \hat{p}_{k:e(k)} \tilde{b}^{(k)}_{i(t)}} \bar{\mathbf{p}}. \tag{7.18}$$

Similar as in (7.12) and (7.14) for the terminal measure, we find for the spot measure:

$$\frac{\partial \bar{p}_{i:e}}{\partial f_{k:e(k)}} = 1_{\{k \geq i+1\}} \bar{p}_{k:e(k)} \sum_{j=i}^{\mu(i,k)} \alpha_j \tilde{b}^{(k)}_{j+1} - \bar{p}_{k:e(k)} \bar{p}_{i:e} \tilde{b}^{(k)}_{i(t)}. \tag{7.19}$$

Substituting (7.19) into (7.17), suppressing the dependency of time, and using

$$\bar{p}_{k:e(k)} f_{k:e(k)} = \bar{b}_k - \bar{b}_{e(k)},$$

we obtain the generic market model SDE under the spot measure:

$$\begin{aligned} \frac{\mathrm{d}f_{i:e}}{f_{i:e}} &= -\frac{1}{\bar{p}_{i:e}} \sum_{k=i(t)}^{n} \left(\bar{b}_k - \bar{b}_{e(k)} \right) \left(1_{\{k \geq i+1\}} \sum_{j=i}^{\mu(i,k)} \alpha_j \tilde{b}^{(k)}_{j+1} - \bar{p}_{i:e} \tilde{b}^{(k)}_{i(t)} \right) \boldsymbol{\sigma}_{k:e(k)} \\ &\quad \cdot \boldsymbol{\sigma}_{i:e} \mathrm{d}t + \boldsymbol{\sigma}_{i:e} \cdot \mathrm{d}\mathbf{w}^{(i(t))}. \end{aligned} \tag{7.20}$$

7.4.3 An example: The LIBOR market model

For illustration, in this section the LIBOR drift terms are calculated starting from the generic market model framework. We stress here that the explicit calculation in this section of the generic expressions of the previous section is *not* required for implementation of the generic market model framework, but is merely performed for illustration only.

First, we derive the LIBOR SDE for the terminal measure, by applying (7.15). In the LIBOR market model, a forward rate $f_{k:e(k)}$ is denoted by f_k. We note that:

(i) $\hat{p}_{i:e(i)} = \hat{p}_{i:i+1} = \alpha_i \hat{b}_{i+1}$,

(ii) $\mu(i,k) = \min(e(i)-1, k-1) = \min(i, k-1) = i$, for $k = i+1, \ldots, n$,

(iii) $\tilde{b}_j^{(k)} = \frac{\hat{b}_j}{\hat{b}_k} 1_{\{j \le k\}} = \frac{\bar{b}_j}{\bar{b}_k} 1_{\{j \le k\}}$,

(iv) $\frac{\hat{b}_k - \hat{b}_{k+1}}{\hat{b}_k} = \frac{\bar{b}_k - \bar{b}_{k+1}}{\bar{b}_k} = 1 - \frac{1}{1+\alpha_k f_k} = \frac{\alpha_k f_k}{1+\alpha_k f_k}$,

(v) $\sum_{j=i}^{\mu(i,k)} \alpha_j \tilde{b}_{j+1}^{(k)} = \frac{\hat{p}_{i:e(i)}}{\hat{b}_k} = \frac{\bar{p}_{i:e(i)}}{\bar{b}_k}$.

Substituting (i)–(v) into (7.15), we obtain,

$$\frac{\mathrm{d}f_i}{f_i} = -\sum_{k=i+1}^{n} \frac{\alpha_k f_k}{1+\alpha_k f_k} \boldsymbol{\sigma}_k \cdot \boldsymbol{\sigma}_i \mathrm{d}t + \boldsymbol{\sigma}_i \cdot \mathrm{d}\mathbf{w}^{(n+1)},$$

which is the familiar expression for the SDE of the LIBOR market model under the terminal measure.

Second, we derive the LIBOR SDE for the spot measure. If we substitute (i)–(v) into (7.20), we see that for $k \ge i+1$, $\sum_{j=i}^{i} \alpha_j \tilde{b}_{j+1}^{(k)}$ cancels against $\bar{p}_{i:i+1} \tilde{b}_{i(t)}^{(k)}$, and for $k \le i$, we are left with $-\bar{p}_{i:i+1} \tilde{b}_{i(t)}^{(k)}$, therefore:

$$\frac{\mathrm{d}f_i}{f_i} = \sum_{k=i(t)}^{i} \frac{\alpha_k f_k}{1+\alpha_k f_k} \boldsymbol{\sigma}_k \cdot \boldsymbol{\sigma}_i \mathrm{d}t + \boldsymbol{\sigma}_i \cdot \mathrm{d}\mathbf{w}^{(i(t))},$$

which is the familiar expression for the SDE of the LIBOR market model under the spot measure.

7.5 Complexity

We study the complexity of the drift calculation over a single time step in a numerical implementation. For generic market models, we show that the complexity is, at worse, of order $\mathcal{O}(n^3)$. For specific market models, such as the LIBOR, swap, and CMS market

Algorithm 5 An $\mathcal{O}(nd)$-algorithm for calculating the forward LIBOR rates for a time step in the LIBOR market model. The number of factors is denoted by d. The log forward rates, $\log \mathbf{f}(t) = (\log f_{i(t)}(t), \ldots, \log f_n(t))$ at time t, and $\log \mathbf{f}(t + \Delta t)$ at time $t + \Delta t$, are denoted by $\boldsymbol{\phi}^{(1)}$ and $\boldsymbol{\phi}^{(2)}$, respectively. Here $\boldsymbol{\Sigma} = (\sigma_{ij})$ governs the volatility, with σ_{ij} the time-t volatility of forward rate f_i with respect to factor j in the model. $\Delta \mathbf{w}$ should be sampled from a $\mathcal{N}(\mathbf{0}, \sqrt{\Delta t}\boldsymbol{I}_d)$ distribution.

Input: n; d $(1 \leq d \leq n)$; $\boldsymbol{\phi}^{(1)}, \boldsymbol{\alpha} \in \mathbb{R}^n$; $\Delta \mathbf{w} \in \mathbb{R}^d$; $\boldsymbol{\Sigma} \in \mathbb{R}^{n \times d}$; Δt.
Output: $\boldsymbol{\phi}^{(2)} \in \mathbb{R}^n$.

1: Set $\boldsymbol{\gamma} \Leftarrow \mathbf{0}$ with $\boldsymbol{\gamma} \in \mathbb{R}^d$.
2: **for** $i = n, \ldots, i(t)$ **do**
3: $\quad \phi_i^{(2)} \Leftarrow \phi_i^{(1)}$.
4: $\quad$ **for** $j = 1, \ldots, d$ **do**
5: $\quad\quad \phi_i^{(2)} \Leftarrow \phi_i^{(2)} + \left(\gamma_j - \frac{1}{2}\sigma_{ij}\right)\sigma_{ij}\Delta t + \sigma_{ij}\Delta w_j$.
6: $\quad\quad \gamma_j \Leftarrow \gamma_j - \frac{\alpha_i \exp\left(\phi_i^{(1)}\right)}{1+\alpha_i \exp\left(\phi_i^{(1)}\right)}\sigma_{ij}$.
7: $\quad$ **end for**
8: **end for**

models, we show that a more efficient implementation is available that renders the order to $\mathcal{O}(nd)$. For CMS market models, this more efficient implementation is approximate.

For generic market models, the results are derived for the terminal measure, but can equally well be derived for the spot measure. Recall (7.12) that occurs in the drift calculation,

$$\frac{\partial \hat{\mathbf{p}}}{\partial f_{k:e(k)}} = -\mathbf{A}\mathbf{U}^{-1}\frac{\partial \mathbf{U}}{\partial f_{k:e(k)}}\mathbf{U}^{-1}\mathbf{c}.$$

The inverse of $\mathbf{U}$ can be calculated in $\mathcal{O}(n^3)$ operations. Subsequently, the 4 consecutive matrix multiplications with a vector require $\mathcal{O}(n^2)$ operations, for each forward rate k, thus in total $\mathcal{O}(n^3)$ operations. Therefore a generic market model has at worse a complexity of $\mathcal{O}(n^3)$.

The LIBOR market model has a special structure that renders the complexity to $\mathcal{O}(nd)$, which has been shown by Joshi (2003*b*). In Algorithm 5 such an $\mathcal{O}(nd)$ algorithm has been displayed that calculates the forward LIBOR rates for a time step under the terminal measure. An algorithm for the spot measure can be defined analogously, by summing from 1 to n and by incrementing γ_j (rather than decrementing) before updating $\phi_i^{(2)}$.

We show that a similar approximate algorithm can be defined for CMS(q) market models, for the terminal measure. The algorithm is shown to be exact for the swap market

model ($q = n$). The following quantity that occurs in the drift term is approximated:

$$\tilde{p}^{(k)}_{i:\mu(i,k)+1} = \tilde{p}^{(k)}_{i:\min(k,i+q)} := \sum_{j=i}^{\min(k,i+q)-1} \alpha_j \tilde{b}^{(k)}_{j+1} \quad (i < k). \tag{7.21}$$

The approximation is based on the assumption that α_i is close to α_{i+q}, for $i = 1, \ldots, n-q$. We note that this assumption is used only to efficiently approximate (7.21) for calculation of drift terms, and this assumption is *not* used in the calculation of contract payoffs. Moreover, if needs be, the drift terms can be calculated exactly by exact calculation of (7.21).

Approximation 1 *Approximately, by assumption of $\alpha_i \approx \alpha_{i+q}$ $(i = 1, \ldots, n-q)$, we have, for $\tilde{p}^{(k)}_{i:\mu(i,k)+1}$ defined in (7.21),*

$$\tilde{p}^{(k)}_{i:\mu(i,k)+1} \approx \alpha_{k-1} \prod_{m=i}^{k-2} \left(1 + \alpha_m f_{m+1:e(m+1)} \right) \quad (i < k). \tag{7.22}$$

Here, an empty product denotes 1. Formula (7.22) is exact for $i > k-q-1$. In particular, (7.22) is exact for any i in the swap market model ($q = n$).

The rationale for Approximation 1, as well as the proof of exactness when $i > k-q-1$, are given in Appendix 7.A. We note that accumulating errors in (7.22) are likely to cancel, since in practice the difference $\alpha_i - \alpha_{i+q}$ is both negative and positive. From (7.15) and Approximation 1, we obtain,

$$\begin{aligned} \frac{\mathrm{d}f_{i:e}}{f_{i:e}} \;\approx\; -\frac{1}{\hat{p}_{i:e}} \sum_{k=i+1}^{n} \Big(\hat{b}_k - \hat{b}_{e(k)}\Big) \alpha_{k-1} \prod_{m=i}^{k-2} \big(1 + \alpha_m f_{m+1:e(m+1)}\big) \boldsymbol{\sigma}_{k:e(k)} \cdot \boldsymbol{\sigma}_{i:e} \mathrm{d}t \\ + \boldsymbol{\sigma}_{i:e} \cdot \mathrm{d}\mathbf{w}^{(n+1)}. \end{aligned} \tag{7.23}$$

Define

$$\mathbf{v}_i = \sum_{k=i+1}^{n} \Big(\hat{b}_k - \hat{b}_{e(k)}\Big) \alpha_{k-1} \prod_{m=i}^{k-2} \big(1 + \alpha_m f_{m+1:e(m+1)}\big) \boldsymbol{\sigma}_{k:e(k)}. \tag{7.24}$$

The proof of the following lemma has been deferred to Appendix 7.B.

Lemma 3 *The quantity $\mathbf{v}_i$ defined in (7.24) satisfies the following recursive formulas:*

- $\mathbf{v}_n = \mathbf{0}$,
- $\mathbf{v}_i = \big(1 + \alpha_i f_{i+1:e(i+1)}\big)\mathbf{v}_{i+1} + \alpha_i \Big(\hat{b}_{i+1} - \hat{b}_{e(i+1)}\Big) \boldsymbol{\sigma}_{i+1:e(i+1)}$.

Algorithm 6 An $\mathcal{O}(nd)$-algorithm for approximately calculating the forward swap rates for a time step in the CMS(q) market model (exact when $q = n$), under the terminal measure. The number of factors is denoted by d. The log forward rates, $\log \mathbf{f}(t) = (\log f_{i(t):e(i(t))}(t), \ldots, \log f_{n:e(n)}(t))$ at time t, and $\log \mathbf{f}(t + \Delta t)$ at time $t + \Delta t$, are denoted by $\boldsymbol{\phi}^{(1)}$ and $\boldsymbol{\phi}^{(2)}$, respectively. Here $\boldsymbol{\Sigma} = (\sigma_{ij})$ governs the volatility, with σ_{ij} the time-t volatility of forward rate $f_{i:e(i)}$ with respect to factor j. Here, $e(\cdot)$ is defined in (7.2). $\Delta \mathbf{w}$ should be sampled from a $\mathcal{N}(\mathbf{0}, \sqrt{\Delta t}\boldsymbol{I}_d)$ distribution.

Input: n; d, q $(1 \leq d, q \leq n)$; $\boldsymbol{\phi}^{(1)}, \boldsymbol{\alpha} \in \mathbb{R}^n$; $\Delta \mathbf{w} \in \mathbb{R}^d$; $\boldsymbol{\Sigma} \in \mathbb{R}^{n \times d}$; Δt.
Output: $\boldsymbol{\phi}^{(2)} \in \mathbb{R}^n$.

1: $\beta_{n+1} \Leftarrow 1$. $\varpi_{n+1} \Leftarrow 0$.
2: **for** $i = n, \ldots, i(t)$ **do**
3: $\quad \varpi_i \Leftarrow \varpi_{i+1} + \alpha_i \beta_{i+1} - 1_{\{i<n \ \& \ e(i)=e(i+1)-1\}} \alpha_{e(i+1)-1} \beta_{e(i+1)}$.
4: $\quad f_i^{(1)} \Leftarrow \exp(\phi_i^{(1)})$.
5: $\quad \beta_i \Leftarrow \varpi_i f_i^{(1)} + \beta_{e(i)}$.
6: $\quad$ If $i = n$, set $\mathbf{v}_n \Leftarrow \mathbf{0} \in \mathbb{R}^d$, else $(i < n)$, set

$$\mathbf{v}_i \Leftarrow \Big(1 + \alpha_i f_{i+1}^{(1)}\Big)\mathbf{v}_{i+1} + \alpha_i \big(\beta_{i+1} - \beta_{e(i+1)}\big)\boldsymbol{\sigma}_{i+1}.$$

7: $\quad \phi_i^{(2)} \Leftarrow \phi_i^{(1)} + \Big(-\frac{1}{\varpi_i}\mathbf{v}_i - \frac{1}{2}\boldsymbol{\sigma}_i \Big) \cdot \boldsymbol{\sigma}_i \Delta t + \boldsymbol{\sigma}_i \cdot \Delta \mathbf{w}$.
8: **end for**

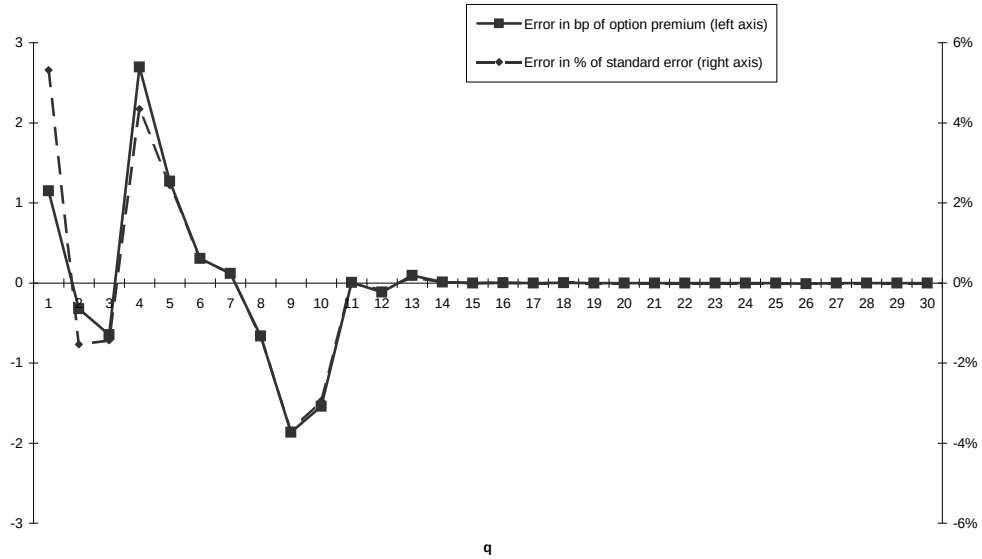

Figure 7.3: Results of the test of exact versus approximate drift terms in CMS(q) models.

Table 7.2: Deal description for the test of exact versus approximate drift terms in CMS(q) models.

Currency:	USD
Market data:	Swap rates and at-the-money swaption volatility
Valuation date:	18 July 2003
Deal:	30 year fixed-maturity Bermudan swaption
Start date:	16 June 2004
Frequency:	Annual
Day count:	ACT/365
Date roll:	Modified following
Fixed coupon:	3.2%

In Algorithm 6 an $\mathcal{O}(nd)$ algorithm, based on Lemma 3, is displayed that approximately calculates the forward swap rates for a time step under the terminal measure, for the CMS(q) market model. This algorithm is exact for the swap market model ($q = n$). Algorithm 6 also calculates time-t values for discount bond prices (denoted by β) and for PVBPs ($p_{i:e(i)}$ is denoted by ϖ_i).

To benchmark the accuracy of Algorithm 6, various fixed-maturity Bermudan swaptions are priced in their corresponding CMS(q) market models, with both exact SDE (7.15) and approximate SDE (7.23). The deal specification is given in Table 7.2. The swap tenor is q years, with $31 - q$ exercise opportunities, at (16 June 2004 + i years), $i = 0, \ldots, 30 - q$, for $q = 1, \ldots, 30$. The difference between the minimum (0.996) and maximum (1.007) attained day count fractions is 0.011. To price fixed-maturity Bermudan swaptions in Monte Carlo, we use the algorithm of Longstaff & Schwartz (2001), with the swap value as explanatory variable x, and basis functions 1, x and x^2. An 8 factor model is used ($d = 8$), with the correlation of the forward CMS(q) rates given by the parametrization of Rebonato (1998, Equation (4.5), page 83), $\exp(-\beta|t_i - t_j|)$, for rates $f_{i:e(i)}$ and $f_{j:e(j)}$, with $\beta = 3\%$. The differences between the prices obtained with exact and approximate drift terms are displayed in Figure 7.3. We note that for $q = n$, equal prices are obtained up to all digits. The results show that the error is small, up to only 3 bp of the option premium, and up to only 6% of the simulation standard error. Moreover, the error fluctuates robustly around 0, since the difference $\alpha_i - \alpha_{i+q}$ is both negative and positive, in practice.

A significant reduction of computational time can thus be attained by selecting a low number of factors d. A result of using a low number of factors is that the instantaneous correlation matrix (ρ_{ij}) cannot be exactly fit to the historically estimated or market

implied correlation matrix. The procedure for fitting a generic market model to correlation is exactly the same as for the LIBOR market model. For fitting a low-factor LIBOR market model to correlation, the reader is referred to Pietersz & Groenen (2004*a*, *b*) (see Chapter 3), Grubišić & Pietersz (2005) (see Chapter 4), Wu (2003) and Rebonato (2002, Section 9) or Brigo (2002).

7.6 Generic calibration to correlation

When each particular interest rate derivative has its own generic market model that is used for its valuation and risk management, then the associated input correlation to those models involves different interest rates. There is a relationship between these correlations, and this relationship allows for netting correlation risk or reserves. Moreover, utilizing the relationship between the correlations means that correlation is determined consistently across different products. In general all interest rate correlations stem from the correlations between different segments of the yield curve. In this section we show how forward LIBOR correlations can be used to determine subsequently the correlations for any of the generic market models specific to certain interest rate products.

The advantage of considering all correlations in this way comes from the fact that one can treat correlation risk (or reserves) in a consistent fashion across all interest rate products. Netting of correlation reserves will subsequently occur naturally. Furthermore only instantaneous forward LIBOR correlations have to be determined and administered.

The key to the method is the well-known fact that, within the LIBOR market model, the instantaneous volatility vector $\boldsymbol{\sigma}_{s:e}(t)$ of a forward swap rate $f_{s:e}$ can be expressed as weighted averages of instantaneous volatility vectors $\boldsymbol{\sigma}_i(t)$ of forward LIBORs,

$$\boldsymbol{\sigma}_{s:e}(t) = \sum_{i=s}^{e-1} w_i^{s:e}(t)\boldsymbol{\sigma}_i(t).$$

An expression for the weights $w_i^{s:e}$ may be found, for example, in Hull & White (2000, page 53). The weights $w_i^{s:e}$ are state dependent. A highly accurate deterministic approximation $\tilde{\boldsymbol{\sigma}}_{s:e}(t)$ for the instantaneous volatility can however be obtained by evaluating the weights at time zero,

$$\tilde{\boldsymbol{\sigma}}_{s:e}(t) = \sum_{i=s}^{e-1} w_i^{s:e}(0)\boldsymbol{\sigma}_i(t).$$

From the preceding considerations it should be clear that the instantaneous forward rate correlation $\rho_{s(1):e(1),s(2):e(2)}(t)$ can be approximately expressed as a function of the instan-

taneous forward LIBOR correlations $\rho_{ij}(t)$,

$$\begin{aligned}\rho_{s(1):e(1),s(2):e(2)}(t) &= \rho\left(\frac{\mathrm{d}f_{s(1):e(1)}(t)}{f_{s(1):e(1)}(t)}, \frac{\mathrm{d}f_{s(2):e(2)}(t)}{f_{s(2):e(2)}(t)}\right) \\ &= \frac{\boldsymbol{\sigma}^T_{s(1):e(1)}(t)\boldsymbol{\sigma}_{s(2):e(2)}(t)}{\sqrt{\boldsymbol{\sigma}^T_{s(1):e(1)}(t)\boldsymbol{\sigma}_{s(1):e(1)}(t)\boldsymbol{\sigma}^T_{s(2):e(2)}(t)\boldsymbol{\sigma}_{s(2):e(2)}(t)}},\end{aligned}$$

where

$$\begin{aligned}\boldsymbol{\sigma}^T_{i:j}(t)\boldsymbol{\sigma}_{k:l}(t) &\approx \tilde{\boldsymbol{\sigma}}^T_{i:j}(t)\tilde{\boldsymbol{\sigma}}_{k:l}(t) \\ &= \sum_{m_1=i}^{j-1}\sum_{m_2=k}^{l-1} w^{i:j}_{m_1}(0)w^{k:l}_{m_2}(0)|\boldsymbol{\sigma}_{m_1}(t)||\boldsymbol{\sigma}_{m_2}(t)|\rho_{m_1m_2}(t).\end{aligned}$$

7.7 Conclusions

In this chapter, a generalization of market models has been studied, whereby arbitrary forward rates are allowed to span the tenor structure relevant to an interest rate derivative. The benefit of such generalization is that straightforward volatility-calibration can be achieved for the fixings of LIBOR or swap rates relevant to the interest rate derivative. Generic market models are therefore particularly apt for pricing and risk management of CMS and hybrid coupon swaps, and callable and cancellable versions thereof, in particular, Bermudan CMS swaptions and fixed-maturity Bermudan swaptions. We showed that the LIBOR and swap market models are special cases of the generic market model framework. The need for a generic specification of market models has been illustrated by counting the admissible market model structures with $n+1$ tenor times. We found $n!$ possible market models. For example, already only for an annual-paying deal of 10 years, there are 10!=3,628,800 market models, thereby establishing the need for a generic specification. Necessary and sufficient conditions were derived for a set of forward swap agreements to provide a unique solution for discount bond prices, essentially regardless of the scenario of attained forward rates. The major novelty of this chapter is the derivation of generic expressions for no-arbitrage drift terms in generic market models. We developed a novel algorithm of order $\mathcal{O}(nd)$ for approximate drift calculations in CMS market models under the terminal measure.

7.A Appendix: Rationale for Approximation 1

We proceed by induction on $i = k-1, \ldots, i(t)$.

- For $i = k-1$: $\tilde{p}^{(k)}_{i:\mu(i,k)+1} = \tilde{p}^{(k)}_{k-1:\min(k,k-1+q)} = \alpha_{k-1}\tilde{b}^{(k)}_k = \alpha_{k-1}$.

- For $i = k-2, \ldots, k-q$, we have $\min(k, i+q) = k$. The quantity $\tilde{b}_{i+1}^{(k)}$ satisfies:

$$\tilde{b}_{i+1}^{(k)} = f_{i+1:e(i+1)}\tilde{p}_{i+1:k}^{(k)}. \tag{7.25}$$

To see this, note that from line 3 of Algorithm 4, we have:

$$\tilde{b}_{i+1}^{(k)} = f_{i+1:e(i+1)}\tilde{p}_{i+1:i+q+1}^{(k)} + \tilde{b}_{i+q+1}^{(k)}. \tag{7.26}$$

From the definition $\tilde{b}_j^{(k)} = (\mathbf{U}^{-1}\mathbf{c}_k)_j$ in (7.13), we deduce that $\tilde{b}_j^{(k)} = 0$ for $j > k$, from which (7.25) follows. We obtain:

$$\begin{aligned}
\tilde{p}_{i:k}^{(k)} &= \tilde{p}_{i:k}^{(k)} = \tilde{p}_{i+1:k}^{(k)} + \alpha_i\tilde{b}_{i+1}^{(k)} = \tilde{p}_{i+1:k}^{(k)}\big(1+\alpha_i f_{i+1:e(i+1)}\big) \\
&\overset{(*)}{=} \alpha_{k-1}\prod_{m=i+1}^{k-2}\big(\,1+\alpha_m f_{m+1:e(m+1)}\,\big)\big(1+\alpha_i f_{i+1:e(i+1)}\big) \\
&= \alpha_{k-1}\prod_{m=i}^{k-2}\big(\,1+\alpha_m f_{m+1:e(m+1)}\,\big),
\end{aligned}$$

where equality $(*)$ follows from the induction hypothesis.

- For $i = k-q-1, \ldots, i(t)$, we have $\min(k, i+q) = i+q$. From (7.26), we deduce:

$$\begin{aligned}
\tilde{p}_{i:\mu(i,k)+1}^{(k)} &= \tilde{p}_{i:i+q}^{(k)} = \alpha_i\tilde{b}_{i+1}^{(k)} - \alpha_{i+q}\tilde{b}_{i+q+1}^{(k)} + \tilde{p}_{i+1:i+q+1}^{(k)} \\
&= \alpha_i\Big(f_{i+1:e(i+1)}\tilde{p}_{i+1:i+q+1}^{(k)} + \tilde{b}_{i+q+1}^{(k)}\Big) - \alpha_{i+q}\tilde{b}_{i+q+1}^{(k)} + \tilde{p}_{i+1:i+q+1}^{(k)} \\
&\overset{(*)}{\approx} \tilde{p}_{i+1:i+q+1}^{(k)}\Big(1+\alpha_i f_{i+1:e(i+1)}\Big) \\
&= \alpha_{k-1}\prod_{m=i}^{k-2}\Big(\,1+\alpha_m f_{m+1:e(m+1)}\,\Big),
\end{aligned}$$

where in approximation $(*)$, we have used $\alpha_i \approx \alpha_{i+q}$. □

7.B Appendix: Proof of Lemma 3

For $i < n$,

$$\begin{aligned}
\mathbf{v}_i &= \sum_{k=i+1}^{n}\Big(\hat{b}_k - \hat{b}_{e(k)}\Big)\alpha_{k-1}\prod_{m=i}^{k-2}\big(1+\alpha_m f_{m+1:e(m+1)}\big)\boldsymbol{\sigma}_{k:e(k)} \\
&= \Big(\hat{b}_{i+1} - \hat{b}_{e(i+1)}\Big)\alpha_i\boldsymbol{\sigma}_{i+1:e(i+1)} + \big(1+\alpha_i f_{i+1:e(i+1)}\big)\times \\
&\qquad \left\{\sum_{k=i+2}^{n}\Big(\hat{b}_k - \hat{b}_{e(k)}\Big)\alpha_{k-1}\prod_{m=i+1}^{k-2}\big(1+\alpha_m f_{m+1:e(m+1)}\big)\boldsymbol{\sigma}_{k:e(k)}\right\} \\
&= \big(1+\alpha_i f_{i+1:e(i+1)}\big)\mathbf{v}_{i+1} + \alpha_i\Big(\hat{b}_{i+1} - \hat{b}_{e(i+1)}\Big)\sigma_{i+1:e(i+1)},
\end{aligned}$$

which was to be shown. □

Chapter 8

Conclusions

In this thesis, innovations on efficient pricing and risk-management of Bermudan-style interest rate derivatives are presented. The main pricing model for these derivatives is the LIBOR market model (see Brace et al. (1997), Jamshidian (1997) and Miltersen et al. (1997)). It allows for efficient calibration to volatility and correlation.

The most outstanding result of the thesis is the development of new market models, named *CMS and generic market models* (Chapter 7). We specify precisely when an arbitrary structure of forward rates is arbitrage-free at all possible (future) states of the model. Via matrix notation, we are able to transform CMS and generic pricing measures to spot and terminal measures, which enables a Monte Carlo implementation of the models. Moreover, we present an efficient algorithm to accurately approximate forward CMS rates over time steps during simulation in CMS market models. CMS and generic market models allow for efficient volatility calibration (i.e., the model parameter is the market implied volatility) of a whole new class of derivatives, such as fixed-maturity Bermudan swaptions and Bermudan CMS swaptions.

A breakthrough on pricing callable products (e.g., Bermudan swaptions) in market models can be found in Chapter 6. There, the least-squares Monte Carlo (MC) algorithm of Longstaff & Schwartz (2001) is studied for estimating the optimal exercise decision for American options with MC. A discontinuity occurs in the least-squares MC algorithm, whereby finite difference estimates of risk sensitivities are inefficient. We propose a modification of the least-squares MC algorithm, named *constant exercise decision method*. Hedge tests with Bermudan swaptions on USD data show that reduction of variance of profit and loss (P&L) is much greater and acceptable when the constant exercise decision method is used.

Chapter 6 contains many more results: First, hedge tests show that jointly delta and vega hedging outperforms delta hedging only. Second, tests show that correlation pricing impact on Bermudan swaptions is significant. It is shown that correlation can be accurately captured in both single-factor models (e.g., the Markov-functional model of

Hunt et al. (2000)) and multi-factor models (e.g., market models). Third, hedge tests show that the following do not significantly impact reduction of variance of P&L: correlation, number of factors, or, use of multi-factor models versus single-factor models. Fourth, tests show that the pricing impact of volatility smile can be much larger than the pricing impact of correlation.

As stated above, correlation still remains an important aspect of pricing derivatives, even though correlation impact on hedging is small and smile is more important (for the empirical findings in Chapter 6). Full-factor market models allow for straightforward calibration to correlation, in the sense that the model parameter is literally the real-world observed correlation value. For low-factor market models however, the situation is different. Here, any model attainable correlation matrix has a rank equal to the number of factors in the model, and this rank restriction usually does not hold for the given real-world correlation matrix. Therefore, we need to find the low-rank correlation matrix closest to the given matrix. This optimization problem is non-convex, and therefore hard to solve. The process of finding the nearest low-rank correlation matrix is called *rank reduction of the correlation matrix*. This thesis includes some of the forefront knowledge on this topic, via Chapters 3 and 4. Two completely different solution algorithms are presented, based on *majorization* and *geometric programming*. In extensive numerical tests, these two algorithms seem to outperform existing algorithms, in terms of computational speed. Both methods enjoy global convergence properties. Geometric Newton has a quadratic rate of convergence, and geometric conjugate gradient has m-steps quadratic convergence, where m is the dimension of the manifold. Moreover, we develop a method to instantly check whether a stationary point (i.e., a point with negligible gradient) is in fact a global minimum, which is quite an uncommon feature for a non-convex programming problem.

A discretization can be thought of as a translation of a continuous-time model to a numerical algorithm aimed to implement the model. For the LIBOR market model, a new and so-called *Brownian bridge* discretization is introduced in Chapter 5. The Brownian bridge is specifically designed for single or large time steps. For single time steps, Brownian bridge is least-squares optimal over all other discretizations (in a certain sense). This is confirmed in an extended version of the numerical LIBOR-in-arrears test of Hunter et al. (2001). Viewed as a multi step scheme, theoretical results show that Brownian bridge converges weakly with order one. Moreover, we show that a mild assumption on volatility, named *separability*, in combination with a single time step scheme, yields much more efficient pricing on a grid or recombining lattice, instead of Monte Carlo simulation.

An important result is given in Chapter 2. Empirical tests highlight the effect of various popular calibration choices on the quality of risk sensitivity estimates of Bermudan swaptions priced with the LIBOR market model. So-called *time-homogeneous* choices lead to poor and unstable estimates of risk, whereas the so-called *constant volatility* choice leads to stable and efficient estimates. The results are important to practitioners that need to

choose a calibration method for market models, with the aim to risk manage Bermudan swaptions and other interest rate derivatives.

Nederlandse samenvatting (Summary in Dutch)

Waarderingsmodellen voor Bermuda-stijl rente derivaten

Bermuda-stijl rente derivaten vormen een belangrijke klasse van opties. Veel bancaire en verzekeringsproducten, zoals hypotheken, vervroegd aflosbare obligaties, en levensverzekeringen, bevatten Bermuda rente opties, die een gevolg zijn van de mogelijkheid tot vervroegde terugbetaling of stopzetting van het contract. Het veel voorkomen van deze opties maakt duidelijk dat het belangrijk is, voor banken en verzekeraars, om de waarde en risico van deze producten op de juiste manier in te schatten. Het juist inschatten van het risico maakt het mogelijk om markt risico af te dekken met onderliggende en regelmatig verhandelde waardes en opties. *Waarderingsmodellen* moeten arbitrage-vrij zijn, en dienen consistent te zijn met (*gekalibreerd te zijn aan*) prijzen van actief verhandelde onderliggende opties. De dynamica van de modellen moet overeen komen met de geobserveerde dynamica van de rente-termijnstructuur, zoals bijvoorbeeld correlatie tussen rentestanden. Bovendien moeten waarderingsalgoritmes *efficiënt* zijn: Financiële beslissingen gebaseerd op derivaten waarderingsberekeningen worden veeleer binnen enkele seconden genomen, dan binnen uren of dagen. In recente jaren is een succesvolle klasse van modellen naar voren gekomen, genaamd *markt modellen*. Dit proefschrift, onder begeleiding van Antoon Pelsser en Ton Vorst, breidt de theorie van markt modellen uit, door: (*i*) een nieuwe, efficiënte en meer nauwkeurige benaderende waarderingstechniek te introduceren, (*ii*) twee nieuwe en snelle algoritmes voor correlatie-kalibratie te presenteren, (*iii*) nieuwe modellen te ontwikkelen die een efficiënte kalibratie toestaan voor een hele nieuwe klasse van derivaten, zoals vaste-looptijd Bermuda rente opties, en (*iv*) nieuwe empirische vergelijkingen te presenteren van bestaande kalibratie technieken en modellen, in termen van reductie van risico.

Bibliography

Abraham, R., Marsden, J. E. & Ratiu, T. (1988), *Manifolds, Tensor Analysis, and Applications*, Springer-Verlag, Berlin.

Al-Baali, M. (1985), 'Descent property and global convergence of the Fletcher-Reeves method with inexact line search', *IMA Journal of Numerical Analysis* **5**, 121–124.

Andersen, L. & Andreasen, J. (2000), 'Volatility skews and extensions of the LIBOR market model', *Applied Mathematical Finance* **7**(1), 1–32.

Andersen, L. & Andreasen, J. (2001), 'Factor dependence of bermudan swaptions: fact or fiction?', *Journal of Financial Economics* **62**(1), 3–37.

Apostol, T. M. (1967), *Calculus*, Vol. 1, 2 edn, John Wiley & Sons, Chichester.

Avellaneda, M. & Gamba, R. (2001), Conquering the Greeks in Monte Carlo: Efficient calculation of the market sensitivities and hedge-ratios of financial assets by direct numerical simulation, *in* 'Proceedings of the First Bachelier Congress', Paris.

Avellaneda, M., Holmes, R., Friedman, C. & Samperi, D. (1997), 'Calibration of volatility surfaces via relative-entropy minimization', *Applied Mathematical Finance* **4**(1), 37–64.

Avramidis, A. N. & Matzinger, H. (2004), 'Convergence of the stochastic mesh estimator for pricing Bermudan options', *Journal of Computational Finance* **7**(4), 73–91.

Baxter, M. W. & Rennie, A. J. O. (1996), *Financial calculus: An introduction to derivative pricing*, Cambridge University Press, Cambridge.

Bennett, M. N. & Kennedy, J. E. (2004), A comparison of Markov-functional and market models: The one-dimensional case, `www2.warwick.ac.uk/fac/sci/statistics/staff/research_students/mbennett/`.

Berridge, S. & Schumacher, J. M. (2003), 'An irregular grid method for high-dimensional free-boundary problems in finance', *Future Generation Computer Systems* **20**(3), 353–362.

Björk, T. (2004), *Arbitrage Theory in Continuous Time*, 2 edn, Oxford University Press, Oxford.

Björk, T., Landén, C. & Svensson, L. (2004), 'Finite-dimensional Markovian realizations for stochastic volatility forward-rate models', *Proceedings of the Royal Society* **460**(2041), 53–83. Series A.

Black, F. (1976), 'The pricing of commodity contracts', *Journal of Financial Economics* **3**(2), 167–179.

Black, F. & Karasinski, P. (1991), 'Bond and option pricing when short rates are lognormal', *Financial Analysts Journal* **47**(4), 52–59.

Black, F. & Scholes, M. (1973), 'The pricing of options corporate liabilities', *Journal of Political Economy* **81**(3), 637–654.

Black, F., Derman, E. & Toy, W. (1990), 'A one-factor model of interest rates and its applications to treasury and bond options', *Financial Analysts Journal* **46**(1), 33–39.

Borg, I. & Groenen, P. J. F. (1997), *Modern Multidimensional Scaling*, Springer-Verlag, Berlin.

Brace, A. & Womersley, R. S. (2000), Exact fit to the swaption volatility matrix using semidefinite programming, presented at the ICBI Global Derivatives Conference, Paris.

Brace, A., Dun, T. & Barton, G. (1998), Towards a central interest rate model, presented at the ICBI Global Derivatives Conference, Paris.

Brace, A., Gątarek, D. & Musiela, M. (1997), 'The market model of interest rate dynamics', *Mathematical Finance* **7**(2), 127–155.

Brennan, M. J. & Schwartz, E. S. (1979), 'A continuous time approach to the pricing of bonds', *Journal of Banking and Finance* **3**(2), 133–155.

Brigo, D. (2002), A note on correlation and rank reduction, `www.damianobrigo.it`.

Brigo, D. & Mercurio, F. (2001), *Interest Rate Models: Theory and Practice*, Springer-Verlag, Berlin.

Broadie, M. & Glasserman, P. (1996), 'Estimating security price derivatives using simulation', *Management Science* **42**(2), 269–285.

Broadie, M. & Glasserman, P. (2004), 'A stochastic mesh method for pricing high-dimensional American options', *Journal of Computational Finance* **7**(4), 35–72.

Cairns, A. J. G. (2004), *Interest Rate Models: An Introduction*, Princeton University Press, New Jersey.

Choy, B., Dun, T. & Schlögl, E. (2004), 'Correlating market models', *Risk Magazine* pp. 124–129. September.

Chu, M. T., Funderlic, R. E. & Plemmons, R. J. (2003), 'Structured low rank approximation', *Linear Algebra and its Applications* **366**, 157–172.

Cox, J. C. & Ross, S. A. (1976), 'The valuation of options for alternative stochastic processes', *Journal of Financial Economics* **3**(2), 145–166.

Cox, J. C., Ingersoll, J. E. & Ross, S. A. (1985), 'A theory of the term structure of interest rates', *Econometrica* **53**(2), 385–408.

Dai, Q. & Singleton, K. (2003), 'Term structure dynamics in theory and reality', *Review of Financial Studies* **16**(3), 631–678.

D'Aspremont, A. (2002), Calibration and Risk-Management Methods for the Libor Market Model Using Semidefinite Programming, PhD thesis, Ecole Polytechnique, Paris.

D'Aspremont, A. (2003), 'Interest rate model calibration using semidefinite programming', *Applied Mathematical Finance* **10**(3), 183–213.

Davies, P. I. & Higham, N. J. (2000), 'Numerically stable generation of correlation matrices and their factors', *BIT* **40**, 640–651.

De Jong, F., Driessen, J. & Pelsser, A. A. J. (2004), 'On the information in the interest rate term structure and option prices', *Review of Derivatives Research* **7**(2), 99–127.

De Leeuw, J. & Heiser, W. J. (1977), Convergence of correction-matrix algorithms for multidimensional scaling, *in* J. C. Lingoes, E. E. Roskam & I. Borg, eds, 'Geometric representations of relational data', Mathesis Press, Ann Arbor, MI, pp. 735–752.

Dedieu, J.-P., Priouret, P. & Malajovich, G. (2003), 'Newton's method on Riemannian manifolds: Covariant alpha-theory', *IMA Journal of Numerical Analysis* **23**(3), 395–419.

Depczynski, U. & Stöckler, J. (1998), A differential geometric approach to equidistributed knots on Riemannian manifolds, *in* C. K. Chui & L. L. Schumaker, eds, 'Approximation Theory IX, Theoretical Aspects', Vol. 1, Vanderbilt University Press, Nashville, TN, pp. 99–106.

do Carmo, M. P. (1992), *Riemannian Geometry*, 12 edn, Birkhäuser, Boston, MA.

Dolan, E. D. & Moré, J. J. (2002), 'Benchmarking optimization software with performance profiles', *Mathematical Programming, Series A* **91**(2), 201–213.

Dothan, L. U. (1978), 'On the term structure of interest rates', *Journal of Financial Economics* **6**(1), 59–69.

Driessen, J., Klaassen, P. & Melenberg, B. (2003), 'The performance of multi-factor term structure model for pricing and hedging caps and swaptions', *Journal of Financial abd Quantitative Analysis* **38**(3), 635–672.

Duistermaat, J. J. & Kolk, J. A. C. (2000), *Lie Groups*, Springer-Verlag, Berlin.

Dykstra, R. L. (1983), 'An algorithm for restricted least squares regression', *Journal of the American Statistical Association* **87**(384), 837–842.

Edelman, A. & Lippert, R. (2000), Nonlinear eigenvalue problems with orthogonality constraints (section 8.3), *in* Z. Bai, J. Demmel, J. Dongarra, A. Ruhe & H. van der Vorst, eds, 'Templates for the Solution of Algebraic Eigenvalue Problems: A Practical Guide', SIAM, Philidelphia.

Edelman, A., Arias, T. A. & Smith, S. T. (1999), 'The geometry of algorithms with orthogonality constraints', *SIAM Journal of Matrix Analysis and its Applications* **20**(2), 303–353.

Fan, R., Gupta, A. & Ritchken, P. (2003), 'Hedging in the possible presence of unspanned stochastic volatility: Evidence from swaption markets', *Journal of Finance* **58**(5), 2219–2248.

Fletcher, R. & Reeves, C. M. (1964), 'Function minimization by conjugate gradients', *Computer Journal* **7**(2), 149–154.

Flury, B. (1988), *Common Principal Components and Related Multivariate Models*, J. Wiley & Sons, New York.

Fournié, E., Lasry, J.-M., Lebuchoux, J., Lions, P.-L. & Touzi, N. (1999), 'Applications of Malliavin calculus to Monte Carlo methods in finance', *Finance and Stochastics* **3**(4), 391–412.

Galluccio, S. & Hunter, C. J. (2004), 'The co-initial swap market model', *Economic Notes* **33**(2), 209–232.

Galluccio, S., Huang, Z., Ly, J.-M. & Scaillet, O. (2004), Theory and calibration of swap market models, Working Paper, June Version.

Gilbert, J.-C. & Nocedal, J. (1992), 'Global convergence properties of conjugate gradient methods for optimization', *SIAM Journal on Optimization* **2**(1), 21–42.

Glasserman, P. (2004), *Monte Carlo Methods in Financial Engineering*, Springer-Verlag, Berlin.

Glasserman, P. & Merener, N. (2003*a*), 'Cap and swaption approximations in LIBOR market models with jumps', *Journal of Computational Finance* **7**(1), 1–36.

Glasserman, P. & Merener, N. (2003*b*), 'Numerical solution of jump-diffusion LIBOR market models', *Finance and Stochastics* **7**(1), 1–27.

Glasserman, P. & Merener, N. (2004), 'Convergence of a discretization scheme for jump-diffusion processes with state-dependent intensities', *Proceedings of the Royal Society* **460**(2041), 111–127. Series A.

Glasserman, P. & Zhao, X. (1999), 'Fast Greeks by simulation in forward LIBOR models', *Journal of Computational Finance* **3**(1), 5–39.

Glasserman, P. & Zhao, X. (2000), 'Arbitrage-free discretization of lognormal forward LIBOR and swap rate models', *Finance and Stochastics* **4**(1), 35–68.

Glunt, W., Hayden, T. L., Hong, S. & Wells, J. (1990), 'An alternating projection algorithm for computing the nearest Euclidean distance matrix', *SIAM Journal of Matrix Analysis and its Applications* **11**(4), 589–600.

Golub, G. H. & van Loan, C. F. (1996), *Matrix Computations*, 3 edn, John Hopkins University Press, Baltimore, MD.

Grubišić, I. (2002), Interest rate theory: BGM model, Master's thesis, Mathematical Institute, Leiden University. `www.math.uu.nl/people/grubisic`.

Grubišić, I. & Pietersz, R. (2005), Efficient rank reduction of correlation matrices, `www.few.eur.nl/few/people/pietersz`.

Han, S.-P. (1988), 'A successive projection method', *Mathematical Programming* **40**, 1–14.

Hayden, T. L. & Wells, J. (1988), 'Approximation by matrices positive semidefinite on a subspace', *Linear Algebra and its Applications* **109**, 115–130.

Heath, D., Jarrow, R. & Morton, A. (1992), 'Bond pricing and the term structure of interest rates: A new methodology for contingent claims valuation', *Econometrica* **60**(1), 77–105.

Heiser, W. J. (1995), Convergent computation by iterative majorization: Theory and applications in multidimensional data analysis, *in* W. J. Krzanowski, ed., 'Recent Advances in Descriptive Multivariate Analysis', Oxford University Press, Oxford, pp. 157–189.

Higham, N. J. (2002), 'Computing the nearest correlation matrix–a problem from finance', *IMA Journal of Numerical Analysis* **22**(3), 329–343.

Ho, T. S. Y. & Lee, S.-B. (1986), 'Term structure movements and pricing interest rate contingent claims', *Journal of Finance* **41**(5), 1011–1029.

Horn, R. A. & Johnson, C. R. (1990), *Matrix Analysis*, Cambridge University Press, Cambridge.

Hughston, L. P. & Rafailidis, A. (2005), 'A chaotic approach to interest rate modelling', *Finance and Stochastics* **9**(1), 43–65.

Hull, J. C. (2000), *Options, Futures, and Other Derivatives*, 4 edn, Prentice-Hall, London.

Hull, J. C. & White, A. (1990), 'Pricing interest-rate-derivative securities', *Review of Financial Studies* **3**(4), 573–592.

Hull, J. C. & White, A. (2000), 'Forward rate volatilities, swap rate volatilities, and implementation of the LIBOR market model', *Journal of Fixed Income* **10**(2), 46–62.

Hunt, P. & Kennedy, J. E. (2000), *Financial Derivatives in Theory and Practice*, John Wiley & Sons, Chichester.

Hunt, P., Kennedy, J. E. & Pelsser, A. A. J. (2000), 'Markov-functional interest rate models', *Finance and Stochastics* **4**(4), 391–408.

Hunter, C. J., Jäckel, P. & Joshi, M. S. (2001), 'Getting the drift', *Risk Magazine*. July.

Jäckel, P. (2002), *Monte Carlo Methods in Finance*, J. Wiley & Sons, Chichester.

Jäckel, P. & Rebonato, R. (2003), 'The link between caplet and swaption volatilities in a Brace-Gątarek-Musiela/Jamshidian framework: approximate solutions and empirical evidence', *Journal of Computational Finance* **6**(4), 41–59.

Jamshidian, F. (1989), 'An exact bond option formula', *Journal of Finance* **44**(1), 205–209.

Jamshidian, F. (1997), 'LIBOR and swap market models and measures', *Finance and Stochastics* **1**(4), 293–330.

Jamshidian, F. (2003), Minimax optimality of Bermudan and American claims and their Monte-Carlo upper bound approximation, NIB Capital Bank, working paper.

Joshi, M. S. (2003*a*), *The Concepts and Practice of Mathematical Finance*, Cambridge University Press, Cambridge.

Joshi, M. S. (2003*b*), 'Rapid computation of drifts in a reduced factor LIBOR market model', *Wilmott Magazine* **5**, 84–85.

Joshi, M. S. & Theis, J. (2002), 'Bounding Bermudan swaptions in a swap-rate market model', *Quantitative Finance* **2**(5), 370–377.

Karatzas, I. & Shreve, S. E. (1991), *Brownian Motion and Stochastic Calculus*, 2 edn, Springer-Verlag, Berlin.

Kerkhof, J. & Pelsser, A. A. J. (2002), 'Observational equivalence of discrete string models and market models', *Journal of Derivatives* **10**(1), 55–61.

Kiers, H. A. L. (2002), 'Setting up alternating least squares and iterative majorization algorithms for solving various matrix optimization problems', *Computational Statistics and Data Analysis* **41**, 157–170.

Kiers, H. A. L. & Groenen, P. J. F. (1996), 'A monontonically convergent algorithm for orthogonal congruence rotation', *Psychometrika* **61**, 375–389.

Kloeden, P. E. & Platen, E. (1999), *Numerical Solution of Stochastic Differential Equations*, Vol. 23 of *Applications of Mathematics*, Springer-Verlag, Berlin.

Kurbanmuradov, O., Sabelfeld, K. & Schoenmakers, J. (2002), 'Lognormal approximations to LIBOR market models', *Journal of Computational Finance* **6**(1), 69–100.

Levenberg, K. (1944), 'A method for the solution of certain non-linear problems in least squares', *Quarterly of Applied Mathematics* **2**, 164–168.

Longstaff, F. A. & Schwartz, E. S. (1992), 'Interest rate volatility and the term structure: A two-factor general equilibrium model', *Journal of Finance* **47**(4), 1259–1282.

Longstaff, F. A. & Schwartz, E. S. (2001), 'Valuing American options by simulation: A simple least-squares approach', *Review of Financial Studies* **14**(1), 113–147.

Longstaff, F. A., Santa-Clara, P. & Schwartz, E. S. (2001), 'Throwing away a billion dollars: the cost of suboptimal exercise strategies in the swaptions market', *Journal of Financial Economics* **62**(1), 39–66.

Marquardt, D. W. (1963), 'An algorithm for least-squares estimation of nonlinear parameters', *Journal of the Society for Industrial and Applied Mathematics* **11**(2), 431–441.

Merton, R. C. (1973), 'Theory of rational option pricing', *Bell Journal of Economics and Management Science* **4**(1), 141–183.

Merton, R. C. (1976), 'Option pricing when underlying stock returns are discontinuous', *Journal of Financial Economics* **3**(1–2), 125–144.

Miltersen, K. R., Sandmann, K. & Sondermann, D. (1997), 'Closed form solutions for term structure derivatives with log-normal interest rates', *Journal of Finance* **52**(1), 409–430.

Morini, M. & Webber, N. (2004), An EZI method to reduce the rank of a correlation matrix, `www.cass.city.ac.facfin/facultypages/nwebber/`.

Munkres, J. R. (1975), *Topology*, Prentice-Hall, London.

Musiela, M. & Rutkowski, M. (1997), 'Continuous-time term structure models: Forward measure approach', *Finance and Stochastics* **1**(4), 261–291.

Øksendal, B. K. (1998), *Stochastic Differential Equations*, 5 edn, Springer-Verlag, Berlin.

Ostrom, D. (1998), 'Japanese interest rates enter negative territory', *Japan Economic Institute Report* (43B), 4–6. `www.jei.org/archive/`.

Ostrovsky, D. (2002), A Markov-functional model consistent with caplet and swaption smiles, Yale University Working Paper.

Pearson, N. D. & Sun, T.-S. (1994), 'Exploiting the conditional density in estimating the term structure: An application to the Cox, Ingersoll, and Ross model', *Journal of Finance* **49**(4), 1279–1304.

Pelsser, A. A. J. (2000), *Efficient Methods for Valuing Interest Rate Derivatives*, Springer-Verlag, Berlin.

Pietersz, R. (2001), The LIBOR market model, Master's thesis, Mathematical Institute, Leiden University. `www.math.leidenuniv.nl/scripties/pietersz.pdf`.

Pietersz, R. & Groenen, P. J. F. (2004*a*), 'A major LIBOR fit', *Risk Magazine* p. 102. December issue.

Pietersz, R. & Groenen, P. J. F. (2004*b*), 'Rank reduction of correlation matrices by majorization', *Quantitative Finance* **4**(6), 649–662.

Pietersz, R. & Pelsser, A. A. J. (2004*a*), 'Risk-managing Bermudan swaptions in a LIBOR model', *Journal of Derivatives* **11**(3), 51–62.

Pietersz, R. & Pelsser, A. A. J. (2004*b*), 'Swap vega in BGM: pitfalls and alternatives', *Risk Magazine* pp. 91–93. March issue.

Pietersz, R. & Pelsser, A. A. J. (2005*a*), A comparison of single factor markov-functional and multi factor market models, SSRN Working Paper.

Pietersz, R. & Pelsser, A. A. J. (2005*b*), Swap vega in BGM: pitfalls and alternatives, *in* N. Dunbar, ed., 'Derivatives Trading and Option Pricing', Risk Books, London, UK, pp. 277–285.

Pietersz, R. & van Regenmortel, M. (2005), Generic market models, SSRN Working Paper.

Pietersz, R., Pelsser, A. A. J. & van Regenmortel, M. (2004), 'Fast drift-approximated pricing in the BGM model', *Journal of Computational Finance* **8**(1), 93–124.

Pietersz, R., Pelsser, A. A. J. & van Regenmortel, M. (2005), 'Bridging Brownian LIBOR', *Wilmott Magazine* **18**, 98–103.

Piterbarg, V. V. (2004), 'TARNs: Models, valuation, risk sensitivities', *Wilmott Magazine* **14**, 62–71.

Polak, E. & Ribière, G. (1969), 'Note sur la convergence de méthodes de directions conjuguées', *Revue Française d'Informatique et de Recherche Opérationnelle* **16**, 35–43.

Rapisarda, F., Brigo, D. & Mercurio, F. (2002), Parametrizing correlations: A geometric interpretation, Banca IMI Working Paper, `www.fabiomercurio.it`.

Rebonato, R. (1998), *Interest Rate Option Models*, 2 edn, J. Wiley & Sons, Chichester.

Rebonato, R. (1999*a*), 'Calibrating the BGM model', pp. 74–79. Risk Magazine.

Rebonato, R. (1999*b*), 'On the simultaneous calibration of multifactor lognormal interest rate models to Black volatilities and to the correlation matrix', *Journal of Computational Finance* **2**(4), 5–27.

Rebonato, R. (1999*c*), *Volatility and Correlation in the Pricing of Equity, FX and Interest-Rate Options*, J. Wiley & Sons, Chichester.

Rebonato, R. (2001), Accurate and optimal calibration to co-terminal European swaptions in a FRA-based BGM framework, Royal Bank of Scotland Working Paper, London.

Rebonato, R. (2002), *Modern Pricing of Interest-Rate Derivatives*, Princeton University Press, New Jersey.

Rebonato, R. (2004*a*), 'Interest-rate term-structure pricing models: a review', *Proceedings of the Royal Society London* **460**(2043), 667–728. Series A.

Rebonato, R. (2004*b*), *Volatility and Correlation: The Perfect Hedger and the Fox*, 2 edn, J. Wiley & Sons, Chichester, UK.

Ritchken, P. & Sankarasubramanian, L. (1995), 'Volatility structures of the forward rates and the dynamics of the term structure', *Mathematical Finance* **5**(1), 55–72.

Rogers, L. C. G. (2002), 'Monte Carlo valuation of American options', *Mathematical Finance* **12**(3), 271–286.

Rubinstein, M. (1983), 'Displaced diffusion option pricing', *Journal of Finance* **38**(1), 213–217.

Santa-Clara, P. & Sornette, D. (2001), 'The dynamics of the forward interest rate curve with stochastic string shocks', *Review of Financial Studies* **14**(1), 149–185.

Schlögl, E. (2002), 'A multicurrency extension of the lognormal interest rate market models', *Finance and Stochastics* **6**(2), 173–196.

Sharpe, W. F. (1964), 'Capital asset prices: A theory of market equilibrium under conditions of risk', *Journal of Finance* **19**(3), 425–442.

Sidenius, J. (2000), 'LIBOR market models in practice', *Journal of Computational Finance* **3**(3), 5–26.

Smith, S. T. (1993), Geometric Optimization Methods for Adaptive Filtering, PhD thesis, Harvard University, Cambridge, MA.

Suffridge, T. J. & Hayden, T. L. (1993), 'Approximation by a Hermitian positive semidefinite Toeplitz matrix', *SIAM Journal of Matrix Analysis and its Applications* **14**(3), 721–734.

Valdez, S. (1997), *An Introduction to Global Financial Markets*, 2 edn, MacMillan Press, London.

Vasicek, O. (1977), 'An equilibrium characterization of the term structure', *Journal of Financial Economics* **5**(2), 177–188.

Weigel, P. (2004), 'Optimal calibration of LIBOR market models to correlations', *Journal of Derivatives* **12**(3).

Williams, D. (1991), *Probability with Martingales*, Cambridge University Press, Cambridge.

Wilmott, P. (1998), *Derivatives: The Theory and Practice of Financial Engineering*, John Wiley & Sons, Chichester.

Wu, L. (2003), 'Fast at-the-money calibration of the LIBOR market model using Lagrange multipliers', *Journal of Computational Finance* **6**(2), 39–77.

Zangwill, W. I. (1969), 'Convergence conditions for nonlinear programming algorithms', *Management Science (Theory Series)* **16**(1), 1–13.

Zhang, Z. & Wu, L. (2003), 'Optimal low-rank approximation to a correlation matrix', *Linear Algebra and its Applications* **364**, 161–187.

Zoutendijk, G. (1970), Nonlinear programming, computational methods, *in* J. Abadie, ed., 'Integer and nonlinear programming', pp. 37–86.

Author index

Curriculum Vitae

Raoul Pietersz was born on 12 June 1978 in Rotterdam, The Netherlands. In 2000, he obtained a Certificate of Advanced Studies in Mathematics (Mathematical Tripos Part III), with distinction, from the University of Cambridge. Over the academic year 1999-2000, he was awarded a title of Cambridge European Trust Scholar, and a retrospective title of Scholar at Peterhouse, Cambridge. In the summer of 2000, he completed internships at UBS Warburg and Dresdner Kleinwort Wasserstein, in London. In 2001, he obtained a first class M.Sc. degree in Mathematics from Leiden University. His Master's thesis entitled "The LIBOR market model" was completed during an internship at ABN AMRO Bank, in Amsterdam. Over the period 1997-2001, he was awarded the Shell International Scholarship for undergraduate studies. His Ph.D. research, under supervision of Antoon Pelsser and Ton Vorst, focuses on the efficient valuation and risk management of interest rate derivatives. He has published articles in The Journal of Computational Finance, The Journal of Derivatives, Quantitative Finance, Risk Magazine and Wilmott Magazine. He has presented his research at various international conferences. His teaching experience includes lecturing taught Master courses on derivatives at the Rotterdam School of Management. Since the start of the Ph.D. period, he has held a part-time position at ABN AMRO Bank, initially at Quantitative Risk Analytics, Risk Management. Since July 2004, he is a Senior Derivatives Researcher, developing front-office pricing models for interest rate derivatives, at Product Development Group, Quantitative Analytics, as part of Structured Derivatives.

Erasmus Research Institute of Management

ERIM Ph.D. Series Resesearch in Management

Appelman, J.H., Governance of Global Interorganizational Tourism Networks: Changing Forms of Co-ordination between the Travel Agency and Aviation Sector, Promotors: Prof. dr. F.M. Go & Prof. dr. B. Nooteboom
EPS-2004-036-MKT, ISBN: 90-5892-060-7, http://hdl.handle.net/1765/1199

Assen, M.F. van, Empirical Studies in Discrete Parts Manufacturing Management, Promotors: Prof. dr. S.L. van de Velde & Prof. dr. W.H.M. Zijm
EPS-2005-056-LIS, ISBN: 90-5892-085-2, http://hdl.handle.net/1765/6767

Berens, G., Corporate Branding: The Development of Corporate Associations and their Influence on Stakeholder Reactions, Promotor: Prof. dr. C. B. M. van Riel
EPS-2004-039-ORG, ISBN: 90-5892-065-8, http://hdl.handle.net/1765/1273

Berghe, D.A.F., Working Across Borders: Multinational Enterprises and the Internationalization of Employment, Promotors: Prof. dr. R.J.M. van Tulder & Prof. dr. E.J.J. Schenk
EPS-2003-029-ORG, ISBN: 90-5892-05-34, http://hdl.handle.net/1765/1041

Bijman, W.J.J., Essays on Agricultural Co-operatives: Governance Structure in Fruit and Vegetable Chains, Promotor: Prof. dr. G.W.J. Hendrikse
EPS-2002-015-ORG, ISBN: 90-5892-024-0, http://hdl.handle.net/1765/867

Boer, N.I., Knowledge Sharing within Organizations: A situated and relational Perspective, Promotor: Prof. dr. K. Kumar
EPS-2005-060-LIS, ISBN: 90-5892-086-0, http://hdl.handle.net/1765/6770

Boer, C.A., Distributed Simulation in Industry, Promotors: Prof. dr. A. de Bruin & Prof. dr. eng. A. Verbraeck
EPS-2005-065-LIS, ISBN: 90-5892-093-3, http://hdl.handle.net/1765/6925

Brito, M.P. de, Managing Reverse Logistics or Reversing Logistics Management?, Promotors: Prof. dr. eng. R. Dekker & Prof. dr. M. B. M. de Koster
EPS-2004-035-LIS, ISBN: 90-5892-058-5, http://hdl.handle.net/1765/1132

Brohm, R., Polycentric Order in Organizations: a dialogue between Michael Polanyi and IT-

consultants on knowledge, morality, and organization, Promotors: Prof. dr. G.W.J. Hendrikse & Prof. dr. H.K. Letiche
EPS-2004-063-ORG, ISBN: 90-5892-095-X, http://hdl.handle.net/1765/6911

Campbell, R.A.J., Rethinking Risk in International Financial Markets, Promotor: Prof. dr. C.G. Koedijk
EPS-2001-005-F&A, ISBN: 90-5892-008-9, http://hdl.handle.net/1765/306

Chen, Y., Labour Flexibility in China's Companies: An Empirical Study, Promotors: Prof. dr. A. Buitendam & Prof. dr. B. Krug
EPS-2001-006-ORG, ISBN: 90-5892-012-7, http://hdl.handle.net/1765/307

Daniševská, P., Empirical Studies on Financial Intermediation and Corporate Policies, Promotor: Prof. dr. C.G. Koedijk
EPS-2004-044-F&A, ISBN: 90-5892-070-4, http://hdl.handle.net/1765/1518

Delporte-Vermeiren, D.J.E., Improving the Flexibility and Profitability of ICT-enabled Business Networks: An Assessment Method and Tool, Promotors: Prof.mr. dr. P.H.M. Vervest & Prof. dr. eng. H.W.G.M. van Heck
EPS-2003-020-LIS, ISBN: 90-5892-040-2, http://hdl.handle.net/1765/359

Dijksterhuis, M., Organizational Dynamics of Cognition and Action in the Changing Dutch and US Banking Industries, Promotors: Prof. dr. eng. F.A.J. van den Bosch & Prof. dr. H.W. Volberda
EPS-2003-026-STR, ISBN: 90-5892-048-8, http://hdl.handle.net/1765/1037

Fenema, P.C. van, Coordination and Control of Globally Distributed Software Projects, Promotor: Prof. dr. K. Kumar
EPS-2002-019-LIS, ISBN: 90-5892-030-5, http://hdl.handle.net/1765/360

Fleischmann, M., Quantitative Models for Reverse Logistics, Promoters: Prof. dr. eng. J.A.E.E. van Nunen & Prof. dr. eng. R. Dekker
EPS-2000-002-LIS, ISBN: 35-4041-711-7, http://hdl.handle.net/1765/1044

Flier, B., Strategic Renewal of European Financial Incumbents: Coevolution of Environmental Selection, Institutional Effects, and Managerial Intentionality, Promotors: Prof. dr. eng. F.A.J. van den Bosch & Prof. dr. H.W. Volberda
EPS-2003-033-STR, ISBN: 90-5892-055-0, http://hdl.handle.net/1765/1071

Fok, D., Advanced Econometric Marketing Models, Promotor: Prof. dr. P.H.B.F. Franses
EPS-2003-027-MKT, ISBN: 90-5892-049-6, http://hdl.handle.net/1765/1035

Ganzaroli , A., Creating Trust between Local and Global Systems, Promotors: Prof. dr. K. Kumar & Prof. dr. R.M. Lee
EPS-2002-018-LIS, ISBN: 90-5892-031-3, http://hdl.handle.net/1765/361

Gilsing, V.A., Exploration, Exploitation and Co-evolution in Innovation Networks, Promotors: Prof. dr. B. Nooteboom & Prof. dr. J.P.M. Groenewegen
EPS-2003-032-ORG, ISBN 90-5892-05-42, http://hdl.handle.net/1765/1040

Graaf, G. de, Tractable Morality: Customer Discourses of Bankers, Veterinarians and Charity Workers, Promotors: Prof. dr. F. Leijnse & Prof. dr. T. van Willigenburg
EPS-2003-031-ORG, ISBN: 90-5892-051-8, http://hdl.handle.net/1765/1038

Hartigh, E. den, Increasing Returns and Firm Performance: An Empirical Study, Promotor: Prof. dr. H.R. Commandeur
EPS-2005-067-STR, ISBN: 90-5892-098-4, http://hdl.handle.net/1765

Hermans. J.M., ICT in Information Services, Use and deployment of the Dutch securities trade, 1860-1970. Promotor: Prof. dr. drs. F.H.A. Janszen
EPS-2004-046-ORG, ISBN 90-5892-072-0, http://hdl.handle.net/1765/1793

Heugens, P.M.A.R., Strategic Issues Management: Implications for Corporate Performance, Promotors: Prof. dr. eng. F.A.J. van den Bosch & Prof. dr. C.B.M. van Riel
EPS-2001-007-STR, ISBN: 90-5892-009-7, http://hdl.handle.net/1765/358

Hooghiemstra, R., The Construction of Reality, Promotors: Prof. dr. L.G. van der Tas RA & Prof. dr. A.Th.H. Pruyn
EPS-2003-025-F&A, ISBN: 90-5892-047-X, http://hdl.handle.net/1765/871

Jansen, J.J.P., Ambidextrous Organizations, Promotors: Prof. dr. eng. F.A.J. Van den Bosch & Prof. dr. H.W. Volberda
EPS-2005-055-STR, ISBN 90-5892-081-X

Jong, C. de, Dealing with Derivatives: Studies on the Role, Informational Content and Pricing of Financial Derivatives, Promotor: Prof. dr. C.G. Koedijk
EPS-2003-023-F&A, ISBN: 90-5892-043-7, http://hdl.handle.net/1765/1043

Keizer, A.B., The Changing Logic of Japanese Employment Practices: A Firm-Level Analysis of Four Industries Promotors: Prof. dr. J.A. Stam & Prof. dr. J.P.M. Groenewegen
EPS-2005-057-ORG, ISBN: 90-5892-087-9, http://hdl.handle.net/1765/6667

Kippers, J., Empirical Studies on Cash Payments, Promotor: Prof. dr. Ph.H.B.F. Franses

EPS-2004-043-F&A, ISBN 90-5892-069-0, http://hdl.handle.net/1765/1520

Koppius, O.R., Information Architecture and Electronic Market Performance, Promotors: Prof. dr. P.H.M. Vervest & Prof. dr. eng. H.W.G.M. van Heck
EPS-2002-013-LIS, ISBN: 90-5892-023-2, http://hdl.handle.net/1765/921

Kotlarsky, J., Management of Globally Distributed Component-Based Software Development Projects, Promotor: Prof. dr. K. Kumar
EPS-2005-059-LIS, ISBN: 90-5892-088-7, http://hdl.handle.net/1765/6772

Kuilman, J., The re-emergence of foreign banks in Shanghai: An ecological analysis, Promotor: Prof. dr. B. Krug
EPS-2005-066-ORG, ISBN: 90-5892-096-8, http://hdl.handle.net/1765/6926

Langen, P.W. de, The Performance of Seaport Clusters: A Framework to Analyze Cluster Performance and an Application to the Seaport Clusters of Durban, Rotterdam and the Lower Mississippi, Promotors: Prof. dr. B. Nooteboom & Prof. drs. H.W.H. Welters
EPS-2004-034-LIS, ISBN: 90-5892-056-9, http://hdl.handle.net/1765/1133

Le Anh, T., Intelligent Control of Vehicle-Based Internal Transport Systems, Promotors: Prof. dr. M.B.M. de Koster & Prof. dr. eng. R. Dekker
EPS-2005-051-LIS, ISBN 90-5892-079-8, http://hdl.handle.net/1765/6554

Le-Duc, T., Design and control of efficient order picking processes, Promotor: Prof. dr. M.B.M. de Koster
EPS-2005-064-LIS, ISBN 90-5892-094-1, http://hdl.handle.net/1765/6910

Liang, G., New Competition: Foreign Direct Investment And Industrial Development In China, Promotor: Prof. dr. R.J.M. van Tulder
EPS-2004-047-ORG, ISBN 90-5892-073-9, http://hdl.handle.net/1765/1795

Loef, J., Incongruity between Ads and Consumer Expectations of Advertising, Promotors: Prof. dr. W.F. van Raaij & Prof. dr. G. Antonides
EPS-2002-017-MKT, ISBN: 90-5892-028-3, http://hdl.handle.net/1765/869

Maeseneire, W., de, Essays on Firm Valuation and Value Appropriation, Promotor: Prof. dr. J.T.J. Smit
EPS-2005-053-F&A, ISBN 90-5892-082-8

Mandele, L.M., van der, Leadership and the Inflection Point: A Longitudinal Perspective, Promotors: Prof. dr. H.W. Volberda, Prof. dr. H.R. Commandeur

EPS-2004-042-STR, ISBN 90-5892-067-4, http://hdl.handle.net/1765/1302

Meer, J.R. van der, Operational Control of Internal Transport, Promotors: Prof. dr. M.B.M. de Koster & Prof. dr. eng. R. Dekker
EPS-2000-001-LIS, ISBN: 90-5892-004-6, http://hdl.handle.net/1765/859

Miltenburg, P.R., Effects of Modular Sourcing on Manufacturing Flexibility in the Automotive Industry: A Study among German OEMs, Promotors: Prof. dr. J. Paauwe & Prof. dr. H.R. Commandeur
EPS-2003-030-ORG, ISBN 90-5892-052-6, http://hdl.handle.net/1765/1039

Moerman, G.A., Empirical Asset Pricing and Banking in the Euro Area, Promotors: Prof. dr. C.G. Koedijk
EPS-2005-058-F&A, ISBN: 90-5892-090-9, http://hdl.handle.net/1765/6666

Mol, M.M., Outsourcing, Supplier-relations and Internationalisation: Global Source Strategy as a Chinese Puzzle, Promotor: Prof. dr. R.J.M. van Tulder
EPS-2001-010-ORG, ISBN: 90-5892-014-3, http://hdl.handle.net/1765/355

Mulder, A., Government Dilemmas in the Private Provision of Public Goods, Promotor: Prof. dr. R.J.M. van Tulder
EPS-2004-045-ORG, ISBN: 90-5892-071-2, http://hdl.handle.net/1765

Muller, A.R., The Rise of Regionalism: Core Company Strategies Under The Second Wave of Integration, Promotor: Prof. dr. R.J.M. van Tulder
EPS-2004-038-ORG, ISBN 90-5892-062-3, http://hdl.handle.net/1765/1272

Oosterhout, J. van, The Quest for Legitimacy: On Authority and Responsibility in Governance, Promotors: Prof. dr. T. van Willigenburg & Prof.mr. H.R. van Gunsteren
EPS-2002-012-ORG, ISBN: 90-5892-022-4, http://hdl.handle.net/1765/362

Pak, K., Revenue Management: New Features and Models, Promotor: Prof. dr. eng. R. Dekker
EPS-2005-061-LIS, ISBN: 90-5892-092-5

Peeters, L.W.P., Cyclic Railway Timetable Optimization, Promotors: Prof. dr. L.G. Kroon & Prof. dr. eng. J.A.E.E. van Nunen
EPS-2003-022-LIS, ISBN: 90-5892-042-9, http://hdl.handle.net/1765/429

Popova. V., Knowledge Discovery and Monotonicity, Promotor: Prof. dr. A. de Bruin
EPS-2004-037-LIS, ISBN: 90-5892-061-5, http://hdl.handle.net/1765/1201

Pouchkarev, I., Performance Evaluation of Constrained Portfolios, Promotors: Prof. dr. J. Spronk & Dr. W.G.P.M. Hallerbach
EPS-2005-052-F&A, ISBN: 90-5892-083-6, http://hdl.handle.net/1765/6731

Puvanasvari Ratnasingam, P., Interorganizational Trust in Business to Business E-Commerce, Promotors: Prof. dr. K. Kumar & Prof. dr. H.G. van Dissel
EPS-2001-009-LIS, ISBN: 90-5892-017-8, http://hdl.handle.net/1765/356

Romero Morales, D., Optimization Problems in Supply Chain Management, Promotors: Prof. dr. eng. J.A.E.E. van Nunen & Dr. H.E. Romeijn
EPS-2000-003-LIS, ISBN: 90-9014078-6, http://hdl.handle.net/1765/865

Roodbergen , K.J., Layout and Routing Methods for Warehouses, Promotors: Prof. dr. M.B.M. de Koster & Prof. dr. eng. J.A.E.E. van Nunen
EPS-2001-004-LIS, ISBN: 90-5892-005-4, http://hdl.handle.net/1765/861

Schweizer, T.S., An Individual Psychology of Novelty-Seeking, Creativity and Innovation, Promotor: Prof. dr. R.J.M. van Tulder
EPS-2004-048-ORG, ISBN: 90-5892-07-71, http://hdl.handle.net/1765/1818

Six, F.E., Trust and Trouble: Building Interpersonal Trust Within Organizations, Promotors: Prof. dr. B. Nooteboom & Prof. dr. A.M. Sorge
EPS-2004-040-ORG, ISBN: 90-5892-064-X, http://hdl.handle.net/1765/1271

Slager, A.M.H., Banking across Borders, Promotors: Prof. dr. D.M.N. van Wensveen & Prof. dr. R.J.M. van Tulder
EPS-2004-041-ORG, ISBN: 90-5892-066-6, http://hdl.handle.net/1765/1301

Speklé, R.F., Beyond Generics: A closer look at Hybrid and Hierarchical Governance, Promotor: Prof. dr. M.A. van Hoepen RA
EPS-2001-008-F&A, ISBN: 90-5892-011-9, http://hdl.handle.net/1765/357

Teunter, L.H., Analysis of Sales Promotion Effects on Household Purchase Behavior, Promotors: Prof. dr. eng. B. Wierenga & Prof. dr. T. Kloek
EPS-2002-016-ORG, ISBN: 90-5892-029-1, http://hdl.handle.net/1765/868

Valck, K. de, Virtual Communities of Consumption: Networks of Consumer Knowledge and Companionship, Promotors: Prof. dr. eng. G.H. van Bruggen, & Prof. dr. eng. B. Wierenga
EPS-2005-050-MKT, ISBN: 90-5892-078-X, http://hdl.handle.net/1765/6663

Verheul, I., Is there a (fe)male approach? Understanding gender differences in entrepreneur-

ship, Prof. dr. A.R. Thurik
EPS-2005-054-ORG, ISBN: 90-5892-080-1, http://hdl.handle.net/1765/2005

Vis, I.F.A., Planning and Control Concepts for Material Handling Systems, Promotors: Prof. dr. M.B.M. de Koster & Prof. dr. eng. R. Dekker
EPS-2002-014-LIS, ISBN: 90-5892-021-6, http://hdl.handle.net/1765/866

Vliet, P. van, Downside Risk and Empirical Asset Pricing, Promotor: Prof. dr. G.T. Post
EPS-2004-049-F&A ISBN: 90-5892-07-55, http://hdl.handle.net/1765/1819

Vromans, M.J.C.M., Reliability of Railway Systems, Promotors: Prof. dr. L.G. Kroon & Prof. dr. eng. R. Dekker
EPS-2005-062-LIS, ISBN: 90-5892-089-5, http://hdl.handle.net/1765/6773

Waal, T. de, Processing of Erroneous and Unsafe Data, Promotor: Prof. dr. eng. R. Dekker
EPS-2003-024-LIS, ISBN: 90-5892-045-3, http://hdl.handle.net/1765/870

Wielemaker, M.W., Managing Initiatives: A Synthesis of the Conditioning and Knowledge-Creating View, Promotors: Prof. dr. H.W. Volberda & Prof. dr. C.W.F. Baden-Fuller
EPS-2003-28-STR, ISBN: 90-5892-050-X, http://hdl.handle.net/1765/1036

Wijk, R.A.J.L. van, Organizing Knowledge in Internal Networks: A Multilevel Study, Promotor: Prof. dr. eng. F.A.J. van den Bosch
EPS-2003-021-STR, ISBN: 90-5892-039-9, http://hdl.handle.net/1765/347

Wolters, M.J.J., The Business of Modularity and the Modularity of Business, Promotors: Prof. mr. dr. P.H.M. Vervest & Prof. dr. eng. H.W.G.M. van Heck
EPS-2002-011-LIS, ISBN: 90-5892-020-8, http://hdl.handle.net/1765/920

Pricing models for Bermudan-style interest rate derivatives

Bermudan-style interest rate derivatives are an important class of options. Many banking and insurance products, such as mortgages, cancellable bonds, and life insurance products, contain Bermudan interest rate options associated with early redemption or cancellation of the contract. The abundance of these options makes evident that their proper valuation and risk measurement are important to banks and insurance companies. Risk measurement allows for offsetting market risk by hedging with underlying liquidly traded assets and options. *Pricing models* must be arbitrage-free, and consistent with *(calibrated to)* prices of actively traded underlying options. Model dynamics need be consistent with the observed dynamics of the term structure of interest rates, e.g., correlation between interest rates. Moreover, valuation algorithms need be efficient: Financial decisions based on derivatives pricing calculations often need to be made in seconds, rather than hours or days. In recent years, a successful class of models has appeared in the literature known as market models. This thesis extends the theory of market models, in the following ways: *(i)* it introduces a new, efficient, and more accurate approximate pricing technique, *(ii)* it presents two new and fast algorithms for correlation-calibration, *(iii)* it develops new models that enable efficient calibration for a whole new range of derivatives, such as fixed-maturity Bermudan swaptions, and *(iv)* it presents novel empirical comparisons of the performance of existing calibration techniques and models, in terms of reduction of risk.

ERIM

The Erasmus Research Institute of Management (ERIM) is the Research School (Onderzoekschool) in the field of management of the Erasmus University Rotterdam. The founding participants of ERIM are RSM Erasmus University and the Erasmus School of Economics. ERIM was founded in 1999 and is officially accredited by the Royal Netherlands Academy of Arts and Sciences (KNAW). The research undertaken by ERIM is focussed on the management of the firm in its environment, its intra- and inter-firm relations, and its business processes in their interdependent connections.

The objective of ERIM is to carry out first rate research in management, and to offer an advanced graduate program in Research in Management. Within ERIM, over two hundred senior researchers and Ph.D. candidates are active in the different research programs. From a variety of academic backgrounds and expertises, the ERIM community is united in striving for excellence and working at the forefront of creating new business knowledge.

ERIM ERASMUS RESEARCH INSTITUTE OF MANAGEMENT

www.erim.eur.nl

ISBN 90-5892-099-2

Design: B&T Ontwerp en advies www.b-en-t.nl Print: Haveka www.haveka.nl